

# Perichromism: a novel technique to distinguish between amorphous and crystalline material

By

**Patrick J. Major**

[BSc (Hons), AMRSC]

A thesis submitted in partial fulfilment of the requirements of the University of  
Greenwich for the degree of Doctor of Philosophy (in Chemistry)

Medway Sciences  
School of Science  
University of Greenwich at Medway  
Chatham Maritime,  
Kent ME4 4TB, UK

**April 2010**



*the*  
UNIVERSITY  
*of*  
GREENWICH

# Abstract

## *Perichromism: A novel technique to distinguish between amorphous and crystalline material*

It is important for the pharmaceutical industry to be able to distinguish between amorphous and crystalline material, as an unexpected change in crystallinity can affect the character, efficacy and even safety of a medicine. There are currently many techniques that are used to distinguish between morphological forms, but these have many drawbacks, including cost and limit of detection. In this context there are currently no techniques that can be adapted for on-line analysis.

To distinguish between amorphous and crystalline material, 0.1% w/w phenol red, was added to sucrose, and dissolved in water. The solution was frozen before being freeze-dried, and the resultant amorphous excipient, with probe incorporated, was split into eight equal masses. The samples were then stored at controlled temperature and at a relative humidity unique to each sample. After storage for one week under these conditions, visual inspection of the samples showed that there were two distinct groups. Each sample was analysed by diffuse reflectance ultraviolet spectroscopy (DRUV) spectroscopy which confirmed the existence of two groups. The amorphous or crystalline nature of each sample tested by DRUV spectroscopy was independently verified by the following techniques: FT-Raman spectroscopy; differential scanning calorimetry; and X-ray diffraction. These techniques were also used to compare the excipient without the probe to that with the probe molecule to ensure that the presence of the probe molecule had not affected the sucrose.

Once the experimentation had been concluded using sucrose as the pharmaceutical excipient, the sample set of excipients was increased to include lactose, trehalose and raffinose. All experiments conducted with the saccharides were in agreement with each other. SEM of amorphous and crystalline trehalose with and without the probe was also performed, which showed that crystalline trehalose with phenol red has a very disrupted surface compared to amorphous trehalose with phenol red, or trehalose without phenol red. Other experiments were conducted into probe choice and concentration, showing that the original choice of concentration for phenol red was the optimum choice. Reichardt's dye was chosen as a comparison probe to phenol red as Reichardt's dye is the most solvatochromic probe so far discovered. Reichardt's dye has very poor aqueous solubility, necessitating a change in method, so a rotary evaporator was used. A change in the wavelength in the DRUV spectra of any of the four saccharides used with phenol red was not observed with Reichardt's dye. DSC was used to confirm that each saccharide with Reichardt's dye had been made amorphous or crystalline.

A mechanism of action for perichromism (the change in wavelength observed) with phenol red is suggested, and that is that perichromism occurs via hydrogen bonding, with potential changes to the planarity of the probe caused by different bonding mechanisms between the amorphous and crystalline surfaces. These studies show that perichromism is a quick, cheap technique that allows for a visual interpretation of morphological form of a pharmaceutical excipient, which could easily be adapted for use as an on-line pharmaceutical manufacturing test.

***Patrick J. Major (BSc (Hons), AMRSC)***

## Acknowledgements

Firstly I would like to thank my supervisors, Dr. Bruce Alexander, Dr. Victoria Cornelius and Professor John Mitchell, without whom I would never have been able to complete this work.

I would also like to thank all my colleagues in Medway Sciences: those who were there when I started – Vanessa Castro-Lopez, Claudia da Costa Matthews, Louise Garcia, Gill Gibson, Saima Jabeen, Natasa Majcen, Summia Naz, Wanessa Russeau, Philip Lansdell-Smith and George Vine and those who joined later – Nighat Kausar, Hani Nur, Kerstin Mader, Vivek Trivedi, Nicola Gaunt, Sam Booth, Tammy Ehiwe, Tracey Ehiwe, Joanna Thorn and Craig Morton.

Thanks also to Amanda Lewis, Prof. Martin Snowden and Prof. Babur Chowdhry for support and advice at various stages of the project and Dr. Laura Waters at the University of Huddersfield for suggesting I should consider a Ph.D. in the first place.

Tony Auffret for his insightful suggestions with probe molecules, John Murphy, Ian Slipper, Vivek Trivedi and Tracey Ehiwe for XRD, Sam Booth for help with EDX.

Pfizer Ltd for funding the project.

Finally, I would like to thank my family for their un-ending support through-out all my studies.

*For Sarah-Jayne and Elliott*

*“Alea iacta est”*

Gaius Julius Caesar, 49BC

# Contents

<b>Title page</b> .....	<b>i</b>
<b>Declaration</b> .....	<b>ii</b>
<b>Abstract</b> .....	<b>iii</b>
<b>Acknowledgements</b> .....	<b>iv</b>
<b>Dedication</b> .....	<b>v</b>
<b>Quote</b> .....	<b>vi</b>
<b>Contents</b> .....	<b>vii</b>
<b>List of figures</b> .....	<b>xi</b>
<b>List of tables</b> .....	<b>xv</b>
<b>List of abbreviations</b> .....	<b>xvi</b>
<b>Chapter 1: Introduction</b> .....	<b>1</b>
1.1 Solvatochromism .....	1
1.1.1 Electron transitions .....	3
1.1.2 The $E_T(30)$ and $E_T^N$ scales of solvent polarity. ....	4
1.2 Amorphous and crystalline solids.....	6
1.2.1 Amorphous solids .....	7
1.2.1.1 Transition temperatures.....	9
1.2.2 Crystalline solids.....	11
1.2.2.1 Polymorphism .....	12
1.2.2.2 Solvates .....	13
1.3 Surface chemistry .....	14
1.3.1 Adsorption.....	14
1.3.2 Surface energy .....	16
1.4 Surface acidity of pharmaceutical excipients .....	17
1.5 The project .....	21
1.5.1 Perichromism .....	22
1.5.1.1 Potential applications.....	23
1.6 References.....	24
<b>Chapter 2: Techniques</b> .....	<b>27</b>
2.1 Introduction.....	27
2.2 Freeze-drying .....	28

2.3	Rotary evaporation.....	29
2.4	Relative humidity.....	30
2.5	UV/vis and Diffuse Reflectance-UV spectroscopy .....	31
2.5.1	Ultraviolet/visible spectroscopy .....	33
2.5.2	The Beer-Lambert law .....	34
2.5.3	Diffuse Reflectance-UV.....	34
2.5.4	The Kubelka-Munk Remission Function.....	36
2.6	FT-Raman spectroscopy .....	37
2.6.1	Fourier transform as used in Raman spectroscopy .....	39
2.7	Differential scanning calorimetry .....	42
2.8	X-ray diffraction .....	44
2.9	Other techniques .....	47
2.9.1	Electron microscopy .....	47
2.9.2	Energy-Dispersive X-ray Analysis .....	48
2.10	Comparison of techniques.....	48
2.11	References.....	56
<b>Chapter 3: Materials and Methods .....</b>		<b>58</b>
3.1	Introduction.....	58
3.2	Dye selection.....	59
3.3	Excipients.....	61
3.3.1	Sucrose .....	61
3.3.2	Lactose .....	62
3.3.3	Trehalose .....	62
3.3.4	Raffinose .....	63
3.4	Equipment.....	64
3.4.1	Freeze-drying .....	64
3.4.2	Relative humidity.....	65
3.4.3	DRUV .....	65
3.4.4	FT-Raman .....	66
3.4.5	DSC.....	66

3.4.6	XRD .....	67
3.4.7	SEM .....	67
3.4.8	EDX .....	67
3.5	Methods.....	67
3.6	References.....	70
<b>Chapter 4: Results and discussion – The saccharides .....</b>		<b>71</b>
4.1	Introduction.....	71
4.2	Selection of probe molecule.....	72
4.3	DRUV spectra of sucrose.....	76
4.4	FT-Raman of sucrose .....	79
4.5	FT-Raman of sucrose without probe.....	80
4.6	DSC of sucrose .....	82
4.7	DSC of sucrose without probe .....	85
4.8	XRD of sucrose.....	86
4.9	XRD of sucrose without probe .....	88
4.10	Summary of sucrose.....	90
4.11	DRUV spectra of lactose .....	92
4.12	FT-Raman of lactose.....	95
4.13	FT-Raman of lactose without probe .....	96
4.14	DSC of lactose .....	97
4.15	DSC of lactose without probe .....	100
4.16	XRD of lactose.....	101
4.17	XRD of lactose without probe .....	102
4.18	Summary of lactose.....	103
4.19	DRUV spectra of trehalose .....	104
4.20	FT-Raman of trehalose .....	108
4.21	FT-Raman of trehalose without probe .....	109
4.22	DSC of trehalose .....	109
4.23	DSC of trehalose without probe.....	111
4.24	XRD of trehalose .....	112
4.25	XRD of trehalose without probe.....	114
4.26	Summary of trehalose .....	115
4.27	DRUV spectra of raffinose .....	116

4.28 DSC of raffinose .....	119
4.29 DSC of raffinose without probe .....	121
4.30 XRD of raffinose.....	122
4.31 XRD of raffinose without probe .....	123
4.32 Summary of raffinose .....	124
4.33 The saccharides.....	125
4.34 References.....	128
<b>Chapter 5: Mechanistic studies and sample set expansion .....</b>	<b>131</b>
5.1 Introduction.....	131
5.2 Control experiments.....	131
5.3 Low-level amorphous content determination of sucrose .....	133
5.4 Effect of mechanical friction on crystallinity .....	136
5.5 Dye concentration .....	139
5.6 Dispersive Raman of trehalose .....	140
5.7 SEM of trehalose.....	141
5.8 EDX of trehalose.....	145
5.9 Perichromism with other materials? .....	145
5.10 Sample preparation .....	150
5.11 Reichardt's dye .....	152
5.11.1 A comparison of the three methods .....	157
5.12 Mechanism.....	157
5.13 References.....	162
<b>Chapter 6: Conclusions and future work .....</b>	<b>164</b>
6.1 Conclusions.....	164
6.2 Future work.....	168
6.3 References .....	172

# List of Figures

Figure	page
1.1 A graphical representation of solvatochromism .....	2
1.2 Electronic energy levels and transitions .....	3
1.3 Reichardt's dye .....	4
1.4 An illustration of a) long-range order in a crystalline material; and b) lack of long-range order in an amorphous material .....	7
1.5 Amorphous solid to liquid (and back again).....	10
1.6 The Bravais lattices .....	11-12
1.7 Energetic favourability of polymorphs .....	13
1.8 An example of a Langmuir adsorption isotherm. ....	15
1.9 Surface and internal energy differences.....	16
2.1 A temperature-pressure phase diagram .....	29
2.2 Light from the light source a) passing through a transparent solution in UV/vis spectroscopy, b) specular reflectance from a mirror, and c) diffuse reflectance from a solid surface, as in DRUV spectroscopy. ....	32
2.3 Schematic of an UV/vis spectrophotometer. ....	33
2.4 Schematic of an integrating sphere. ....	35
2.5 Rayleigh and Raman scatter.....	38
2.6 Stokes, and anti-Stokes Raman scattering.. ....	39
2.7 Schematic of a standard interferometer in an FT-Raman spectrometer.. ....	41
2.8 a) constructive interference of two waves, b) total destructive interference and c) partial destructive interference.....	41
2.9 Schematic of a Differential Scanning Calorimeter .....	43
2.10 DSC thermogram for an amorphous and a crystalline material.....	44
2.11 X-ray diffractogram of a crystalline sample and an amorphous sample showing the characteristic "halo" .....	45
2.12 An electron micrograph of crystalline raffinose. ....	48
3.1 Methyl red.....	59
3.2 Methyl green. ....	60
3.3 Phenol red. ....	61
3.4 Sucrose.....	62

3.5	Lactose.....	62
3.6	Trehalose.....	63
3.7	Raffinose.....	64
4.1	Diffuse-reflectance UV spectra of sucrose with 0.5 % w/w methyl green.....	73
4.2	Diffuse-reflectance UV spectra of lactose with 0.5 % w/w methyl green. ....	73
4.3	Diffuse-reflectance UV spectra of sucrose with methyl red.....	75
4.4	Diffuse-reflectance UV spectra of lactose with methyl red.....	75
4.5	Eight samples of sucrose with 0.1 % w/w phenol red after storage for one week at 25° C and controlled %RH.....	77
4.6	DRUV spectra of sucrose with 0.1 % w/w phenol red after storage for one week at 25° C and controlled %RH.....	78
4.7	First derivative diffuse-reflectance UV spectra of sucrose with 0.1 % w/w phenol red after storage for one week at 25° C and controlled %RH.....	78
4.8	FT-Raman spectra of sucrose with 0.1 % w/w phenol red after storage for one week at 25° C and controlled %RH. ....	80
4.9	FT-Raman spectra of sucrose after storage for one week at 25° C and controlled %RH. ....	82
4.10	DSC thermograms of sucrose with 0.1 % w/w phenol red after storage for one week at 25° C and controlled %RH. ....	83
4.11	DSC thermograms of sucrose after storage for one week at 25° C and controlled %RH. ....	85
4.12	XRD diffractograms of sucrose with 0.1 % w/w phenol red after storage for one week at 25° C and controlled %RH. ....	87
4.13	XRD diffractograms of sucrose stored for one week at 25° C and controlled %RH. ....	89
4.14	DRUV spectra of sucrose with 0.1 % w/w phenol red after storage for one week at 25° C and controlled %RH. ....	91
4.15	Eight samples of lactose with 0.1 % w/w phenol red after storage for one week at 25° C and controlled %RH. ....	93
4.16	DRUV spectra of lactose with 0.1 % w/w phenol red after storage for one week at 25° C and controlled %RH. ....	93
4.17	First derivative DRUV spectra of lactose with 0.1 % w/w phenol red after storage for one week at 25° C and controlled %RH.....	94
4.18	FT-Raman spectra of lactose with 0.1 % w/w phenol red after storage for one week at 25° C and controlled %RH. ....	95
4.19	FT-Raman spectra of lactose after storage for one week at 25° C and controlled %RH. ....	97

4.20 DSC thermograms of lactose with 0.1 % w/w phenol red after storage for one week at 25° C and controlled %RH. ....	98
4.21 DSC thermograms of lactose after storage for one week at 25° C and controlled %RH. ....	100
4.22 XRD diffractograms of lactose with 0.1 % w/w phenol red after storage for one week at 25° C and controlled %RH. ....	102
4.23 XRD diffractograms of lactose after storage for one week at 25° C and controlled %RH. ....	103
4.24 Photographs of trehalose with 0.1 %w/w phenol red, freeze-dried and stored for one week at 25° C and controlled %RH.....	106
4.25 DRUV spectra of trehalose with 0.1 %w/w phenol red after storage for one week at 25° C and controlled %RH. ....	106
4.26 First derivative DRUV spectra of trehalose with 0.1 % w/w phenol red after storage for one week at 25° C and controlled %RH.....	107
4.27 FT-Raman spectroscopy of trehalose with 0.1 %w/w phenol red after storage for one week at 25° C and controlled %RH.....	108
4.28 DSC of trehalose with 0.1 %w/w phenol red stored for one week at 25° C and controlled %RH.....	110
4.29 DSC of trehalose stored for one week at 25° C and controlled %RH.....	111
4.30 XRD of trehalose with 0.1 %w/w phenol red stored for one week at 25° C and controlled %RH.....	113
4.31 XRD of trehalose stored for one week at 25° C and controlled %RH. ....	114
4.32 DRUV spectra of raffinose with 0.1 %w/w phenol red stored for one week at 25° C and controlled %RH. ....	117
4.33 First derivative DRUV spectra of raffinose with 0.1 % w/w phenol red after storage for one week at 25° C and controlled %RH.....	118
4.34 DSC of raffinose with 0.1% w/w phenol red, stored for one week at 25° C and controlled %RH.....	119
4.35 DSC of raffinose stored for one week at 25° C and controlled %RH. ....	121
4.36 XRD of raffinose with 0.1% w/w phenol red, stored for one week at 25° C and controlled %RH.....	122
4.37 XRD of raffinose stored for one week at 25° C and controlled %RH.....	123
4.38 A comparison of four amorphous saccharides, each with 0.1 %w/w phenol red. ....	126
4.39 A comparison of four crystalline saccharides, each with 0.1 %w/w phenol red. ....	127
5.1 DRUV spectra of freeze-dried phenol red stored for one week at constant temperature (25° C) and %RH. ....	132

5.2	DRUV spectra of mixtures of amorphous and crystalline sucrose .....	133
5.3	Correlation between amorphous content of sucrose and the ratios of crystalline peak intensity to amorphous peak intensity.....	135
5.4	DRUV spectra of sucrose with 0.1 %w/w phenol red, each spectrum taken after grinding in a mortar in pestle.....	137
5.5	XRD of ground, and crystalline sucrose with 0.1 %w/w phenol red.....	138
5.6	DRUV spectra of amorphous sucrose with various concentrations of phenol red. ...	139
5.7	Dispersive Raman of trehalose with 0.1 %w/w phenol red stored for one week at 25° C and 57 %RH.....	141
5.8	SEM of a) amorphous trehalose with 0.1 %w/w phenol red; b) amorphous trehalose; c) crystalline trehalose with 0.1 %w/w phenol red; and d) crystalline trehalose. ....	142-143
5.9	Solution UV/Vis spectra of phenol red at four different pH values. ....	146
5.10	Electronic Absorbance spectra of phenol red in aqueous solution .....	147
5.11	DRUV spectra of four excipients with 0.1 %w/w phenol red that were used in the literature to examine “pH-equivalence”.....	148
5.12	Comparison between processing methods for sucrose, with 0.1 %w/w phenol red..	151
5.13	DRUV spectra of four saccharides with 0.1 %w/w Reichardt’s dye, freeze dried and stored for 1 week at 25° C and controlled %RH.....	154
5.14	DSC of four saccharides with 0.1 %w/w E <sub>T</sub> (30), stored for one week at 25° C and controlled %RH.....	155
5.15	DRUV spectra of E <sub>T</sub> (30).....	156
5.16	Phenol red. ....	160
5.17	Neutral red.. ....	161

## List of tables

Table	page
1.1 A sample of techniques used to determine low-levels of amorphous content in a predominantly crystalline solid .....	9
1.2 The “pH-equivalences” of some common pharmaceutical excipients .....	20
2.1 Techniques used to determine amorphous content .....	50-54
3.1 Some classes of excipient that might be used in tablet manufacture .....	59
3.2 List of saturated salt solutions to control relative humidity.....	65
4.1 Peaks from the DSC thermograms of sucrose with 0.1 % w/w phenol red after storage for one week at 25° C and controlled %RH. ....	84
4.2 Summary of results for sucrose by technique and storage %RH .....	90
4.3 Peaks in the thermograms of lactose .....	98
4.4 Summary of results for lactose by technique and storage %RH.....	104
4.5 Summary of results for trehalose by technique and storage %RH .....	116
4.6 $T_g$ and $T_m$ peak onset values for amorphous raffinose and raffinose pentahydrate. ..	120
4.7 Summary of results for trehalose by technique and storage %RH .....	124
4.8 Wavelength (nm) of maximum reflectance of four different saccharides, with 0.1 %w/w phenol red, after lyophilisation and storage for one week at 25° C and controlled %RH.....	128
5.1 Peak ratios of amorphous and crystalline material in figure 5.2.....	134
5.2 A comparison between predicted and actual DRUV spectra .....	148
5.3 A comparison between literature and predicted “pH-equivalence” values. ....	149

## List of abbreviations

Symbol	Description
%RH	Relative humidity
° C	Degree(s) centigrade
$\Delta$	Change
A	Absorbance
$\alpha$ L <sub>mono</sub>	$\alpha$ -lactose monohydrate
API	Active pharmaceutical ingredient
$\beta$ L	$\beta$ -lactose anhydrous
<i>ca.</i>	<i>Circa</i> (approximately)
cm <sup>-1</sup>	Wavenumber(s)
DMA	Dynamic mechanical analysis
DRUV	Diffuse reflectance ultraviolet spectroscopy
DSC	Differential scanning calorimetry
EDX	Energy dispersive x-ray analysis
<i>e.g.</i>	<i>Exempli gratia</i> (for example)
$E_T^N$	Normalised $E_T(30)$ value(s)
$E_T(30)$	Solvent polarity scale measured using Reichardt's dye
F(R)	Reflectance, after Kubelka-Munk remission theory applied
FT	Fourier transform
FT-Raman	Fourier transform Raman spectrscopy
g	Gram(s)
H <sub>0</sub>	Hammett acidity function
HOMO	Highest occupied molecular orbital
HSDSC	High speed differential scanning calorimetry
i.d.	Internal diameter
<i>i.e.</i>	<i>Id est</i> (that is)
IGC	Inverse gas chromatography
IMC	Isothermal microcalorimetry
IR	Infra-red

ITC	Isothermal calorimetry
kcal	Kilocalory(ies)
kV	Kilovolt
$\lambda_{\max}$	Wavelength of maximum absorbance
$L\alpha_H$	$\alpha$ -lactose anhydrous (hygroscopic)
$L\alpha_S$	$\alpha$ -lactose anhydrous (stable)
LUMO	Lowest unoccupied molecular orbital
mbar	Millibar
mg	Milligram
$\text{min}^{-1}$	<i>Per</i> minute
mL	Millilitre
Mol	Mole
Nd:YAG	Neodymium-doped yttrium aluminium garnet
NF	National Formulary
NIRS	Near infra-red spectroscopy
nm	Nanometer(s)
NMR	Nuclear magnetic resonance
pA	Pico ampere(s)
PAT	Process analytical technique
pH	Inverse log of the concentration of hydrogen ions.
“pH-eq”	“pH-equivalence”
$\text{pK}_a$	Inverse log of acid dissociation constant
ppm	Part(s) per million
PSP	Phenolsulphonphthalein
$\text{s}^{-1}$	Per second
SEM	Scanning electron microscopy
Sol Cal	Solution calorimetry
SSNMR	Solid state nuclear magnetic resonance spectroscopy
$T$	Temperature
$T_c$	Crystallisation temperature
$T_g$	Glass transition temperature
TGA	Thermal gravimetric analysis
$T_m$	Melting temperature

<b>TMS</b>	<b>Tetramethylsilane</b>
<b>USP</b>	<b>United States pharmacopoeia</b>
<b>UV/vis</b>	<b>Ultraviolet/visible</b>
<b>W</b>	<b>Watt(s)</b>
<b>w/v</b>	<b>Weight/volume</b>
<b>w/w</b>	<b>Weight/weight</b>
<b>XRD</b>	<b>X -ray diffraction</b>

# Chapter 1

## Introduction

### 1.1 Solvatochromism

The stability of molecular orbitals is influenced by the surrounding medium that a molecule is in. This affect on stability will be reflected in electronic absorption spectra. Solvatochromism is observed when a change in solvent causes a change in the position and/or intensity of an absorption band.<sup>[1, 2]</sup> The word solvatochromism is slightly misleading, as it suggests that the effect of the media is only applicable to change in polarity in the liquid state, when polarity change in solid and gaseous media can also be observed and measured.<sup>[3, 4]</sup>

Solvatochromism is caused by differential solvation of the ground and excited state of a chromophore.<sup>[4]</sup> A chromophore is a feature in a molecule where the energy difference between two molecular orbitals occur within the visible light range.<sup>[5]</sup> When light is absorbed, an electron can be excited from its ground state to an excited state.<sup>[5]</sup> Chromophores, are usually either metal complexes or, in organic materials, an unsaturated functional group (often caused by conjugated  $\pi$  systems, which are alternating single and double bonds).<sup>[6]</sup> An example of a chromophore is an azo dye, which contains a N=N bond (each nitrogen also being bonded to either an aromatic ring or a carbon chain), such as  $\text{CH}_3\text{N}=\text{NCH}_3$  which has a maximum absorbance ( $\lambda_{\text{max}}$ ) of 339 nm in water.<sup>[7]</sup>

There are two possible solvatochromic shifts. A bathochromic (blue) shift with increasing solvent polarity is negative solvatochromism, caused by the ground-state being stabilized, or the excited-state being destabilised. It follows that a hypsochromic (red) shift is positive solvatochromism with the (de)stabilization effects on the electronic states reversed.<sup>[4]</sup> (Figure 1.1).

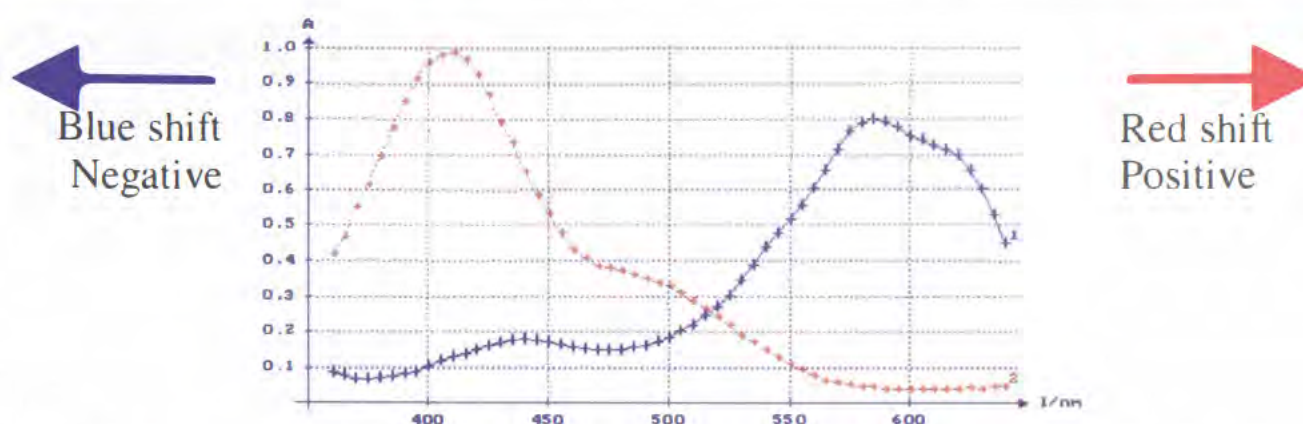


Figure 1.1. A graphical representation of solvatochromism. Two distinct spectra for one solvatochromic molecule in two solvents of differing polarity.

An electron in its ground state, is at its lowest possible energy level, the excited state, is any where the energy level is greater than the ground. Electron excitations are very short-lived events, typically in the femtosecond region.<sup>[4]</sup> Excitations can be caused by the adsorption of photons, if the energy increase from the photon is too great, the electron will be ejected, and no longer be part of the original system. Relaxation from the excited state is accompanied by the release of a photon.<sup>[5]</sup>

Only some electronic excitations are possible.<sup>[5]</sup> Selection rules show which electron transitions are allowed, and which are forbidden (although forbidden transitions can still occur). Some selection rules state that, the spin quantum number of the electron can not be changed during a transition, and that there is a limit to the number of electrons that can be excited at any one time.<sup>[5]</sup>

Solvatochromic dyes can also be used as probes for the determination of pH<sup>[8]</sup> because they exhibit colour change, not only with respect to solvent polarity, but often with pH. A pH indicator is usually a weak acid or base that changes the colour of a solution when it is either protonated or de-protonated, effectively because the indicator will be sensitive to the presence of H<sup>+</sup> or OH<sup>-</sup> ions. The electron configuration of the indicator will change when it binds to one of these ions, which is observed as the colour change in the solution. Examples of pH indicators include phenol red (yellow below pH 6.8 and red above pH 8.2)<sup>[7]</sup> methyl red (pink/red below pH 4.4, yellow above 6.2)<sup>[7]</sup> and phenolphthalein (colourless below pH 8.3, pink/purple above pH 10.0).<sup>[7]</sup> Note that these transitions are dependent upon solvent used.

The solvatochromic shift that is observed is dependent on the chemical structures and physical properties of both the chromophore and the solvent. Dye molecules with a large change in their permanent dipole upon excitation exhibit larger solvatochromic shifts.<sup>[4]</sup> Other potentially strongly solvatochromic probes are able to donate or accept hydrogen ions.<sup>[4]</sup>

### 1.1.1 Electron transitions.

As a molecule absorbs energy, an electron is promoted from an occupied molecular orbital to an unoccupied molecular orbital<sup>[5]</sup> (Figure 1.2.). It requires less energy to promote an electron from the highest occupied molecular orbital (HOMO) to the lowest unoccupied molecular orbital (LUMO) than for any other electron transition, and, depending on selection rules, this is the most commonly observed promotion in UV/vis spectroscopy. The electron in the HOMO means the molecule is in the ground state, and when the electron is promoted to the LUMO, the molecule is in the excited-state.<sup>[4]</sup>

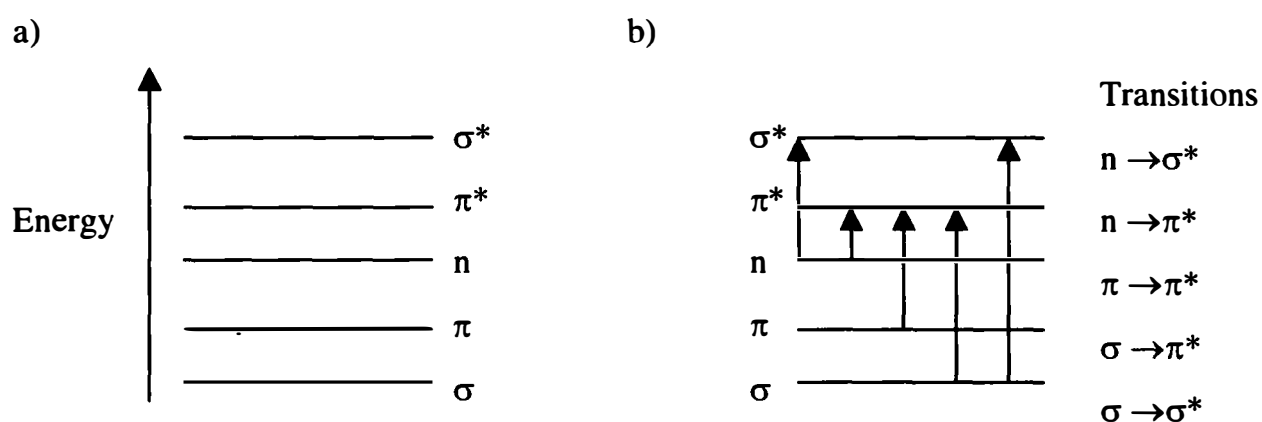


Figure 1.2. a) Electronic energy levels and b) transitions.

The occupied molecular orbitals are  $\sigma$ ,  $\pi$  and  $n$ , and the unoccupied are  $\pi^*$  and  $\sigma^*$  antibonds.<sup>[5]</sup> From Figure 1.2, it is apparent that a HOMO to LUMO transition of  $n\text{-}\pi^*$  for example in carbonyl compounds,<sup>[5]</sup> will require less energy, than any other transition (for the same molecule).

For an organic material to appear in a UV/vis spectrum, it must have a chromophore, which contains electrons of low excitation energy so that one or more of the above transitions can occur.<sup>[5]</sup> The reason why the observed

spectrum is a band rather than a single sharp peak is because the molecule is both vibrating and rotating during the irradiation/electronic excitation. These effects of motion can then be manifest in the electronic absorption spectrum.<sup>[7]</sup> In a solution, freedom to rotate is mostly lost, but the energy of vibrational levels are, particularly for polar solvents like water, modified irregularly, the result is a Gaussian distribution of the energy of a molecule.<sup>[7]</sup> The spectrophotometer is unable to distinguish between the small differences in energy, and the result is a broad band in the solution spectra.<sup>[5, 7]</sup>

### 1.1.2 The $E_T(30)$ and $E_T^N$ scales of solvent polarity.

There are many solvatochromic probes that have been researched.<sup>[4]</sup> 2,6-(Diphenyl-4-(2,4,6-triphenyl-1-pyridino phenolate) betaine dye, also called Reichardt's dye, (Figure 1.3) is the most investigated of the solvatochromic probes,<sup>[9]</sup> having a very large negative solvatochromic shift. In water Reichardt's dye has a  $\lambda_{\max}$  of 453 nm and in diphenyl ether, 810 nm<sup>[4, 9, 10]</sup> caused by a  $\pi$ - $\pi^*$  electron transition.<sup>[4]</sup> Other solvatochromic probe molecules include Nile red, a positively solvatochromic probe, which has wavelengths of 390 nm in hexane and 593 nm in water, and the negatively solvatochromic merocyanine 540 nm, which has wavelengths of 574 nm in benzene and 537 nm in water.

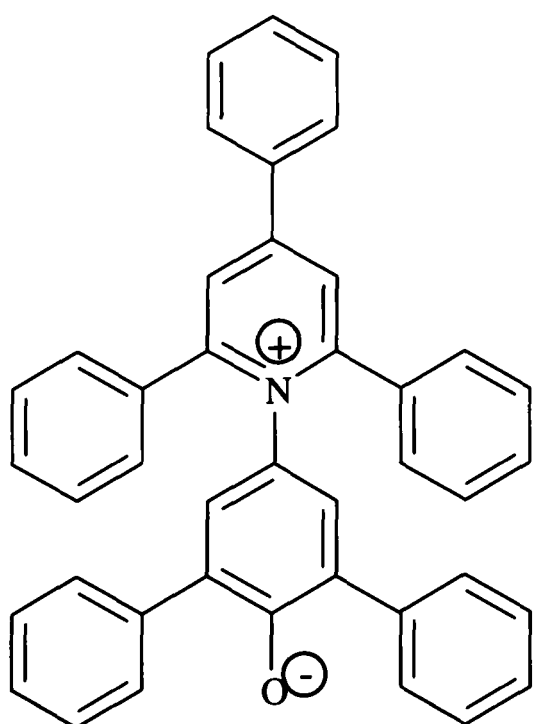


Figure 1.3. Reichardt's dye.

Reichardt's dye can be protonated, in acidic solvents, for example acetic acid.<sup>[4]</sup> However, in the form shown in Figure 1.3. as a dipolar zwitterionic molecule, it exhibits a large permanent dipole moment.<sup>[4, 11]</sup> It has been shown that Reichardt's dye can exhibit, along with solvatochromism, *piezochromism* (colour change with pressure) *thermochromism* (colour change with temperature) and *halochromism* (colour change with pH).<sup>[12]</sup> The solvatochromic absorption band, due to a  $\pi$ - $\pi^*$  transition, for Reichardt's dye lies within the visible spectrum, allowing for a visual estimation of the polarity of the solvent,<sup>[1]</sup> the dye is red in methanol,<sup>[4]</sup> green in acetone,<sup>[4]</sup> and blue in isoamyl alcohol (3-methyl-1-butanol).<sup>[4]</sup>

The  $E_T(30)$  scale is an empirical scale for measuring solvent polarities, based on Reichardt's dye.<sup>[10]</sup> The name means electron transition, and the (30) derives from the fact that Reichardt's dye had the number 30 in the original publication, and  $E_T$  is used to denote triplet energy.<sup>[4]</sup>  $E_T(30)$  values are the molar electronic transition energies of dissolved Reichardt's dye (kcal/mol) at 25°C and 1 bar pressure<sup>[4]</sup> as given by equation 1.<sup>[4, 13]</sup>

$$\begin{aligned} E_T(30) &= hc\tilde{\nu}_{max} N_A \\ &= (2.8591 \times 10^{-3})\tilde{\nu}_{max}(\text{cm}^{-1}) \\ &= 28591/\lambda_{max}(\text{nm}) \end{aligned}$$

Equation 1.

Where  $\tilde{\nu}_{max}$  is frequency, in wavenumbers, of the peak maxima,  $\lambda_{max}$  the wavelength of the lowest energy  $\pi$ - $\pi^*$  absorption band of Reichardt's dye,  $h$  is Planck's constant,  $c$  is the speed of light and  $N_A$  is Avagadro's number.

Normalized  $E_T^N$  values have also been introduced.  $E_T^N$  values are dimensionless and are based on a scale of two extremes of polarity, a polar solvent (water) and non-polar solvent (tetramethylsilane, TMS). Values for  $E_T^N$  range from 0.0 for TMS to 1.0 for water, and are calculated according to equation 2.<sup>[4]</sup>

$$E_T^N = \frac{E_T(\text{solvent}) - E_T(\text{TMS})}{E_T(\text{water}) - E_T(\text{TMS})}$$

$$E_T^N = \frac{E_T(\text{solvent}) - 30.7}{32.4}$$

Equation 2.

Either  $E_T(30)$  or  $E_T^N$  values can be used. A high value for either is indicative of a polar solvent.  $E_T(30)$  values give a facile comparison of the magnitude of the solvent effect, the  $E_T^N$  scale gives a better insight into the polarity of multi-component solvent systems.<sup>[4, 14]</sup>

## 1.2 Amorphous and crystalline solids

Pharmaceutical products can be administered in many different ways, from intravenous injection of liquids, to topical administration of creams, and oral administration of solutions and tablets. Depending on the route of administration for the drug, the medicine will be in either the solid, liquid or gaseous phase. The most common form of pharmaceutical administration is as a tablet, because it is stable, easy to administer, and maintain dosing regimens and has good patient compliance.<sup>[15]</sup> Tablets are an example of solid dosage design; other examples include capsules and dry-powder inhalers. It is essential for the pharmaceutical industry to know the exact parameters of their formulations, in order to understand the pharmacodynamics and pharmacokinetics of the medicine. Pharmacodynamics is the study of what the drug does to the body, pharmacokinetics being the study of what the body does to the drug. For solid drugs, this means understanding the morphological form of both the active pharmaceutical ingredient (API) and *all* the excipients in the formulation.

All solids have, theoretically, the possibility of existing as either a crystalline or an amorphous form.<sup>[15]</sup> A crystal is any material that has a regular repeating pattern of molecules in three-dimensional space, an amorphous solid has a random arrangement.<sup>[15]</sup> Some solid material falls outside of these definitions, for example quasicrystals, which are solids where the molecules are ordered, but do not have total long-range order.<sup>[16]</sup> For this work, crystal (or crystalline) and

amorphous will mean a material that fulfils the relevant, aforementioned definition.

When a material is cooled from a liquid phase to the solid, then the material may crystallise exhibiting long-range order.<sup>[17]</sup> However, if the cooling rate is greater than the crystallisation rate, then there will not be enough time to form this long-range order and the sample will be amorphous<sup>[18]</sup> (Figure 1.4.).

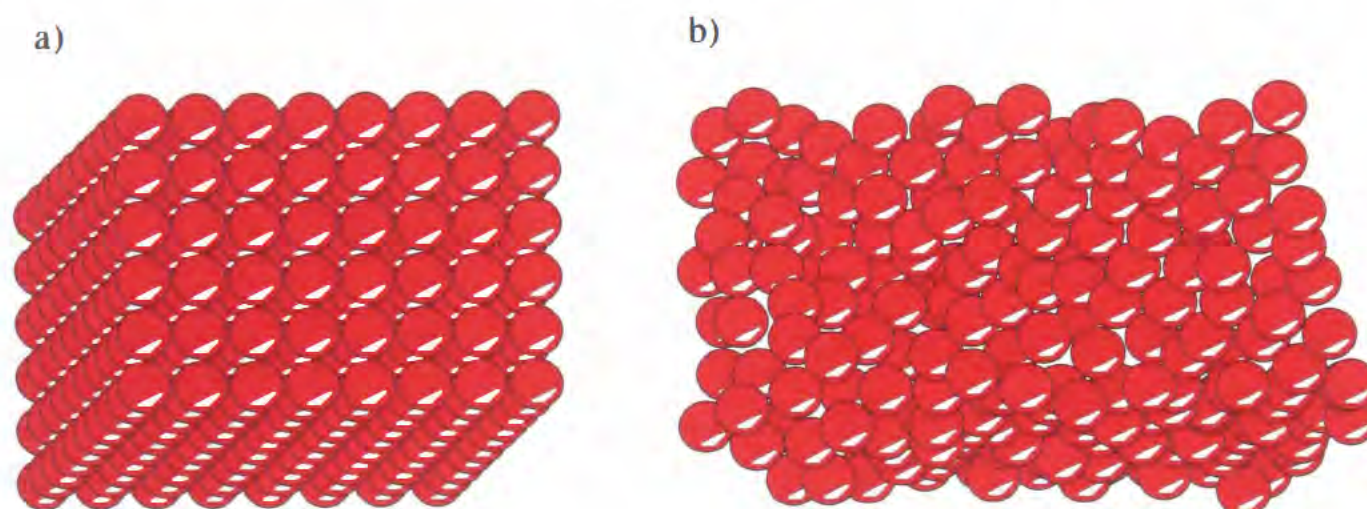


Figure 1.4. An illustration of a) long-range order in a crystalline material; and b) lack of long-range order in an amorphous material.

There are many pronounced differences between the properties of amorphous and crystalline solids, and these will be discussed in detail. Amorphous materials are said to exhibit short-range order,<sup>[18]</sup> this means molecules in an amorphous solid are not totally randomly arranged (as in a gas for example), but there is little to no repetition in the orientation of molecules, and therefore no symmetry.<sup>[18]</sup> It is also important to remember that an amorphous material can re-crystallize and a crystalline solid can be made amorphous (section 1.2.1).

### 1.2.1 Amorphous solids

Amorphous materials are common in many everyday materials, from glass to polymers and are important in a range of fields including food and pharmaceuticals.<sup>[18]</sup> It is of great importance to the pharmaceutical industry to be able to determine the presence of amorphous material in a drug.<sup>[19-22]</sup> Much of this importance stems from the fact that it is often neither advantageous nor

desirable to have amorphous material present in a pharmaceutical product. There are several reasons for this, those of interest for pharmaceutical companies relating to physico-chemical stability, dissolution rates and bioavailability.<sup>[18]</sup> Amorphous material is often less physically and chemically stable,<sup>[23]</sup> has greater solubility and dissolution,<sup>[24]</sup> and is more hygroscopic<sup>[25, 26]</sup> than its crystalline counterpart. An amorphous drug may have a different bioavailability than a crystalline one.<sup>[27]</sup> Other differences include the fact that an amorphous material, due to the absence of long-range order, and the random positioning of molecules, does not have a defined shape (crystal lattice) and from this, no definite melting point (breakage of the crystal lattice).<sup>[15]</sup> See section 1.2.1.1 for further information.

Amorphous material, usually being more hygroscopic than crystalline material, may aggregate as a result. Aggregation, of either the API or an excipient, is a serious problem for the pharmaceutical industry, especially for the inhalation route of administration<sup>[28]</sup> as the medicine will be unable to reach the target. If amorphous material in a drug crystallizes, then the bioavailability of the drug will be different,<sup>[27]</sup> effecting efficacy and safety. Crystallization may occur due to the lower stability and higher molecular mobility of amorphous material, with similar, unintended changes occurring to the pharmacodynamics of the drug.<sup>[29]</sup>

During manufacturing, amorphous material can be inadvertently produced. Common causes for this are processes that apply a mechanical force or cause particle-particle collisions, for example, jet-milling, tableting, spray-drying and freeze-drying,<sup>[19]</sup> where a solution is frozen, and the water then removed, the solute remains arranged randomly (*i.e.* as if still dissolved in a liquid) once all the water is removed, the solid material will not have the molecular mobility to form long range order and will remain amorphous, dependent on storage conditions. In many processes, the generation of amorphous material is unintended, and affects only the surface of the sample.<sup>[30]</sup>

The presence of amorphous material at the surface, gives a disproportionate influence compared to the percentage of the sample that has remained crystalline, because the surface is the area exposed to any external influence. This means a

product may change quite dramatically over time. Undesirable amorphous material is often generated as a small percentage of the total material, therefore many authors are attempting to find suitable methods for analysing very low fractions of amorphous content in a predominantly crystalline material<sup>[31-37]</sup> (Table 1.1.). Chapter 2 will discuss these, and other techniques, in greater detail.

Technique	Reference
X-Ray Diffraction (XRD)	35
Differential Scanning Calorimetry (DSC)	36
Raman Spectroscopy	33
Nuclear Magnetic Resonance (NMR)	32
Isothermal Calorimetry (ITC)	37
High speed DSC (HSDSC)	38
Near Infra-Red Spectroscopy (NIRS)	32

Table 1.1. A sample of techniques used to determine low-levels of amorphous content in a predominantly crystalline solid.

### 1.2.1.1 Transition Temperatures

Sometimes the amorphous form is preferred to the crystalline, usually to improve solubility. Unfortunately, due to the weaker physico-chemical stability of the amorphous form, it may crystallize during certain storage conditions.<sup>[38]</sup> The re-crystallisation of an amorphous solid is governed by several factors; temperature, relative humidity (%RH), pressure and time. The loosely packed amorphous material has very low molecular mobility, as one or more of the aforementioned factors is increased, the molecular mobility will also increase. When a specific mobility, for a given amorphous material, has been reached, the sample crystallises. The point where the molecular mobility is great enough for re-crystallisation is called the glass transition temperature ( $T_g$ ). When the storage temperature is above the  $T_g$ , re-crystallisation may occur. Increasing the pressure or relative humidity (water acts as a plasticiser, and increases molecular mobility) will cause the  $T_g$  to be lowered. This change in  $T_g$  can be very

pronounced, for example amorphous lactose stored at 0 %RH has a  $T_g$  of 104 °C<sup>[26]</sup> and at 57 %RH, the  $T_g$  is 25 °C.<sup>[34]</sup>

As stated earlier (section 1.2.) rapid cooling of a melt will cause a material to solidify as an amorphous “glass”.<sup>[39]</sup> If the sample is heated (or exposed to elevated humidity lowering the  $T_g$ ) the glass will become softer upon passing through the glass transition temperature and enter a “rubbery” state. From the rubbery state, the molecules, having increased molecular mobility,<sup>[18]</sup> may either pass the crystallization temperature ( $T_c$ ) and become a crystalline solid, or reform an amorphous material. If the crystalline solid is heated enough it will reach the melting temperature ( $T_m$ ) and become a liquid again. (Figure 1.5.) Melting is achieved by the molecules gaining sufficient energy to break the attractive forces that hold the crystal together.<sup>[15]</sup> The stronger the attractive forces, for example hydrogen bonds as opposed to van der Waals forces, holding the crystal together, the higher the melting temperature will be.

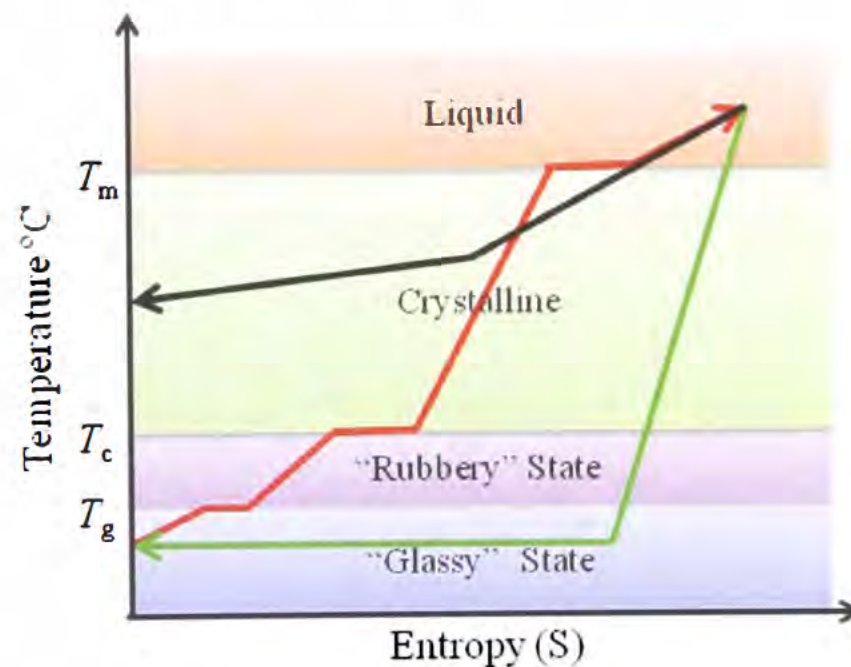
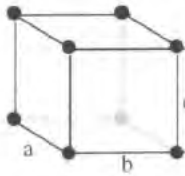
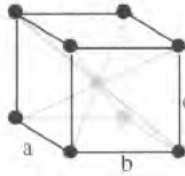
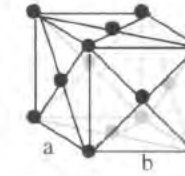
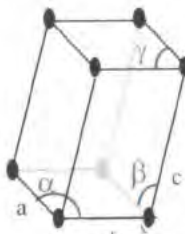


Figure 1.5. Amorphous solid to liquid (and back again). → Amorphous solid to liquid. → Very rapid cooling rate, there is not enough time for long-range order to form, so the liquid sample solidifies as an amorphous solid. → Slower cooling rate, long-range order forms, and the liquid solidifies to a crystalline material.

## 1.2.2 Crystalline solids

Unlike amorphous solids, crystalline solids have a definite shape and melting point.<sup>[15]</sup> A crystalline solid is one where structural units are arranged in a specific order over three-dimensional space,<sup>[40]</sup> giving a crystal lattice (Figure 1.4.). The basic structural unit is called the unit cell, and has defined dimensions and volume. A unit cell is a box, or compartment, containing one or more sets of atoms arranged in a particular way (motif) from which the structure of the entire crystal can be constructed. The dimensions of the unit cell are formed by the lattice parameters, defined by the length of the edges of the cell, along with the internal angles.<sup>[41]</sup> There are 14 possible arrangements, called Bravais lattices<sup>[41]</sup> (Figure 1.6.). The Bravais lattices are in one of seven geometric shapes, some of which have more than one possible Bravais lattice depending on the possibility of face centring, body centring and base centring. The seven geometric shapes are cubic, triclinic, monoclinic, orthorhombic, tetragonal, hexagonal and rhombohedral. It should be noted that even if two different crystals (*e.g.* different molecules) have face-centred cubic unit cells, the atoms might be arranged differently in them.

Geometric Shape	Bravais lattices'			
Cubic $a = b = c$ $\alpha, \beta, \gamma = 90^\circ$	Simple 	Body-centred 	Face-centred 	
Triclinic $a \neq b \neq c$ $\alpha, \beta, \gamma \neq 90^\circ$				
Monoclinic $a \neq b \neq c$ $\alpha \neq 90^\circ, \beta, \gamma = 90^\circ$	Simple 	Base-centred 		

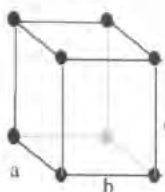
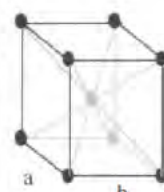
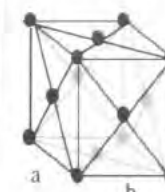
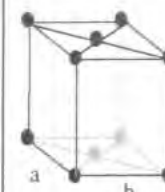
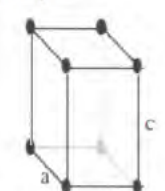
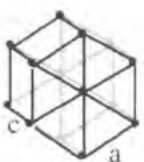
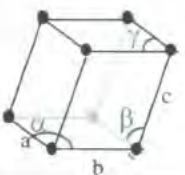
Orthorhombic $a \neq b \neq c$ $\alpha, \beta, \gamma = 90^\circ$	Simple 	Body-centred 	Face-centred 	Base-centred 
Tetragonal $a = b \neq c$ $\alpha, \beta, \gamma = 90^\circ$	Simple 	Body-centred 		
Hexagonal $a \neq c$				
Rhombohedral $a = b = c$ $\alpha, \beta, \gamma \neq 90^\circ$				

Figure 1.6. The Bravais lattices

### 1.2.2.1 Polymorphism

A solid may be able to crystallise into more than one crystal structure.<sup>[15]</sup> These different possible crystal structures from a material are called polymorphs. A polymorph has the same chemical properties as another polymorph of the same material, but its physical properties, for example, solubility and melting temperature can be quite different.<sup>[15]</sup> Polymorphism can arise in three distinct ways, different crystal packing, conformation (cause by rotation around a bond) and the introduction of a solvate, (section 1.2.2.2) this is called pseudopolymorphism,<sup>[40]</sup> as the chemistry of the crystal has been modified by the entrapment of a molecule in the crystal lattice.

The most energetically favourable polymorph is the most stable, less energetically favourable polymorphs are called metastable, and under certain conditions (similar to the re-crystallisation of an amorphous solid) can re-arrange to form the most energetically favourable polymorph (Figure 1.7). A well-known

polymorph is diamond, which is a metastable form of carbon – the stable form being graphite, however, it requires extremes of temperature and/or pressure to convert diamond to graphite. Pharmaceutical polymorphs may have a much lower activation energy barrier, and in some cases, may easily convert to the most stable form.

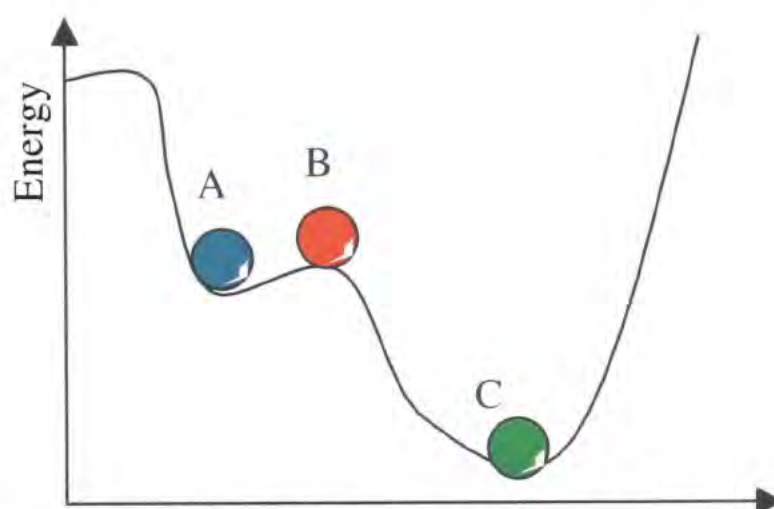


Figure 1.7. A) a metastable morph. B) Upon addition of energy, “A” will become B) an unstable morph, which may re-arrange to either “A” or to C) a more stable morph. The reason for the greater stability being the much greater energy requirement to convert “C” to “B” than for “A” to “B”, although it is still possible.

### 1.2.2.2 Solvates

Solvates arise when solvent molecules are incorporated into a crystal structure during crystallization. If the solvent is water, then it is said to be a hydrate. Hydrates are common in pharmaceutical products.<sup>[42]</sup> This incorporation of a solvent alters the physical properties of the solid.<sup>[40]</sup> It is also possible to produce a “desolvated solvate”<sup>[40]</sup> – *i.e.* removal of the solvent but the crystal retains the properties of the solvated form. Desolvated solvates are difficult to analyse, as they have the properties of the solvate, but the chemical composition of the original crystal form.<sup>[40]</sup>

Solvates differ in crystal packing and lattice energy, which often causes large changes in their physical properties, including solubility, melting point and density.<sup>[15]</sup> Changes to solubility can also affect the bioavailability of a drug.

Solvates may be formed more easily than the non-solvated crystal, for example the only commercially available form of lactose is  $\alpha$ -lactose monohydrate,<sup>[43]</sup> which all other lactose polymorphs are derived from.<sup>[43]</sup>

### 1.3 Surface Chemistry

Solid materials can be thought to exist as a bulk material covered by a surface layer. The majority of the solid will be in the bulk, but it is the material at the surface, being the initial contact, that will govern the chemical interactions of the solid.<sup>[7, 44]</sup> In practice, many surface analysis techniques are not sensitive enough to probe a 'monolayer' of a solid material; there is always going to be some level of penetration into the bulk material.

Surface chemistry is an umbrella term for all chemical interactions between two interfaces, which is how all chemical reactions, involving one or more solids, occur<sup>[44]</sup>. A solid can easily react with a liquid or a gas, but when mixed directly with another solid, there is usually no reaction, and the original products can be recovered, for example, mixing sugar with sand, the reagents can be recovered by adding water, where the sugar dissolves but the sand does not. To chemically react one solid with another, a solvent is usually required. Solvatochromic probes can be dissolved in a solvent, added to an excipient, and the solvent removed, bonding the probe to the excipient. Relative humidity (to lower the  $T_g$ , of the amorphous excipient) is also a solid-liquid interaction. There are many properties at the surface of a solid that can be examined, including adsorption,<sup>[15]</sup> and surface energy.<sup>[45]</sup>

#### 1.3.1 Adsorption

Adsorption is the accumulation on a solid surface of either a gas or a liquid. Adsorption can be either by chemisorption or physisorption. Chemisorption is adhesion through the creation of a chemical bond.<sup>[15]</sup> Physisorption is adhesion through much weaker (intermolecular) van der Waals forces.<sup>[15]</sup> Physisorption also allows for multi-layer accumulation of the adsorbate species, chemisorption

requires bond-formation, which may not be as quick, is not as easily reversed and can only form a monolayer of the adsorbate.<sup>[15]</sup> The reverse process is called desorption. Adsorption should not be confused with absorption, which may include penetration of the absorbent into the bulk layer. Adsorption arises as a consequence of surface energy. Unlike atoms in the bulk material, those at the surface are not wholly surrounded by other atoms, and therefore are able to attract, and bind to adsorbates.

Water that is part of the crystal lattice of a hydrate is called essential water. Water adsorbed onto the surface of a crystal is non-essential, and is not present in a stoichiometric proportion. Non-essential water is present on all solids.<sup>[7]</sup> Logically, for a material that will adsorb, the greater the surface area available, the more adsorption can take place.<sup>[46]</sup> So a disorganised (and potentially larger) surface of an amorphous material may be more likely to adsorb than the more structured (and smaller) surface of the crystal face. However, adsorption of water is controlled by the environmental conditions, being dependent on temperature and humidity.<sup>[7]</sup> An adsorption isotherm can be constructed by plotting the weight of, for example, water adsorbed on the surface of a solid against the partial pressure of water in the surrounding atmosphere.<sup>[7]</sup> A Langmuir adsorption isotherm (Figure 1.8) will reveal the level of adsorption for a given pressure (for adsorption of gases) or concentration (liquids).<sup>[7]</sup>

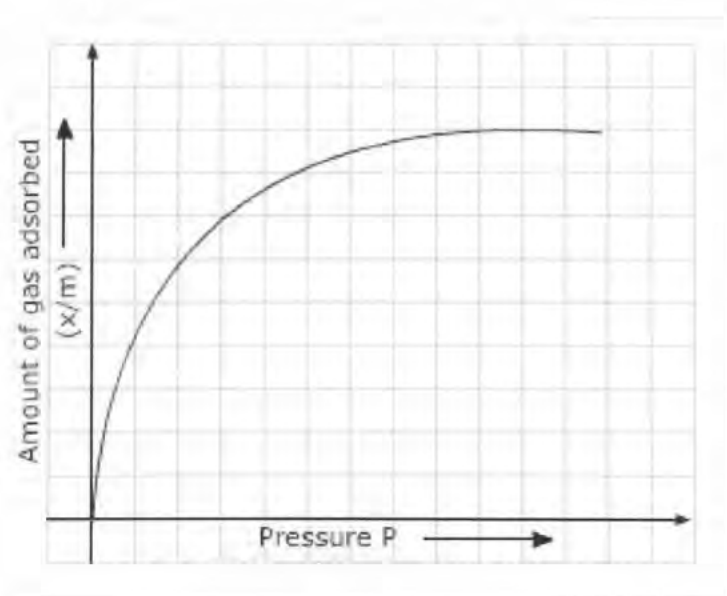


Figure 1.8.

An example of a Langmuir adsorption isotherm.

### 1.3.2 Surface Energy

The surface properties are described in terms of surface free energy, usually just called surface energy.<sup>[47]</sup> Generally, higher surface energy corresponds to a greater chance for interactions to occur.<sup>[47]</sup> Processes such as milling can cause the surface of a material to become amorphous. This can have a major factor on the surface energy. It has also been argued that these processes may alter surface energy by exposing new crystal faces to the surface.<sup>[44]</sup>

Surface energy arises from the inward force exerted on the molecules at the surface by molecules in the bulk material<sup>[15]</sup> (Figure 1.9). Surface interactions are dependent on these forces, and if unfavourable, interactions are unlikely to occur. The surface energy of solids is far more difficult to calculate than for liquids, primarily because every crystal face will have different internal forces affecting it and the possibility of crystal defects. From this it is logical that different crystals, for example hydrates, of a solid have very different surface energies. In the case of an amorphous material, the randomness of atoms present at the surface,<sup>[15]</sup> and greater freedom of mobility, which could lead to a change in surface energy with time, make calculating the surface energy even more difficult.

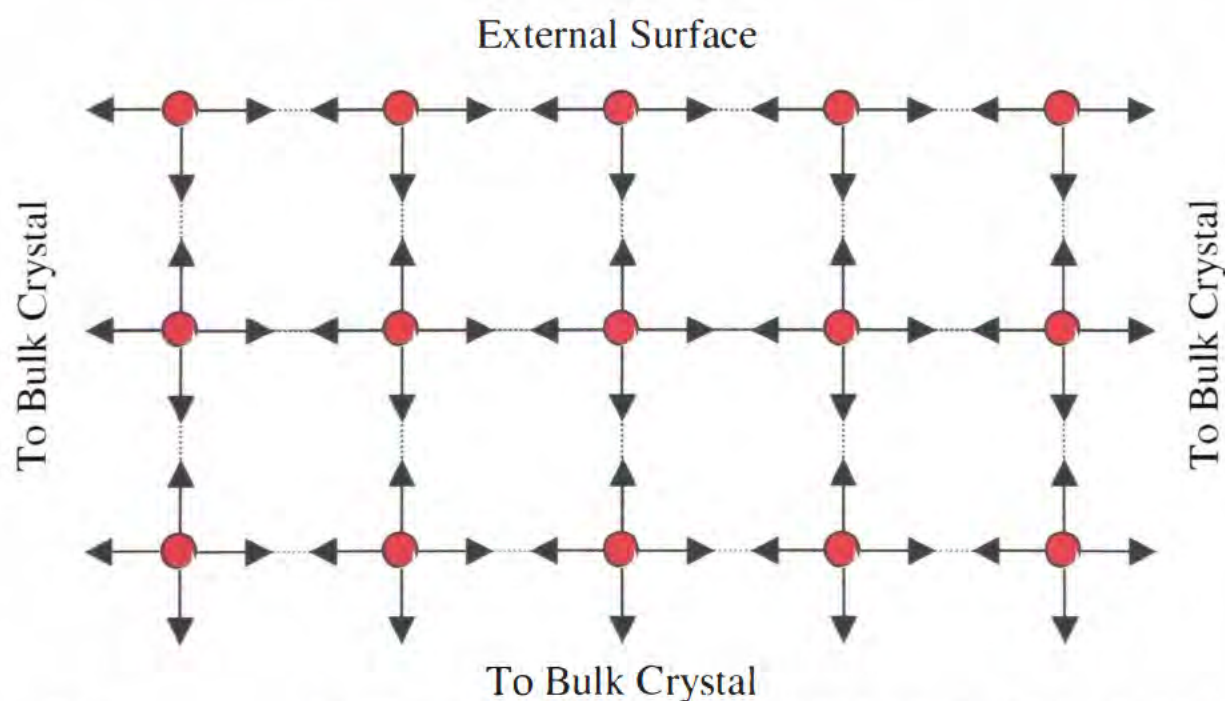


Figure 1.9 A simplified diagram showing that the intermolecular forces of molecules present at the surface are different to those in the bulk material.

Inverse gas chromatography (IGC) is able to determine the surface energy of amorphous materials and how they can be affected by their environment, for example, the surface energy of amorphous lactose is altered by relative humidity.<sup>[48]</sup> As the relative humidity increases, a decrease from the high-energy amorphous state to the lower energetic state of crystalline lactose is observed. IGC is, as the name suggests, a form of gas chromatography, however, rather than analysing the separation of a mixture of gases by a standard stationary phase as in normal gas chromatography, in IGC the column contains a known mass of the solid sample under investigation and a single gas is injected into it. The gas will interact with the powder column surface, and the surface energy of the powder can be calculated from the retention time of the gas in the column.<sup>[44]</sup> IGC assumes that the surface area of the powder is known, and that orientation of the powder does not affect adsorption of the gas, similar to preferred orientation in XRD (discussed in section 2.8)

As the surface energy of a solid is dependant on the surface being shown, it stands to reason that the surface acidity will show similar dependence as well, as different atoms will be present at the surface (certainly it is plausible that there could be a difference between an amorphous and a crystalline solid). Solids, unlike liquids have no easy way of determining acidity. For most solutions it is a common, and simple, method to measure the pH by either using a pH electrode, or adding a pH indicator, or using indicator paper. Little is known about the acidic or basic properties of solid pharmaceutical excipients,<sup>[49]</sup> because there is no simple method to measure the pH of a solid – none of the techniques for measuring solution pH are suitable. However, as discussed in the next section, there have been recent attempts made at developing methods to analyse surface acidity by other techniques.

#### **1.4 Surface acidity of pharmaceutical excipients.**

Calculating the surface acidity of a solid material is not as straightforward as measuring the pH of a solution. The surface acidity of a solid pharmaceutical excipient will have an effect on how the excipient reacts with other excipients,

and also with the active pharmaceutical ingredient (API). These effects could either stabilize or destabilize the formulation.<sup>[50]</sup>

The surface energy of a solid material is affected by whether or not the sample is amorphous or crystalline, and which crystal face is measured (section 1.3.2.). This suggests that the surface acidity will be affected in much the same way, depending on which atoms of the molecule are present at the surface of each crystal face, or amorphous area, probed. A current method for calculating surface acidity is to use pH indicators as probes for determining the Hammett acidity function.<sup>[51]</sup>

The Hammett acidity function ( $H_0$ ) is used to measure the acidity of extremely concentrated solutions, where the Henderson-Hasselbalch equation no longer applies due to activity co-efficients that deviate from ideal behaviour.<sup>[51, 52]</sup> In equation 3,  $H_0$  replaces pH,  $a_{H^+}$  is the activity of the hydrogen ion and  $f_B/f_{BH^+}$  is the ratio between the activity co-efficients of an uncharged base and its conjugate acid<sup>[52, 53]</sup>.

$$H_0 \equiv -\log a_{H^+} f_B/f_{BH^+}$$

Equation 3.

From the Hammett acidity function, a similar definition was applied to solid surfaces by Cheves Walling in 1950: “The ability of the surface to convert an absorbed base to its conjugate acid.”<sup>[52]</sup> If the base forms a complex with the surface, because the surface acts as a Lewis acid, then equation 3 can now be written as equation 4,<sup>[52]</sup> where  $\alpha_A$  is the activity of the Lewis acid.

$$H_0 = -\log \alpha_A f_B/f_{AB}$$

Equation 4.

If this definition of acidity applies to surfaces, which requires that there be a single scale for surface acidities, independent of base involved, then it is possible to measure the acidity of the surface by adsorbing acid-base indicators on the

surface. The appearance of the colour of the acidic form of the indicator would correspond to  $H_0$  being lower than the  $pK_a$  of the indicator.<sup>[52]</sup> From this, adsorbing enough indicators, with a range of  $pK_a$  values, should be able to give the acidity of the surface.

In recent years, this approach has been adapted utilising diffuse reflectance ultraviolet/visible spectroscopy (DRUV). Firstly, a solution profile of the acid-base indicator is taken at regular pH intervals in solution. The indicator is then adsorbed on the surface of a pharmaceutical solid from a stock solution, where the indicator is dissolved in a suitable solvent that also acts as an anti-solvent to the excipient (*i.e.* the excipient will not dissolve in the solvent). After evaporation of the solvent, a DRUV spectrum of the coated surface is obtained. The concentration of the probe molecule varies slightly by author and with probe indicator, but remains as a very dilute concentration, to avoid losing spectral information about the surface interaction between probe and excipient.

The ratio of the intensities of the protonated and un-protonated indicator species determined from the DRUV spectrum is then compared to the corresponding ratios of intensity in the solution UV/vis spectra. The pH of the solution spectrum that corresponds with the solid spectrum is termed the “pH-equivalence”, often shortened to “pHeq” which is claimed to be the surface acidity.<sup>[49-51, 53, 54]</sup> Table 1.2. is a list of some “pH-equivalences” for some common excipient surfaces.

Surface	Indicator	“pH-eq”	Reference
Avicel 101	Bromophenol Blue	3.88	49
Avicel 102	Bromophenol Blue	3.94	49
Sorbitol >350µm	Bromophenol Blue	4.14	49
Sorbitol 90-180µm	Bromophenol Blue	4.23	49
Lactose 200M	Bromophenol Blue	3.42	49
Lactose mono-hydrate NF*	Bromocresol Green	4.24	50
Calcium Carbonate USP	Phenol Red	7.69	50
Citric acid	<i>p</i> -xylenol blue	1.45	49
Magnesium Stearate NF	Phenol Red	7.45	50

Table 1.2. The “pH-equivalences” of some common pharmaceutical excipients. \* = spray dried.

In addition to Table 1.2, there has been a publication with a graphical representation of the reproducibility of “pH-equivalence” values.<sup>[53]</sup> Whilst actual figures like those given in the table are absent, it is clear from the comparison of the six materials that lack of reproducibility is a significant problem, for example magnesium stearate in one study has a “pH-eq” of *ca.* 5, and in a later study *ca* 7.5. This difference in “pH-eq” suggests that to quote any “pH-eq” value to 2 decimal places is unwarranted.

In some of the literature, the reason for “pH-equivalence” is attributed to Hammett acidity function, and therefore surface acidity. In other literature, particularly for lyophilised samples, it is attributed to “pH-memory”.<sup>[50, 54]</sup> The term “pH-memory” suggests that either the lyophilite has retained a memory of the pH of the solution before freeze-drying, or, that the indicator has been “frozen” in either it’s acidic or basic form depending on the solution pH and has been unable to convert to its usual solid state by virtue of being adsorbed on the surface of the sample. The ambiguity of this term is unfortunate, leading to possible misconceptions about the scientific value of this research, and what is actually being measured, as the term also implies it is the acidity or basicity of the solution rather than the surface acidity of the solid, suggesting that the

authors purporting “pH-memory” could have simply taken the pH of the solution!

It should be remembered that “pH-equivalence” is measured by comparing the *intensities* of the protonated and un-protonated indicator peaks in the solution UV/vis spectra with the DRUV spectrum. A DRUV spectrum measures reflectance, not absorbance, is dependant on particle size and scattering coefficients, and should be analysed using the Kubelka-Munk remission function.<sup>[55]</sup> It has been stated in the literature, that particle size (within a range) does not influence the determination of surface acidities.<sup>[49]</sup> However, data from the same paper<sup>[49]</sup> (Sorbitol in Table 1.2) shows that particle size **has** changed the “pH-equivalence”. A final obstacle in comparing a solid DRUV spectrum with a solution UV/vis spectrum is that the concentration of the analyte is directly proportional to the absorbance but not the reflectance (to be discussed in chapter 2), meaning that any small changes in the analyte concentration from the two experiments, will have disparate effects in the final spectra. If the pH of the indicator solution is changed by addition of acid or base to the solution, then, the indicator will be diluted as the experiment continues, and if fresh solution is prepared for each pH in the UV/vis spectra, then errors in weighing will affect the intensities observed in each spectrum.

Similar methods have been utilised to examine gels with a pH-indicator.<sup>[56]</sup> Another method is correlating chemical reactivity with Hammett acidity function.<sup>[51]</sup> To do this, Reichardt’s dye has been adsorbed onto the surface of multi-component amorphous sucrose systems, using a derivatized Hammett acidity function equation. Reichardt’s dye has also been used to determine the polarity of silica.<sup>[57]</sup>

## 1.5 The project

The “pH-equivalence” data for lactose (Table 1.2) show that changing the indicator can also give a large change in the “pH-equivalence” value, or, that spray drying lactose has caused the “pH-equivalence” to become less acidic. Assuming that the intensities from the two spectra have been correlated without

any of the variables (section 1.4) causing a deviation, then from surface energy information (section 1.3.2.) it would appear that spray drying, which would have rendered the lactose amorphous, could indeed change the surface acidity. To the author's knowledge, an acid-base indicator has never been employed to distinguish between the surface acidity of a pharmaceutical excipient of its crystalline and amorphous states.

### 1.5.1 Perichromism

Perichromism was originally suggested as an alternative name for solvatochromism, because solvatochromism suggests that the position or intensity change of an absorption band is only observed in liquids.<sup>[4]</sup> However, this was rejected because the name solvatochromism was already established.<sup>[4]</sup> To distinguish between solution phase and solid state interactions, the term perichromism is used instead of solvatochromism. Perichromism is the employment of an acid-base indicator to distinguish between an amorphous and a crystalline surface. The practicalities of perichromism will have to encompass the adsorption of a probe dye onto the surface of a solid as well as being able to inter-convert the solid between amorphous and crystalline. Due to the problems inherent in comparing solution UV/vis and DRUV spectra, rather than examine a change in the intensities (which are effectively incomparable between the solid and solution states) of the two spectra, an approach, which gives more confidence, would be one that only uses DRUV spectroscopy and shows that an indicator adsorbed on an amorphous surface has a different *wavelength* of maximum absorption to the same indicator adsorbed onto a crystalline surface of the same material.

A change in the wavelength of an adsorbed indicator on an amorphous surface to that of a crystalline surface is reminiscent of solvatochromism (section 1.1). However, instead of probing solvent polarity, the indicator will be probing a property of the solid surface, presumably a difference in surface acidity caused by a change in what exposed surface available to adsorb the indicator. Assuming that there is a large enough difference in surface acidity, and a dye with a  $pK_a$  in between the acidities of the two surfaces is chosen, the dye would be expected to

show a  $\lambda_{\max}$  for its protonated form for one surface, and the  $\lambda_{\max}$  of the unprotonated form for the other surface.

Producing a stock concentration of indicator, and applying a known volume of this stock to a known weight of different surfaces may have the potential for errors to occur. If it is possible to prepare a large volume of sample with indicator adsorbed, and then to convert this to either amorphous or crystalline, the concentration of indicator should be identical throughout all known volumes of sample. This method will also be a more realistic simulation of possible amorphous to crystalline transitions that would occur in the manufacture of a drug product in a pharmaceutical industry.

#### **1.5.1.1 Potential applications**

The industrial value of perichromism lies in the possibility of developing a process analytical technique (PAT) capable of monitoring the development of undesirable amorphous or crystalline material during a manufacturing process of a medicine, thereby enabling the causes of the production of unwanted material to be identified. Once problems are identified, changes can be implemented to the manufacturing process that will mean that only the desired morphological form of the drug product will be produced, improving product knowledge, and confidence in the quality of the medicine. It will also stop situations arising where a drug is marketed, only to be withdrawn later due to changes in crystallinity occurring, improving profitability, and more importantly, consumer confidence.

Perichromism could also, potentially, be adapted to be used on-line as a quality control for the manufacture of medicines, whereby the acid-base indicator would become an ingredient in the formulation. For this to be possible, the indicator must be non-toxic, edible and safe.

**1.6 References.**

- [1] C. Reichardt, *Pure Applied Chemistry* **2004**, 76, 1903.
- [2] E. B. Tada, L. P. Novaki, O. A. El Seoud, *Journal of Physical Organic Chemistry* **2000**, 13, 679.
- [3] F. L. Dickert, U. Geiger, P. Lieberzeit, U. Reutner, *Sensors and Actuators B* **2000**, 70, 263.
- [4] C. Reichardt, *Chemical Reviews* **1994**, 94, 2319.
- [5] D. L. Pavia, G. M. Lampman, G. S. Kriz, *Introduction to Spectroscopy*, Third ed., Harcourt College Publishers, **2001**.
- [6] J. McMurray, *Organic Chemistry*, Fifth ed., Brooks/Cole, **2000**.
- [7] D. A. Skoog, D. M. West, F. J. Holler, in *Fundamentals of Analytical Chemistry*, Seventh ed., Saunders College Publishing, **1997**.
- [8] N. A. Vodolazkaya, N. O. Mchedlov-Petrosyan, G. Heckenkemper, C. Reichardt, *Journal of Molecular Lipids* **2003**, 107, 221.
- [9] K. Stadnicka, P. Milart, A. Olech, P. Olszewski, *Journal of Molecular Structure* **2002**, 604, 9.
- [10] N. O. Mchedlov-Petrosyan, N. A. Vodolazkaya, C. Reichardt, *Colloids and Surfaces A: Physicochemical and Engineering Aspects* **2002**, 205, 215.
- [11] C. Zhang, K. S. Suslick, *Journal of the American Chemical Society* **2005**, 127, 11548.
- [12] C. Reichardt, *Chemical Society Reviews* **1992**, 21, 147.
- [13] K. A. Fletcher, I. A. Storey, A. E. Hendricks, S. Pandey, S. Pandey, *Green Chemistry* **2001**, 3, 210.
- [14] D. J. Macquarrie, S. J. Tavener, G. W. Gray, P. A. Heath, J. S. Rafelt, S. I. Saulzet, J. J. E. Hardy, J. H. Clark, P. Sutra, D. Brunel, F. di Renzo, F. Fajula, *New J. Chem.* **1999**, 23, 725.
- [15] M. E. Aulton, *Pharmaceutics the science of dosage form design*, Second ed., Churchill Livingstone, **2002**.
- [16] X. Fu, X. Zhang, Z. Hou, *Journal of Non-Crystalline Solids* **2008**, 354, 1740.
- [17] L. S. Taylor, G. Zografì, *Journal of Pharmaceutical Sciences* **1998**, 87, 1615.
- [18] L. Yu, *Advanced Drug Delivery Reviews* **2001**, 48, 27.
- [19] J. J. Seyer, P. E. Luner, M. S. Kemper, *Journal of Pharmaceutical Sciences* **2000**, 89, 1305.
- [20] M. Lappalainen, I. Pitkanen, P. Harjunen, *International Journal of Pharmaceutics* **2006**, 307, 150.
- [21] D. Al-Hadithi, G. Buckton, S. Brocchini, *Thermochimica Acta* **2004**, 417, 193.
- [22] E. Katainen, P. Niemela, P. Harjunen, J. Suhonen, K. Jarvinen, *Talanta* **2005**, 68, 1.
- [23] D. Gao, J. H. Rytting, *International Journal of Pharmaceutics* **1997**, 151, 183.
- [24] P. Niemela, M. Paallysaho, P. Harjunen, M. Koivisto, V.-P. Lehto, J. Suhonen, K. Jarvinen, *Journal of Pharmaceutical and Biomedical Analysis* **2005**, 37, 907.
- [25] Y. Roos, M. Karel, *Biotechnology Progress* **1991**, 7, 49.

- [26] A. A. Elamin, T. Sebhatu, C. Ahlneck, *International Journal of Pharmaceutics* **1995**, 119, 25.
- [27] Y. Aso, S. Yoshioka, S. Kojima, *Journal of Pharmaceutical Sciences* **2001**, 90, 798.
- [28] B. M. Murphy, S. W. Prescott, I. Larson, *Journal of Pharmaceutical and Biomedical Analysis* **2005**, 38, 186.
- [29] Y. Aso, S. Yoshioka, *Journal of Pharmaceutical Sciences* **2006**, 95, 318.
- [30] R. Ramos, S. Gaisford, G. Buckton, *International Journal of Pharmaceutics* **2005**, 300, 13.
- [31] A. Gombas, I. Antal, P. Szabo-Revesz, S. Marton, I. Eros, *International Journal of Pharmaceutics* **2003**, 256, 25.
- [32] M. Kacurakova, M. Mathlouthi, *Carbohydrate Research* **1996**, 284, 145.
- [33] C. J. Kedward, W. MacNaughtan, J. R. Mitchell, *Carbohydrate Research* **2000**, 329, 423.
- [34] G. Buckton, P. Darcy, *International Journal of Pharmaceutics* **1995**, 123, 265.
- [35] S. E. Hogan, G. Buckton, *International Journal of Pharmaceutics* **2000**, 207, 57.
- [36] A. Saleki-Gerhardt, G. Zograf, *Pharmaceutical Research* **1994**, 11, 1166.
- [37] N. Drapier-Beche, J. Fanni, M. Parmentier, M. Vilasi, *Journal of Dairy Science* **1997**, 80, 457.
- [38] J. T. Cartensen, K. Van Scoik, *Pharmaceutical Research* **1990**, 7, 1278.
- [39] D. Q. M. Craig, P. G. Royall, V. L. Kett, M. L. Hopton, *International Journal of Pharmaceutics* **1999**, 179, 179.
- [40] S. R. Vippagunta, H. G. Brittain, D. J. W. Grant, *Advanced Drug Delivery Reviews* **2001**, 48, 3.
- [41] H. H. Read, J. Watson, in *Introduction to Geology. Volume I. Principles*, Second (reprinted) ed., The MacMillan Press Ltd, **1979**.
- [42] S. R. Byrn, Academic Press, **1982**.
- [43] J. H. Kirk, S. E. Dann, C. G. Blatchford, *International Journal of Pharmaceutics* **2007**, 334, 103.
- [44] G. Buckton, H. Gill, *Advanced Drug Delivery Reviews* **2007**, 59, 1474.
- [45] P. Rousset, P. Sellappan, P. Daoud, *Journal of Chromatography A* **2002**, 969, 97.
- [46] Z. Wu, L. You, H. Xiang, J. Y., *Journal of Colloid and Interface Science* **2006**, 303, 346.
- [47] V. Swaminathan, J. Cobb, I. Saracovan, *International Journal of Pharmaceutics* **2006**, 312, 158.
- [48] H. E. Newell, G. Buckton, D. A. Butler, F. Thielmann, D. R. Williams, *International Journal of Pharmaceutics* **2001**, 217, 45.
- [49] C.-A. Scheef, D. Oelkrug, P. C. Schmidt, *European Journal of Pharmaceutics and Biopharmaceutics* **1998**, 46, 209.
- [50] R. Govindarajan, A. Zinchuk, B. Hancock, E. Y. Shalaev, R. Suryanarayanan, *Pharmaceutical Research* **2006**, 23, 2454.
- [51] K. Chatterjee, E. Y. Shalaev, R. Suryanarayanan, R. Govindarajan, *Journal of Pharmaceutical Sciences* **2008**, 97, 274.
- [52] C. Walling, *Journal of the American Chemical Society* **1950**, 72, 1164.
- [53] A. Zinchuk, B. Hancock, E. Y. Shalaev, R. D. Reddy, R. Govindarajan, E. Novak, *European Journal of Pharmaceutics and Biopharmaceutics* **2005**, 61, 158.

- [54] R. Govindarajan, K. Chatterjee, L. Gatlin, R. Suryanarayanan, E. Y. Shalaev, *Journal of Pharmaceutical Sciences* **2006**, 95, 1498.
- [55] S. Lacombe, H. Cardy, N. Soggiu, S. Blanc, J. L. Habib-Jiwan, S. J.Ph., *Microporous and Mesoporous Materials* **2001**, 46, 311.
- [56] C. Rottman, G. Grader, Y. De Hazan, S. Melchior, D. Avnir, *Journal of the American Chemical Society* **1999**, 121, 8533.
- [57] S. Spange, A. Reuter, E. Vilsmeier, *Colloid Polymer Science* **1996**, 274, 59.

## Chapter 2

### Techniques

#### **2.1 Introduction**

The novel PAT for the detection of perichromism, as discussed in section 1.5, is dependant on diffuse-reflectance UV/visible spectroscopy (DRUV). However, this is not a technique usually used to discriminate between polymorphs, indeed a search of the literature revealed no instance of this occurring. Therefore, results from DRUV spectroscopy will require corroboration from other analytical techniques. These techniques will be described and evaluated after appraising the experimental methods used to generate, or develop, the polymorphic samples that will be used.

One method for addition of a probe molecule to an excipient, is to apply a “pH-equivalent” indicator in a solution in an anti-solvent to the pharmaceutical excipient which is then removed by placing the sample in a vacuum oven, evaporating the solvent.<sup>[1, 2]</sup> In this method the indicator is soluble in the solvent, but the excipient is not. The drawback to this method is that a suitable solvent for the indicator needs to be found that has no effect on the excipient to be examined. With perichromism, the indicator could be added this way, but a better way would be to add the perichromic probe before subjecting the excipient to the processes required to generate different polymorphic forms. This will remove the need for an anti-solvent, and any possibility that there could be some small interaction between excipient and anti-solvent. The probe is integrated to the excipient by dissolving it in an aqueous solution of the excipient, and then freeze-drying, to produce an amorphous pharmaceutical excipient with the indicator incorporated throughout. To convert this amorphous material to a crystalline one requires storage at either elevated temperature or relative humidity. Amorphous and crystalline samples can then be compared by DRUV.

To be certain that the material being probed is amorphous or crystalline, many other techniques can be employed, and will be discussed throughout this chapter (sections 2.6 to 2.10 inclusive).

## 2.2 Freeze drying

Freeze-drying, or lyophilisation, is a common technique used to dehydrate a sample<sup>[3]</sup> that will also render it amorphous.<sup>[4, 5]</sup> This is a two-step process: the sample material is frozen, before being placed under vacuum to allow for the sublimation of ice to water vapour. The method used to freeze the sample is dependent upon the sample itself, in particular the melting point of the solvent used. Freezing in a laboratory can be accomplished by placing the material in a conventional freezer, which will cool the material to  $-18^{\circ}\text{C}$ , or, if a colder temperature is required, the sample can be stored in dry ice ( $-77^{\circ}\text{C}$ ) or quench-cooled in liquid nitrogen ( $\approx -200^{\circ}\text{C}$ ). The faster the freezing process, the greater the level of solvent trapped inside the crystal matrix, so selecting the optimum freezing parameters is important. The aim of freezing the sample is to cool the eutectic material below its eutectic point (the coldest temperature at which the liquid and solid phase can co-exist) to allow for sublimation of frozen water directly to gaseous water.<sup>[3]</sup>

Once frozen, the sample is placed in an atmosphere of reduced pressure to allow the frozen water to sublime. Water vapour is collected by re-freezing on a condenser plate, otherwise the pressure would increase and sublimation would cease to occur.<sup>[3]</sup>

Sublimation is the transformation of matter from the solid state to the gaseous without becoming a liquid at any point (the opposite process is called deposition, *e.g.* frost formation). The possible processes (involving the solid phase) are best viewed in a phase diagram (Figure 2.1.)

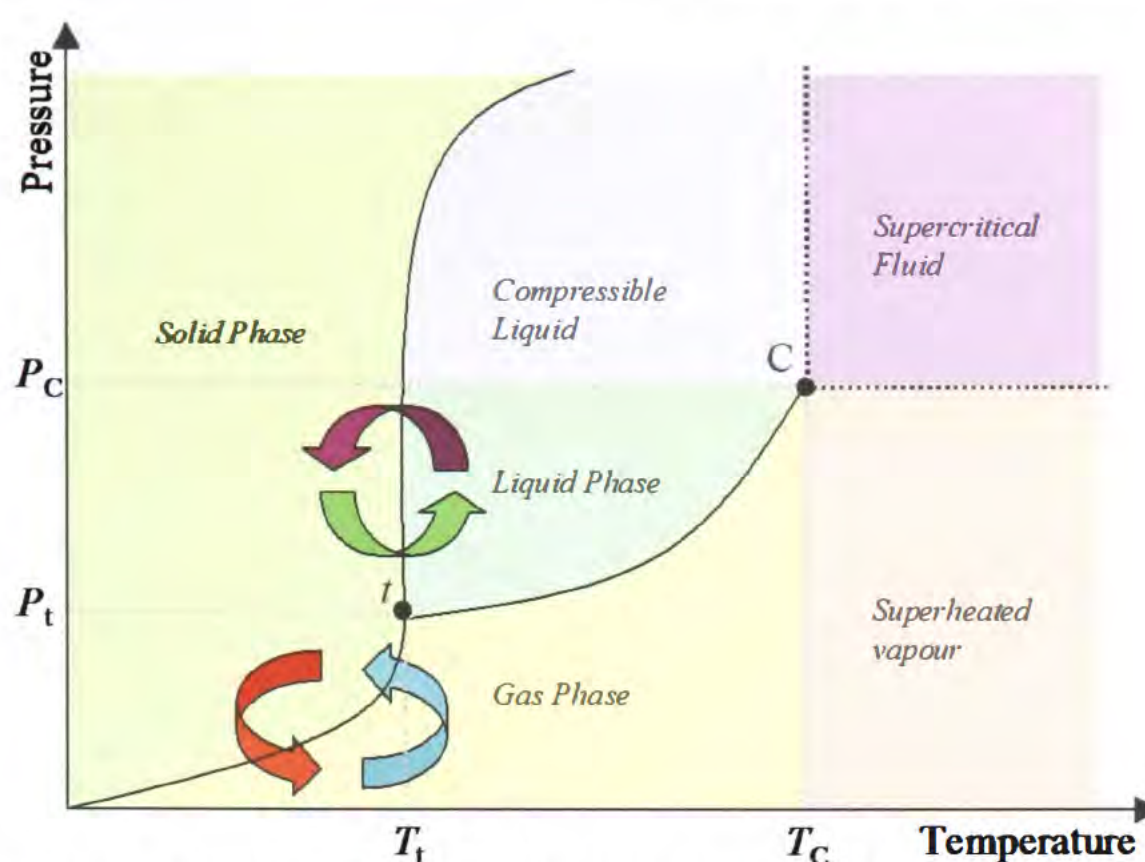


Figure 2.1. A temperature-pressure phase diagram. Where  $\rightarrow$  is sublimation,  $\rightarrow$  is deposition,  $\rightarrow$  is melting,  $\rightarrow$  is freezing,  $t$  is the triple point (where a material co-exists as solid, liquid and gas) and  $C$  is the critical point.

There are several disadvantages to freeze-drying in the lab: it is very slow; unsuitable to volatile organic solvents (which commonly corrupt the seals of the vacuum pump, although a solvent-trap can negate this); and the generated material is very hygroscopic,<sup>[5]</sup> meaning it has to be stored carefully. However, freeze-drying remains a common method for the removal of water from a system, particularly for heat-sensitive products.<sup>[6]</sup>

### 2.3 Rotary Evaporation

The method for calculating “pH-memory” and the incorporation of indicators in to (or on to) solids to calculate the Hammett acidity function (section 1.4.) require a vacuum oven,<sup>[1, 2, 7]</sup> which dries the sample under vacuum at elevated temperature. A rotary evaporator may also be used where a flask containing the sample is in contact with a water bath at elevated temperature. Both methods allow for the evaporation of a solvent. It should be noted that rotating the sample in the case of rotary evaporation reduces the surface tension of the solvent, allowing for easier evaporation.

Rotary evaporation could be viewed as a similar process to freeze drying, as it is also the removal of a solvent from a system. The solvent is again converted to a gaseous phase prior to removal under vacuum. Unlike freeze drying however, the conversion to the gaseous phase is achieved by raising the temperature of the system, under vacuum, boiling the solvent, which is made easier by the reduced surface tension, and then trapping it as a liquid through a condenser.

The solvent removed is usually an anti-solvent to the desired product, which is, herein, a pre-determined polymorph of a pharmaceutical excipient that exists as either a precipitate or solid particulates in the system. The sample is placed in a round-bottomed flask, and heated in a water bath, whilst being rotated under vacuum. Rotary evaporation is faster than freeze-drying, but is usually carried out on a much-reduced scale. It is also not particularly practical for the removal of water, due to the comparatively high boiling point of water compared to other solvents, such as methanol, as even under vacuum the required temperature may cause undesirable changes to occur in the product.

Rotary evaporation has been used as a technique to remove from the system the solvent in which the probe molecule has been dissolved. The rotation and the fact that the excipient is insoluble in the solvent should allow for an even coating of the probe molecule across the surface of any chosen polymorphic surface during the initial stages of rotation when there is a large volume of solvent.

## 2.4 Relative Humidity

Relative humidity (%RH) is defined as the ratio between the vapour pressure of water in the atmosphere to the vapour pressure of water in air that is saturated with moisture.<sup>[6]</sup> The vapour pressure of water in saturated air, at 25 °C, is 31.67 mbar.<sup>[6]</sup> When air contains a vapour pressure of, for example, 14 mbar, then the relative humidity is  $14/31.67 \times 100 = 44.2$  %RH.

Following the genesis of amorphous material by lyophilisation, carefully controlled storage of the product is required, due to the hygroscopic nature of the sample. If the sample is not stored at low relative humidity, then it will sorb

water. Sorbed water acts as a plasticiser, which lowers the glass transition temperature ( $T_g$ ).<sup>[8]</sup> This may allow the sample to “cake” (*i.e.* to collapse under its own weight and harden), and then undergo a phase transition, thereby randomly altering the morphology of the sample.

To maintain a sample in an amorphous state the product is stored at low temperature and/or low relative humidity. The exact conditions will vary for each material, based on its  $T_g$ ; indeed, the  $T_g$  will vary with ambient %RH. The method for storage chosen throughout this work is to use desiccators with different saturated salt solutions at constant temperature, which allow for the selection, and control, of different relative humidity within each desiccator.<sup>[9]</sup> Samples were stored for one week, as previously used in the literature,<sup>[10, 11]</sup> in a desiccator of controlled temperature and %RH to allow the sample to equilibrate to the storage conditions. The equilibration time is an important factor, because for a given temperature, there is often a %RH that will enable a phase transition to occur. However, storage at an %RH just above the minimum required for a phase transition, will mean that the transition is slow to occur.<sup>[12]</sup>

The salt solutions were chosen to give a range of samples where the  $T_g$  was both above and below room temperature for each sample (for details of salts used, see section 3.4.2). This means that, for samples stored at low relative humidity, the  $T_g$  is above room temperature and the sample will remain amorphous. At higher relative humidity, the sample should crystallise, because the  $T_g$  is now below room temperature.

## 2.5 UV/vis and Diffuse Reflectance-UV spectroscopy

UV/vis absorption spectroscopy is routinely applied to transparent liquids,<sup>[6]</sup> but will not work for an opaque solid, which will block light of all wavelengths from being transmitted through it. However, a UV/vis spectrophotometer can be adapted so that a solid material can be analysed using an integrating sphere, which collects all of the light reflected from a solid sample. As the name suggests, in DRUV the diffuse reflectance of light from the surface is measured, rather than directly measuring the absorption (Figure 2.2). Two types of

reflectance are possible: specular and diffuse. Specular reflection is reflection where incident light approaching at an angle  $\theta$  from the surface normal is reflected back at angle  $\theta$ , for example when light strikes a mirror. Diffuse reflectance occurs when light is reflected back in many different directions occurring when light strikes an uneven surface.

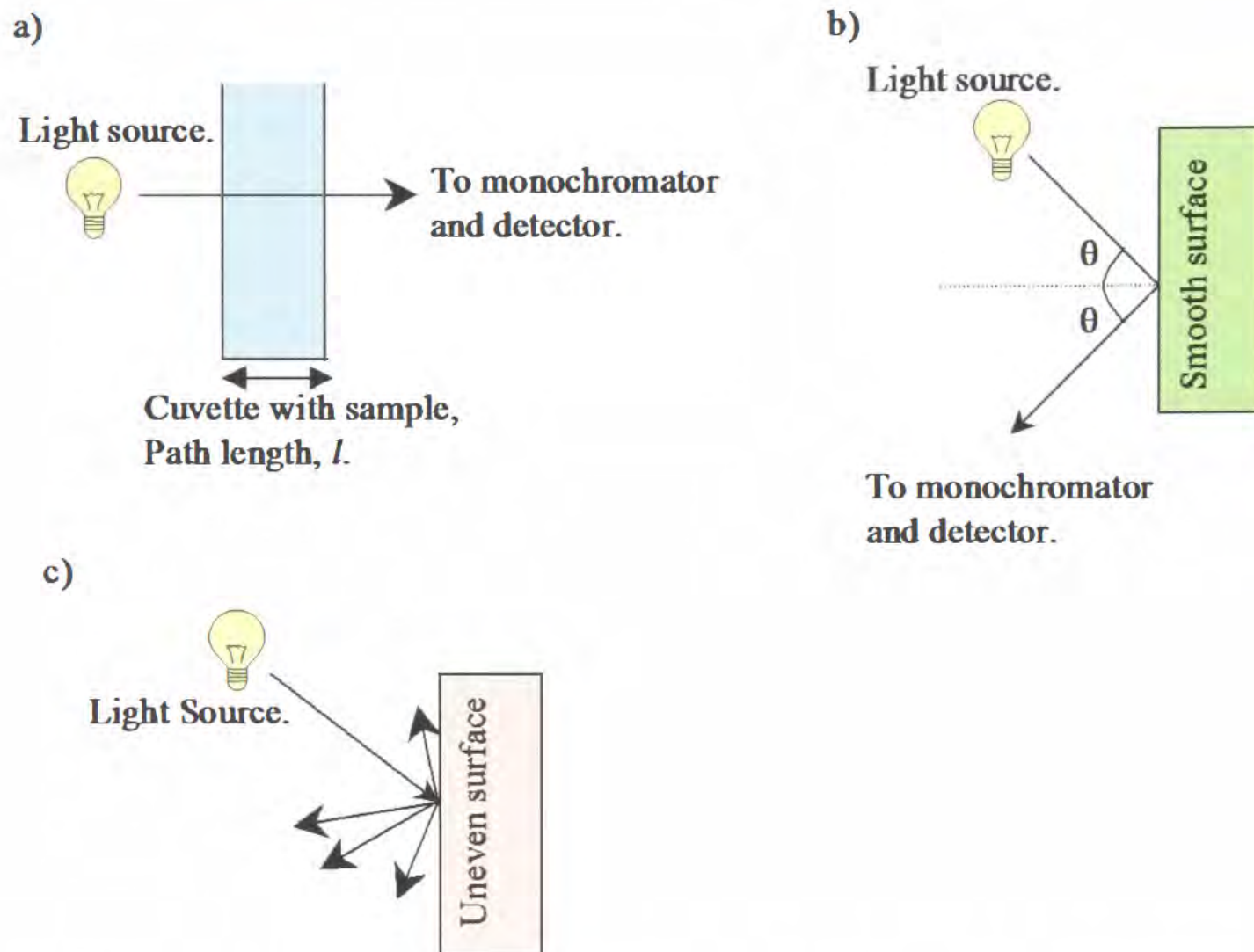


Figure 2.2. Light from the light source a) passing through a transparent solution in UV/vis spectroscopy, b) specular reflectance from a mirror, and c) diffuse reflectance from a solid surface, as in DRUV spectroscopy. The light diffusely reflected needs to be collated before reaching the monochromator

### 2.5.1 Ultraviolet/Visible spectroscopy

Ultraviolet/visible spectroscopy (UV/vis spectroscopy) can be used for identification of an unknown compound, but is usually used for quantitative analysis of a known analyte. The spectrophotometer consists of three basic components, a light source, a monochromator and a detector.<sup>[6]</sup> The light source usually consists of two lamps to cover a large spectral window: a deuterium lamp (200-350 nm); and a tungsten lamp (350-800 nm).<sup>[6]</sup> The monochromator separates the different wavelengths of light, and the detector collates the information about the intensity of light of different wavelengths. The sample is placed in a cuvette between the light source and the entrance slit of the monochromator (Figure 2.3). This sample must be fully dissolved (*i.e.* any particulates need to be removed by filtration), and free of bubbles, to reduce light scattering. The sample absorbs some radiation from the light source, corresponding to electron transitions<sup>[13]</sup> and this absorption of light manifests itself in the spectrum as a broad absorption band.

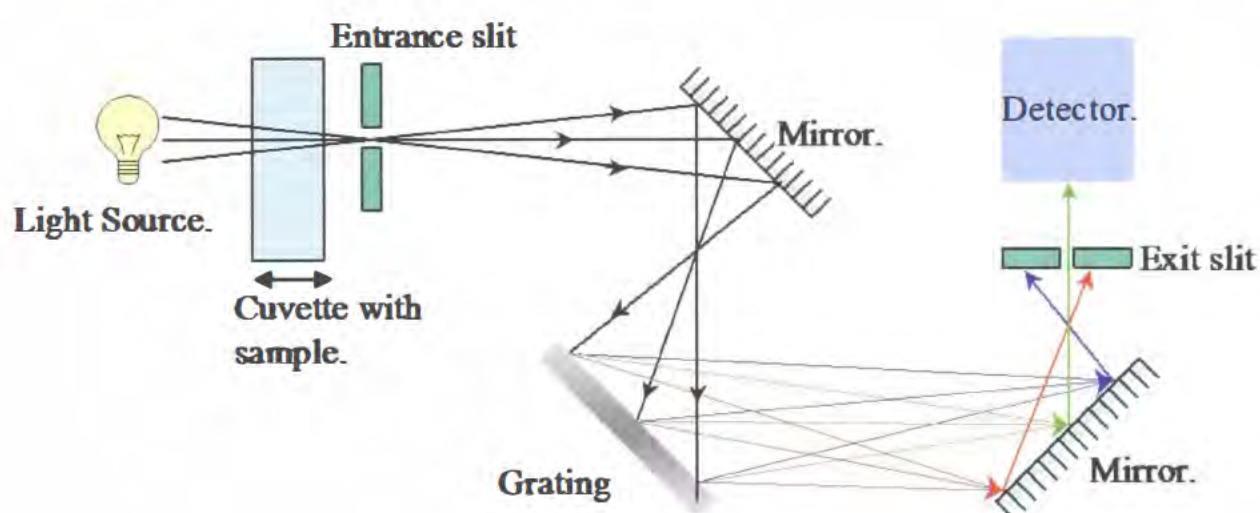


Figure 2.3 Schematic of an UV/vis spectrophotometer.

For a sample to give a UV/vis spectrum, it must have a chromophore. A chromophore is a functional group that absorbs light in the ultraviolet or visible range.<sup>[6]</sup> The bonding present in a chromophore will determine the possible electronic transitions, which in turn, will affect the absorption observed in a UV/vis spectrum. Chromophore absorption peak position and intensities are dependant on the transition involved, and also the solvent used.<sup>[6]</sup>

### 2.5.2 The Beer-Lambert Law

A UV/vis spectrophotometer measures the intensity of light ( $I$ ) that passes through a sample. This is compared to a reference of the intensity of light that is incident to a sample ( $I_0$ ). The ratio  $I/I_0$  gives the transmittance ( $T$ ), and from this the absorbance ( $A$ ) can be calculated (Equation 5).<sup>[14]</sup>

$$T = I/I_0$$

$$A = -\log(T) \qquad \text{Equation 5.}$$

The more molecules present that absorb light at a given wavelength, the greater the level of absorption of that light. Some molecules will also be more, or less, effective than other molecules at absorbing light of a certain wavelength depending on structure and chromophore present.<sup>[15]</sup> From these principles (and also the path-length, *i.e.* the distance the light travels through the sample), it can be seen that absorption of light is related to the concentration of the light absorbing species. This relationship (for single species causing the observed absorption) forms the Beer-Lambert law<sup>[14]</sup> (equation 6).

$$A = \epsilon cl \qquad \text{Equation 6.}$$

Where  $A$  = Absorbance,  $\epsilon$  = molar absorptivity,  $l$  = path length of the cell and  $c$  = molar concentration of the solute.

### 2.5.3 Diffuse Reflectance-UV

Solvatochromism (as discussed in section 1.1) can be considered as an indirect measure of solvent polarity using UV/vis spectroscopy. The resultant spectra of the indicator in different solvents have a range of  $\lambda_{\max}$ , with a blue shift (*i.e.* a shorter wavelength) corresponding to an increased solvent polarity,<sup>[15]</sup> and a red shift corresponding to decreased solvent polarity. The principles of diffuse reflectance-UV spectroscopy are similar to those of absorption UV/vis spectrometry applied to a solution, except instead of measuring the absorbance of

a solution; it measures the reflectance of a solid (Figure 2.2. *vide supra*), therefore DRUV also contains information on the absorbance, as whatever light is not reflected, must have been absorbed by the sample. To be able to measure reflectance, an integrating sphere is added to the DRUV spectrophotometer enabling the collection of all light reflected from the sample. The sample is now placed in a sample holder, rather than a cuvette.

An integrating sphere (Figure 2.4)<sup>[16]</sup> is a hollow spherical chamber, ranging in size from a diameter of a couple of centimetres, to metres, depending on the application.<sup>[16, 17]</sup> The interior of the sphere is coated with a highly reflective, inert and stable material. A possible mechanical problem with integrating spheres is the generation of “hot-spots”.<sup>[17]</sup> This can be overcome by the addition of baffles to the sphere. Baffles are small wedges that are placed at certain points of the sphere and are coated in the same material as the rest of the sphere. The sphere (usually) has 3 ports,<sup>[17]</sup> as shown by figure 2.4: the illumination port, where the light source enters; the sample port, where the incident light reflects off the surface of the sample; and the measurement port, where the light leaves the integrating sphere *en route* to the monochromator. These ports should be as small as possible, typically less than 5% of the area of the sphere.<sup>[17]</sup>

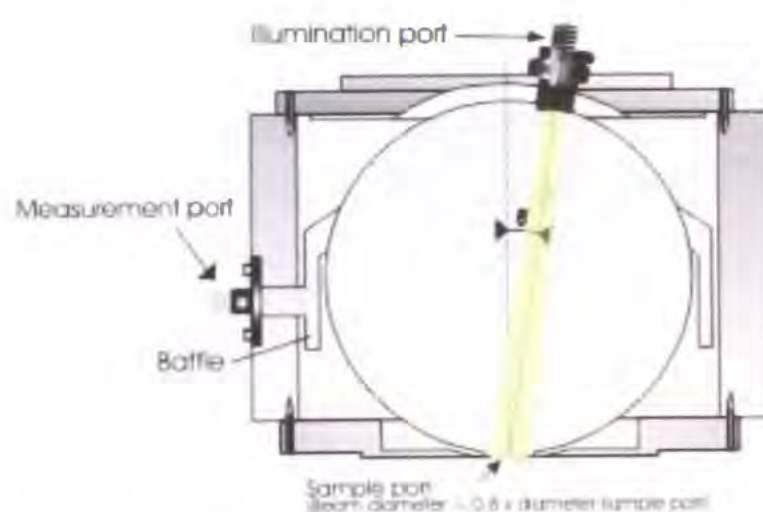


Figure 2.4. Schematic of an integrating sphere.

The integrating sphere has a uniform scattering effect;<sup>[17]</sup> light that is diffusely reflected by the sample will be reflected evenly to all points on the integrating sphere, and reach the detector as an integrated signal.<sup>[17]</sup> The sample will not have the same reflectivity as the coating material of the integrating sphere. Some

wavelengths will be scattered by interaction with the sample, and, the resultant electronic transition(s) will be observed.

To calculate the absorbance of a sample, it is necessary to obtain both  $I$  and  $I_0$ .  $I_0$  is measured by recording the absorbance of the solvent, and  $I$  by recording the absorbance of the sample. The measurement of  $I_0$  is known as the reference measurement, and as it gives the baseline, must be completed before the measurement of the absorbance of any sample. For a DRUV spectrophotometer the reflectance is the reflectivity of a highly reflective (over 80%)<sup>[17]</sup>, non-absorbing species such as Spectralon™.<sup>[16]</sup> In reality 100% reflectivity is not possible, because of this, light reflected from the blank sample should not be reflected directly to the detector, because it will give a higher signal strength than the attenuated light that has reflected via the integrating sphere.<sup>[17]</sup> Throughout this thesis, reference spectra were obtained by measuring the absorbance of the empty sample holder, which, like the integrating sphere, was coated in Spectralon™.

The advantages to using DRUV spectroscopy are that it is quick, easy and cost effective. These are very desirable qualities within industrial applications, including the detection of amorphous content, where there is definite potential to improve on the current techniques available. The disadvantage is that the sample must contain a chromophore to be observed. All analytical techniques used to determine amorphous content have advantages and disadvantages to their use; the sensitivity of the technique is called its “limit of detection” which differs from sample to sample within any technique employed. The limit of detection of DRUV spectroscopy will be estimated for different excipients as part of the work on the viability of perichromism as an industrial technique.

#### **2.5.4 The Kubelka-Munk Remission Function**

DRUV measures the reflectance of light, rather than directly measuring the absorption. Absorbance of solutions can be directly measured experimentally. In contrast, the diffuse reflectance of light from a sample is influenced by a number of factors, such as packing density, particle size and inhomogeneity of the

surface.<sup>[18]</sup> The use of the Kubelka-Munk remission function, (equation 7)<sup>[18, 19]</sup> accounts for these variables.

$$F(R) = \frac{(1-R)^2}{2R} \quad \text{Equation 7.}$$

Where  $F(R)$  is the Kubelka-Munk remission function, and  $R$  is the fraction of light reflected from the sample surface.

The Kubelka-Munk equation may be re-written to show that  $F(R)$  is directly proportional to analyte concentration (equation 8)<sup>[2]</sup> which is analogous to the Beer-Lambert law (equation 6) for solution UV/vis spectral data.

$$F(R) = \frac{k}{S} = \frac{\epsilon'c}{S} \quad \text{Equation 8.}$$

Where  $k$  is the absorption co-efficient,  $S$  is the scattering co-efficient,  $\epsilon'$  is the extinction co-efficient of the analyte, and  $c$  is the concentration of the analyte.

## 2.6 FT-Raman Spectroscopy

Raman spectroscopy (both dispersive and FT) is used to study vibrational and rotational motion.<sup>[20]</sup> It is dependant on inelastic Raman scattering of light by a sample. The difference in the energies of the incident and the scattered light reveals information about the molecular vibrations in a solid material. However, as can be seen in figure 2.5, there are two types of scatter possible when a photon interacts with a molecule. By far the most common scattering process is Rayleigh scattering, which is elastic scattering, where the scattered photon has the same energy as the incident irradiation. The other possibility is Raman scattering.<sup>[21]</sup> The energy of the scattered photon may be either lower (Stokes), or greater (anti-Stokes), than the incident light, but not the same. Stokes scattering is the more common form of Raman scatter, as it is caused by the incident light exciting an

electron into having greater vibrational energy, and the initial 'relaxed' state is more favourable.<sup>[21]</sup>

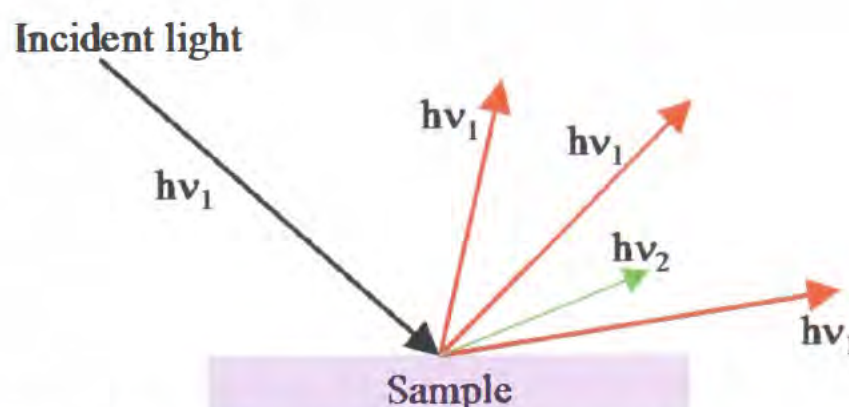


Figure 2.5. Rayleigh and Raman scatter. Where  $\rightarrow$  is the incident light,  $\rightarrow$  is Rayleigh scattering and  $\rightarrow$  is Raman scattering.

A Raman spectrometer usually contains a laser as a light source, which illuminates a sample. Light scattered from the sample is collected then enters an element that separates the photons according to their energy, *e.g.* a monochromator, and (if desired) a notch filter, which filters out the unwanted Rayleigh scattered light. Any light that originates from Raman scattering is able to pass through to the detector.

Raman scatter occurs when incident light interacts with the electron cloud of bonds within a molecule.<sup>[22]</sup> Photons cause the molecules to be excited from the ground vibrational electronic state to a virtual state before relaxing into an excited vibrational state of the ground electronic level then it is called Stokes scattering. If the photon causes the electron to be excited from the ground electronic, but a higher vibrational state into a virtual state and then relax into a ground vibrational electronic state, then it is anti-Stokes scattering (Figure 2.6).<sup>[22]</sup> In Stokes scattering, the molecule absorbs energy, so the scattered photon has a lower energy level than the incident light, the reverse is true for anti-Stokes scatter.

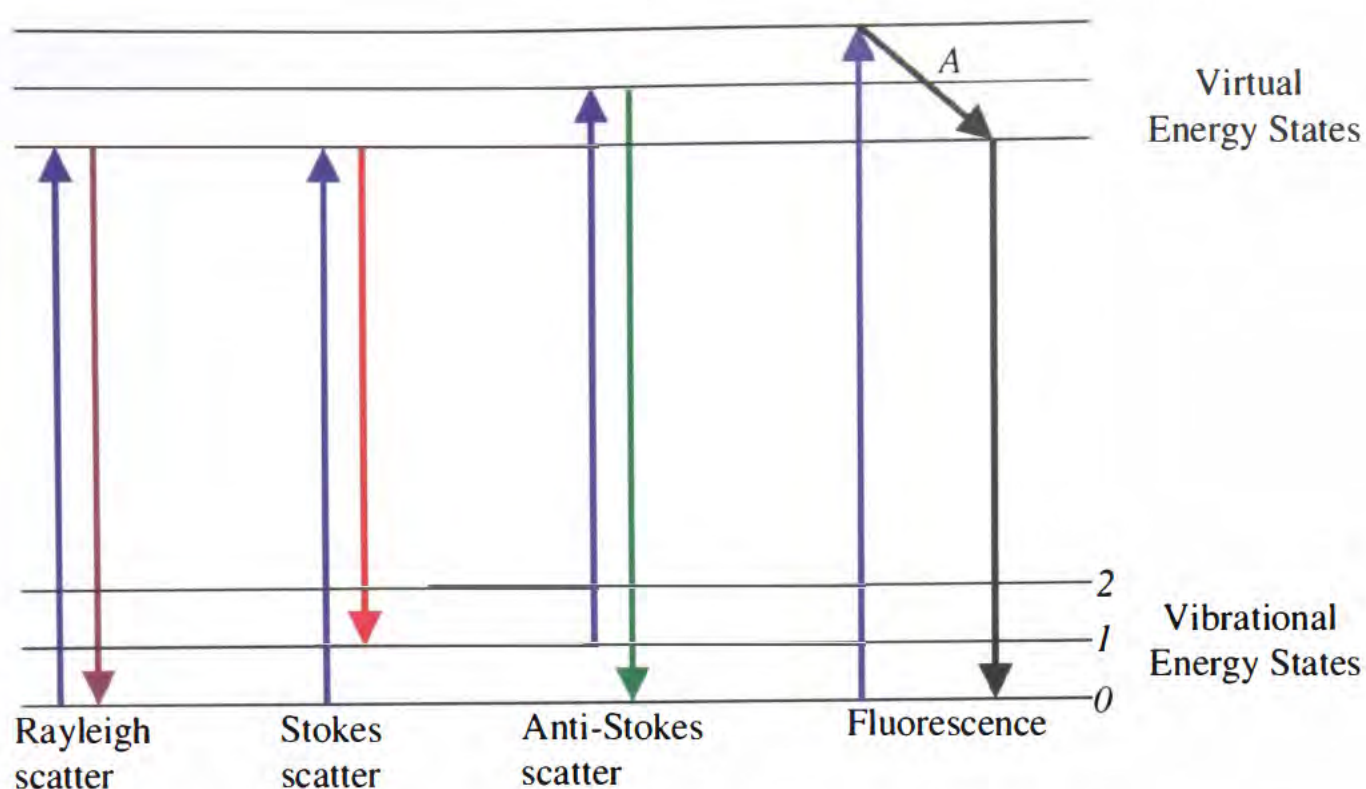


Figure 2.6. Stokes, and anti-Stokes Raman scattering. Where  $\rightarrow$  is excitation energy,  $\rightarrow$  is Rayleigh scatter,  $\rightarrow$  is Stokes Raman scatter,  $\rightarrow$  is anti-Stokes Raman scatter, and  $\rightarrow$  is fluorescence. A is the energy lost as heat before the emission of a photon.

From the information in Figure 2.6, it can be seen that for anti-Stokes scattering to occur, the molecule that the incident photon interacts with must already be in a higher vibrational state than the ground and then lose this energy to the photon. This is less common than for the molecule to be in the most energetically favourable, *i.e.* ground state and/or to gain energy from the photon.

### 2.6.1 Fourier-Transform as used in Raman spectroscopy

Fourier transform spectroscopy is applicable to many types of spectroscopy, for example Raman and infra-red spectroscopy.<sup>[23]</sup> The main disadvantage with dispersive Raman spectroscopy is that the spectra generated are obscured if the sample fluoresces. Many probe molecules, such as those used for perichromism fluoresce when irradiated by visible light sources such as used in conventional dispersive Raman spectroscopy, but not when irradiated by the longer wavelength of light from *e.g.* IR lasers, commonly utilised in FT-Raman spectrometers. FT spectroscopy also allows for the simultaneous collection of a

spectrum across a wide spectral region, rather than the much slower conventional technique.<sup>[21]</sup>

To perform Fourier-transform spectroscopy, an interferometer is required to enable a time-delay to be applied to half of the radiative source, usually a laser.<sup>[23]</sup> This allows for the generation of spectra where one wavelength of light irradiates the sample, but a wide range of wavelengths can be detected simultaneously. For FT-Raman spectroscopy, the usual wavelengths detected are  $3700\text{ cm}^{-1}$  to  $400\text{ cm}^{-1}$ . Due to the Fourier transformation, the spectra for this entire range can be generated in seconds using a single incident wavelength,<sup>[23]</sup> while a dispersive Raman would not be able to do this.

In FT-Raman spectroscopy, the light from the source is split into two beams by a half-silvered mirror (a beam-splitter). One of the beams is reflected from a stationary mirror, and the other from a mobile mirror (Figure 2.7),<sup>[24]</sup> The motion of the mobile mirror creates a difference in path-length of the two beams, consequently introducing a time-delay between the two paths. This splitting of the incident light and reflection from either a mobile or stationary mirror is the basis for a Michelson interferometer.<sup>[23, 24]</sup> If the two mirrors are equidistant from the beam-splitter, the re-joining of the two waves will be at the same point on each wave (*i.e.* the crest of the wave) and interfere constructively, allowing for maximal signal amplitude.<sup>[23]</sup> If the mobile mirror is, for example, 125% the distance of the stationary mirror from the beam-splitter, then the light that reflects from the mobile mirror travels a total of 50% further. The crest of one wave will meet the trough of the other wave, causing total destructive interference. No light will reach the detector.<sup>[23]</sup> If the mobile mirror is any other distance, the waves will interfere destructively, but not negate each other (Figure 2.8).<sup>[23]</sup> The resulting interference pattern is called an interferogram.

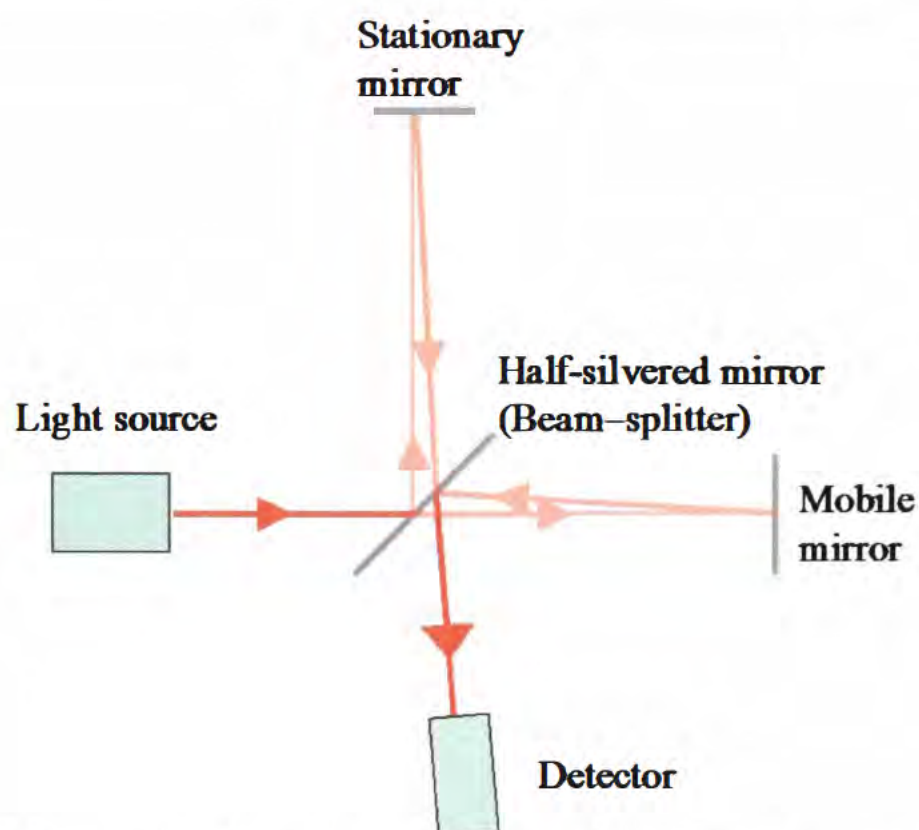


Figure 2.7 Schematic of a standard interferometer in an FT-Raman spectrometer. Showing how the interferogram is generated.

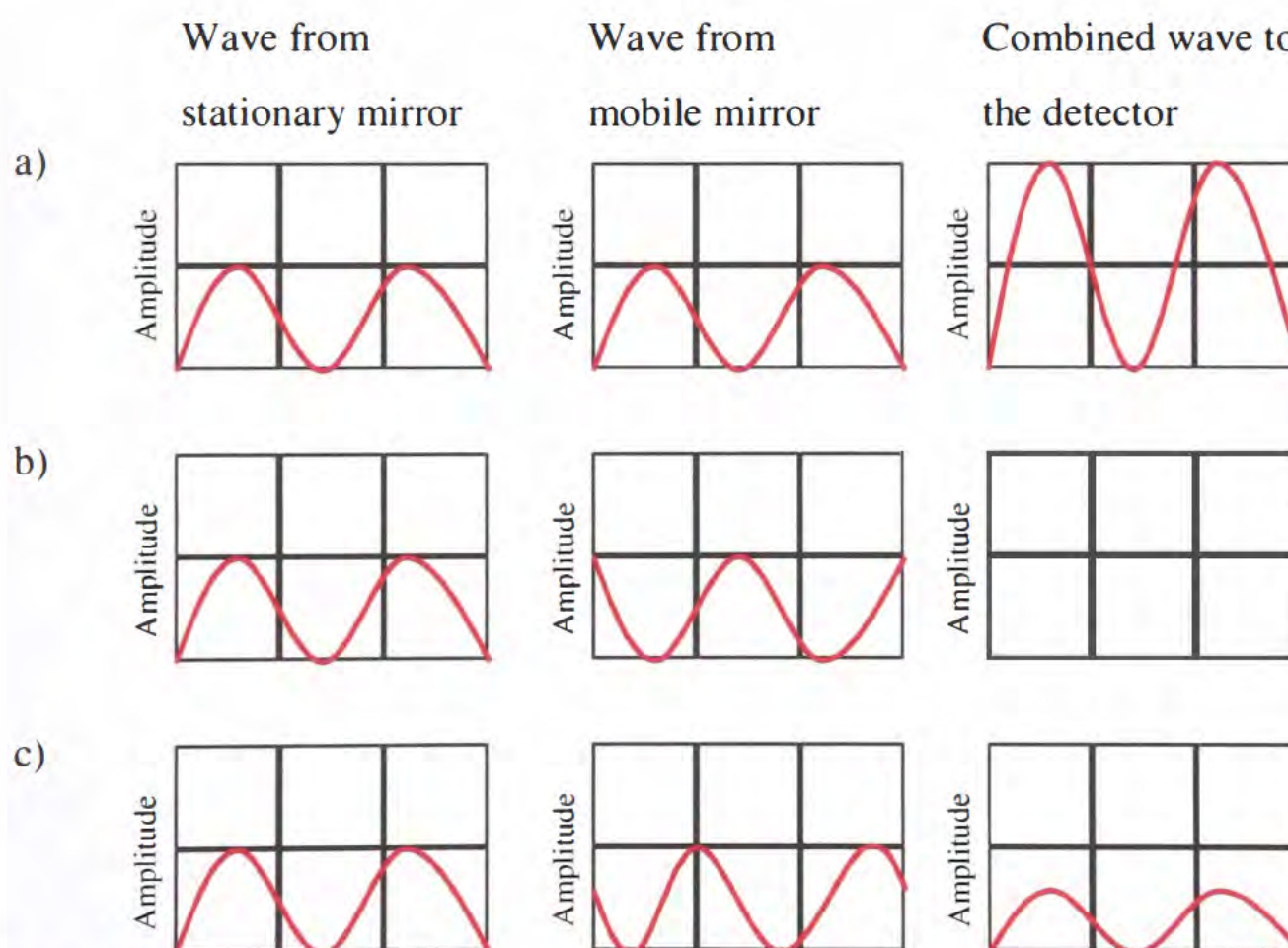


Figure 2.8 a) constructive interference of two waves, b) total destructive interference and c) partial destructive interference.

Raman spectroscopy gives information on the chemical bonds within a system. It is complementary to infrared spectroscopy (NIRS), but Raman spectroscopy has the advantage that the sample can be wet. Water, because it is very polar is a

strong IR absorber; hence if water is present in the sample, the IR spectrum will be largely obscured. Water is, however, a poor Raman scatterer,<sup>[23]</sup> so does not appear strongly in a Raman spectrum. The disadvantage of Raman is that the spectrum is totally obscured if the sample fluoresces. It has a limit of detection of about 1%.<sup>[25]</sup> FT-Raman has the same advantages as Raman spectroscopy, suffering less from fluorescence,<sup>[23]</sup> and has a similar limit of detection.

## 2.7 Differential Scanning Calorimetry

Differential scanning calorimetry (DSC) is a thermo-analytical technique where the properties of a sample are inferred from how heat flows into and out of a sample with changing temperature. The sample is weighed into a sample pan, either aluminium or steel, and then sealed. The reference pan is made of the same material as the sample pan, and treated identically to it, except that it remains empty.

The sample pan is heated at the same rate as the reference pan. As the sample undergoes physical or chemical changes, it will either require more heat (endothermic) or less heat (exothermic) than the reference pan to maintain the same temperature of the sample. The difference in energy required to maintain constant heating in both pans is recorded as a thermogram against the temperature of the pans.<sup>[26]</sup>

When measuring a DSC thermogram, the atmosphere inside the calorimeter can be air, nitrogen, or another inert gas, for example, argon. The advantage to having an inert atmosphere is that the sample cannot oxidise upon heating. However, as the sample is in a hermetically sealed pan, and the reference material is air (if a nitrogen atmosphere is used, and the reference pan is not properly sealed the reference material will become nitrogen as diffusion of the atmosphere gas into the reference pan will occur) it is sufficient to use an ambient air atmosphere if oxidation is unlikely. A differential scanning calorimeter has the basic design shown in Figure 2.9.<sup>[26]</sup>

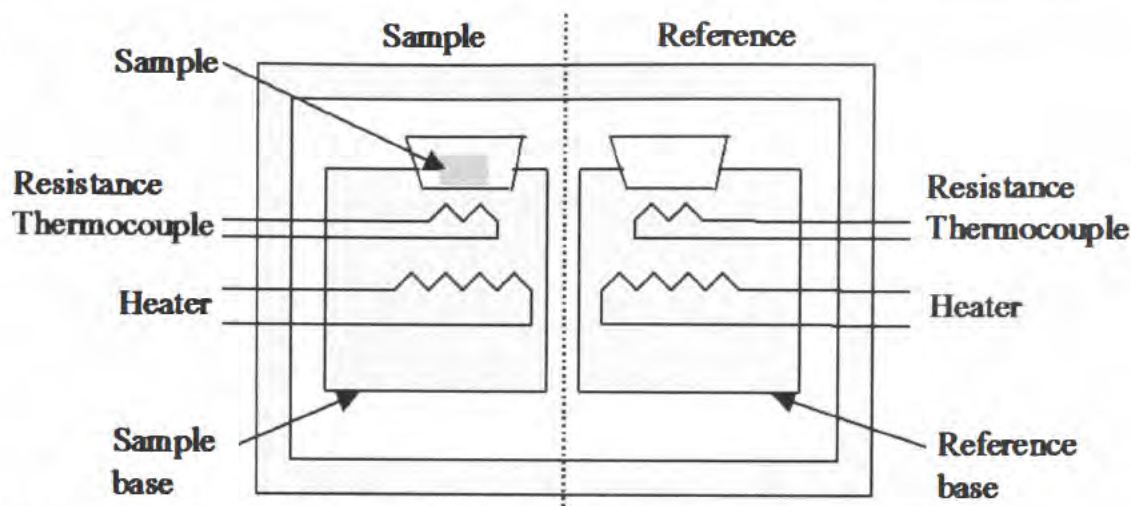


Figure 2.9 Schematic of a Differential Scanning Calorimeter.

Just as DSC experiments are recorded during heating, information may also be obtained during the subsequent cooling of the sample back to the start temperature. Re-heating of this sample will show, if upon cooling, the sample has become amorphous, crystallised into its original form, or crystallised into a new form.<sup>[27]</sup> The original heating cycle may also remove water from the sample, which, when cooled, will form a solid from the melt, but not necessarily re-incorporate the expelled water, meaning the sample may now be anhydrous, which will also change the properties of the sample.<sup>[27]</sup>

Heating rates for DSC can vary, but the standard rate for pharmaceutical samples appears to be  $10\text{ }^{\circ}\text{C min}^{-1}$ .<sup>[3, 28, 29]</sup> A phase transition occurs over a small temperature range. This is observed in the thermogram as a narrow peak. At low scan speeds, this peak shape is preserved, but at higher rates, it is sacrificed to observe more easily where the transition appears in the thermogram. Scan rates can be as low as  $0.1\text{ }^{\circ}\text{C min}^{-1}$ ; high speed DSC (HSDSC) can utilise scan rates of up to  $500\text{ }^{\circ}\text{C min}^{-1}$ .<sup>[25]</sup>

Information from a DSC thermogram is dependant on the sample. For a crystalline product a melting temperature ( $T_m$ ) will be observed. Peaks due to dehydration and decomposition may also be observed. An amorphous material will have the same peaks in the thermogram as a crystalline material, but in addition to these, there should be a glass transition temperature ( $T_g$ ) assuming that the DSC experiment started below the  $T_g$  of the sample, and a crystallisation temperature ( $T_c$ ).

Below the  $T_g$  the sample is in the “glassy” amorphous state, below the  $T_c$  it is in the “rubbery” amorphous state, below the  $T_m$  it is in the crystalline state (and hence, from this point onwards, the thermogram for the amorphous and crystalline material should now look identical) and above the  $T_m$  the sample is in the liquid state. A typical thermogram for an amorphous and a crystalline material is as follows (Figure 2.10).<sup>[26]</sup>

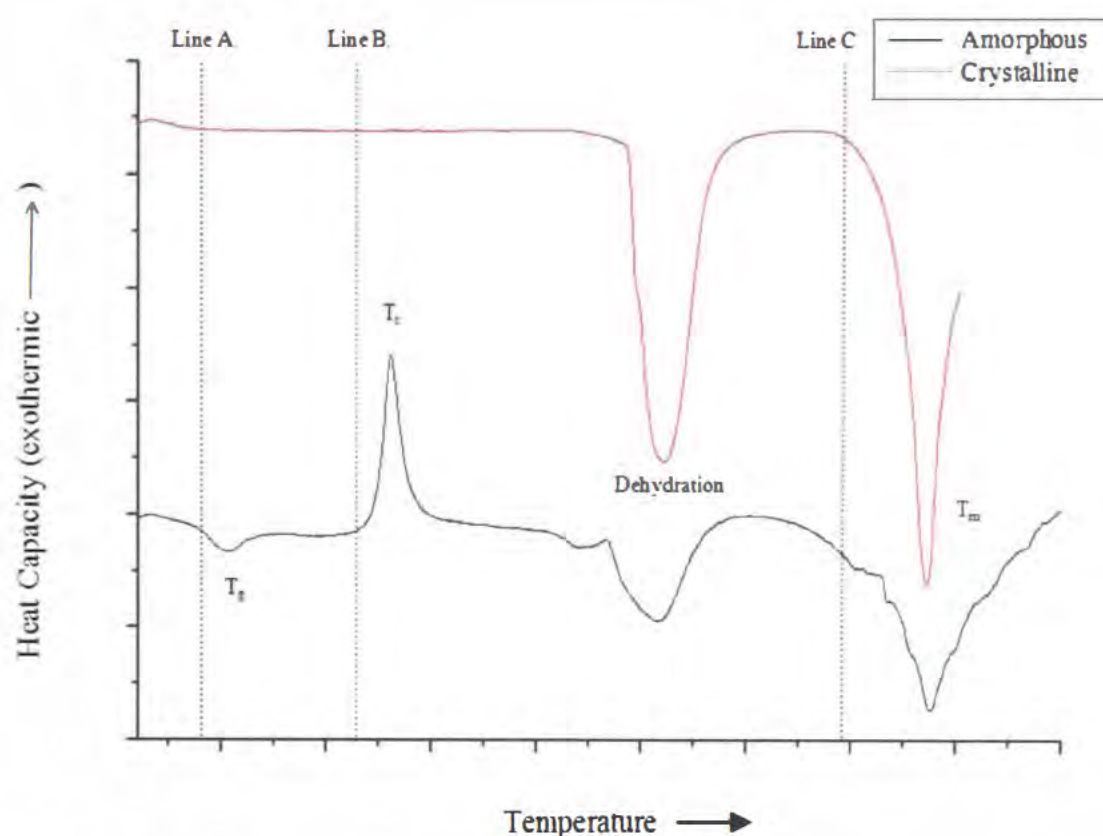


Figure 2.10 A DSC thermogram for an amorphous and a crystalline material. Line A is the onset of the  $T_g$  for the amorphous material, Line B is the onset of the  $T_c$  for the amorphous material, Line C is the onset of the  $T_m$ .

DSC allows for observation of phase transitions. However, unlike some of the other techniques discussed, these observations are for the entirety of the material present and not just the surface of the sample. The limit of detection of DSC is about 10%,<sup>[30]</sup> but for HSDSC this can be reduced to 1%.<sup>[25]</sup>

## 2.8 X-Ray Diffraction

The primary use of x-ray diffraction (XRD) is the identification and characterisation of crystalline solids. Every material has a unique diffractogram, and the positions and intensities of a peak, are representative of d-spacing in a crystal and therefore are characteristic of what phase the material is in. A

diffraction pattern is a graph of photon counts of radiation versus diffraction angle  $2\theta$  degrees. There are three main areas where information of the sample is observed in the diffraction pattern. These are peak position, which relates to crystalline material present in the sample, peak intensity, which is a quantification of the crystalline material, and the half-width of the peak, relates to the crystallite size. A diffraction pattern is obtained by reflecting x-rays off a sample. The sample, once inside the sample holder, needs to be carefully flattened. The sample is then either slowly rotated, whilst undergoing x-ray bombardment or is stationary whilst the x-ray source and detector rotate around it. X-rays that are reflected are then collected and counted by a detector.

For a crystalline product, the diffraction pattern is a series of sharp peaks, but if amorphous, then all that is observed is a single broad expanse, known as the “halo” effect<sup>[31]</sup> as in figure 2.11. This very obvious difference in the diffraction patterns makes XRD particularly useful in ascertaining whether a sample is crystalline or not. For a multi-component sample, the diffraction pattern of each sample will be superimposed, allowing for the quantification of the relative concentrations of each analyte present.

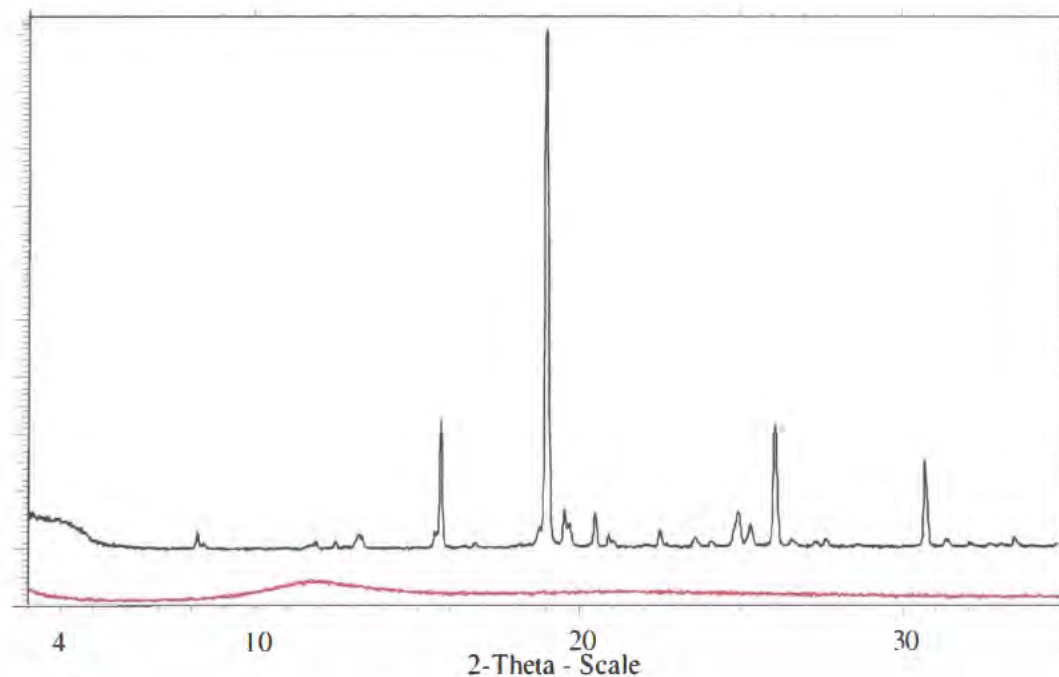


Figure 2.11 X-ray diffraction pattern of → a crystalline sample and → an amorphous sample showing the characteristic “halo”.

The Bragg condition is that for the reflection of x-rays, only crystals that are in specific orientations with respect to both the x-ray source and the detector will reflect x-rays. Reflection will only be observed when constructive interference of the x-ray beam occurs.<sup>[32]</sup> The diffracted beam makes an angle of  $2\theta$  with the incident beam. A finely ground crystalline powder contains a very large quantity of small crystals, known as crystallites. Crystallites will have a random orientation within the powder, this is important, as if the sample is not rotated then the preferred orientation of the crystallites will be shown, which may not give accurate information for the sample. The powder is placed into the monochromatic x-ray beam and crystallites that are orientated at the correct angle will fulfil the Bragg condition.<sup>[32]</sup> The sample is rotated, so that all crystallites will at some point fulfil this condition.<sup>[32]</sup> If the sample is presented to the x-ray along a single plane, then preferred orientation effects will occur, which will greatly reduce the quantitative information from the diffractogram, but not affect the qualitative data (rotating the sample should avoid the preferred orientation effect by allowing all orientations to be measured).

The intensity of the peak in the diffractogram is based on how many crystallites reflect the x-ray. The width of each peak is caused by incomplete destructive interference. As the crystallite size decreases, the width of the peak will increase. Any x-ray beams diffracted at either side of the Bragg angle will destructively interfere, but in small crystallites there is not enough planes for complete destructive interference causing peak broadening in the diffractogram.<sup>[32]</sup> For an amorphous powder, there are no crystallites present, so the Bragg condition cannot be fulfilled, resulting in the halo effect, as shown in figure 2.11 above.

The advantages of XRD are the obvious differences between an amorphous and a crystalline diffractogram, the high quality of the data and the amount of information that can be derived from the diffractogram, making XRD a favoured technique in industry. The disadvantages are that it is very expensive and requires a highly qualified technician and there is little information in a diffractogram of an amorphous material (except that it is amorphous). The limit of detection for XRD is approximately 5-10%.<sup>[33]</sup>

Finally, there is one important experimental factor to note. To generate the polycrystalline powder suitable for XRD analysis, a sample must be ground; therefore it is subject to mechanical stress. This will generate amorphous material, but, generally at a concentration too low to be detected by the diffractometer.

## **2.9 Other Techniques**

There are many other techniques that are employed within pharmaceutical sciences that are capable of distinguishing between amorphous and crystalline material, a more complete list can be found in section 2.10. There is, however, another technique that has been used, for a different purpose. Scanning electron microscopy (SEM) is a surface analytical technique employed, in the case of this work, to analyse differences in surface morphologies between an amorphous and crystalline sample of the same material, and more importantly, to ascertain if the indicator probe has disrupted the surface of the material. The surface being of particular importance throughout this work, as DRUV, FT-Raman and XRD are all techniques where the incident beam predominantly comes into contact with only the surface of the material to be analysed. DSC analyses all material present equally.

### **2.9.1 Electron Microscopy**

Electron microscopy is a technique for examining the surface topography, homogeneity, crystal morphology and surface defects by scanning with a high-energy beam of electrons.<sup>[34]</sup> Electron microscopes can be either transmission, or reflectance in design. Transmission electron microscopy (TEM) requires the sample to be thin; otherwise the electrons are absorbed by the sample. This often requires extensive sample preparation, for example ultra high vacuum, which may alter the surface of the sample, thinning techniques include ion bombardment. The most common type of reflection instrumentation is the scanning electron microscope (SEM). Samples that are poor electrical conductors need to be coated in a thin film of an electrically conductive material, often gold, to prevent charge build up on the sample surface.<sup>[34]</sup> The beam of electrons are

reflected either elastically by the atoms in the sample or inelastically, emitting secondary electrons. From this scatter, the image is generated.<sup>[32]</sup> Magnification of the surface can be anywhere from 25 times, to 250,000 times. Secondary electrons are generated as ionisation products from the primary electron beam. An example of a scanning electron micrograph and the level of detail available are shown in Figure 2.12.



Figure 2.12 An electron micrograph of crystalline raffinose<sup>[35]</sup>

### 2.9.2 Energy-Dispersive X-ray Analysis

Energy-dispersive x-ray analysis (EDX) is a technique to determine elemental composition at the surface of a sample. Elements present will emit characteristic x-rays upon bombardment by an electron beam. These are separated by a silicon-lithium detector, and amplified and corrected for absorption. EDX gives both a qualitative and a quantitative analysis of the elements in the sample, provided that they are present above the limit of detection (10%) and they have an atomic number higher than 11 (*i.e.* all elements after sodium).<sup>[32]</sup>

### 2.10 Comparison of techniques

The preceding sections (2.5-2.9 inclusive) show the techniques that are going to be used throughout this work, and explain what each technique reveals about the sample. However, each of the techniques has their strengths and weaknesses, there are also many other techniques that are used in material sciences that have

not been mentioned thus far. Table 2.1 is a list of these techniques. This list will detail the name of each technique, the main advantage and disadvantage of using it, whether or not it is destructive, and the limit of detection. For a technique to be destructive, the sample that is being analysed has to be changed in some way, or rendered impossible to recover.

Technique		Advantages	Disadvantages	Destructive	Limit of detection
Diffuse-Reflectance spectroscopy (DRUV)	UV	Very fast. Cheap. Easy to use, and prepare sample. May be adaptable for quality control.	Sample must have a chromophore.	No	To be investigated.
Dispersive Spectroscopy	Raman	Fast, reproducible. <sup>[37]</sup> Very little sample required. <sup>[31]</sup> Ease of sample preparation. <sup>[31]</sup> Sample can be wet.	May suffer from fluorescence and photodecomposition. <sup>[31]</sup>	No	1% <sup>[25]</sup> (A)
FT-Raman Spectroscopy		As above, fluorescence generally avoided. <sup>[24, 31]</sup>	As above, although less sensitive, due to wavelength of light used. Water can cause problems.	No	1% <sup>[36]</sup> (A)
Differential Calorimetry (DSC)	Scanning	Can observe the $T_g$ , $T_c$ and $T_m$ . Well recorded in literature.	Assumes no structural change during heating, thermolabile samples are problematic. <sup>[28]</sup>	Yes	10% <sup>[25, 30]</sup> (A)

Technique	Advantages	Disadvantages	Destructive	Limit of detection
X-Ray Diffraction (XRD)	Industrially preferred method. Qualification of multi-component systems.	Quantification difficult or unreliable if preferred orientation is present. <sup>[28]</sup> Sample is ground.	No – although grinding during preparation may be destructive.	5-10% <sup>[30]</sup> (A)
High-Speed Scanning Differential Calorimetry (HSDSC)	Same as DSC with increased limit of detection. Experimentally rapid form of DSC.	Same as DSC. Reduced quantification possible with higher scan speeds.	Yes	1.5% <sup>[25]</sup> (A)
Atomic Force Microscopy (AFM)	Maps amorphous regions on the surface of the sample. <sup>[38]</sup> Gives surface morphology of a sample.	Sample must be compared to crystalline or amorphous sample. <sup>[38]</sup>	No, unless sample crystallised to get comparison. <sup>[38]</sup>	Above 0.5% <sup>[38]</sup> (B)
Dynamic Mechanical Analysis (DMA)	Characterises phase behaviour and measures the activation energy of the $T_g$ <sup>[39]</sup>	Expensive, technique still to be optimised. <sup>[39]</sup>	Yes	2% or better <sup>[39]</sup> (A)

Technique	Advantages	Disadvantages	Destructive	Limit of detection
Thermal Gravimetric Analysis (TGA)	Gives more detailed decomposition data than DSC. <sup>[34]</sup>	Results dependant on weight change and atmosphere. <sup>[34]</sup>	Yes	1% <sup>[33, 40]</sup> (A)
Solid State Nuclear Magnetic Resonance Spectroscopy (SSNMR)	Gives structural information for multi-component systems. <sup>[41, 43]</sup>	Expensive. Slower technique. <sup>[43]</sup>	No	Up to 0.5% <sup>[41]</sup> (A)
Isothermal Microcalorimetry (IMC)	Very low limit of detection observed in many different systems for amorphous content quantification. <sup>[28]</sup>	Only amorphous samples that crystallise under certain %RH can be studied. <sup>[28]</sup>	Yes	Below 0.5-1% <sup>[28, 33, 41]</sup> (A)
Solution Calorimetry (Sol Cal)	Very good limit of detection.	Requires 100% amorphous and 100% crystalline standards. <sup>[28]</sup>	Yes	1% or better <sup>[42]</sup> (A)

Technique	Advantages	Disadvantages	Destructive	Limit of detection
Inverse Gas Chromatography (IGC)	Extremely surface sensitive, very low limit of detection. <sup>[46]</sup>	Routine analysis difficult. Expensive.	Yes	1% or better <sup>[44]</sup> (A)
Gravimetric Vapour Sorption	Capable of distinguishing between samples of very low amorphous content. <sup>[33]</sup>	Quantification is poor. <sup>[33]</sup>	Yes	0.5% although has been stated as 0.05% <sup>[33]</sup> (A)
Near Infrared Spectroscopy (NIRS)	Gives chemical and physical information of the sample at molecular level. <sup>[47]</sup> Qualitative data. <sup>[47]</sup>	Sample needs to be dry.	No	1 % or better <sup>[45]</sup> (C)
Scanning Electron Microscopy (SEM)	Gives a visual result of the surface morphology.	Sample needs to be conductive so often coated. Also needs to be smooth, hence polished.	Yes. Sample needs to be coated.	Can visualise amorphous regions

Technique	Advantages	Disadvantages	Destructive	Limit of detection
Transmission Electron Microscope (TEM)	Detection of defects within a crystal structure.	Sample must be able to withstand high vacuum, and be prepared as thin film. Complex micrographs. Slow.	Structural change may occur during sample preparation.	

Table 2.1 Techniques used to determine amorphous content

(A) = Amorphous lactose in crystalline lactose.

(B) = Amorphous budesonide in crystalline budesonide

(C) = Amorphous raffinose in crystalline raffinose.

There are many techniques used to quantify amorphous content as Table 2.1 shows. They all have advantages and disadvantages, and it is suggested in some cases<sup>[37]</sup> that it is better to use more than one technique. The fact that there is no one individual technique that can unequivocally state that a sample is, for example, 0.1% amorphous, means that new methods for low level amorphous content quantification are still being sought. Many of these techniques are tested against current standard techniques, noticeably XRD and DSC. The disadvantage with most of these techniques is that they are expensive and/or difficult for non-experts to use, leading to problems obtaining facile, routine analyses as required.

Perichromism, using DRUV spectroscopy is a different approach, the equipment is comparatively inexpensive, and the technique is easy to use. DRUV spectroscopy can analyse small samples (in the milligram range) and, depending on the size of the integrating sphere, could be scaled up to be a quality control process during various stages of drug manufacture. The one serious disadvantage is the need of a chromophore. However, if the indicator probe added to the material is edible, either already used in a pharmaceutical compound, or a food stuff, then it may, in the visible region, act as a self-indicating system. Having a drug that is already coloured would also eliminate the need to add colourants to the product, which are added to cover batch differences, and for aesthetic reasons.

The techniques chosen to show that the sample is either amorphous or crystalline (along with DRUV) are FT-Raman, DSC and XRD. DSC and XRD were chosen for the fact that they are used extensively in the literature (as already discussed) and FT-Raman as it has a good limit of detection is non-destructive, fast, the sample can be wet and it was available for use. The other techniques mentioned have not been used because they did not fulfil one or more of these criteria, this will be discussed in greater detail in the conclusions and future work (chapter 6).

## 2.11 References

- [1] C.-A. Scheef, D. Oelkrug, P. C. Schmidt, *European Journal of Pharmaceutics and Biopharmaceutics* **1998**, *46*, 209.
- [2] R. Govindarajan, A. Zinchuk, B. Hancock, E. Y. Shalaev, R. Suryanarayanan, *Pharmaceutical Research* **2006**, *23*, 2454.
- [3] M. E. Aulton, *Pharmaceutics the science of dosage form design*, Second ed., Churchill Livingstone, London, UK, **2002**.
- [4] L. Yu, *Advanced Drug Delivery Reviews* **2001**, *48*, 27.
- [5] M. K. Haque, Y. H. Roos, *Carbohydrate Research* **2005**, *340*, 293.
- [6] D. A. Skoog, D. M. West, F. J. Holler, *Fundamentals of Analytical Chemistry*, Seventh ed., Saunders College Publishing, Orlando, USA, **1997**.
- [7] K. Chatterjee, E. Y. Shalaev, R. Suryanarayanan, R. Govindarajan, *Journal of Pharmaceutical Sciences* **2008**, *97*, 274.
- [8] Y. Roos, M. Karel, *Biotechnology Progress* **1991**, *7*, 49.
- [9] L. Greenspan, *Journal of Research at the National Bureau of Standards A*. **1977**, *81A*, 89.
- [10] M.-A. Ottenhof, W. MacNaughtan, I. A. Farhat, *Carbohydrate Research* **2003**, *338*, 2195.
- [11] L. Norgaard, M. T. Hahn, L. B. Knudsen, I. A. Farhat, S. B. Engelsen, *International Dairy Journal* **2005**, *15*, 1261.
- [12] D. J. Burnett, F. Thielmann, J. Booth, *International Journal of Pharmaceutics* **2004**, *287*, 123.
- [13] D. L. Pavia, G. M. Lampman, G. S. Kriz, *Introduction to Spectroscopy*, Third ed., Harcourt College Publishers, **2001**.
- [14] P. W. Atkins, *Physical Chemistry*, 5th ed., Oxford University Press, Oxford, UK, **1995**.
- [15] C. Reichardt, *Chemical Reviews* **1994**, *94*, 2319.
- [16] R. Yeo, in *Workshop at Photonics Cluster (UK)*, Anson University, **2005**.
- [17] I. Lindseth, A. Bardal, R. Spooren, *Optics and Lasers in Engineering* **1999**, *32*, 419.
- [18] ProLite Technologies, *Diffuse Reflectance - Theory and Applications*, **2005**.
- [19] S. Lacombe, H. Cardy, N. Soggiu, S. Blanc, J. L. Habib-Jiwan, S. J.Ph., *Microporous and Mesoporous Materials* **2001**, *46*, 311.
- [20] M. Kacurakova, M. Mathlouthi, *Carbohydrate Research* **1996**, *284*, 145.
- [21] C. N. Banwell, E. M. McCash, *Fundamentals of Molecular Spectroscopy*, Fourth ed., McGraw-Hill, **1994**.
- [22] S. Elliott, *The physics and chemistry of solids*, Wiley, Chichester, UK, **1998**.
- [23] G. Xue, *Prog. Polymer Science* **1997**, *22*, 313.
- [24] S. Wartewig, R. H. H. Neubert, *Advanced Drug Delivery Reviews* **2005**, *57*, 1144.
- [25] M. Saunders, K. Podlunii, S. Shergill, G. Buckton, P. Royall, *International Journal of Pharmaceutics* **2004**, *274*, 35.
- [26] P. W. Atkins, J. de Paula, *Elements of Physical Chemistry*, 4th ed., Oxford University Press, Oxford, UK, **2005**.
- [27] H. Nagase, T. Endo, H. Ueda, M. Nakagaki, *Carbohydrate Research* **2002**, *337*, 167.

- [28] D. Gao, J. H. Rytting, *International Journal of Pharmaceutics* **1997**, *151*, 183.
- [29] B. M. Murphy, S. W. Prescott, I. Larson, *Journal of Pharmaceutical and Biomedical Analysis* **2005**, *38*, 186.
- [30] A. Saleki-Gerhardt, G. Zografi, *Pharmaceutical Research* **1994**, *11*, 1166.
- [31] M. E. Auer, U. J. Griesser, J. Sawatzki, *Journal of Molecular Structure* **2003**, *661-662*, 307.
- [32] L. E. Smart, E. A. Moore, *Solid state chemistry an introduction*, 3rd ed., CRC/Taylor and Francis Group, **2007**.
- [33] G. Buckton, P. Darcy, *International Journal of Pharmaceutics* **1995**, *123*, 265.
- [34] A. R. West, *Solid State Chemistry and its applications*, Wiley, **1985**.
- [35] K. Kajiwara, F. Franks, P. Echlin, A. L. Greer, *Pharmaceutical Research* **1999**, *16*, 1441.
- [36] L. S. Taylor, G. Zografi, *Pharmaceutical Research* **1998**, *15*, 755.
- [37] J. H. Kirk, S. E. Dann, C. G. Blatchford, *International Journal of Pharmaceutics* **2007**, *334*, 103.
- [38] M. D. Jones, P. M. Young, D. Traini, J. Shur, S. Edge, R. Price, *International Journal of Pharmaceutics* **2008**, *357*, 314.
- [39] P. G. Royall, C.-y. Huang, S.-w. J. Tang, J. Duncan, G. Van-de-Velde, M. B. Brown, *International Journal of Pharmaceutics* **2005**, *301*, 181.
- [40] H. Larhrib, X. M. Zeng, G. P. Martin, C. Marriott, J. Pritchard, *International Journal of Pharmaceutics* **1999**, *191*, 1.
- [41] C. Gustafsson, H. Lennholm, T. Iversen, C. Nystrom, *International Journal of Pharmaceutics* **1998**, *174*, 243.
- [42] S. E. Hogan, G. Buckton, *International Journal of Pharmaceutics* **2000**, *207*, 57.
- [43] R. K. Harris, *Nuclear Magnetic Resonance Spectroscopy. A physicochemical view.*, Pitman Books Limited, **1983**.
- [44] H. E. Newell, G. Buckton, D. A. Butler, F. Thielmann, D. R. Williams, *International Journal of Pharmaceutics* **2001**, *217*, 45.
- [45] S. E. Hogan, G. Buckton, *International Journal of Pharmaceutics* **2001**, *227*, 57.
- [46] M. D. Ticehurst, P. York, R. C. Rowe, S. K. Dwivedi, *International Journal of Pharmaceutics* **1996**, *141*, 93.
- [47] A. Gombas, I. Antal, P. Szabo-Revesz, S. Marton, I. Eros, *International Journal of Pharmaceutics* **2003**, *256*, 25.

## **Chapter 3**

### **Materials and Methods**

#### **3.1 Introduction**

Perichromism, as described herein, is designed to distinguish between amorphous and crystalline material, by detecting changes in the DRUV spectrum of a probe molecule added to a pharmaceutically important excipient. This requires a careful, informed choice of probe molecule. Parameters that should be considered include safety or edibility of the probe molecule, which also exhibits a large wavelength (perichromic) shift between the amorphous and crystalline forms of an excipient.

The materials that have been chosen to examine perichromism are a selection of pharmaceutical excipients. A medicine consists of both the active pharmaceutical ingredient (API), and often many, different excipients. The API is the part of a medicine that actually cures/treats the disease or ailment. Excipients are added to this for a variety of reasons, such as: improving the bioavailability (by increasing aqueous solubility) of the medicine; preserving the medicine to increase shelf-life (and therefore profitability); improving processing and manufacturing variables (flowability, grinding, compaction *etc.*); and taste masking to improve patient compliance. The API was not chosen for study for the following reasons: they are difficult to obtain in a pure form; they are usually more complicated molecules than excipients; they are often very expensive; and, there has been little work published revealing information on them as they are often covered by patents by pharmaceutical companies as intellectual property to protect companies' products from being manufactured as cheaper generic or alternatively branded medicines. This lack of information makes it considerably more difficult to determine if a result observed is due to a change in polymorphic form, or is a feature inherent to the API. Excipients suffer from few of these

disadvantages, and often make up the majority of the medicine that is taken by the patient. Table 3.1 details some common areas where a pharmaceutical excipient might be required in manufacturing a tablet.<sup>[1]</sup>

Excipient	Usage
Anti-adherent	Prevent medicine sticking to machinery
Glidant	Improve powder flow
Lubricant	Prevent tablets from adhering to die
Preservative	Improve shelf-life
Coating	Improve taste and therefore patient compliance
Disintegrant	Improve drug dissolution
Binder	Prevent tablet from breaking apart
Filler	Make tablet a suitable size for patient to take

Table 3.1 Some classes of excipient that might be used in tablet manufacture.

### 3.2 Dye selection

Two probes were initially chosen: methyl red and methyl green. Methyl red (Figure 3.1) is an (aryl) azo dye and a pH indicator, in aqueous solutions below pH 4.4 it is red, and above pH 6.2 it is yellow<sup>[2, 3]</sup>, suggesting that it may be applicable as a solvatochromic dye.<sup>[4]</sup> Methyl red was purchased from Sigma-Aldrich. Batch number 094K3732, and used as received.

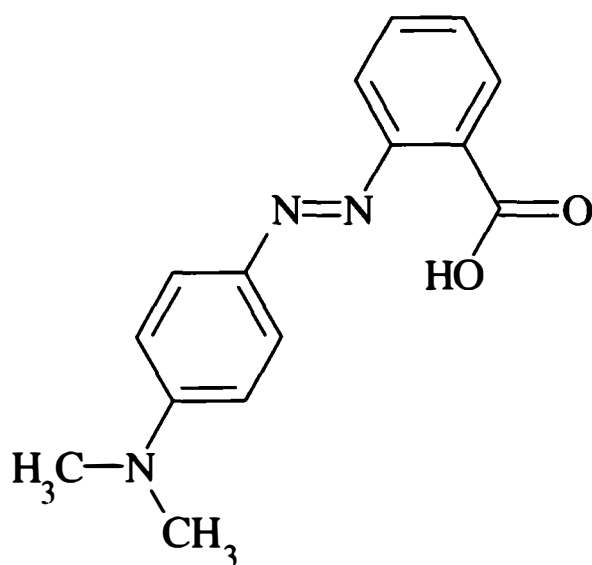


Figure 3.1 Methyl red

Methyl green was also considered and investigated concurrently with methyl red to ascertain which might be more perichromic. Methyl green (Figure 3.2) has the chemical formula  $C_{26}H_{33}N_3Cl_2$  and is also a pH indicator. In aqueous solutions it is yellow below pH 0.1 and blue above pH 2.3. Methyl green, general purpose grade was purchased from Fisher Scientific. Batch number 0587434, and used as received.

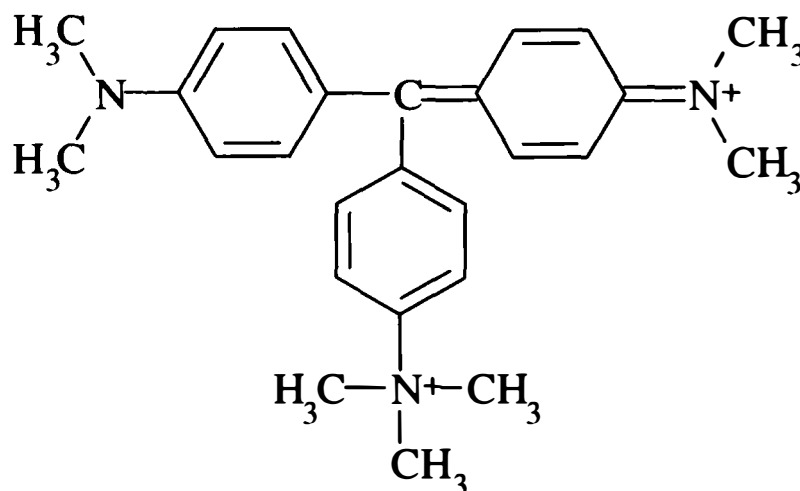


Figure 3.2 Methyl green.

It should be noted here that neither methyl red nor methyl green was purified before use – methyl green can be washed in chloroform to remove crystal violet - but this was considered unnecessary, as any impurity would total approximately 1 % of a probe entailing 0.1 % (*i.e.* the impurity would be 0.001% or 1 ppm) of the total mass of material to be investigated.

The third dye chosen was phenol red (Figure 3.3), which has the molecular structure  $C_{19}H_{14}O_5S$ ,<sup>[2]</sup> and is used in the PSP test and in an intravenously administered test for renal function,<sup>[5]</sup> making phenol red an ideal candidate for testing perichromism, as it is safe for human use. Phenol red, also called phenolsulphonphthalein, is a dark red crystalline dye, and is an acid-base indicator. In aqueous solutions below pH 6.8, phenol red is yellow, and above pH 8.2 it is pink or fuchsia,<sup>[2]</sup> between these two pH values, the colour of the solution is orange-red. Phenol red, general-purpose grade, was purchased from Fisher Scientific, batch 0566600, and used as received.

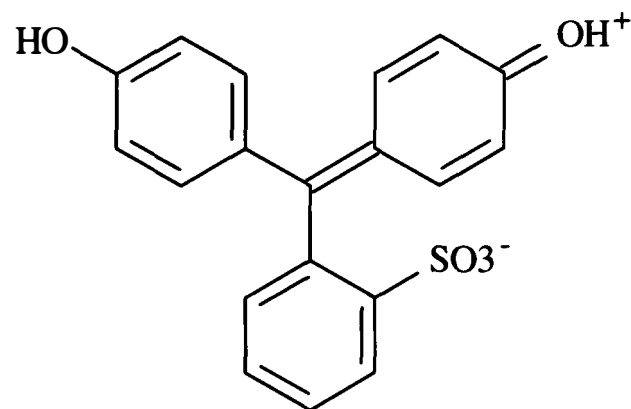


Figure 3.3 Phenol Red

The fourth and final dye, which was used to test a known, highly solvatochromic probe for perichromic purposes, was Reichardt's dye (section 1.1).

### 3.3 Excipients

The best method to distinguish between amorphous and crystalline material is to prepare a 100% amorphous and a 100% crystalline form of each sample. However, it is seldom possible to produce 100% purity (*i.e.* 100% amorphous). Therefore material examined by DRUV spectroscopy should be validated by other techniques. Excipients that are used extensively in the literature, as well as in pharmaceutical formulations, were chosen as model compounds, to test the possibility of developing the concept of perichromism into a PAT test.

#### 3.3.1 Sucrose

Sucrose (Figure 3.4) is a natural disaccharide produced in plants, particularly sugar cane.<sup>[6]</sup> It has the molecular formula C<sub>12</sub>H<sub>22</sub>O<sub>11</sub>,<sup>[7]</sup> and consists of two monosaccharides,  $\alpha$ -glucose and fructose,<sup>[8]</sup> joined by a glycosidic bond. Sucrose has a sweet taste, and is used expansively in the food industry.<sup>[9-11]</sup> In the pharmaceutical industry, sucrose is used as a taste-masking agent, and as a solution binder or filler.<sup>[1]</sup> Sucrose, analytical grade, was purchased from FSA, batch 25453451.

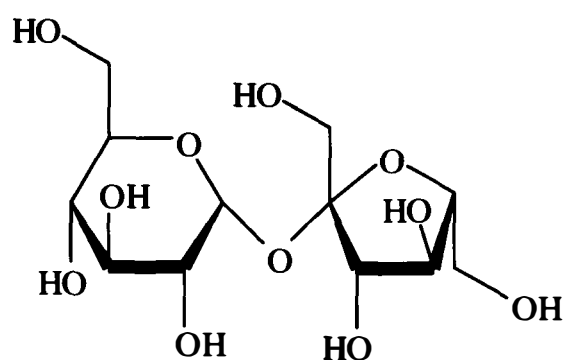


Figure 3.4 Sucrose

### 3.3.2 Lactose

Lactose (Figure 3.5) is another natural disaccharide, commonly produced by mammals. Like sucrose it has the molecular formula  $C_{12}H_{22}O_{11}$ .<sup>[12]</sup> Lactose also consists of two monosaccharides; these are  $\beta$ -D-galactose and  $\beta$ -D-glucose bonded by a  $\beta$ -(1-4) glycosidic link.<sup>[13]</sup> Lactose is also commonly used in the food industry.<sup>[14, 15]</sup> In pharmaceuticals, lactose has a greater role than sucrose, as it is the most common filler used in tablets,<sup>[1]</sup> and can, for example, be used as a carrier powder for dry powder inhalers.<sup>[16]</sup> Lactose,  $\alpha$ -lactose monohydrate, analytical reagent grade, was purchased from Sigma-Aldrich, Lot 110K0282

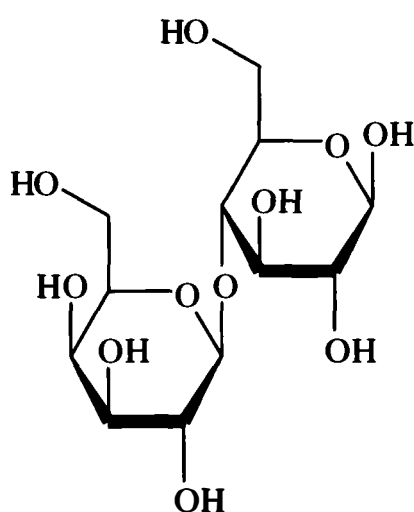


Figure 3.5 Lactose

### 3.3.3 Trehalose

Trehalose (Figure 3.6) is the third isomer of  $C_{12}H_{22}O_{11}$ <sup>[17]</sup> to be utilised. Trehalose like sucrose and lactose, consists of two monosaccharides, in this case two  $\alpha$ -glucose units bonded by an  $\alpha$ -(1-1) glycosidic link.<sup>[18]</sup> It is believed that

trehalose plays an important role in the ability of animals and plants to survive long periods of drought.<sup>[19]</sup> This has also led to trehalose being used as a bioprotectant in freeze drying, particularly of proteins,<sup>[18]</sup> and to increase drug stability.<sup>[20]</sup> Trehalose, D-(+)-Trehalose dihydrate, was purchased from Sigma-Aldrich, batch 027K7350

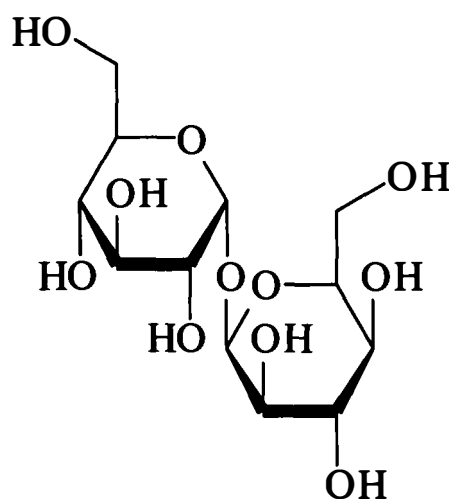


Figure 3.6 Trehalose

### 3.3.4 Raffinose

Raffinose (Figure 3.7) is a trisaccharide with the molecular formula  $C_{18}H_{32}O_{16}$ .<sup>[21, 22]</sup> The three constituent monosaccharides of raffinose ( $\beta$ -D-fructofuranosyl-*O*- $\alpha$ -D-galactopyranosyl-(1-6)- $\alpha$ -glucopyranoside)<sup>[23]</sup> are fructose, galactose and glucose. Raffinose is used less frequently in pharmaceuticals than other carbohydrates, as humans do not have the necessary enzyme required to metabolise it. However, it has been shown that it, like trehalose, can stabilise proteins during freezing,<sup>[19, 24]</sup> probably by acting as a desiccant. Raffinose is more complex than the disaccharides used, as it has more possible hydrates, and is useful for gaining knowledge of techniques used to determine amorphous content,<sup>[23]</sup> although it is not extensively covered in the literature. Raffinose pentahydrate, reagent grade, was purchased from Fisher Scientific batch 0560795

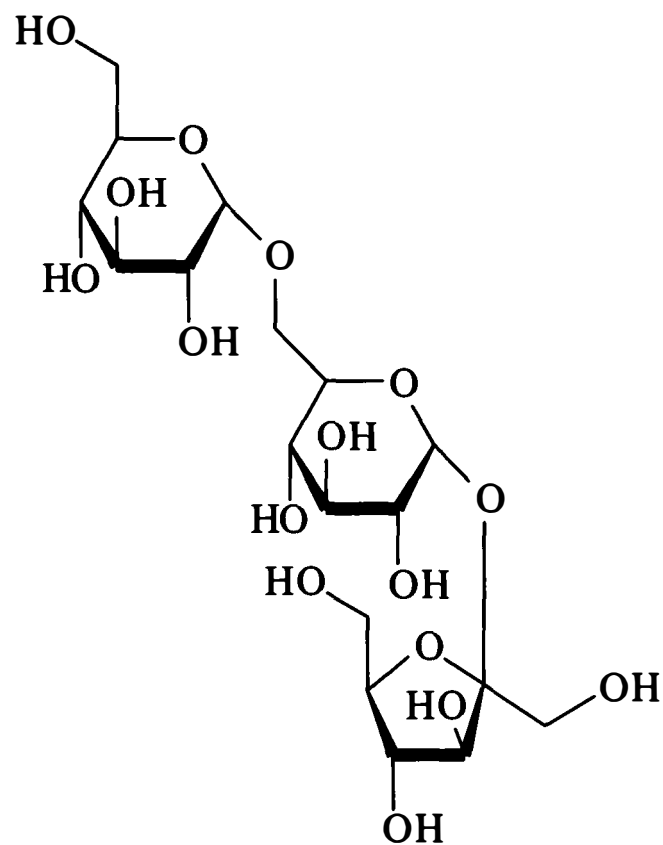


Figure 3.7                      Raffinose

### 3.4                      Equipment

The aims of this work require equipment to do the following: prepare amorphous material; maintain amorphous material during storage or to allow it to crystallise; analyse the extent of crystallisation of the material. The first two requirements are met by using one technique for each (freeze drying and desiccators of controlled temperature and relative humidity); the analysis of crystallinity requires a number of techniques. The reasons for their selection have already been covered in the previous chapter.

#### 3.4.1                      Freeze drying

Freeze drying was performed using an Edwards Modulyo freeze drier. Samples were placed in broad containers to maximise surface area and increase the rate of freeze drying, then frozen in a conventional freezer at  $-18^{\circ}\text{C}$  for at least 18 hours. The sample was then freeze dried at  $-40^{\circ}\text{C}$  for 48 hours, and then split into eight, equal-weight aliquots before storage in a desiccator of controlled relative humidity and temperature.

### 3.4.2 Relative Humidity

Following the freeze-drying process, the samples had been rendered amorphous. They were then stored under temperature and %RH controlled conditions to allow some aliquots to remain amorphous, and others to crystallise. To this end, samples were kept in desiccators over saturated salt solutions to allow atmospheres of various relative humidity to be created. All samples were maintained at 25° C and were stored under these conditions for one week. A list of the saturated salt solutions used, and the resultant relative humidity is given in table 3.2.<sup>[25]</sup>

Salt	%RH
Dryrite*	0
LiCl	11.3
CH <sub>3</sub> COOK	22.5
MgCl <sub>2</sub>	32.8
K <sub>2</sub> CO <sub>3</sub>	43.1
NaBr	57.6
KI	68.9
KCl	84.3

Table 3.2 List of saturated salt solutions to control relative humidity.

\* A hygroscopic solid, generating *ca.* 0 to 1 %RH. Note that these humidity values are only true when the temperature of the solution is 25° C.<sup>[25]</sup>

Relative humidity and temperature of the desiccators was monitored using Testo 608-H2 hygrometers which are accurate to  $\pm 2$  %RH and  $\pm 0.1^\circ$  C. Due to this level of accuracy of the hygrometers all %RH values from this point are as whole numbers  $\pm 2$  %RH, and that at 0 %RH may be as high as 2 %RH.

### 3.4.3 DRUV

Diffuse reflectance UV analysis was performed on an Agilent 8453 UV/visible spectrophotometer fitted with an integrating sphere (Labsphere RSA-HP-8453)

with an internal surface constructed of Spectralon™. Samples were placed in a custom-built sample holder, drilled from Spectralon™. The dimensions of the sample holder are: 6 mm i.d. x 2 mm. The spectrophotometer was calibrated before use by taking a reference spectrum of the blank Spectralon™ holder. Spectra were obtained in under 30 seconds for each sample, during which time the sample was open to ambient conditions within the laboratory.

#### **3.4.4 FT-Raman**

FT-Raman spectroscopy was performed on a Thermo Electron NXR FT-Raman module attached to a Thermo Electron FTIR Nexus. The sample was placed in an NMR tube, which was held in the viewstage of the FT-Raman spectrometer. Spectra were obtained using a Nd:YAG laser ( $\lambda_{\text{ex}}$  1064 nm, power 1.1 W) interferograms were collected on an NXR Genie (germanium) detector, pre-cooled with liquid nitrogen. Each spectrum is the result of 64 scans. An interferogram was obtained before scanning, using either methyl red or sulphur to focus the spectrometer. Calibration is performed automatically before each session of use.

The top of the sample in the NMR tube was open to ambient conditions inside the FT-Raman spectrometer during the scans (*ca.* 2 minutes).

#### **3.4.5 DSC**

Differential scanning calorimetry was performed using a Mettler Toledo FP85 TA cell connected to a Mettler Toledo FP90 central processor. Samples were weighed (between 2 and 5 mg) and sealed in an aluminium pan. The reference pan is in-built into the FP85. The sample pan was heated to 28° C at 1° C min<sup>-1</sup> (to allow for fluctuations in laboratory temperature) and then at 10° C min<sup>-1</sup>. The end temperature differed according to each sample and finished approximately 20° C above the greatest literature melting point for the most thermodynamically stable polymorph of a given sample. The differential scanning calorimeter was calibrated using indium on a regular basis.

### **3.4.6 XRD**

X-ray diffractograms were collected using a Philips PW1729 x-ray diffractometer. The x-ray source is a copper anode x-ray tube. Scan speeds of  $0.05^\circ \text{ s}^{-1}$   $2\theta$  were used and the results detected by using a Philips PW 1050 / 25 Goniometer.

### **3.4.7 SEM**

Scanning electron micrographs were collected on a Cambridge Stereoscan 360 scanning Electron Microscope. Samples were sputter-coated with gold before analysis to ensure sample conductivity. The electron beam was provided by a tungsten filament, and detected by a secondary electron detector. Micrographs were collected with an acceleration voltage of 25 kV. The probe current can range between 10pA and 200 pA.

### **3.4.8 EDX**

Energy dispersive x-ray analysis was performed using an Oxford instruments ISIS 300 attached to a JEOL JSM-5310LV scanning electron microscope. As with SEM samples have to be conductive for EDX, so were also sputter-coated with gold. The electron beam was supplied by a tungsten filament and secondary and backscattered electrons could be detected. An acceleration voltage of 25 kV was used. The probe current can not be measured on this instrument.

## **3.5 Methods**

This work is focussed on the use of probe molecules to distinguish between amorphous and crystalline samples of a material. To do this, two factors must be considered. These are the addition of the probe molecule, and the generation of amorphous and crystalline material. This was approached in several different ways, but in all cases (except a re-creation of the “pH-equivalence” experiments) the probe molecule was added to the excipient before rendering amorphous or

crystallising. This is different to the “pH-equivalence” methodology<sup>[26]</sup>, where a sample was prepared, and a known amount of dye was then added. The method(s) described below were chosen specifically to ensure that no further, unexpected transformation occurred to the sample to be studied, which may not be the case with the “pH-equivalence” method.

**Method 1a.** Preparation of an amorphous material.

10.00 g of the excipient to be analysed was accurately weighed before being dissolved in 100 mL of distilled water. 50.00 mg of the probe molecule was added to this solution. The resultant solution (of fully dissolved excipient and probe – this was facilitated by stirring with a magnetic flea) was placed in a conventional freezer (*ca.* -18° C) for a minimum of six hours. The sample was then freeze dried (section 3.4.1), and the lyophilised product was stored at 0 %RH and low temperature (< 5° C)

**Method 1b.** Preparation of a crystalline material.

10.00 g of the excipient to be analysed was accurately weighed before being dissolved in 100 mL of distilled water at 55° C, stirred gently with a magnetic flea. 50.00 mg of the probe molecule was added to this solution. A 10 mL aliquot of this sample was taken and to this 90 mL of ethanol at 55° C was added. The sample was covered and left at ambient temperature for 12 hours without stirring. The resultant crystals were filtered and stored in an oven at 70° C for a minimum of 12 hours.

This protocol proved to be problematic. The re-crystallisation of the analyte was successful, but unfortunately, the probe molecule did not adsorb fully to the analyte and remained in the filtrate, meaning that the concentration of the probe molecule when analysing the sample could not be ascertained.

**Method 2.** Generation of amorphous material with conversion to crystalline.

This method was only slightly adapted from method 1a, which did produce amorphous material. However, the probe concentration was too great, and the period of time left in the freezer was not sufficient to ensure a totally solid sample pre-lyophilisation. The volume of water to be moved was also excessive, (taking far too long to be fully removed) so this was also reduced.

5.00 g of the excipient to be analysed was accurately weighed before being dissolved in 50 mL of distilled water. 5.00 mg of the probe molecule was added to this solution. The resultant solution was placed in a conventional freezer (*ca.* -18° C) for a minimum of 18 hours, ensuring that the sample was fully solidified before placing in the freeze drier. The sample was then freeze dried, and upon completion of this, was split into eight equal masses, each of which was stored for one week in a desiccator maintained at 25° C (rather than the low temperatures previously used in method 1a) over a saturated salt solution to generate a controlled relative humidity.

**Method 3.** Addition of the probe molecule to a pre-prepared surface.

Method 3 was similar to the “pH-equivalence” experiments (sections 1.4 and 2.3) to prepare the samples. Method 2 was followed with the exception of adding the probe molecule. This was added to the required pre-prepared amorphous or crystalline sample as follows:

A known mass of probe indicator (5.00 mg) was dissolved in 50 mL of a suitable solvent (for example methanol). A ‘suitable solvent’ is one in which the probe molecule is soluble, but the excipient is not. This solution was added as an anti-solvent to 5.00 g of the excipient to be analysed, before being removed by rotary evaporation.

**3.6 References**

- [1] M. E. Aulton, *Pharmaceutics the science of dosage form design*, Second ed., Churchill Livingstone, **2002**.
- [2] F. J. Green, *The Sigma-Aldrich Handbook of Stains, Dyes and Indicators*, **1991**.
- [3] D. A. Skoog, D. M. West, F. J. Holler, in *Fundamentals of Analytical Chemistry*, Seventh ed., Saunders College Publishing, **1997**.
- [4] C. Reichardt, *Chemical Reviews* **1994**, *94*, 2319.
- [5] *The Pharmaceutical Codex*, 11th ed., The Pharmaceutical Press, London, **1979**.
- [6] D. Le Botlan, F. Casseron, F. Lantier, *Analysis* **1998**, *26*, 198.
- [7] J. Kroll, J. Darmo, K. Unterrainer, *Vibrational Spectroscopy* **2007**, *43*, 324.
- [8] L. S. Taylor, G. Zografu, *Journal of Pharmaceutical Sciences* **1998**, *87*, 1615.
- [9] N. Faria, M. N. Pons, S. Feyo de Azevedo, F. A. Rocha, H. Vivier, *Powder Technology* **2003**, *133*, 54.
- [10] I. Hopkinson, R. A. L. Jones, P. J. McDonald, B. Newling, A. Lecat, S. Livings, *Polymer* **2001**, *42*, 4947.
- [11] H. D. Goff, E. Verespej, D. Jermann, *Thermochimica Acta* **2003**, *399*, 43.
- [12] J. H. Kirk, S. E. Dann, C. G. Blatchford, *International Journal of Pharmaceutics* **2007**, *334*, 103.
- [13] N. Drapier-Beche, J. Fanni, M. Parmentier, M. Vilasi, *Journal of Dairy Science* **1997**, *80*, 457.
- [14] L. Norgaard, M. T. Hahn, L. B. Knudsen, I. A. Farhat, S. B. Engelsen, *International Dairy Journal* **2005**, *15*, 1261.
- [15] J. Bronlund, T. Paterson, *International Dairy Journal* **2004**, *14*, 247.
- [16] B. M. Murphy, S. W. Prescott, I. Larson, *Journal of Pharmaceutical and Biomedical Analysis* **2005**, *38*, 186.
- [17] A. B. Richards, S. Krakowka, L. B. Dexter, H. Schmid, A. P. M. Wolterbeek, D. H. Waalkens-Berendsen, A. Shigoyuki, M. Kurimoto, *Food and Chemical Toxicology* **2002**, *40*, 871.
- [18] M. Takahashi, Y. Kawazoe, Y. Ishikawa, H. Ito, *Chemical Physics Letters* **2006**, *429*, 371.
- [19] A. Moran, G. Buckton, *International Journal of Pharmaceutics* **2007**, *343*, 12.
- [20] S. S. Pinto, H. P. Diogo, J. J. Moura-Ramos, *Journal of Chem. Thermodynamics* **2006**, *2006*, 1130.
- [21] W.-T. Cheng, S.-Y. Lin, *Carbohydrate Polymers* **2006**, *64*, 212.
- [22] G. A. Jeffrey, D.-b. Huang, *Carbohydrate Research* **1990**, *206*, 173.
- [23] S. E. Hogan, G. Buckton, *International Journal of Pharmaceutics* **2001**, *227*, 57.
- [24] J. H. Crowe, F. A. Hoekstra, K. H. N. Nguyen, L. M. Crowe, *Biochimica et Biophysica Acta* **1996**, *1280*, 187.
- [25] L. Greenspan, *Journal of Research at the National Bureau of Standards A* **1977**, *81A*, 89.
- [26] R. Govindarajan, A. Zinchuk, B. C. Hancock, E. Y. Shalaev, R. Suryanarayanan, *Pharmaceutical Research* **2006**, *23*, 2454.

## **Chapter 4**

### **Results and discussion: The Saccharides**

#### **4.1 Introduction**

Solvatochromism is measured by detecting changes in the UV spectra of a material in media of different polarity. It is envisaged that by adapting this to measure diffuse reflectance UV spectra of solid material attached to solid media of different morphologies, differences in the DRUV spectra will be observed. This is designed to allow facile identification of the morphological phase that a probe is attached to. However, to be able to validate the technique many other experiments have to be undertaken. Identification of an unknown sample, or unknown morphological phase, can be achieved by using one of many techniques including FT-Raman, DSC and XRD as detailed in Chapter 2.

Due to the nature of this project the results and discussion section has been split into two chapters. Chapter 4 details how perichromism can be observed with a range of pharmaceutical excipients, and then, using the techniques mentioned above, identifying the morphological form of the excipient being examined. Chapter 5 will detail the control experiments that are essential to connect the DRUV spectrum to a particular polymorph and any conclusions that can be drawn from them are caused by a difference in the polymorphs being measured. Once this has been demonstrated the chapter will continue with the further experimentation that is required to form a theory for the mechanism of perichromism and any other examinations that are undertaken.

The ultimate goal of this is to produce a facile and inexpensive “test” for discovering if a change in morphological form is occurring in pharmaceutically important excipients.

## 4.2 Selection of probe molecule

The initial experimentation investigating perichromism was performed using methyl green (Figure 3.2) as the probe molecule. This is because it is an acid-base indicator with a visible transition (yellow below pH 0.1, blue above pH 2.3). Methyl green is used primarily as a stain, rather than a pH indicator. It has seven methyl groups, one of which is easily lost, causing the dye to convert to crystal violet.<sup>[1]</sup> It can also be converted to another dye, ethyl green, where the seventh methyl group is changed to an ethyl group.<sup>[1]</sup>

Amorphous and crystalline sucrose and then lactose with a 0.5% w/w loading of methyl green were prepared. Studies into the determination of amorphous content of pharmaceutical excipients focus intensely on lactose and to a slightly lesser degree sucrose, which is a simpler model than lactose as it can only exist as either an amorphous powder, or an anhydrous crystalline solid. There are three possible crystalline polymorphs of lactose, as well as an amorphous powder.

The incorporation of methyl green into a specific polymorphic form was via method 1a (freeze dry a 10% w/v aqueous solution of lactose with 0.5% w/w methyl green (with respect to lactose)) or method 1b (re-crystallisation with 0.5% w/w methyl green to lactose present) to produce a) amorphous and b) crystalline sucrose or lactose with the probe incorporated. Once spectra had been gathered, they were converted using the Kubelka-Munk remission function to obtain data on reflection rather than absorbance.

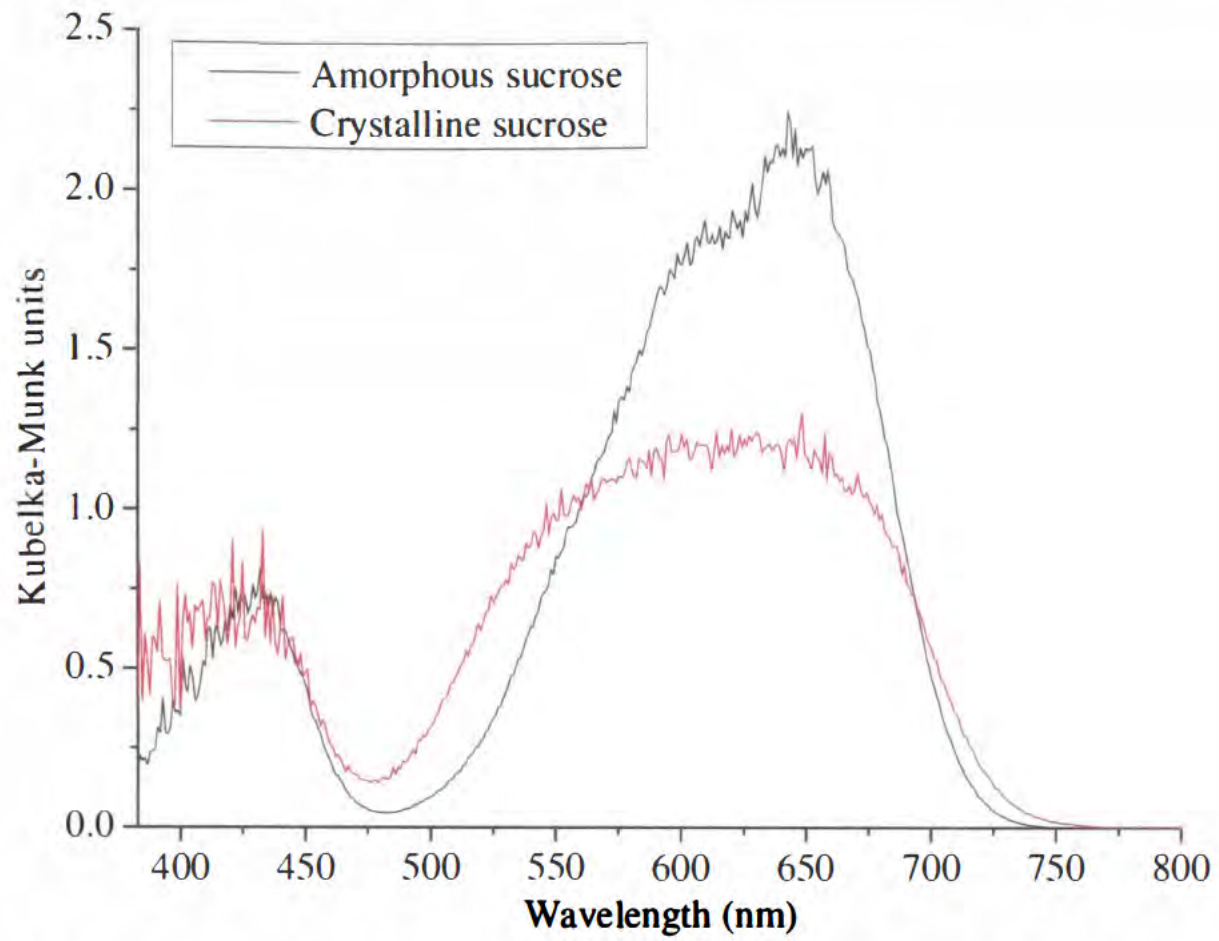


Figure 4.1 Diffuse-reflectance UV spectra of sucrose with 0.5 % w/w methyl green.

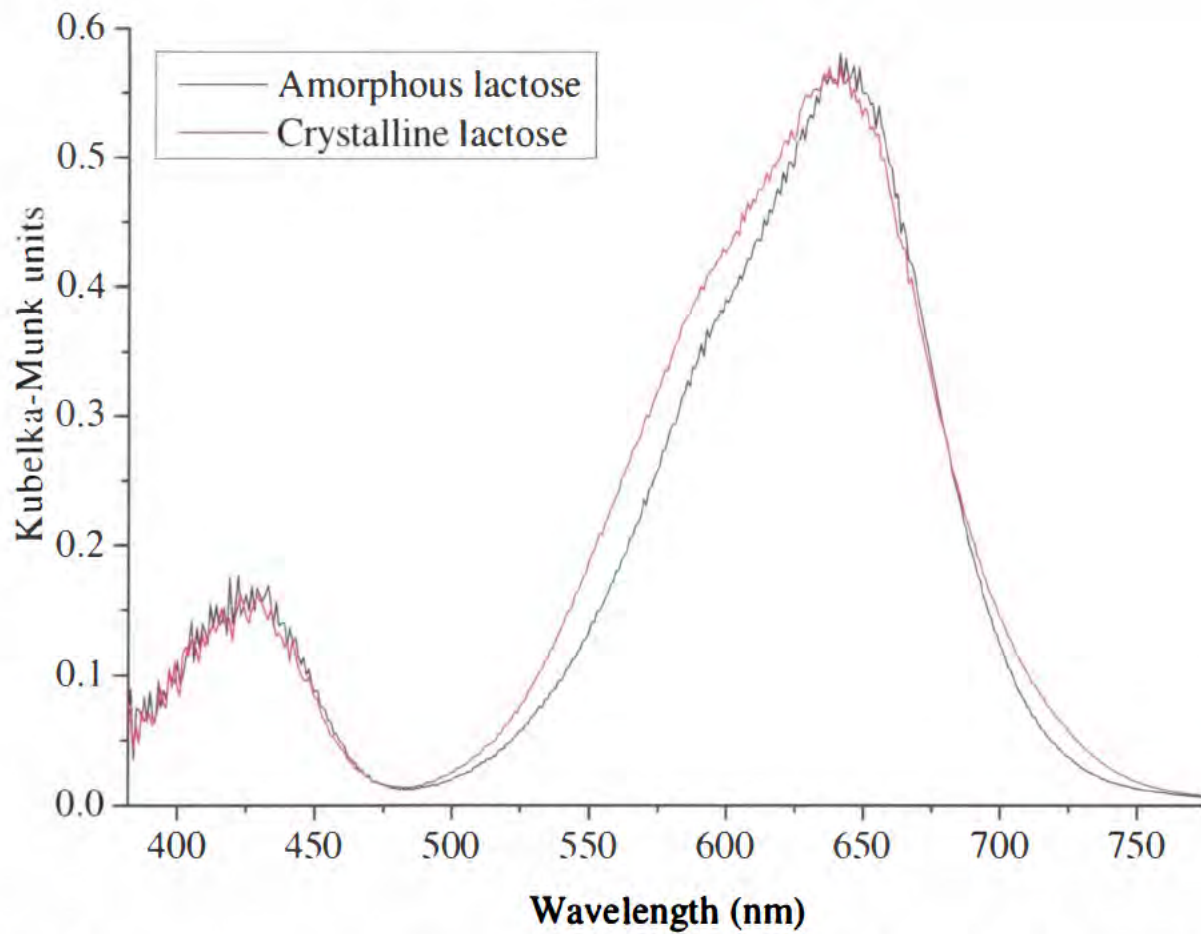


Figure 4.2 Diffuse-reflectance UV spectra of lactose with 0.5 % w/w methyl green.

As can be seen from figures 4.1 and 4.2, showing data for sucrose and lactose respectively, the two phases of each sample show little difference in their diffuse-reflectance UV spectra, and importantly, there is no change in the wavelength of the peaks between the two phases of each sample. The intensities of the two spectra (Figure 4.2) are nearly identical. From these results it can be said that using methyl green as the probe molecule, with methods 1a and 1b to prepare polymorphs have not shown perichromism. This could be due to the method choice or the probe molecule; methyl green as discussed in section 3.2 is subject to inter-conversion to crystal violet.<sup>[1]</sup> Importantly, this uncertainty surrounding the identity of the probe and the similarity of the spectra for the two phases of lactose caused methyl green to be discarded in favour of a different probe molecule.

To determine whether methyl green or methods 1a and 1b were responsible for the failure to observe a perichromic shift, methyl red was chosen to determine whether a change in the spectra of the different samples could be observed. If a change in the spectra was observed then method 1a and 1b would be capable of detecting of perichromism. This would suggest that methyl red, but not methyl green, is perichromic, although it could be possible that neither dye is perichromic. If perichromism was not observed then either both probes used were not perichromic or method 1 was not capable of incorporating the probe material in such a way that perichromism could be observed (or both). Methyl red was chosen because it is an inexpensive dye that is used in biological applications, *i.e.* the methyl red test<sup>[2]</sup> - which is used to determine acid formation by fermentation in bacteria. The probe was added in the same way that methyl green had been, and at the same concentration. Again, both sucrose (Figure 4.3) and lactose (Figure 4.4) were used as pharmaceutical excipients.

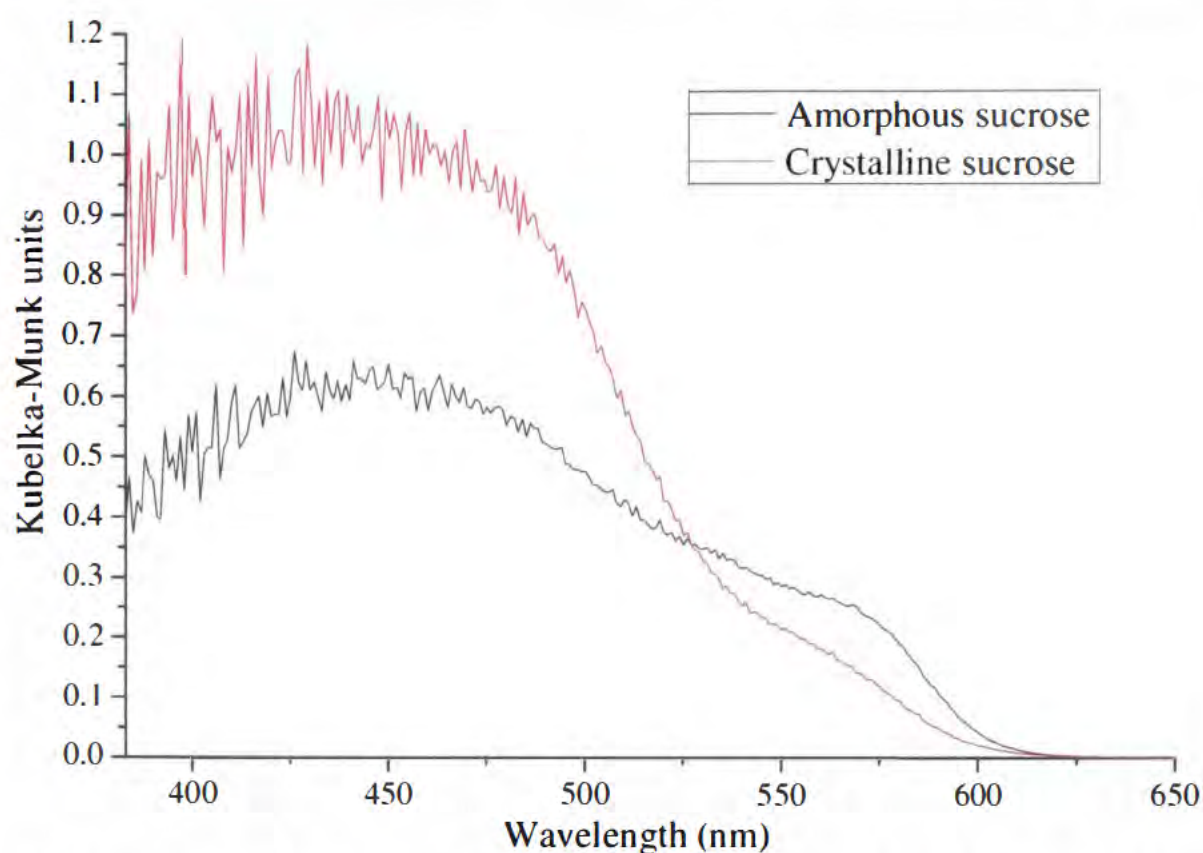


Figure 4.3. Diffuse-reflectance UV spectra of sucrose with methyl red.

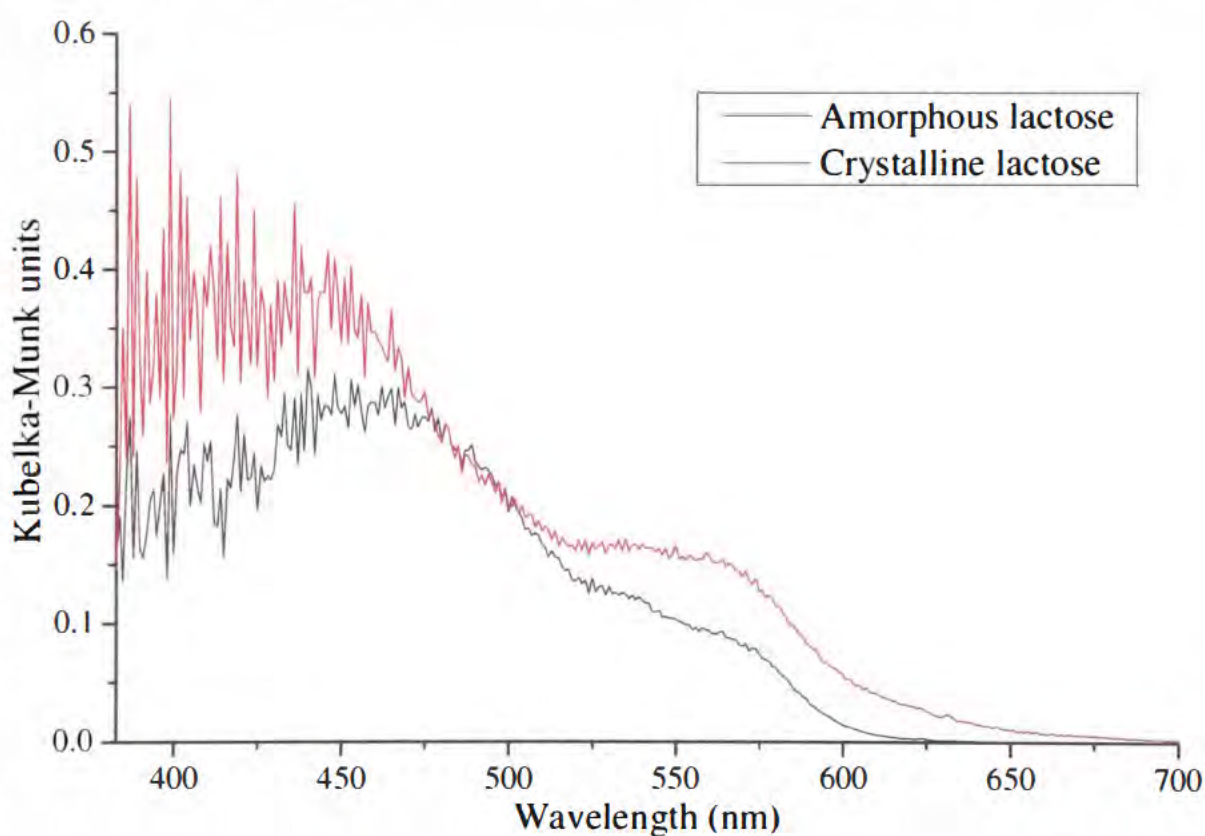


Figure 4.4. Diffuse-reflectance UV spectra of lactose with methyl red.

Methyl red also showed only limited potential for perichromism, and the fact that it is very easily reduced<sup>[1]</sup> meaning the usefulness of the probe is again called in to question, limit its use both as a pH indicator and as a perichromic probe molecule. Methyl red was only used with methods 1a and 1b, and no change in wavelength of any bands in the DRUV spectra produced was observed. A large change in intensity is shown in Figures 4.3 and 4.4, and in both cases the

spectrum for the crystalline polymorph is more intense than the spectrum for the amorphous powder, however, this change in intensity did not prove to be reproducible (in particular the ratio of the difference in intensity was subject to large change). A change in probe molecule in conjunction with a method developmental procedure was decided upon. The method was altered to method 2 (section 3.5) freeze drying an aqueous sample, and then storing at controlled humidity and temperature. Based on both literature evidence of storing sucrose at different %RH<sup>[3]</sup> and method 1a for producing amorphous material by freeze-drying, meaning that both crystalline and amorphous samples were treated identically with the sole exception of storage humidity which could be easily controlled.

Alongside the change in method, a change in probe molecule was decided upon. After careful consideration, phenol red was selected, as it is a stable acid-base indicator with a visual colour transition between pH 6.8 and pH 8.2. It is also non-toxic, and has been intravenously injected to test renal function<sup>[4]</sup> as mentioned in section 3.2. The concentration of the probe, 0.1 % w/w was maintained, as it allowed for easily observed spectra, and does not appear to be too strongly absorbing.

### 4.3 DRUV spectra of sucrose

It was decided that the first pharmaceutical excipient to be analysed was sucrose. The reason for the selection of sucrose is in theory it should be the simplest model compound, as it has only one known crystalline phase. Sucrose is readily available and important in many fields, not least pharmaceuticals. It has no known hydrates or polymorphs<sup>[5]</sup> and exists as either an amorphous powder or an anhydrous crystal; both of which can be generated and maintained easily.<sup>[3]</sup> This has led to sucrose being a common choice for amorphous content determination of techniques to examine polymorphism.<sup>[3, 5-15]</sup> Examples of common techniques used as comparisons include XRD, DSC<sup>[12]</sup> and Raman spectroscopy.<sup>[15]</sup>

The probe molecule was added to the sample before the sample was rendered amorphous (method 2). The sample was then split into eight equal portions, each stored as detailed in Chapter 3. Samples stored at low %RH should remain amorphous, and those at high %RH should crystallise as the increased relative humidity lowers the glass transition temperature of a sample, therefore enabling crystallisation to occur at lower temperature, *i.e.* at, or below, room temperature. Thus for perichromism to be measured for sucrose, it is sufficient for crystalline samples to have a peak at one  $\lambda_{\max}$ , and amorphous materials, a peak at a different wavelength.

Sucrose was stored in a desiccator of controlled temperature ( $^{\circ}\text{C}$ ) and %RH (given in the key of each experiment *e.g.* Figure 4.6) for seven days before analysis. After storage, both the colour and consistency (the crystalline samples had “caked”) of the samples stored at high relative humidity had visually changed, as can be seen in Figure 4.5. This gave great confidence that perichromism would be observed using this probe and method 2. The diffuse-reflectance UV spectrum for sucrose stored at each %RH is shown in figure 4.6.

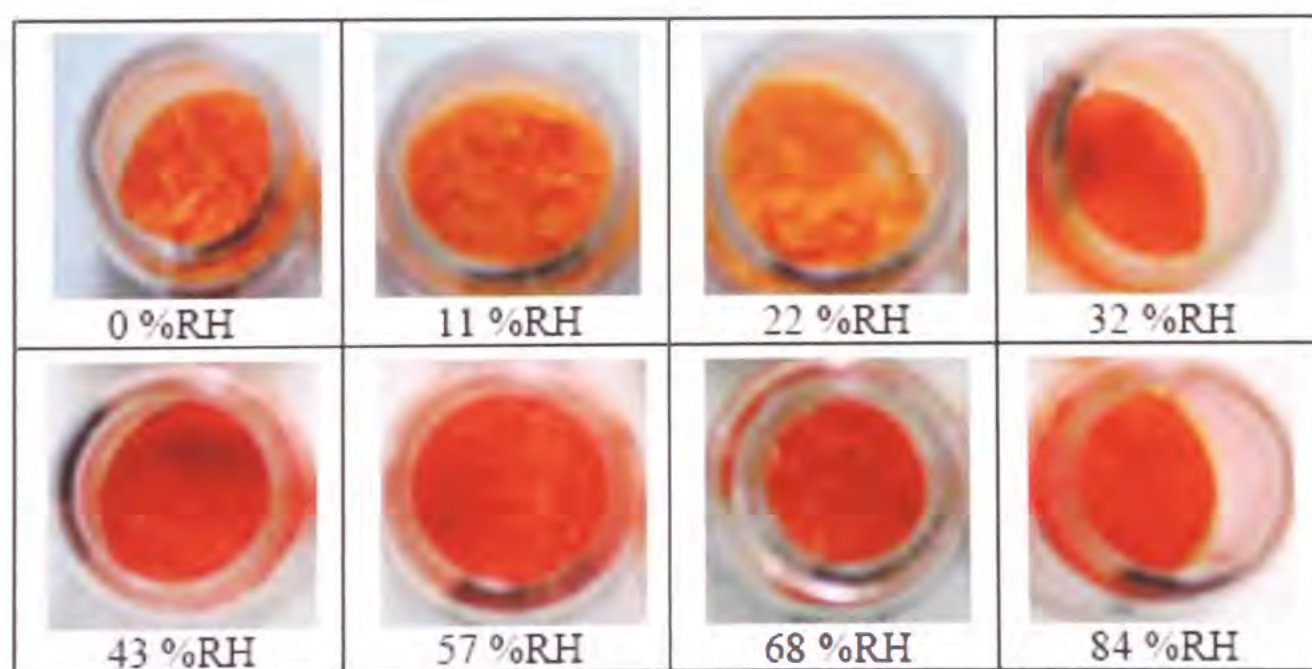
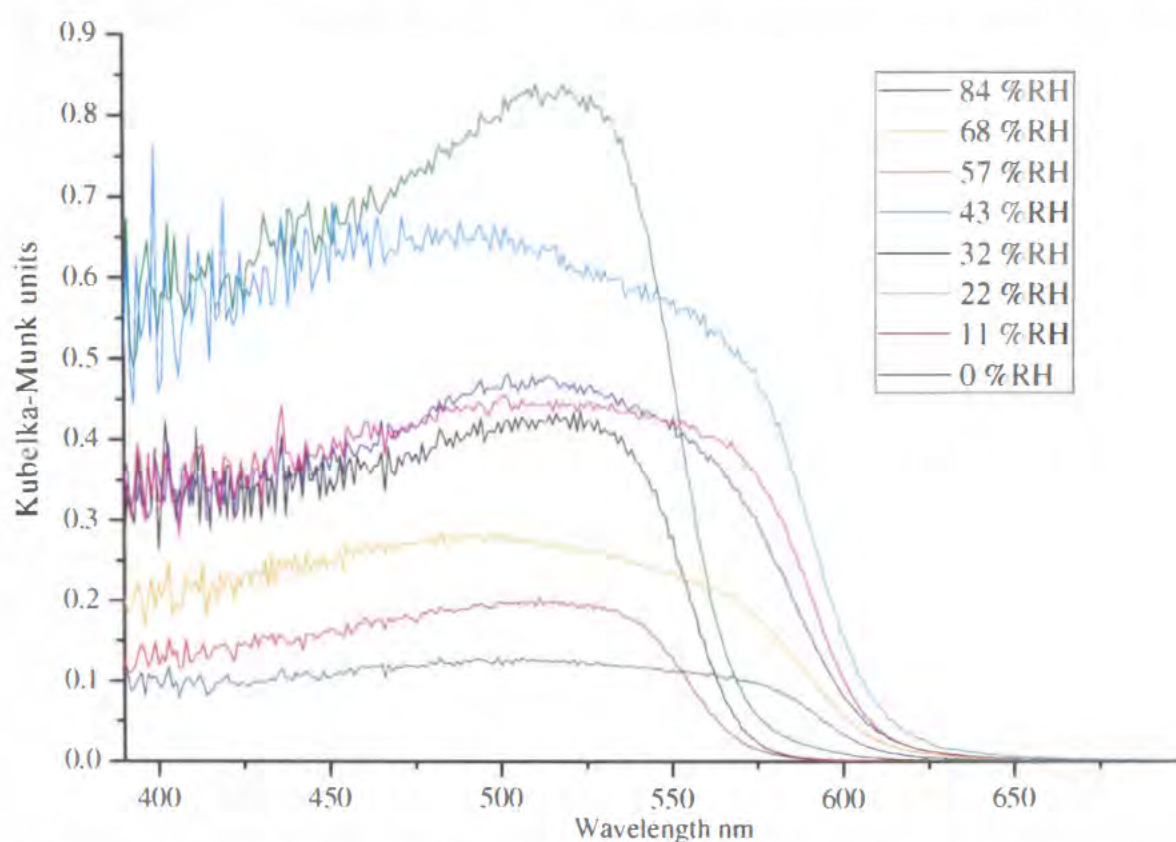
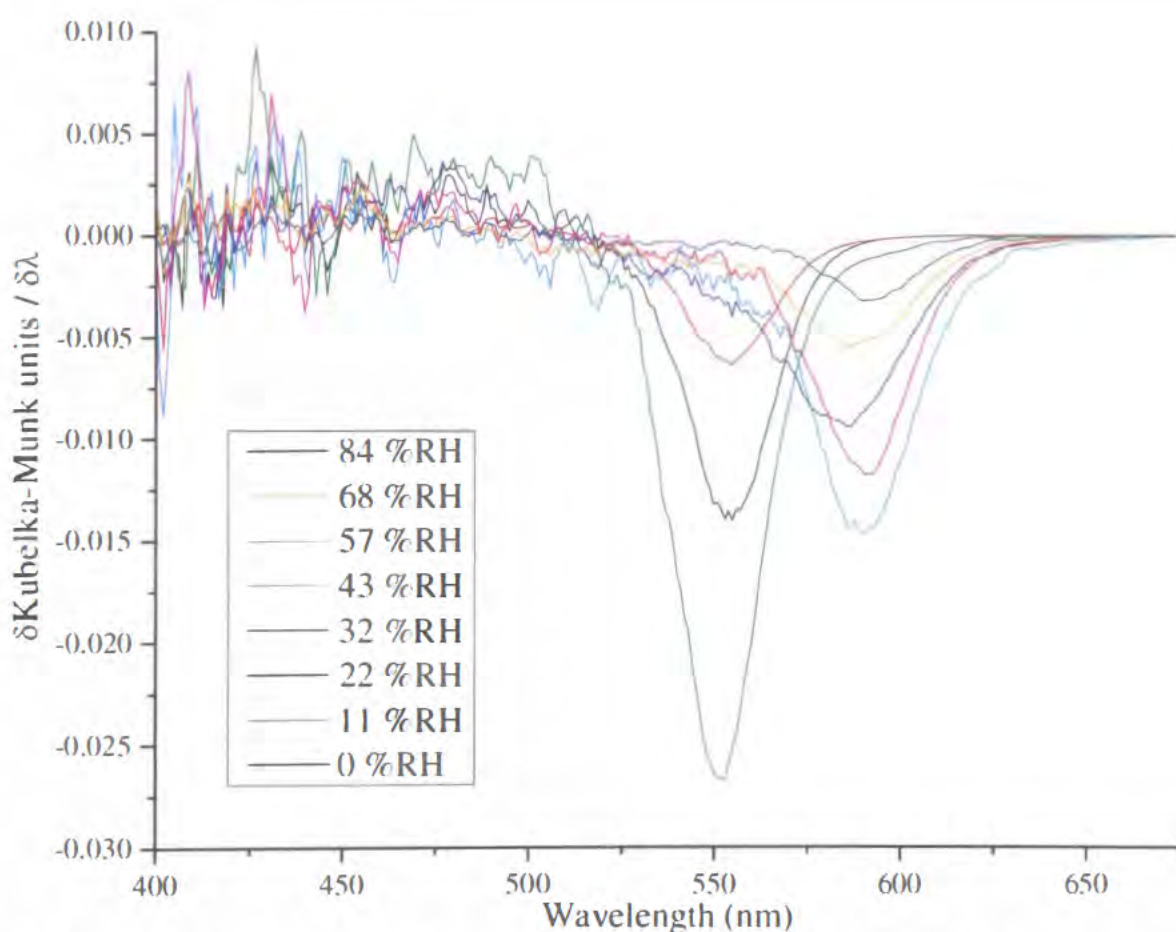


Figure 4.5 Eight samples of sucrose with 0.1 % w/w phenol red after storage for one week at 25° C and controlled %RH.



**Figure 4.6** DRUV spectra of sucrose with 0.1 % w/w phenol red after storage for one week at 25° C and controlled %RH. Spectra collected more than five times; a single, representative result set is shown.



**Figure 4.7** First derivative diffuse-reflectance UV spectra of sucrose with 0.1 % w/w phenol red after storage for one week at 25° C and controlled %RH.

From figure 4.6 it can be seen that the intensity of the reflectance of the three samples maintained at the lowest %RH approach zero at  $\approx 570\text{nm}$ . Samples

stored at 32 %RH and above all approach zero intensity at  $\approx 620\text{nm}$ . As stated earlier, sucrose exists as either an amorphous powder, or an anhydrous crystal. All samples that were placed into the desiccator had been directly removed from the freeze-drier and then split before storage; so all eight samples were identical when first placed into the desiccators. This means that either the samples stored above, or those stored below 32 %RH had undergone a change. It is most likely that the change was the crystallisation from amorphous powder to anhydrous crystalline solid at higher %RH. This was corroborated by the consistency of the samples stored above this humidity. This crystallisation of amorphous sucrose occurring at and above 32 %RH is in agreement with the literature,<sup>[3]</sup> and the two distinct groups observed in the DRUV spectra are strong evidence to suggest that it may be used to determine if an amorphous solid has crystallised. If this is the case, the surface of crystalline and amorphous sucrose may be chemically different, thereby affecting the probe, thus the spectra.

#### 4.4 FT-Raman of sucrose

Figure 4.6 suggests that changes in crystallinity can influence the DRUV spectra. However, it is important to independently verify if the crystallinity is indeed changing, *i.e.* at low %RH amorphous, and at higher %RH crystalline. FT-Raman spectroscopy has been used to distinguish between amorphous and crystalline disaccharides,<sup>[15-17]</sup> including sucrose<sup>[15]</sup> so is an ideal technique to show that the two possible forms of sucrose have indeed been generated. The Raman spectrum for amorphous sucrose is characterised by the absence of sharp, well-defined peaks in the range of  $350 - 1550\text{ cm}^{-1}$ . Crystalline sucrose, in the same range has many well-defined peaks.

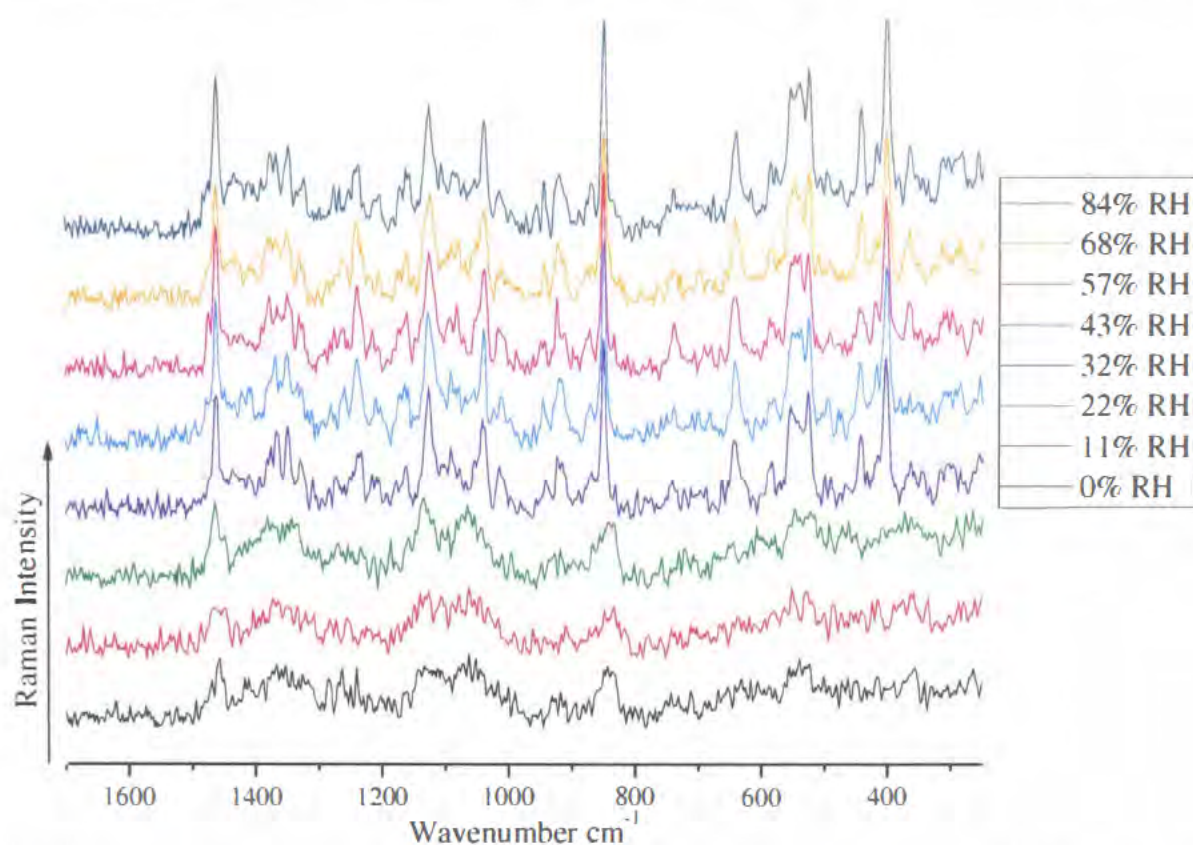


Figure 4.8 FT-Raman spectra of sucrose with 0.1 % w/w phenol red after storage for one week at 25° C and controlled %RH. Spectra collected four times, single result set shown.

It can be seen that from Figure 4.8 that the FT-Raman spectra are in agreement with the DRUV spectra (Figure 4.6). At 32 %RH and above the FT-Raman spectra for the sucrose samples are characterised by sharp, well-defined peaks, characteristic of a crystalline solid.<sup>[15]</sup> For samples below 32 %RH, the peaks in the FT-Raman spectra are broad and ill defined, indicative of an amorphous powder, which is also seen in the literature.<sup>[15]</sup> Importantly there is no fluorescence observed, which would be likely to have occurred with dispersive Raman spectroscopy of a dye by its excitation in the visible range, which indeed will be seen later (section 4.26). Comparing Figure 4.8 with a literature spectrum for amorphous and crystalline sucrose,<sup>[15]</sup> no new peaks (*i.e.* from phenol red) could be observed.

#### 4.5 FT-Raman without dye

The DRUV spectra of sucrose with 0.1% w/w phenol red show that perichromism has some potential to be used to differentiate between crystalline and amorphous sucrose. However it is, still important to determine if phenol red is causing amorphous sucrose to crystallise differently. This can be achieved by

comparing the FT-Raman spectra, DSC thermograms and XRD diffractograms of amorphous and crystalline sucrose with the data for the presence and absence of phenol red. If differences in the data are observed, then the perichromism observed may be being caused by the probe molecule, rather than being a report of the surface of the pharmaceutical excipient.

The DRUV spectra of the pharmaceutical excipient without the probe molecule present (and therefore no chromophore present) will not be comparable to the DRUV spectra with the probe molecule present. A DRUV spectrum of the pharmaceutical excipient would effectively be a reference spectrum although it is not as reflective as the coating of the integrating sphere. This was attempted with sucrose (data not shown) and, was effectively a repeat reference spectrum.

Amorphous sucrose (without the probe) was generated following the same protocol, but without the addition of the probe. After freeze-drying, the sample was split into eight equal portions, and stored alongside the samples with the probe in each desiccator. FT-Raman spectra were taken of these samples after they had equilibrated in the desiccator for the same length of time as samples with the probe (Figure 4.9). All samples were measured under identical conditions *i.e.* concurrently on the same day, to limit possible influences caused by changes in the ambient temperature and humidity of the laboratory.

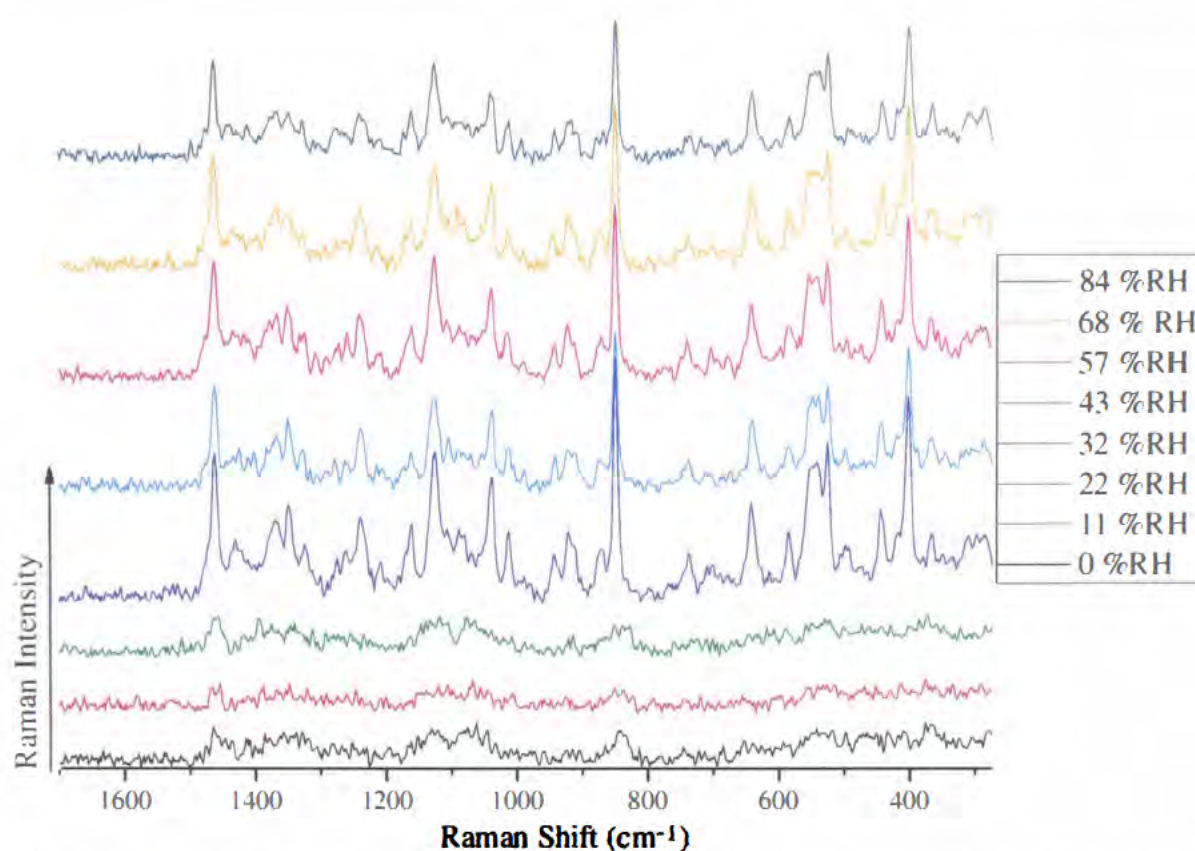


Figure 4.9. FT-Raman spectra of sucrose after storage for one week at 25° C and controlled %RH. Spectra collected four times, single result set shown.

It is apparent from comparing figure 4.9 with figure 4.8 that the FT-Raman spectra of sucrose are not influenced by the presence of the probe molecule. This would suggest that the probe does not affect the crystallinity of the sample. As FT-Raman is a surface technique (irradiation is scattered from the top layers of a sample – admittedly the laser does penetrate a very short, but variable distance into the bulk material, but this is true for all surface techniques) it is not able to measure any possible differences occurring within the bulk material. Both series of FT-Raman spectra agree with literature spectra for sucrose,<sup>[15]</sup> and there does not appear to be any peaks in the spectra for crystalline sucrose that could be caused by the probe, meaning the probe is below the limit of detection by FT-Raman spectroscopy.

#### 4.6 DSC of sucrose

Differential scanning calorimetry is regularly utilised to quantify low-level amorphous content in a predominantly crystalline sample.<sup>[12]</sup> For this to be successful there must be clear differences between the thermograms of an amorphous and a crystalline polymorph of the same material. The thermogram of an amorphous sample is characterised by the presence of a  $T_g$  and a  $T_c$ , which are

always absent from the thermogram of a crystalline solid.<sup>[18]</sup> DSC will give information on what is occurring within the bulk of the material, rather than being surface specific. Although for perichromism the surface of the solid is important in that any change in morphological form will first occur at the surface due to the manufacturing processes, it is important to discover if the presence of the probe molecule is causing any changes anywhere throughout the sample.

Published DSC thermograms<sup>[12]</sup> of sucrose show that both crystalline and amorphous sucrose have a melting endothermic peak ( $T_m$ ) at 180° C. The amorphous samples also have an exothermic peak ( $T_c$ ) at 110° C and an endothermic peak ( $T_g$ ) at 60° C, which is variable, dependent on storage conditions.

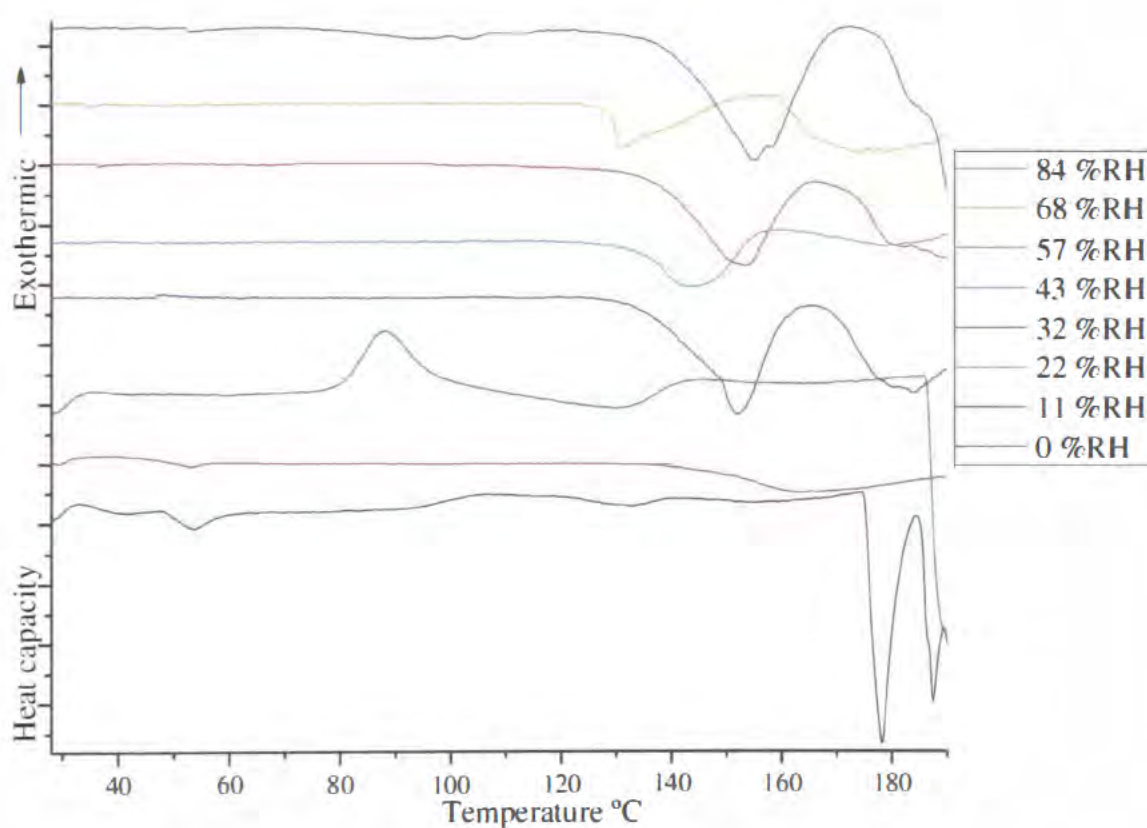


Figure 4.10. DSC thermograms of sucrose with 0.1 % w/w phenol red after storage for one week at 25° C and controlled %RH. Thermograms collected four times, single result set shown.

The DSC thermograms shown in Figure 4.10 are not as clear to interpret as might have been wished for. One possible reason for this might be the presence of the probe molecule, and therefore DSC of sucrose without the probe will also be undertaken to determine if the probe is having a detrimental effect on the DSC thermograms. Nevertheless, from figure 4.10 it can still be observed that samples

stored below 32 %RH have a  $T_g$  or a  $T_c$  present, confirming that they are amorphous. Samples stored at 32 %RH and above have neither a  $T_g$  nor a  $T_c$ , so are crystalline. The crystalline samples, which were stored at higher % RH, show an endothermic peak, onset at *ca.* 130° C, which would correspond to loss of water. For a full listing of peaks, see table 4.1, note decomposition occurs at  $T > 185^\circ \text{C}$ .

Sample	Peaks
0 %RH	48° C = $T_g$ ; 175° C = $T_m$
11 %RH	47° C = $T_g$ .
22 %RH	77° C = $T_c$ ; 185° C = $T_m$
32 – 84 %RH	128-135° C probably loss of water; $\approx 180^\circ \text{C} = T_m$

Table 4.1. Peaks from the DSC thermograms of sucrose with 0.1 % w/w phenol red after storage for one week at 25° C and controlled %RH.

The endothermic peak at  $\approx 130^\circ \text{C}$  in the crystalline samples is interesting, as it shows that the sample probably contains non-essential water, *i.e.* water that is not part of the chemical composition of the sample, and not present in a stoichiometric ratio. This (along with storage at elevated humidity) was the reason that FT-Raman spectroscopy was chosen ahead of IR spectroscopy, as water is well-known to obscure IR spectra,<sup>[19]</sup> but does not affect Raman spectra to the same extent. It also makes sense for the water to be present, as the literature<sup>[3, 20]</sup> reveals that as amorphous sucrose is exposed to elevated humidity, it takes in water, which is then expelled as the anhydrous crystal is formed, suggesting that there must be water present on, or near, the surface of sucrose crystallised in this way.<sup>[21]</sup>

The data from these thermograms compare reasonably well with the literature:<sup>[12]</sup> the  $T_m$  is almost identical – ranging from 175° C to 185° C, whilst the literature value is 186° C. The  $T_g$  that are present are slightly lower than reported, but that is due to the presence of water, which acts as a plasticiser, and reduces  $T_g$ , and is also the reason the  $T_m$  are slightly lower. The only real difference is that the  $T_c$  is considerably lower,  $\approx 40^\circ \text{C}$  than reported in the literature,<sup>[12]</sup> but the sample in

the literature was dry, whereas the  $T_c$  recorded here was for a sample that had been stored at 22 %RH, which could quite easily account for such a large change in  $T_c$ . The other difference is the endothermic peaks at  $\approx 130^\circ\text{C}$ , the cause of which has already been discussed.

#### 4.7 DSC of sucrose without dye

As with FT-Raman, an examination of sucrose that had been prepared identically to the samples already examined, but without the probe molecule was performed to determine if the probe molecule affected the DSC thermograms. The thermograms for sucrose with the probe molecule (Figure 4.10) are not as easy to interpret as either the DRUV or FT-Raman spectra or published thermograms for amorphous<sup>[13]</sup> and crystalline<sup>[12]</sup> sucrose, but they are reproducible, allowing for the comparison of thermograms of sucrose with (Figure 4.10) and without the probe (Figure 4.11).

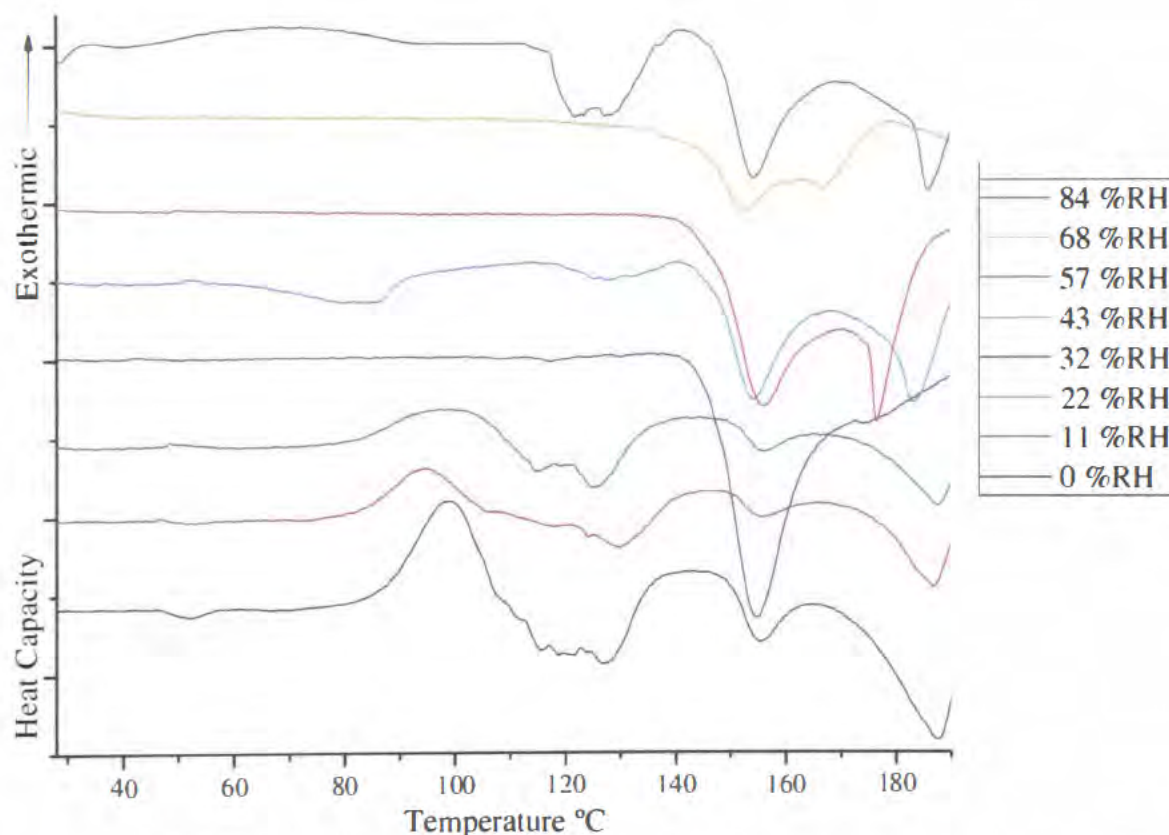


Figure 4.11 DSC thermograms of sucrose after storage for one week at  $25^\circ\text{C}$  and controlled %RH. Thermograms collected four times, single result set shown.

The thermograms of sucrose without the probe are noticeably more difficult to interpret than those with, meaning that the probe molecule is not having a detrimental effect on the thermograms, indeed, just examining these two figures

could lead to the argument that the probe is stabilising the excipient. Repeatability of both series of thermograms in figures 4.10 and 4.11 was poor, suggesting that sucrose itself is a poor, but not impossible, candidate for DSC. However, as can be seen from figure 4.11, samples stored between 0 and 22 %RH have a  $T_c$ , meaning that they are amorphous. Samples stored above 22 %RH have neither a  $T_c$  nor a  $T_g$  and are therefore crystalline. DSC has unfortunately not given particularly high quality data for sucrose; this could be caused by many reasons including sample pans used, the presence or absence of “pin-holes” in the sample lid or water in the sample, scan speed, contamination *et cetera*. The process is slower than both DRUV and FT-Raman spectroscopy, making it less favourable for online monitoring, the results are harder to interpret and the technique destroys the sample. DSC however is a common technique for determining amorphous content and shall be continued for the other excipients, as literature for sucrose includes high quality, informative DSC thermograms.<sup>[12]</sup>

#### 4.8 XRD of sucrose

A common theme in the literature, when presenting a case for a new technique to determine amorphous content, is to highlight the fact that XRD has a poor limit of detection (at least 10% amorphous content is required in some cases) and that the new technique must be an improvement on this<sup>[22]</sup> or another perceived drawback.<sup>[23]</sup> The reason for this is that XRD is considered by the pharmaceutical industry to be one of the most important techniques available for determining polymorph identity, as well as amorphous content, because, as already mentioned, each crystalline polymorph of every material has a unique diffractogram, greatly aiding in identification.

The XRD diffractogram of crystalline sucrose<sup>[24]</sup> reveals that crystalline sucrose is a monoclinic crystal with a cell volume of  $711.5 \text{ \AA}^3$ . However, for the purposes of this work, all that is required from the XRD diffractogram is a qualification between the crystalline form and the amorphous, this should be evidenced by the “halo” effect in the amorphous, and peaks in the crystalline diffractogram.

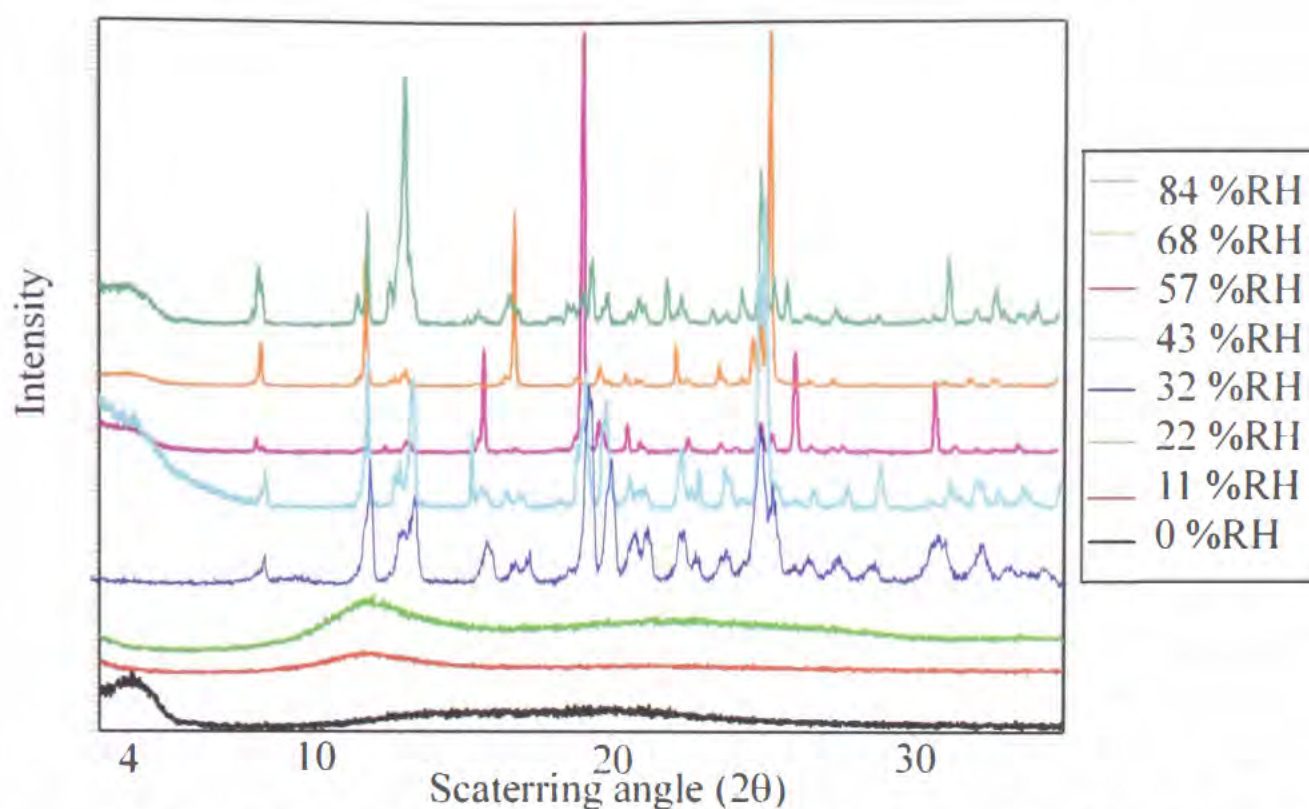


Figure 4.12. XRD diffractograms of sucrose with 0.1 % w/w phenol red after storage for one week at 25° C and controlled %RH. Diffractograms collected once.

The diffractograms for sucrose (above), with the probe molecule present are, at first glance, easily interpreted. Samples stored at 22 %RH and below all exhibit the “halo effect”, and have no peaks, therefore these samples are amorphous. Samples stored at 32 %RH and above all have sharp, well-defined peaks characteristic of a crystalline material. However, it appears that both the 43 %RH and the 84 %RH have a possible halo below 7° 2θ. A possible reason for this is sample contamination (otherwise it would have been expected in all of the crystalline samples and not the most and least exposed to elevated humidity) A more probable explanation for this observation occurs during sample preparation, discussed below.

Closer examination of figure 4.12 reveals that some of the peaks have shifted between diffractograms, in some cases by up to 1° (notably between 15–18° and above 25°). This is unexpected, as the sample identity is known: sucrose with 0.1% w/w phenol red. The probe is present at quantities that are a thousand-fold less than the sucrose, and at a uniform concentration throughout all samples, suggesting that any change to the peak positions should also be uniform. It is also

very unlikely to be caused by different polymorphs, as sucrose has only one crystalline polymorph. The sample was rotated meaning preferred orientation effects are unlikely to have arisen. The cause of the changes in peak position must therefore be due to one of three possible factors: 1) the presence of the probe affecting different samples differently, 2) the change in humidity causing the sample to behave differently when being prepared for XRD, or 3) the sample preparation for XRD requires the sample to be ground into a fine powder. This will cause the generation of amorphous regions on the surface of the sample, which theoretically, could cause different ratios of crystal faces between samples. However, this would be more likely to affect peak height (similarly to preferred orientation effects) than peak position. Grinding for preparation of XRD samples may be a factor in further XRD diffractograms (sections 4.24 and 5.4)

Another interesting phenomenon in figure 4.12 is the peak shapes for the sample at 32 %RH are wider, and less well defined than for the sucrose samples stored at higher %RH. This is also true, to a lesser extent, for the sample stored at 43 %RH. This may be being caused by the fact that the  $T_g$  for sucrose in this humidity range is very close to room temperature (25° C). This would mean that crystallisation will be a lot slower, and either the sample has not fully crystallised (very unlikely given other data) or a change in sample that has not been detected by the other techniques has occurred, smaller crystallites are also possible. Both could be caused by sample preparation.

#### **4.9 XRD of sucrose without dye**

The XRD diffractograms for sucrose with 0.1 %w/w phenol red show that storage at 22 %RH (and 25° C) will maintain an amorphous sample of sucrose. Storage at 32 %RH and above will cause the sample to crystallise within seven days – the greater the relative humidity (above 32 %RH) the faster crystallisation occurs. Due to all materials having a unique diffractogram, XRD is an ideal candidate to determine if the presence of the probe molecule has caused a change to the sample. The diffractograms of the crystalline samples of sucrose with probe (Figure 4.12) all differ slightly, which although unlikely, could be a result of the probe, although it is present at a concentration below the usual limit of

detection for XRD. The diffractograms of sucrose, without the probe molecule, but otherwise prepared and stored identically, are shown in Figure 4.13 to determine if the probe has had any bearing on the small peak positional changes in the XRD diffractograms with the probe (Figure 4.12).

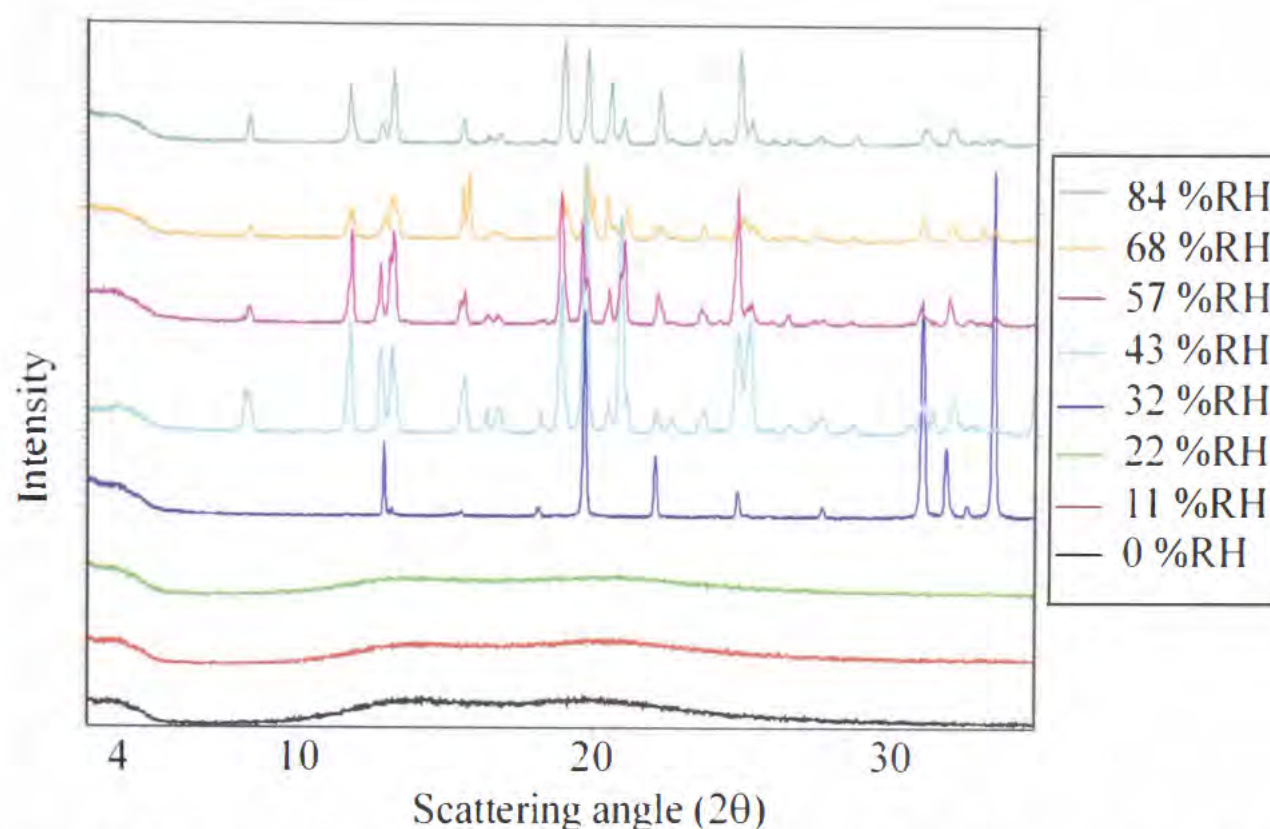


Figure 4.13. XRD diffractograms of sucrose stored for one week at 25° C and controlled %RH. Diffractograms collected once.

Firstly, the general behaviour of the diffractogram pattern is the same for samples of sucrose without the probe as it is for those with, *i.e.* storage at 22 %RH and below has maintained amorphous sucrose and at 32 %RH and above has caused crystallisation to occur. The individual diffractograms for sucrose without the probe (Figure 4.13) again slightly differ from one another, with the exception of the sample stored at 32 %RH which is considerably different. This means that the slight differences observed between diffractograms in Figure 4.12 are not caused by the presence of the probe. The reason for the difference in the diffractogram for the sample stored at 32 %RH in Figure 4.13 is not known, but possibilities include that the sample was subject to preferred orientation, that it was partially amorphous, or, two unlikely possibilities, the samples were contaminated or an intermediate morphological form occurring as sucrose crystallises into its well described crystalline form.<sup>[22]</sup>

#### 4.10 Summary of sucrose.

It has proven possible to prepare amorphous sucrose, both with and without a perichromic probe incorporated by freeze-drying an aqueous solution of sucrose. The amorphous product has then been stored at different %RH, and constant temperature for one week. This allows for amorphous sucrose to either remain amorphous, or crystallise, depending on the relative humidity of the desiccator. The probe molecule does not appear to be exerting any measurable influence on the sucrose (Figures 4.8 to 4.13). The four techniques used give good agreement for each sample, as shown in Table 4.2.

%RH	DRUV	FT-Raman		DSC		XRD	
	With Probe	With Probe	Without Probe	With Probe	Without Probe	With Probe	Without Probe
0	Am	Am	Am	Am	Am	Am	Am
11	Am	Am	Am	Am	Am	Am	Am
22	Am	Am	Am	Am	Am	Am	Am
32	Cryst	Cryst	Cryst	Cryst	Cryst	Cryst	Cryst
43	Cryst	Cryst	Cryst	Cryst	Cryst	Cryst	Cryst
57	Cryst	Cryst	Cryst	Cryst	Cryst	Cryst	Cryst
68	Cryst	Cryst	Cryst	Cryst	Cryst	Cryst	Cryst
84	Cryst	Cryst	Cryst	Cryst	Cryst	Cryst	Cryst

Table 4.2. Summary of results for sucrose by technique and storage %RH.

Am = Amorphous; Cryst = Crystalline.

The addition of a probe molecule appears to allow the observation of perichromism. Amorphous sucrose has a different DRUV spectrum than anhydrous crystalline sucrose (Figures 4.6 and 4.7). It should be noted that this is, so far, only for (effectively) 100% amorphous and 100% crystalline material. Section 5.3 will detail amorphous content determination of amorphous sucrose in a predominantly crystalline material. Before this, it is necessary to discover if perichromism is a measure of the surface of the excipient, or a property of the probe.

Although not shown in the DRUV spectra so far presented, the range of the wavelengths that can be examined reach into the near-IR range, up to 1100 nm. The start of the range where data is useful is at  $\approx 380$  nm (the start of the visible range of the electromagnetic spectrum). When examining the spectra for sucrose, an interesting development was noticed above 1000 nm, as shown in Figure 4.14.

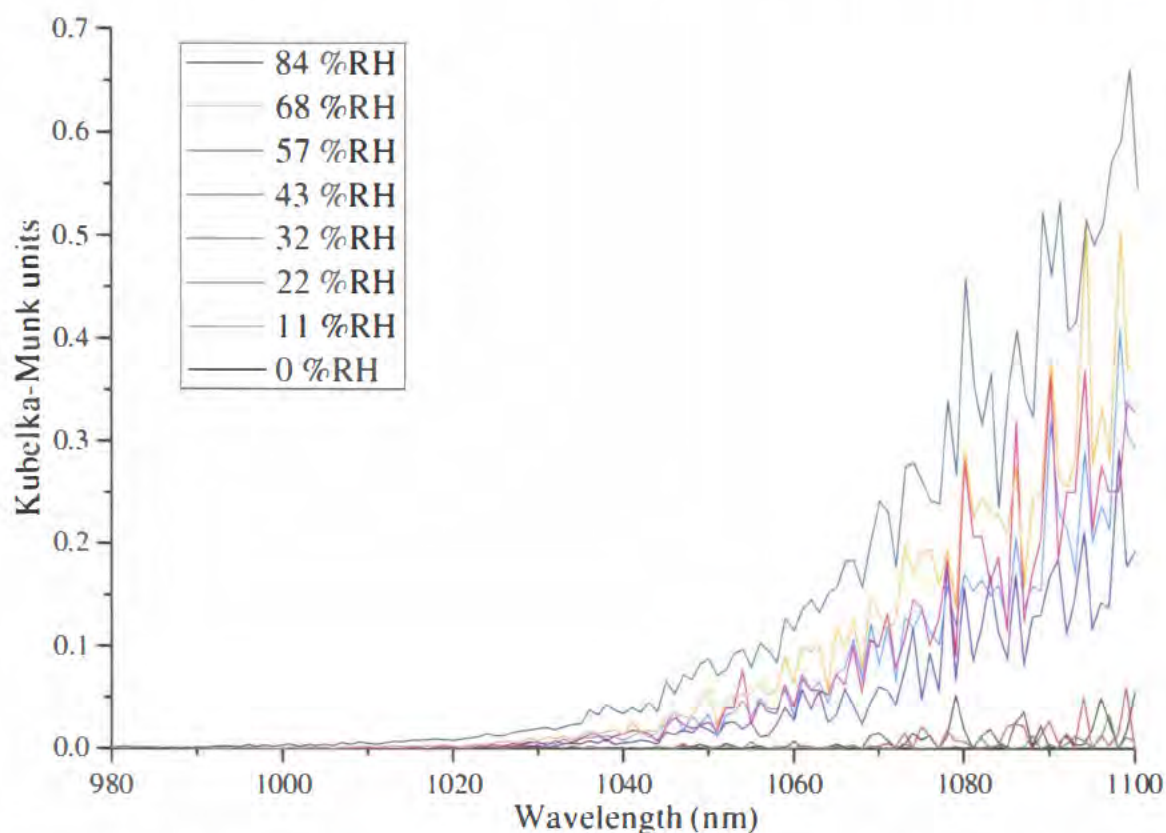


Figure 4.14. DRUV spectra of sucrose with 0.1 % w/w phenol red after storage for one week at 25° C and controlled %RH.

It can clearly be seen from Figure 4.14 that the amorphous samples and the crystalline samples divide into two separate groups. Initially, this was considered an interesting, but not repeatable occurrence, but as more data was gathered, it was noticed that this occurs in every DRUV spectrum where a disaccharide has been stored at different %RH, and in most cases, like figure 4.14, the intensity of the increase is proportional to the %RH. On searching the literature, no explanation for this was discovered. However, the possible relationship to humidity is very intriguing, being roughly in the middle of the near infra-red region (780-1400nm) of the electromagnetic spectrum, but not being reflected in the FT-Raman – even though the laser used operates in this region (1064nm).

It was decided to concentrate on only the visible region because that is why the probe was originally added. It would be very interesting, given more time, to investigate if this region allows for a measure of how relative humidity affects

solid surfaces, possibly measuring how “wet” the sample is. See future work (section 6.2) for how this area could be further explored.

#### 4.11 DRUV of lactose

Having observed perichromism in response to the crystallisation of sucrose, it was decided to ascertain whether a more complex polymorphic system would yield similar results. Lactose has more polymorphs than sucrose, existing as an amorphous powder or potentially four crystalline solids.<sup>[17, 25]</sup>  $\alpha$ -lactose monohydrate ( $L\alpha \cdot H_2O$ ),  $\beta$ -lactose ( $\beta L$ ) anhydrous and one stable form of  $\alpha$ -lactose anhydrous, ( $L\alpha_S$ ) and, potentially, one unstable, hygroscopic form ( $L\alpha_H$ ). There is some debate whether there really are two anhydrous forms of  $\alpha$ -lactose, however to produce either requires a dehydration of  $L\alpha \cdot H_2O$  by either a solvent or an elevated temperature. All samples (in this work) have been stored under controlled relative humidity and temperature, and as lactose should only crystallise at elevated humidity it is expected that the availability of water will cause lactose to crystallise as  $L\alpha \cdot H_2O$ . Despite (or perhaps, because of) the range of polymorphic forms of lactose available, it is still a common choice for determination of amorphous content.<sup>[13, 17, 20, 22, 25-37]</sup>

The probe molecule was added to an aqueous solution of lactose, which is then freeze-dried to produce the amorphous powder (method 2). This is then stored in the desiccators at the same controlled %RH and temperature as that used for sucrose with the aim of forcing some of the lactose (*i.e.* that stored at high %RH) to crystallise. A visual difference in the samples after storage for one week was again observed (figure 4.15). The DRUV spectra of the lactose samples that had been stored in these desiccators for seven days can be seen in figure 4.16 and the first derivatives in figure 4.17.

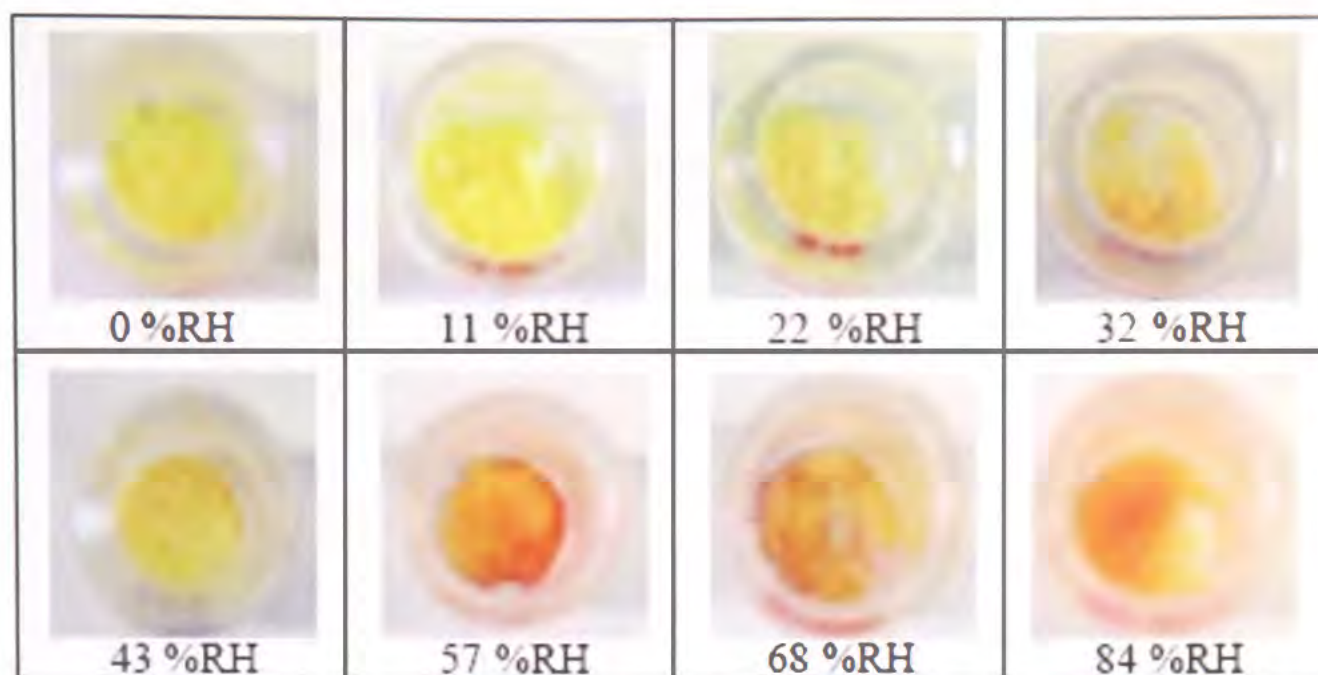


Figure 4.15 Eight samples of lactose with 0.1 % w/w phenol red after storage for one week at 25° C and controlled %RH.

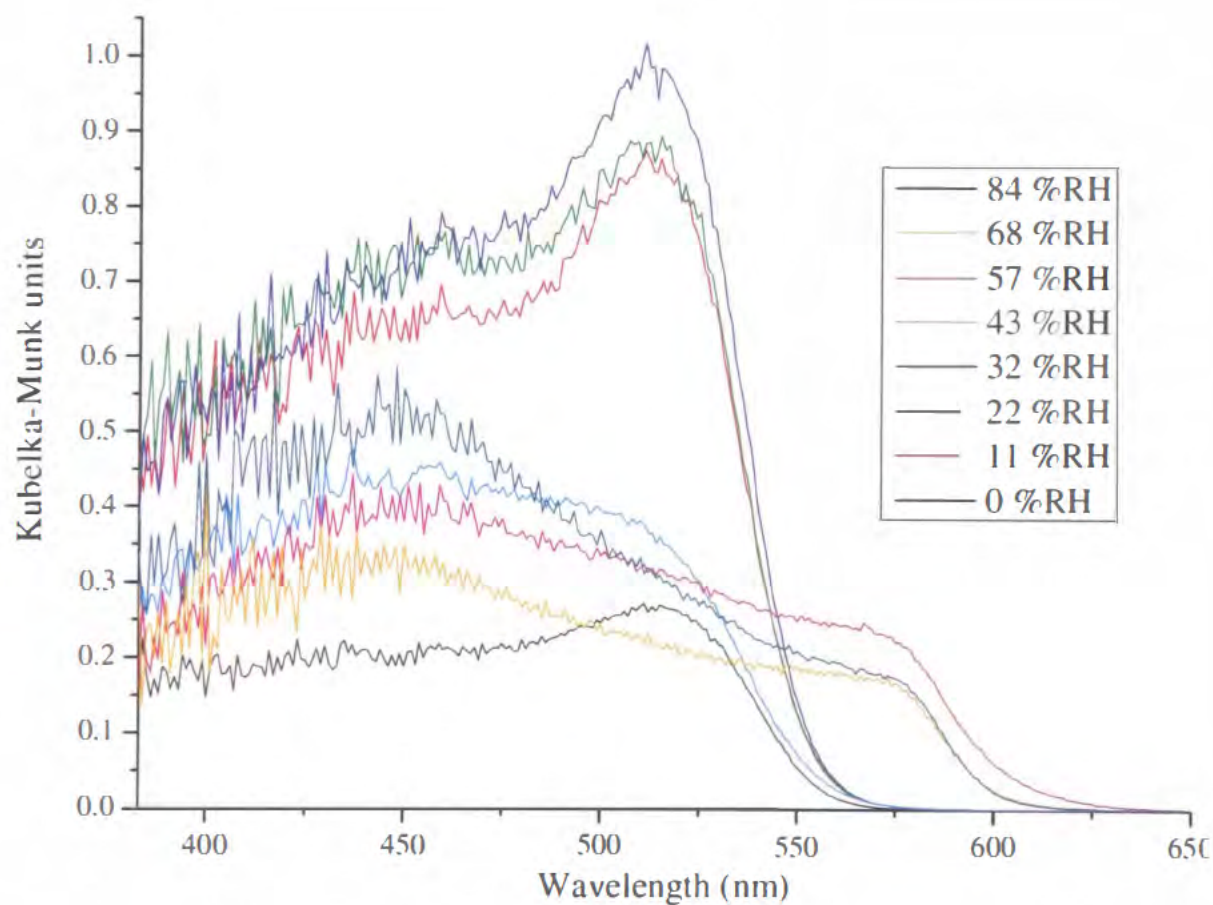


Figure 4.16 DRUV spectra of lactose with 0.1 % w/w phenol red after storage for one week at 25° C and controlled %RH. Spectra collected four times, single result set shown.

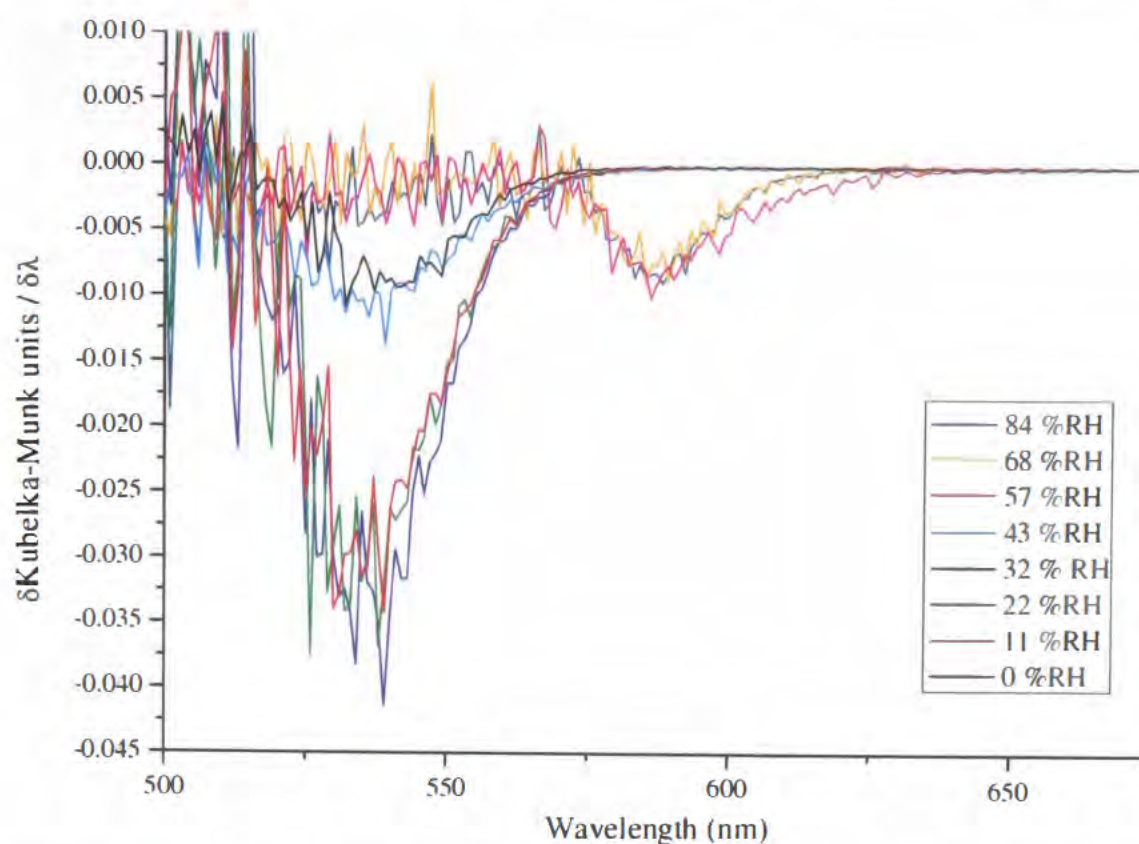


Figure 4.17 First derivative DRUV spectra of lactose with 0.1 % w/w phenol red after storage for one week at 25° C and controlled %RH.

The DRUV spectra of lactose reveal that samples stored at 43 %RH and below have one peak, at 515 nm. The samples stored at 57 %RH and above have two peaks, the first at 448 nm and the second at 573 nm. This grouping agrees with the visual grouping that could be made from figure 4.15. The fact that the samples that have a peak at 515 nm include those stored at very low relative humidity suggests that this peak is characteristic for amorphous lactose - this in turn suggests that the samples with a peak at 573 nm are crystalline, although the exact nature of the polymorph cannot be determined by DRUV alone, and will be discussed further in the following sections.

The peak position of 515 nm for amorphous lactose is identical to that for amorphous sucrose (Figure 4.6). It will be discovered later in this work (section 4.33) whether all amorphous samples give the same spectra (note that this is different to the spectra of phenol red, section 5.2) or if only amorphous disaccharides give the same DRUV spectra. Either way trehalose, another disaccharide with the same chemical formula is predicted to have exactly the same DRUV spectra for the *amorphous* polymorph, raffinose, a trisaccharide, may or may not be different.

Crystalline lactose, having two peaks, one at 448 nm and the other at 573 nm differs slightly from crystalline sucrose (for a full comparison see figures 4.38 and 4.39). This is because there is now long-range order present, and the samples are now structurally different.

#### 4.12 FT-Raman of lactose

There are, as discussed for sucrose, several techniques that will be used to identify the crystalline polymorph of each excipient, and in particular the polymorph of lactose that has resulted in the DRUV spectra observed in figure 4.16. There are significant differences in the Raman spectra (Figure 4.18), between 200 and 1500  $\text{cm}^{-1}$  of the three polymorphic forms of lactose  $\text{L}\alpha\cdot\text{H}_2\text{O}$ ,  $\beta\text{L}$  and  $\text{L}\alpha_{\text{S}}$ .<sup>[17]</sup>  $\text{L}\alpha_{\text{H}}$  gives poor reproducibility and spectral resolution.<sup>[17]</sup> Characteristic Raman bands for each of the three polymorphs are:  $\alpha\text{L}_{\text{mono}}$  at 355, 375, 475 and 1086  $\text{cm}^{-1}$ ;  $\beta\text{L}$  at 359, 437 and 1115  $\text{cm}^{-1}$ ;  $\text{L}\alpha_{\text{S}}$  at 485 and 875  $\text{cm}^{-1}$ , although this form looks similar to  $\alpha\text{L}_{\text{mono}}$  with some amorphous material causing lower peak intensities.<sup>[17]</sup>

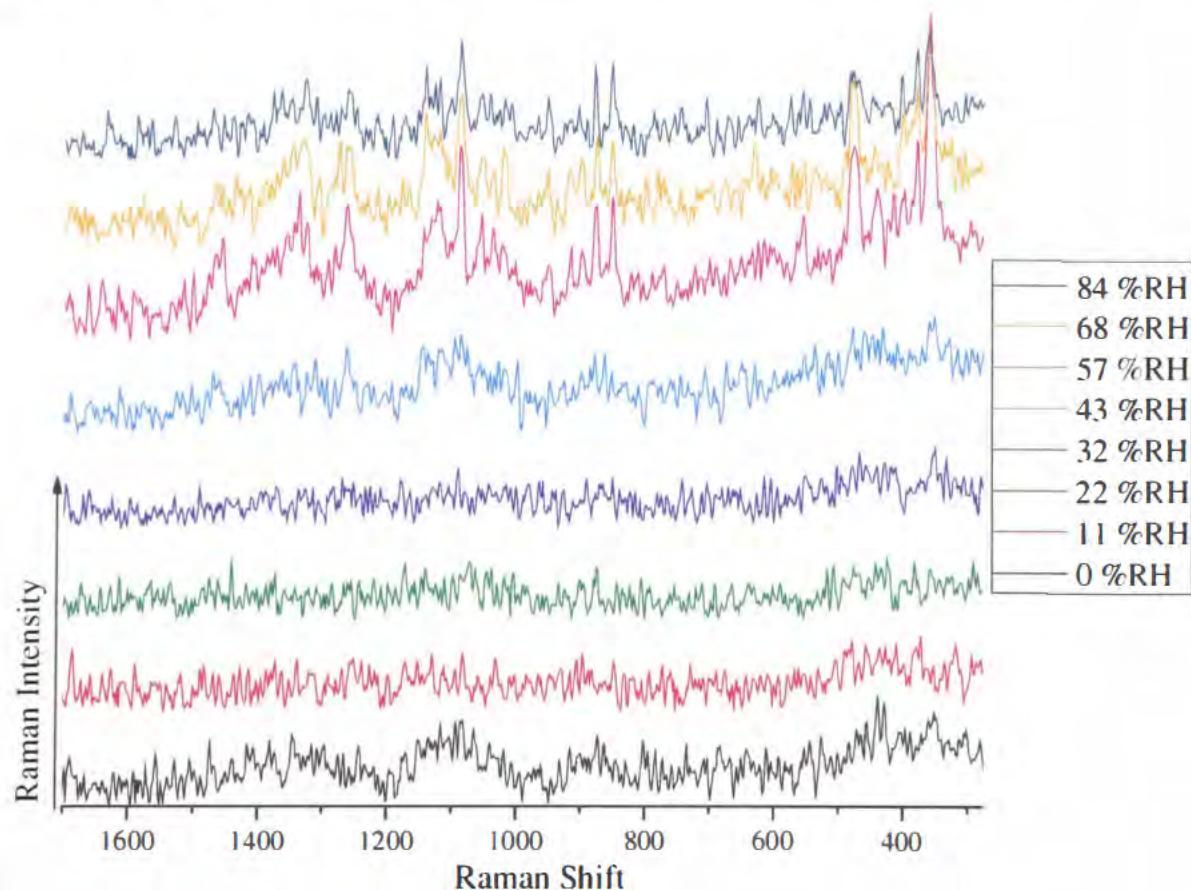


Figure 4.18 FT-Raman spectra of lactose with 0.1 % w/w phenol red after storage for one week at 25° C and controlled %RH. Spectra collected four times, single result set shown.

From the peaks that are unique in the Raman spectra of lactose, it is very hard to determine which polymorph of crystalline lactose is present. This is because the unique peaks occur at wavenumbers very close to other, non-unique peaks. Each spectrum (57-84 %RH) contains a large peak at  $475\text{ cm}^{-1}$  and  $1086\text{ cm}^{-1}$  that are indicative of  $\alpha$ -lactose monohydrate. The presence of both of these peaks eliminates the possibility of the identity of the sample being any other polymorphic form. The identification of all three crystalline samples as the same polymorph agrees with the DRUV spectra of the samples, which show two groupings, one for amorphous lactose and the other for (crystalline)  $\alpha$ -lactose monohydrate.

The two amorphous disaccharides have nearly identical DRUV spectra, but the two different crystalline materials have slightly different DRUV spectra. It is suggested that this change in the crystalline spectra may be due to a property on the surface of the crystalline disaccharide, one possible difference is surface acidity, another is the state of hydration. This will be investigated by the DRUV of trehalose which can exist as a dihydrate crystal (section 4.19), and raffinose, which can exist as a pentahydrate crystal (section 4.27).

#### **4.13 FT-Raman of lactose without dye**

To ascertain that the addition of the probe molecule has had no influence on the crystallisation of amorphous lactose, samples of lyophilised lactose, without the probe molecule, were also prepared. These were stored alongside the samples with the probe molecule inside the desiccators, and then analysed by the same techniques. The FT-Raman spectra of these samples can be seen in figure 4.19.

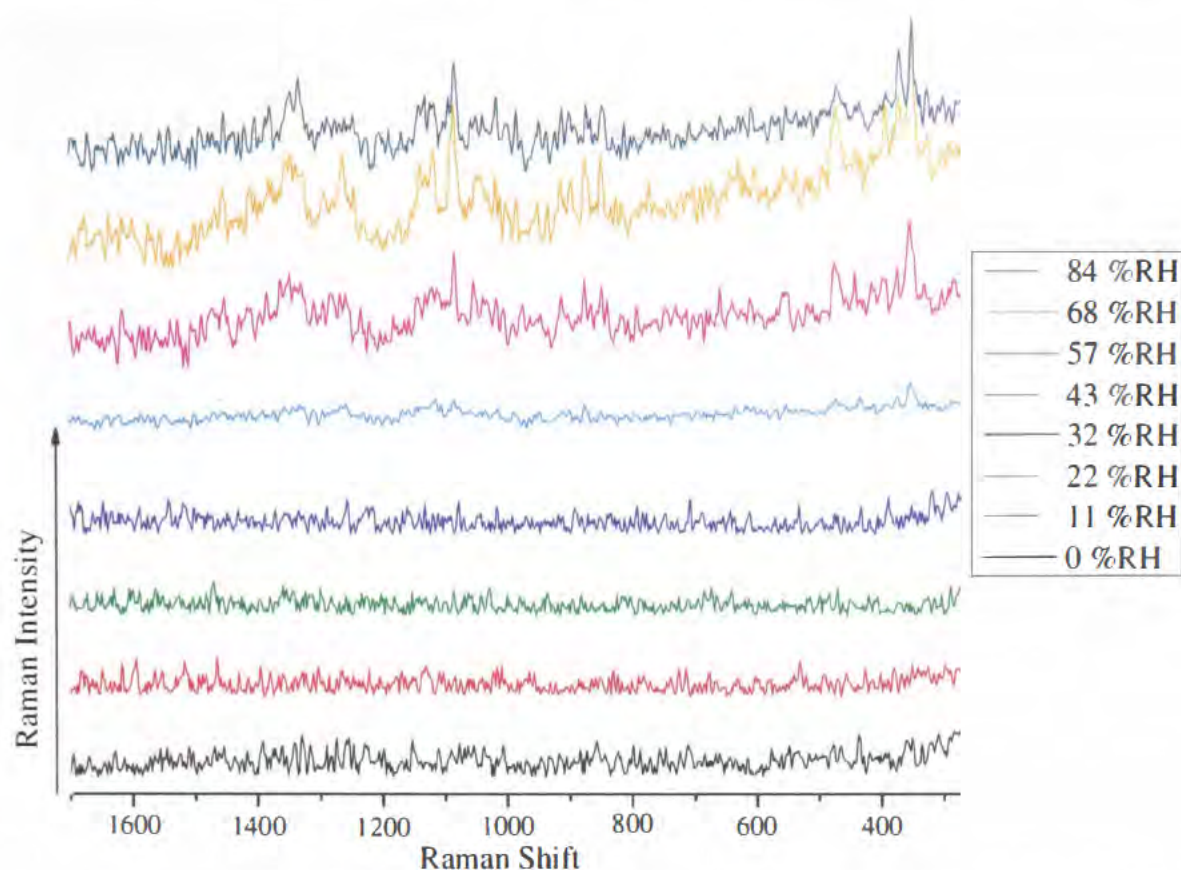


Figure 4.19 FT-Raman spectra of lactose after storage for one week at 25° C and controlled %RH. Spectra collected four times, single result set shown.

The spectra of the crystalline polymorphs of lactose in figure 4.19 also have peaks at 475 and 1086  $\text{cm}^{-1}$ . The fact that all major peaks are unchanged between figures 4.18 and 4.19, is suggestive that the presence of the probe molecule is not being detected by FT-Raman spectroscopy, nor is it affecting the crystallisation of amorphous lactose.

#### 4.14 DSC of lactose

The third technique used to identify the polymorph of lactose present in the crystalline samples is differential scanning calorimetry. This had the added aim of determining how effective DSC is at distinguishing between amorphous and crystalline material, after the poor quality of the thermograms of sucrose (Figures 4.10 and 4.11). The DSC thermograms of each form of lactose are also different, as detailed below. Amorphous lactose exhibits a  $T_g$  and a  $T_c$  (dependent on storage %RH and temperature) that the crystalline forms do not. The (endothermic)  $T_g$  for amorphous lactose stored at 0 %RH and 25° C occurs at 93° C and the (exothermic)  $T_c$  at 154° C.<sup>[13]</sup> If amorphous lactose is stored at 33 %RH and 25° C then the  $T_g$  and  $T_c$  occur at 27° C and 72° C respectively.<sup>[13]</sup>  $\alpha$ -lactose

monohydrate melts at 211° C, anhydrous  $\alpha$ -lactose melts slightly higher (215° C)<sup>[29]</sup> and  $\beta$ -lactose melts at 220° C.<sup>[29]</sup>  $\alpha$ -lactose monohydrate also has an exothermic peak that the anhydrous form does not have at *ca.* 140° C that is attributed to the loss of the water from the monohydrate, hence both forms of  $\alpha$ -lactose melt at the same temperature.<sup>[29]</sup> DSC thermograms for lactose can be seen in figure 4.20. The peaks present are also displayed in table 4.3.

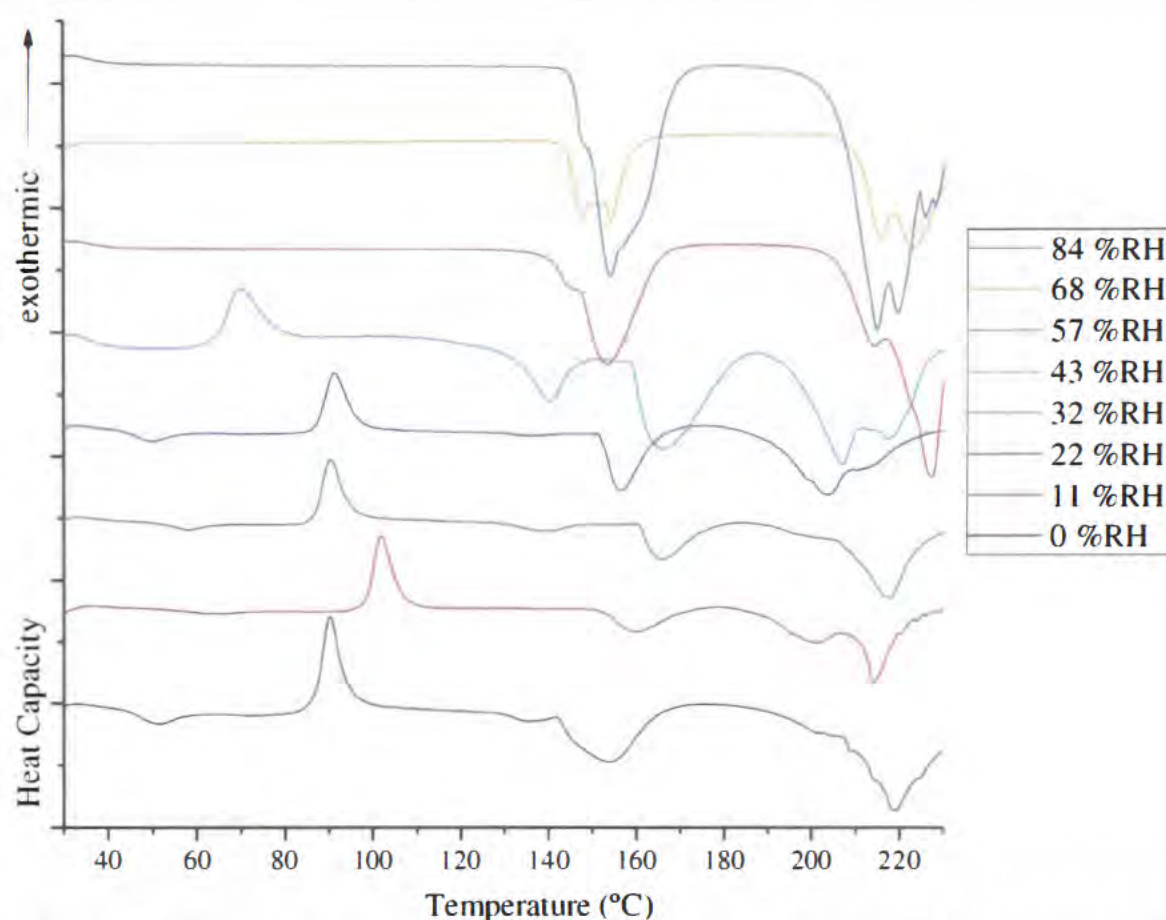


Figure 4.20 DSC thermograms of lactose with 0.1 % w/w phenol red after storage for one week at 25° C and controlled %RH. Thermograms collected four times, single result set shown.

%RH	$T_g$ (°C)	$T_c$ (°C)	Dehydration (°C)	$T_m$ (°C)
0	43.1	81.2	142.4	207.3
11	57.9	94.2	149.7	209.7
22	54.3	83.8	160.3	207.6
32	43.3	84.4	150.6	*
43	-	60.0	130.8 and/or 159.1	*
57	-	-	138.4	204.8
68	-	-	142.4	210.6
84	-	-	142.9	204.2

Table 4.3. Peaks in the thermograms of lactose. \* = Degrades at *ca.* 195 ° C

The result of the DSC of lactose is in agreement with the conclusions drawn from the DRUV and FT-Raman spectra. Samples stored at 43 %RH and below have remained amorphous, as evidenced by the presence of either a  $T_g$  and/or a  $T_c$  in the thermogram. The three samples of lactose that have been stored above 43 %RH are crystalline, as they only contain a  $T_m$  (and a dehydration peak). According to peaks in the FT-Raman spectra, the three samples that have crystallised, have formed  $\alpha$ -lactose monohydrate. The DSC thermograms, having very similar dehydration and melting temperatures appear to be of the same polymorph. The literature contains melting points for each polymorph of lactose, and the thermograms of the samples present here, have a melting point very similar to that of  $\alpha$ -lactose (anhydrous and monohydrate), 211° C.<sup>[29]</sup>  $\beta$ -lactose melts at 220° C;  $\alpha$ -lactose anhydrous at 215° C and amorphous lactose melts at 230° C.<sup>[29]</sup> However, exposure to relative humidity will decrease all of these expected melting points as water acts as a plasticiser – indeed the  $T_m$  for amorphous lactose can be reduced by over 20° C by “rehydration for 30 hours”.<sup>[29]</sup> Hence the slightly lower values reported for the melting temperatures here.

The DSC thermograms of lactose show decomposition as the sample melts. The fact that neither the  $T_g$  nor the  $T_c$  decrease as the storage %RH increases from 0 %RH to 11 %RH is surprising. Theoretically water acts as a plasticiser, and lowers both the  $T_g$  and the  $T_c$ . It was earlier stated (section 3.4.2) that the 0 %RH desiccator was probably not 0 %RH but *ca.* 1 %RH, but the DSC results suggest that it may be a lot higher. However, all experiments show that this desiccator is maintained at a suitably low relative humidity to maintain amorphous lactose (and sucrose), and not to allow crystallisation to occur, the hygrometers maintained that the % RH of this desiccator never surpassed  $0.9 \pm 2$  % RH.

All samples show a dehydration exotherm. This was not expected for the amorphous samples, but has almost certainly arisen from non-essential water accumulating on the sample over the seven days where the sample equilibrates to the artificial environment within the selected desiccator.

#### 4.15 DSC of lactose without dye

The surprising result for the DSC of lactose without the probe molecule (Figure 4.21) is that even though each sample was stored alongside the lactose with the probe molecule, the 0 %RH sample appears to be considerably drier than the sample that had the probe stored in it, as evidenced by the considerably smaller dehydration exotherm at *ca.* 130° C. Otherwise the thermograms for lactose with, and without, the probe molecule show melting temperatures, glass transitions, crystallisation temperatures and dehydration exotherms occurring at approximately the same temperature for samples stored at the same humidity, and that the samples that have crystallised, have probably crystallised as  $\alpha$ -lactose monohydrate, as determined by the melting temperature and dehydration exotherms.

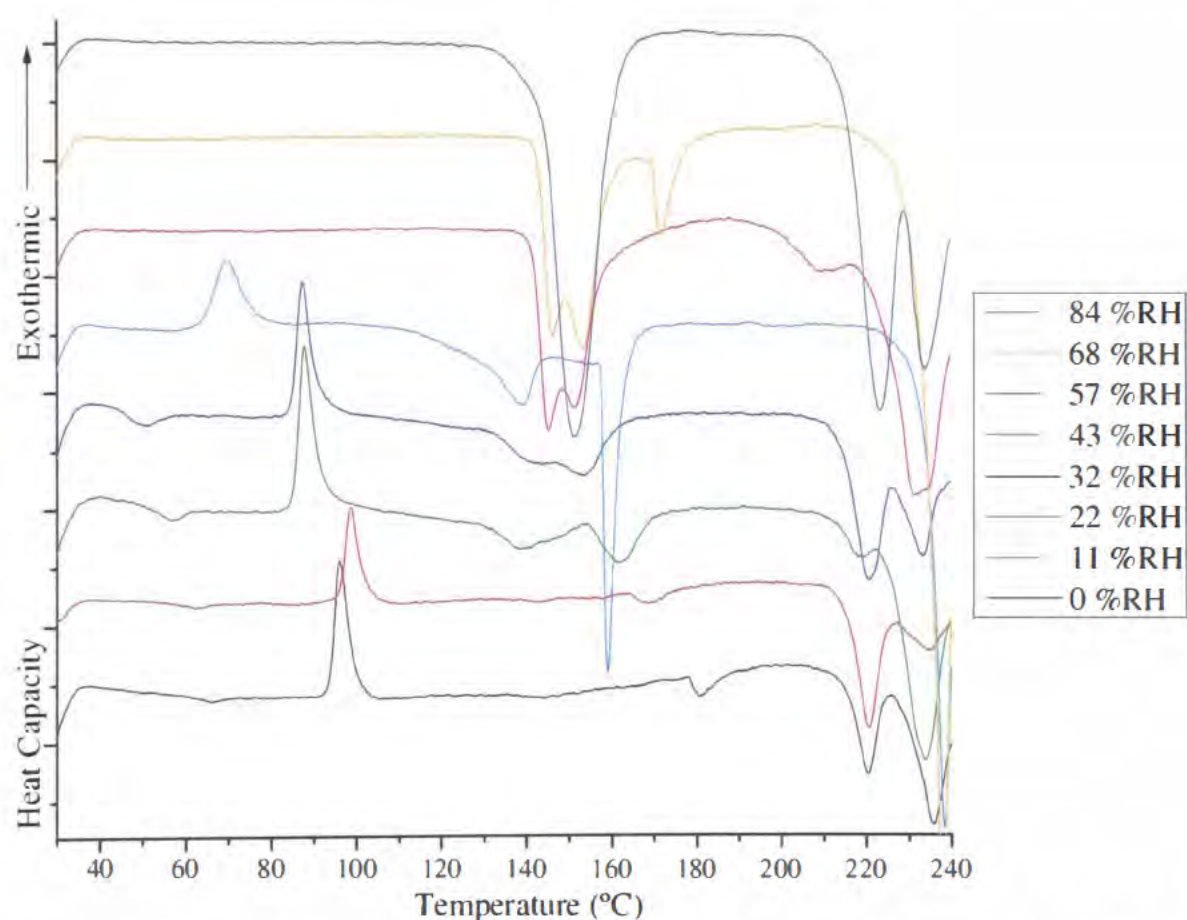


Figure 4.21 DSC thermograms of lactose after storage for one week at 25° C and controlled %RH. Thermograms collected four times, single result set shown.

#### 4.16 XRD of Lactose

Powder x-ray diffraction was performed on the eight samples of lactose with phenol red (Figure 4.22). The literature XRD diffractograms of lactose show that  $\alpha$ -lactose monohydrate,  $\beta$ -lactose anhydrous and the hygroscopic  $\alpha$ -lactose anhydrous all crystallise with monoclinic unit cells<sup>[17]</sup> and the stable  $\alpha$ -lactose anhydrous form apparently crystallises with a triclinic unit cell.<sup>[17]</sup> The diffractograms of the different hydrates of  $\alpha$ -lactose are similar, differing more in peak intensity than position, but a characteristic peak for  $\beta$ -Lactose is at  $10.5^\circ$   $2\theta$ .<sup>[17]</sup>

Even though FT-Raman and DSC could both identify the crystalline polymorph of lactose produced as  $\alpha$ -lactose monohydrate, the FT-Raman spectra are a little noisy, and the intensities quite weak. Furthermore the DSC thermograms have quite poor peak shapes that do not perfectly agree with the literature, and identification from  $T_m$  alone is a little ambiguous. XRD should not suffer from either of these problems. However, as can be observed in figure 4.22, even the XRD of lactose with the probe molecule contains a worse signal-to-noise ratio compared to the XRD of sucrose (with the probe). At first, this was thought to be possible contamination of the sample, but on repeating the experiment, the quality of the spectra, thermograms and diffractograms did not noticeably change. It is interesting that the DRUV spectra for lactose show a greater difference between the amorphous and crystalline samples, as compared to sucrose, even though there was only one polymorph of lactose detected. It is impossible, as yet, to say how well DRUV spectroscopy might distinguish between two crystalline polymorphs of lactose.

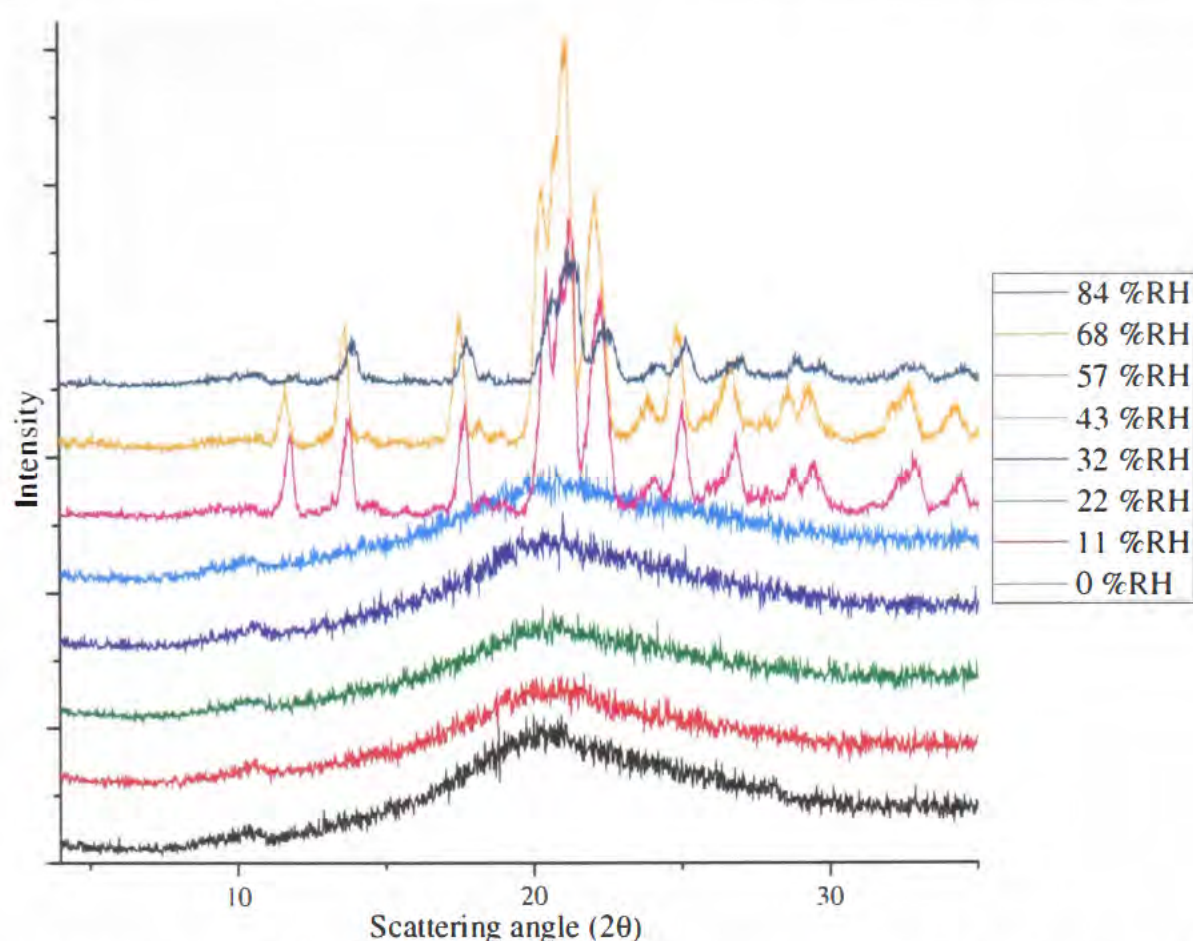


Figure 4.22 XRD diffractograms of lactose with 0.1 % w/w phenol red after storage for one week at 25° C and controlled %RH. Diffractograms collected once.

Each polymorph of lactose has distinct diffractograms.<sup>[17]</sup> The major reflections for each polymorph occur close to peaks in other polymorphs, for example the major reflection of  $\alpha$ -lactose monohydrate is  $2\theta = 19.88^\circ$ , but there is a peak at  $2\theta = 19.91^\circ$  in  $\beta$ -lactose anhydrous. As there is no peak near the characteristic peak of  $\beta$ -lactose at  $2\theta = 10.5^\circ$  (the nearest being at over  $2\theta = 14^\circ$ ) it is possible to rule out this polymorph as a possible identity of the crystalline samples. This means that the peak at *ca.*  $2\theta = 19.9^\circ$  must be caused by  $\alpha$ -lactose monohydrate rather than  $\beta$ -lactose anhydrous. The above diffractograms, although not a perfect match for literature diffractograms of  $\alpha$ -lactose monohydrate are very unlikely to have been produced from any other polymorph of lactose.

#### 4.17 XRD of lactose without dye

The diffractograms of lactose without the probe molecule were also collected (Figure 4.23). These were compared to the diffractograms with the probe, as well as with the literature, and reveal that the polymorphic form of lactose is  $\alpha$ -lactose

monohydrate. This means that the presence of the probe, at a concentration of 0.1 %w/w, is not affecting the lactose such that it can be observed by any technique employed herein.

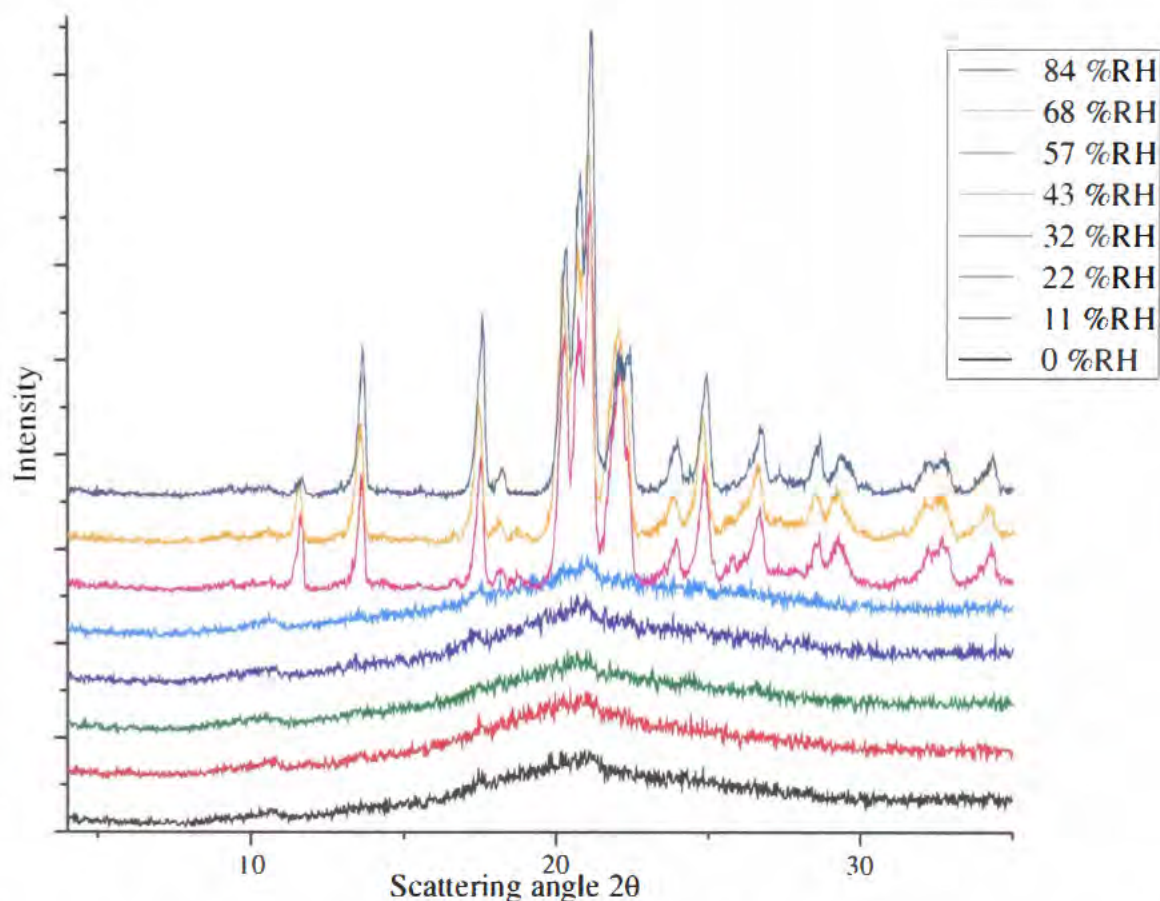


Figure 4.23 XRD diffractograms of lactose after storage for one week at 25° C and controlled %RH. Diffractograms collected once.

#### 4.18 Summary of lactose

Amorphous lactose was prepared by freeze-drying an aqueous solution of lactose. A probe molecule can be added pre-lyophilisation. Storage of the freeze-dried product at, or above 57 %RH (at 25° C) will cause amorphous lactose to crystallise into  $\alpha$ -lactose monohydrate, the identity of the polymorph being determined from FT-Raman spectroscopy, DSC and XRD. Storage at 43 %RH and below will maintain the amorphous polymorph. The presence of the probe molecule does not appear to cause amorphous lactose to crystallise differently. DRUV spectra of the samples of lactose (with the probe) distinguish between amorphous and crystalline lactose, but, because only one of the three possible polymorphs of lactose have been produced, it is, as yet, impossible to state whether perichromism can distinguish between different crystalline polymorphs

of the same material. However, perichromism is in agreement with the other three techniques, as shown in table 4.4.

%RH	DRUV	FT-Raman		DSC		XRD	
	With Probe	With Probe	Without Probe	With Probe	Without Probe	With Probe	Without Probe
0	Am	Am	Am	Am	Am	Am	Am
11	Am	Am	Am	Am	Am	Am	Am
22	Am	Am	Am	Am	Am	Am	Am
32	Am	Am	Am	Am	Am	Am	Am
43	Am	Am	Am	Am	Am	Am	Am
57	Cryst	$\alpha L_{\text{mono}}$					
68	Cryst	$\alpha L_{\text{mono}}$					
84	Cryst	$\alpha L_{\text{mono}}$					

Table 4.4. Summary of results for lactose by technique and storage %RH.

Am = Amorphous; Cryst = Crystalline.  $\alpha L_{\text{mono}}$  =  $\alpha$ -lactose monohydrate.

As was discussed for sucrose (figure 4.14) when examining the DRUV spectra for lactose, in the range of 1000 nm to 1100 nm (not shown) the samples separate based on storage %RH, generally the greater the storage %RH, the greater the intensity increase over this range of wavelength – although no distinct separation into two groups of amorphous and crystalline samples seems to occur. Lactose has also proved to be a more difficult pharmaceutical excipient to characterise than sucrose. This is because the identity of the crystalline polymorph needed to be determined, and each polymorph gives data that is similar to the other two by the techniques available, signal-to-noise ratios for FT-Raman and XRD data meant it was difficult to differentiate between certain polymorphs.

#### 4.19 DRUV of trehalose

The third sugar to be investigated was  $\alpha,\alpha$ -trehalose. This is the naturally occurring form of trehalose. Two forms of trehalose can be produced synthetically. These are  $\alpha,\beta$ -trehalose (neotrehalose) and  $\beta,\beta$ -trehalose

(isotrehalose).<sup>[38]</sup>  $\alpha,\alpha$ -trehalose can exist either as an amorphous powder, or in two crystalline forms. These forms are  $\alpha,\alpha$ -trehalose anhydrous and  $\alpha,\alpha$ -trehalose dihydrate.<sup>[39]</sup> A possible third form, which has a distinct diffractogram and is another anhydrate, has been reported.<sup>[40]</sup> This third form is produced from the dihydrate under specific conditions (heating at 50° C under vacuum for 48 hours) and would not have been produced by the methods used in this work. There have been claims made (although most of these have been later refuted) of several other forms of anhydrous  $\alpha,\alpha$ -trehalose.<sup>[40]</sup> Trehalose has recently become the focus of many studies into polymorphic determination,<sup>[39-47]</sup> mainly because of its bioprotectant behaviour, and recent advances made in preparing pure trehalose.

The DRUV of sucrose and lactose suggests that differences observed in the spectra may be caused by level of hydration. Sucrose being an anhydrous crystal, and lactose was determined to be  $\alpha$ -lactose monohydrate. If trehalose crystallises as  $\alpha,\alpha$ -trehalose dihydrate, then a comparison of the DRUV spectra of the three disaccharides can be made, and the effect of the level of hydration can be discovered. If it crystallises as  $\alpha,\alpha$ -trehalose anhydrate, and the DRUV spectra are different from the DRUV spectra of sucrose, then hydration is not the cause of the changes in wavelength of the probe. It will also be interesting to see if the crystallisation of amorphous trehalose allows for the formation of both crystalline polymorphs of trehalose, or if like lactose, there will only be the most hydrated polymorph present. The probe molecule was added to an aqueous solution of trehalose, which is then freeze-dried to produce the amorphous powder (method 2) which is then stored in one of eight desiccators of controlled temperature and relative humidity. The photographs for trehalose are shown in figure 4.24 and the DRUV and first derivative spectra in figure 4.25, and 4.26 respectively.

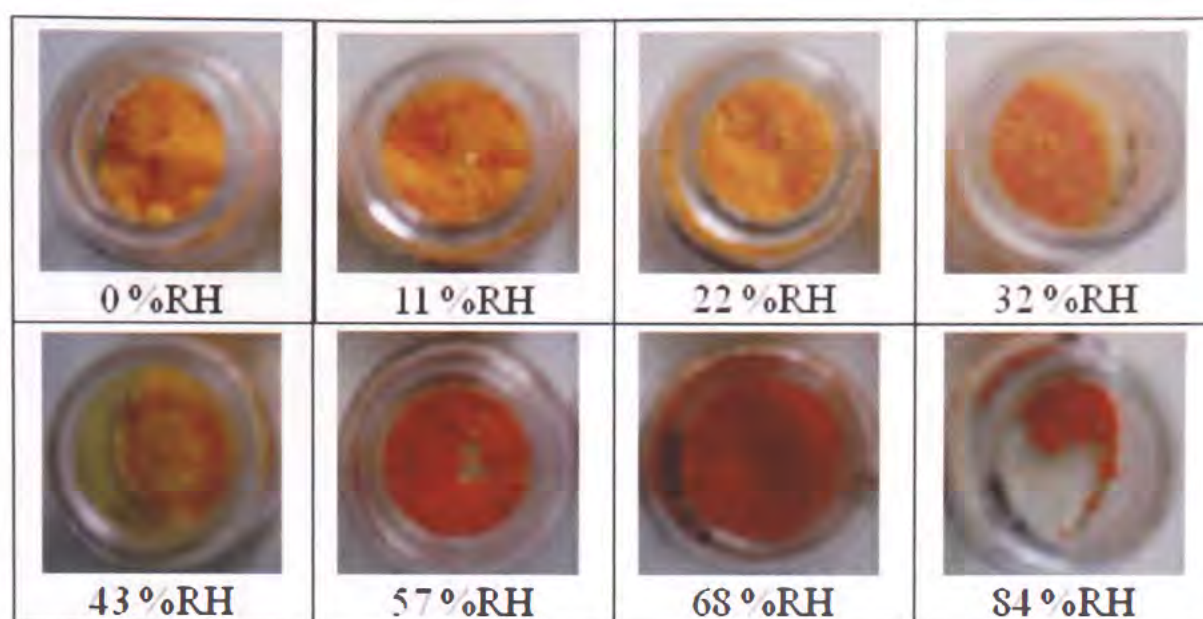


Figure 4.24. Photographs of trehalose with 0.1 %w/w phenol red, freeze-dried and stored for one week at 25° C and controlled %RH.

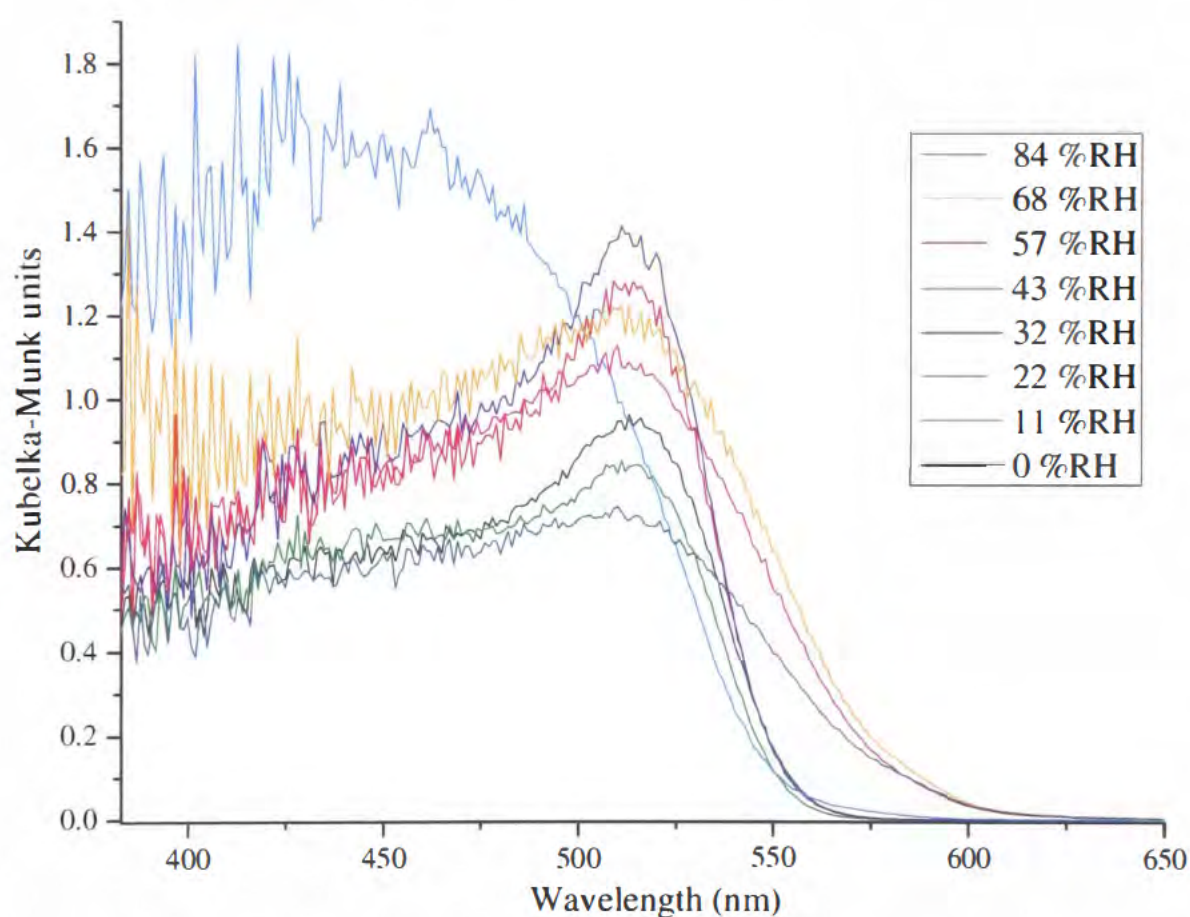


Figure 4.25 DRUV spectra of trehalose with 0.1 %w/w phenol red after storage for one week at 25° C and controlled %RH. Spectra collected once.

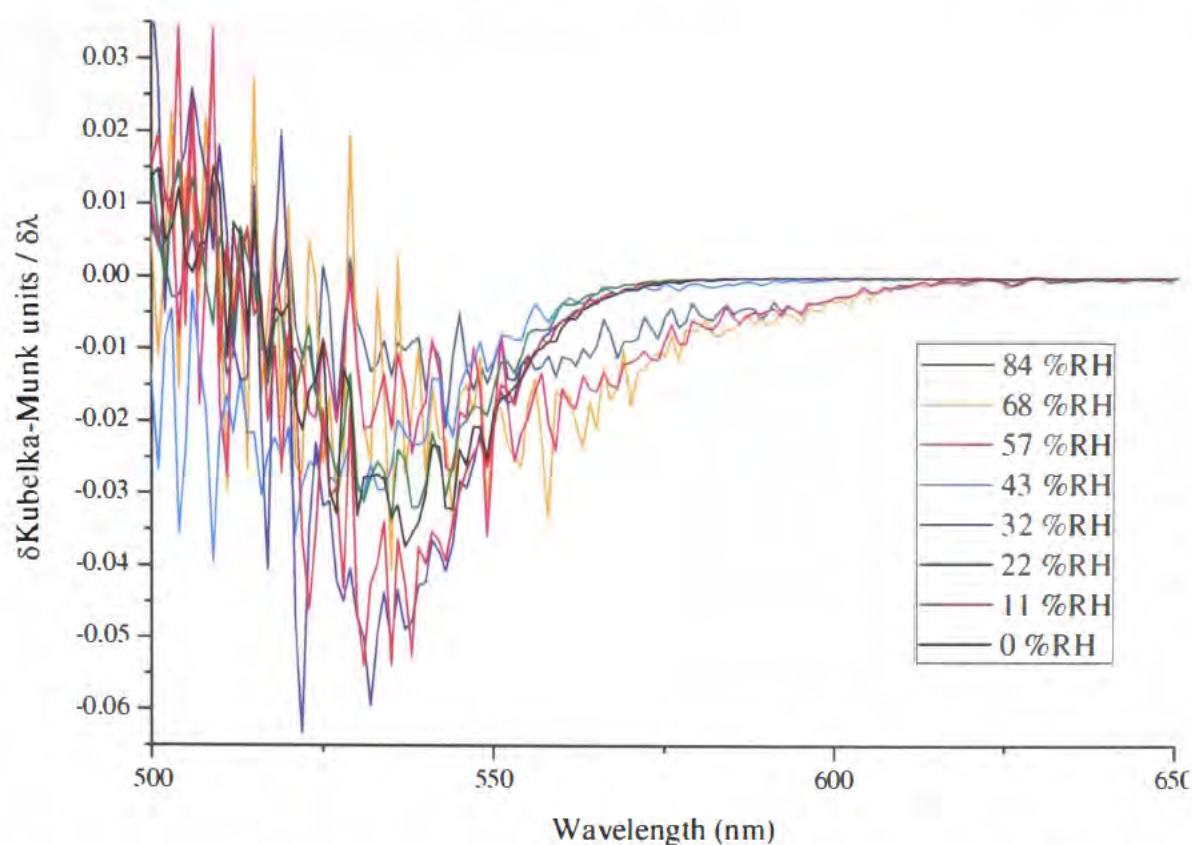


Figure 4.26 First derivative DRUV spectra of trehalose with 0.1 %w/w phenol red after storage for one week at 25° C and controlled %RH.

It would appear from the photographs (Figure 4.24) there are two distinct forms of trehalose being generated under these storage conditions, similar observations were made with both sucrose and lactose. The first of these forms is visually the same as when the amorphous trehalose was removed from the freeze-drier. The second form (57 %RH and above) is noticeably darker. It is also a much denser material, suggesting the amorphous trehalose has undergone a phase transition and caked before crystallising. This would suggest that only one crystalline polymorph of trehalose has been produced. The DRUV spectra concur with the photographs. The main difference between spectra occurs after 550 nm. Samples that have been stored at 43 %RH and below have zero intensity above this wavelength. Samples stored above 43 %RH have an appreciable absorption up to 600 nm. However, all spectra (except for trehalose stored at 43 %RH) contain a main peak at the same wavelength, and it is only after this point that the spectra diverge.

The sample at 43 %RH is intriguing, as although it does not have a peak at *ca.* 525 nm, the point at which the spectrum reaches the baseline is identical to samples that have been stored at lower relative humidity. This could mean that trehalose stored at 43 %RH has crystallised into a different polymorphic form

than if it had been stored at greater humidity. This would most likely be the anhydrous polymorph, as the presence of greater levels of humidity should, in theory, be conducive to the generation of more hydrated morphological forms. However, visually, this sample has not caked and *appears* amorphous. This would be consistent with the fact that the spectrum reaches the baseline at a similar point to the samples stored below 43 %RH. This sample requires identification by other techniques (*i.e.* FT-Raman, DSC and XRD).

#### 4.20 FT-Raman of trehalose

The first technique used to determine the polymorphic forms of trehalose that were analysed by DRUV spectroscopy (Figure 4.25) was FT-Raman spectroscopy. The literature Raman spectra of trehalose shows that different polymorphs can be identified by their respective Raman spectra.<sup>[47]</sup> Amorphous trehalose, will assumedly have, like all amorphous sugars, a very poor Raman cross section, and will be characterized by an ill-defined spectrum, the FT-Raman spectra can be seen in figure 4.27.

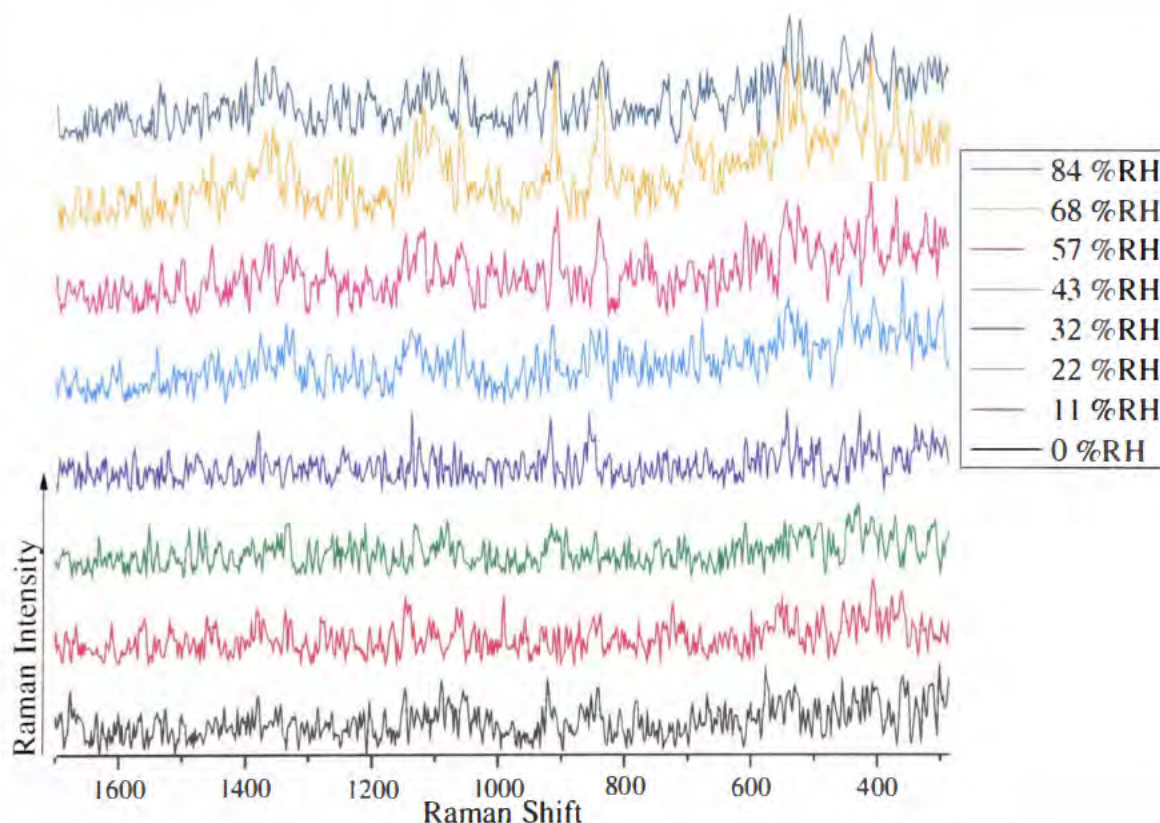


Figure 4.27 FT-Raman spectroscopy of trehalose with 0.1 %w/w phenol red after storage for one week at 25° C and controlled %RH. Spectra collected several times.

The FT-Raman spectra of trehalose are disappointing. The Raman intensity of the peaks are broad and ill-defined, and may be easily confused with background noise. However, the sample at 68 %RH gives the best-defined bands (which also seem to appear in the other crystalline samples) at  $912\text{ cm}^{-1}$  and  $840\text{ cm}^{-1}$  which would suggest that the sample is  $\alpha,\alpha$ -trehalose dihydrate.<sup>[16]</sup> All samples stored below 32% RH appear amorphous – the sample at 32% RH is inconclusive. Due to the fact the intensities of the Raman spectrum are so weak, it is very difficult and probably unwise, to try to determine which morphological forms are present from the spectra in figure 4.27. This was unexpected as FT-Raman had been very useful in determining polymorphs that were present for both sucrose and lactose.

#### 4.21 FT-Raman of trehalose without dye

The FT-Raman of the trehalose samples without the probe molecule was attempted (not included). The result of this was the immediate realisation that there had been an equipment failure. Unfortunately, the liquid nitrogen cooled Germanium detector had failed, and the InGaAs detector did not prove to be capable of showing Raman scatter in any of the samples (*i.e.* trehalose, sucrose and lactose). Literature spectra of the Raman spectra for both trehalose and raffinose (the next saccharide to be examined) show clear spectra for both samples, making the loss of this technique as a tool to identify crystalline polymorphic form highly disappointing, however identification should still be possible using DSC and XRD. The possibility of using dispersive Raman spectroscopy will be discussed in Chapter 5.

#### 4.22 DSC of trehalose

The two crystalline forms of  $\alpha,\alpha$ -trehalose can easily be distinguished by DSC. The anhydrous polymorph melts at  $215^\circ\text{ C}$ , and the dihydrate at  $97^\circ\text{ C}$ .<sup>[48]</sup> The  $\alpha,\beta$  and the  $\beta,\beta$  forms melt at  $210^\circ\text{ C}$  and  $135^\circ\text{ C}$  respectively.<sup>[48]</sup> The amorphous form of trehalose has a  $T_g$  at  $115^\circ\text{ C}$ .<sup>[49]</sup> This very obvious difference in the thermograms will determine which polymorph, or polymorphs, of trehalose have been generated. It is important that DSC is able to do this given the difficulties

encountered with FT-Raman spectroscopy. DSC thermograms for trehalose are given in figure 4.28.

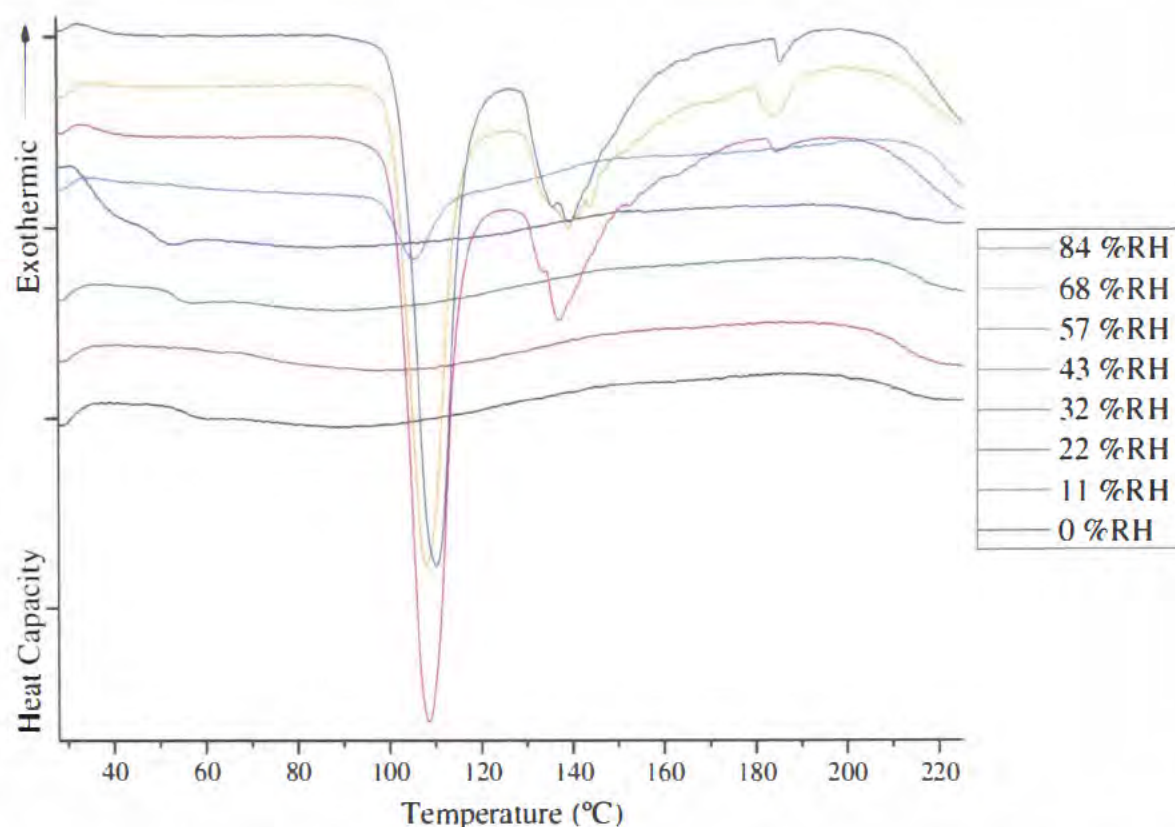


Figure 4.28 DSC of trehalose with 0.1 %w/w phenol red stored for one week at 25° C and controlled %RH. Thermograms collected once.

From the above DSC thermograms (Figure 4.28) it is apparent that the samples stored at 32 %RH and below are amorphous. The samples stored above this all have a  $T_m$  with a peak onset at 96 - 97° C, identifying them as  $\alpha,\alpha$ -trehalose dihydrate. The sample stored at 43 %RH has a  $T_m$  for  $\alpha,\alpha$ -trehalose dihydrate, but this is weaker than for the samples stored at higher relative humidity. It is possible that this sample has not fully crystallised, and is mostly amorphous trehalose with a small amount of trehalose dihydrate. It was shown in the DRUV spectra earlier (Figure 4.25) that this sample was noticeably different from the others, and this could be explained if this sample is a mixture of two amorphous and crystalline forms. It does not however explain why the peak at 525 nm in the DRUV spectrum is missing when it is present in all other DRUV spectra of trehalose.

### 4.23 DSC of trehalose without dye

Amorphous trehalose, with 0.1 %w/w phenol red, stored for one week at 25° C and 43 %RH appears to be the first sample examined which is not totally amorphous or crystalline. It is important to discover if the presence of the probe has impeded, aided, or had no effect upon the crystallisation of amorphous trehalose. Therefore, the DSC thermograms of trehalose, without the probe molecule were measured (Figure 4.29). If the sample at 43 %RH is identified as purely amorphous, or the size of the exotherm matches those for trehalose dihydrate, then phenol red might have altered the crystallisation behaviour of trehalose. If the thermogram is very similar for trehalose both with and without the presence of phenol red, then it would be indicative that the  $T_g$  of amorphous trehalose, at 43 %RH is very close to 25° C, and that very small fluctuations in either humidity, or temperature can result in a different product, giving similar, but not identical results.

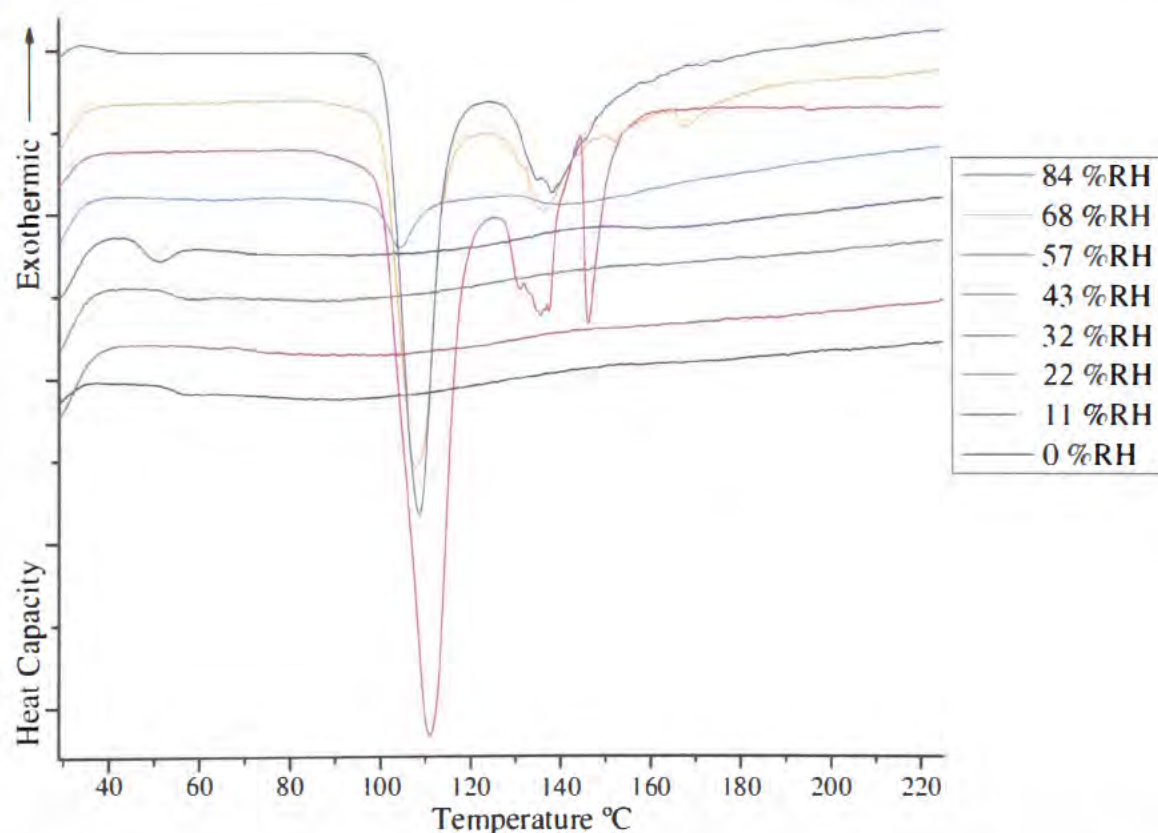


Figure 4.29 DSC of trehalose stored for one week at 25° C and controlled %RH. Thermograms collected once.

The DSC thermograms for trehalose without the probe molecule (Figure 4.29) are the same as those for trehalose with the probe (Figure 4.28). Therefore the probe molecule is not affecting the crystallisation of trehalose. It is most likely

that the sample stored at 43 %RH is partially crystalline. It was earlier shown that the percentage of amorphous material of sucrose in a predominantly crystalline material could be accurately measured by the ratios of the peak heights of amorphous and crystalline sucrose (section 4.12). However, for trehalose, stored at 43 %RH (Figure 4.25), there are no apparent peaks for the ratio to be calculated which makes determining the percentage amorphous content from this method impossible. It might be possible to measure the peak height ratios of the DSC, allowing for quantification of amorphous content, but this would need to be tested by measuring the thermograms of known levels of amorphous content in trehalose. However, as the peak heights for the crystalline trehalose vary widely between crystalline samples, (*i.e.* trehalose stored at 57 %RH has a greater heat capacity than trehalose stored at 68 %RH), the accuracy of this approach is predicted to be too poor to allow for any confidence in the result.

#### 4.24 XRD of trehalose

Powder x-ray diffraction was performed on the eight samples of trehalose (Figure 4.30). The XRD of the different polymorphs of trehalose are available in the literature<sup>[50]</sup> and show that the anhydrous polymorph has peaks at (amongst others)  $2\theta = 17.3^\circ$  and  $25.1^\circ$ , and the dihydrate at  $2\theta = 16.4^\circ$  and  $23.7^\circ$ . The halo effect in the diffractogram identifies amorphous polymorphs.

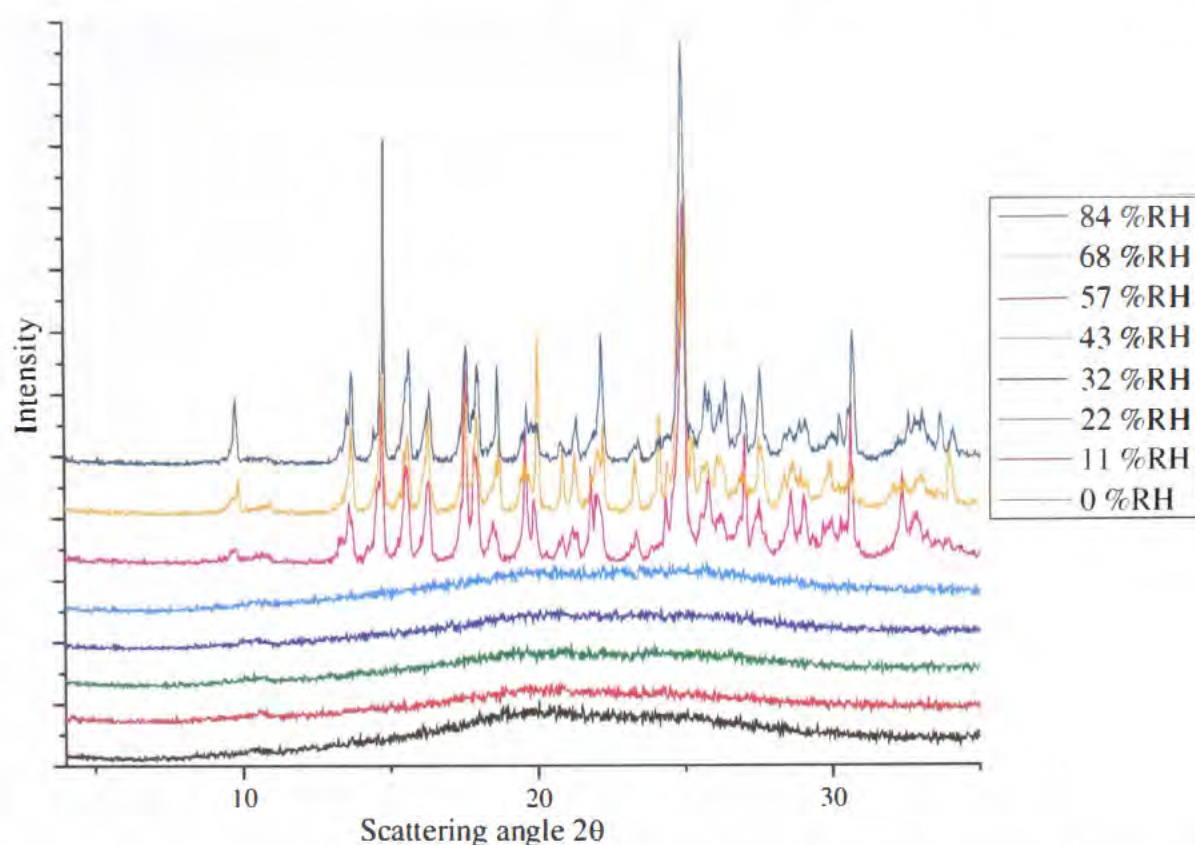


Figure 4.30. XRD of trehalose with 0.1 %w/w phenol red stored for one week at 25° C and controlled %RH. Diffractograms collected once

The first thing that is apparent from the diffractograms shown above (Figure 4.30) is that the trehalose sample stored at 43 %RH has no visible peaks, and is therefore predominantly amorphous, as determined by XRD. This is in contrast to the DSC thermogram, which suggested that there may be some trehalose dihydrate in this sample (see figure 4.29). This difference could have arisen if one of the techniques (DSC) is much more sensitive to the presence of crystalline  $\alpha,\alpha$ -trehalose dihydrate than the other (XRD). Furthermore, this may be an extension of the argument that grinding the sample into a powder before the powder can be introduced to the diffractometer is producing amorphous material (see section 4.8), and that the sample is crystalline in the DSC thermogram and amorphous (at least on the surface) in the XRD diffractogram. The other diffractograms show that the samples stored between 0 and 32 %RH are amorphous. The samples stored at 57 %RH and above are crystalline, and due to peaks present at 16.4° and 23.7°  $2\theta$ , along with others mentioned in the literature<sup>[50]</sup> it is certain that these samples are  $\alpha,\alpha$ -trehalose dihydrate. It should be noted that the relative peak intensities of peaks in the diffractogram for  $\alpha,\alpha$ -trehalose dihydrate shown in this work (Figure 4.30) significantly differ from those found in the literature<sup>[50]</sup>, but the peak positions are the same, this may be

caused by preferred orientation, or the generation of amorphous material as the samples are prepared.

#### 4.25 XRD of trehalose without dye

The presence of the probe molecule in amorphous trehalose has given rise to the first possible scenario where the probe is affecting the crystallisation behaviour of the excipient. The DSC thermograms of trehalose with and without the probe, and to some extent, the XRD of trehalose with the probe have suggested that this is not actually the case. Although as mentioned above, it appears that the sample stored at 43 %RH might be partially crystalline below the level of detection of XRD. It is imperative that the XRD diffractograms of trehalose without the probe molecule (Figure 4.31) prove to be the same as the diffractograms shown in Figure 4.30. If this is not the case, then the probe is hindering crystallisation of amorphous trehalose.

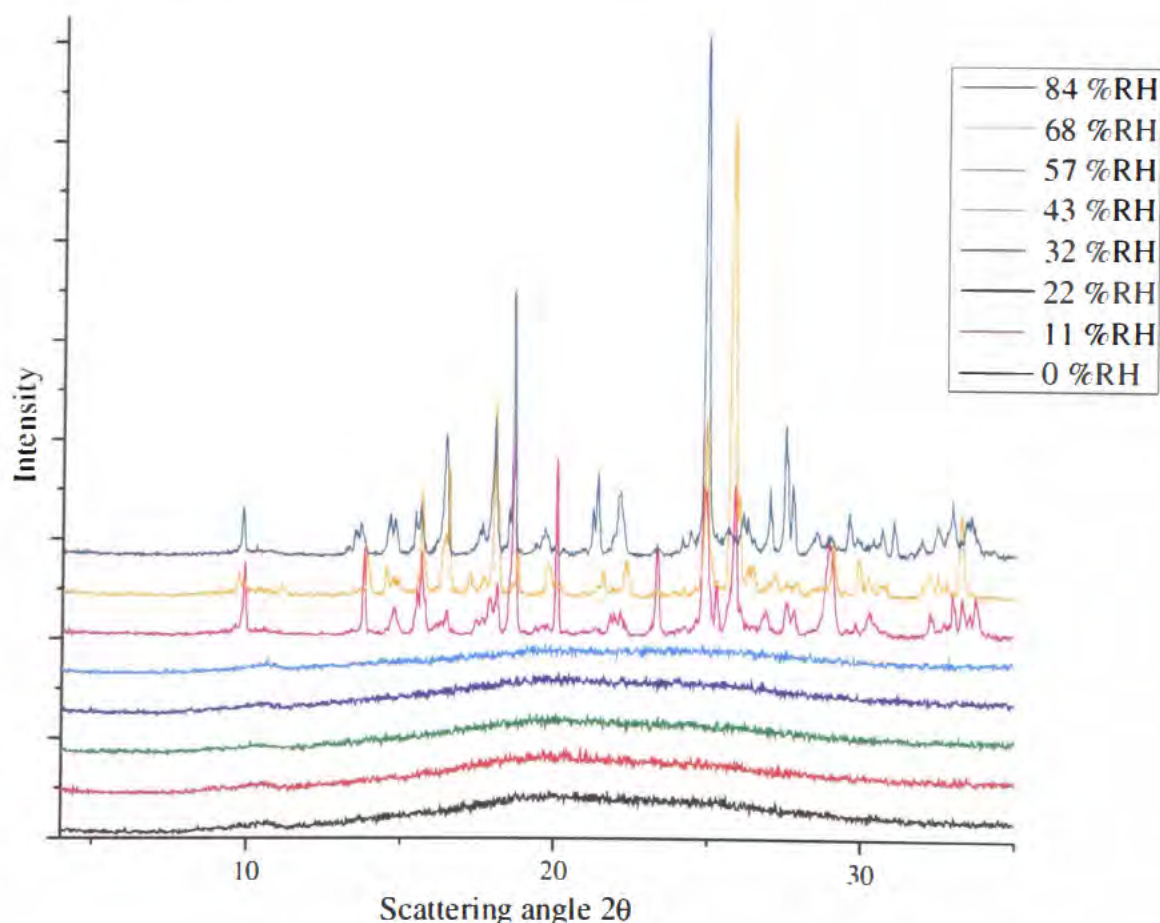


Figure 4.31. XRD of trehalose stored for one week at 25° C and controlled %RH. Diffractograms collected once.

The diffractograms for trehalose without the probe molecule (Figure 4.31) are similar to those with the probe (Figure 4.30). This means that the probe molecule

has no discernible effect upon the crystallisation of amorphous trehalose, as both samples (with and without the probe) are giving the same result from two different techniques, *i.e.* crystallisation appears to occur in samples stored at 57 %RH and above.

It is interesting to note that the technique favoured by industry to determine amorphous content and/or polymorphism, XRD, appears less sensitive to detecting different polymorphs of the same powder than DSC (for example, see sample stored at 43 %RH in figures 4.28 and 4.29 compared to figures 4.30 and 4.31). A possible reason for this could be the sample preparation for XRD, which requires the sample to be ground, generating amorphous material at the surface, which is the part of the sample that XRD measures. The results presented in this thesis thus far show that it is wiser to investigate amorphous content and/or polymorph determination by more than one technique, to obtain greater insight into the solid material being investigated. Perichromism has proven to be extremely successful at qualitatively analysing disaccharides. DSC of disaccharides has been of variable utility dependant on excipient. For sucrose, the DSC results were poor and gave limited information, but for trehalose, they were excellent.

#### **4.26 Summary of trehalose**

Amorphous trehalose was prepared by freeze-drying a 10 %w/v aqueous solution of trehalose dihydrate. A probe molecule (0.1 %w/w phenol red) could be added to this solution prior to lyophilisation. Storage at 25° C and 57 %RH and above for one week causes amorphous trehalose to crystallise in to  $\alpha,\alpha$ -trehalose dihydrate. Storage at 25° C and 32 %RH and below will maintain amorphous trehalose; but 43 %RH may cause a degree of crystallisation to occur, as shown by DRUV and DSC, although this appears to be below the limit of detection of XRD. Trehalose is the first excipient where a disagreement in the results has occurred (*i.e.* a possible difference in morphological phase on one or more of the techniques used on an identical sample). However, this is most probably caused by the differing limits of detection of the techniques used, XRD requiring the

greatest percentage of a polymorph present to observe it in the diffractogram – also the sample is ground for XRD which will further reduce the level of crystallinity within the sample.

 %RH	DRUV	DSC		XRD	
	With Probe	With Probe	Without Probe	With Probe	Without Probe
0	Am	Am	Am	Am	Am
11	Am	Am	Am	Am	Am
22	Am	Am	Am	Am	Am
32	Am	Am	Am	Am	Am
43	Part	Part	Part	Am	Am
57	Cryst	Tre2H <sub>2</sub> O	Tre2H <sub>2</sub> O	Tre2H <sub>2</sub> O	Tre2H <sub>2</sub> O
68	Cryst	Tre2H <sub>2</sub> O	Tre2H <sub>2</sub> O	Tre2H <sub>2</sub> O	Tre2H <sub>2</sub> O
84	Cryst	Tre2H <sub>2</sub> O	Tre2H <sub>2</sub> O	Tre2H <sub>2</sub> O	Tre2H <sub>2</sub> O

Table 4.5. Summary of results for trehalose by technique and storage %RH.

Am = Amorphous; Cryst = Crystalline; Part = part amorphous, part trehalose dihydrate; Tre2H<sub>2</sub>O =  $\alpha,\alpha$ -trehalose dihydrate.

No FT-Raman spectra for trehalose could be recorded, which is unfortunate, as it has the lowest *proven* limit of detection of any of the techniques used, and would have greatly strengthened the argument for a low percentage of crystalline material being present in the sample stored at 43 %RH.

#### 4.27 DRUV of raffinose

The fourth excipient, and sugar, to be used to investigate perichromism is raffinose. Raffinose, unlike the other three sugars used so far is a trisaccharide. Raffinose exists as a crystalline pentahydrate, or an amorphous solid. It has been claimed that it can exist as a crystalline solid and all possible lower levels of hydration (*i.e.* anhydrous, mono-, di-, tri- and tetra-hydrate)<sup>[51]</sup> even though none have been positively identified as yet.<sup>[52]</sup> There are a few examples in the literature of raffinose being used for determination of amorphous content.<sup>[51, 53, 54]</sup>

Examples of techniques used to study raffinose include DSC,<sup>[53]</sup> FT-IR<sup>[53]</sup> and Raman spectroscopy, in aqueous solution.<sup>[55]</sup> As a pentahydrate, raffinose has the highest level of hydration of any of the oligosaccharides.<sup>[56]</sup> Note that this does not include carbohydrates such as starch, as an oligosaccharide is defined as consisting of between three and 10 component sugars, and starch contains more than 10. Raffinose, therefore is probably the best option amongst the sugars to crystallise into more than one hydrated form, hopefully allowing perichromism to distinguish between polymorphs of the same material, as storage at eight different humidity levels, may allow for a lower level of hydration of raffinose to occur.

Again, amorphous raffinose with 0.1 %w/w phenol red is produced by freeze-drying an aqueous solution (method 2). This is then stored in eight desiccators at controlled temperature and humidity. The DRUV spectrum of each sample is then measured (Figure 4.32) and the first derivatives are also shown (Figure 4.33).

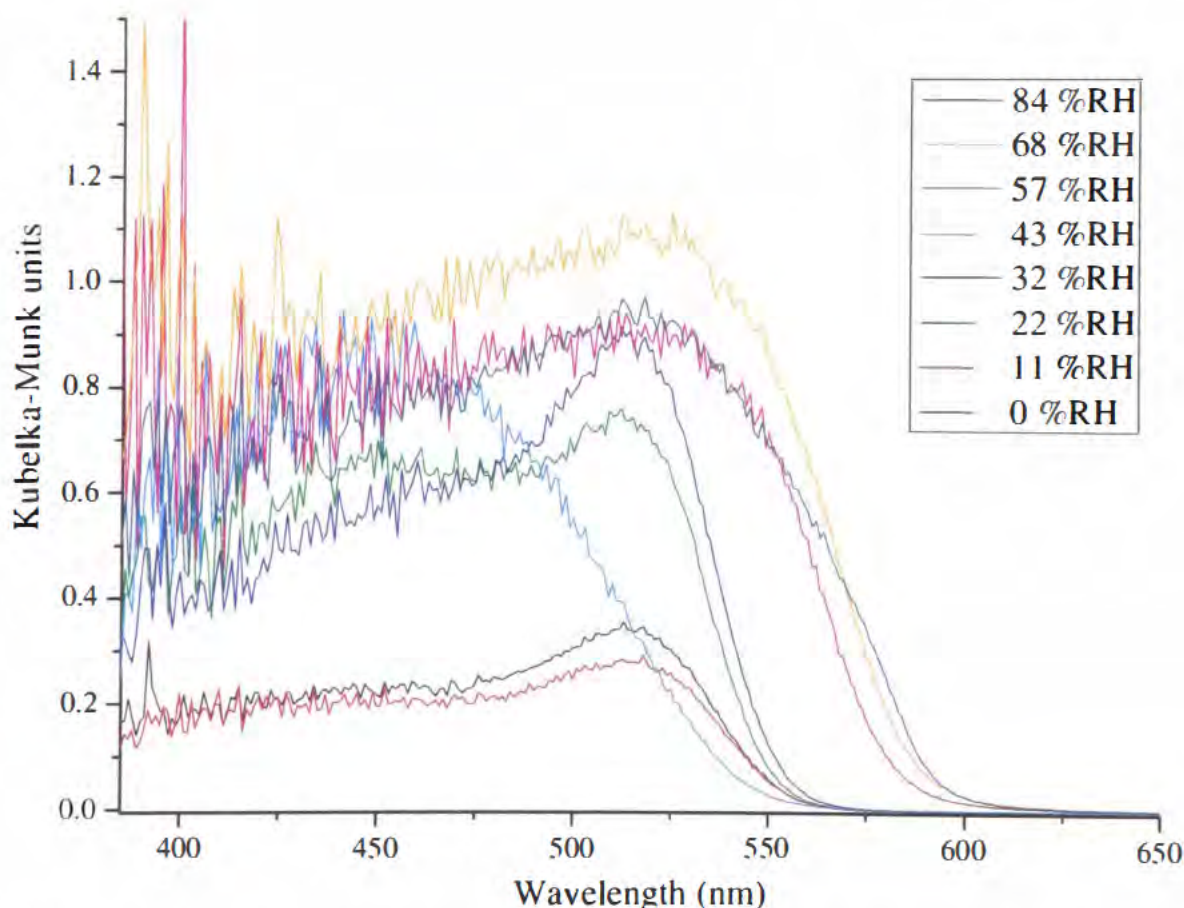


Figure 4.32. DRUV spectra of raffinose with 0.1 %w/w phenol red stored for one week at 25° C and controlled %RH. Spectra collected once.

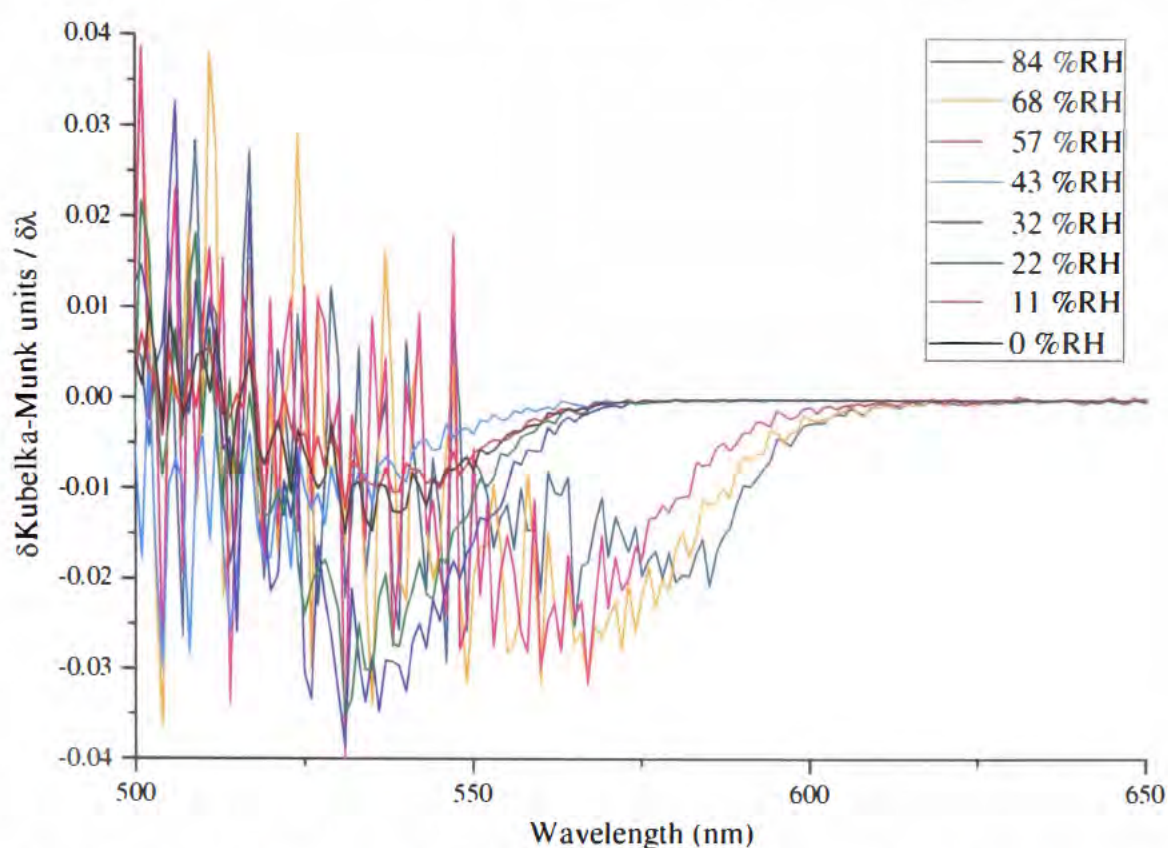


Figure 4.33. First derivative DRUV spectra of raffinose with 0.1 %w/w phenol red stored for one week at 25° C and controlled %RH.

Raffinose, like trehalose has three distinct spectra. For samples stored at 32 %RH and below, a peak at 510 nm can be observed; the intensity has tailed to zero by 560 nm. For samples stored at 57 %RH and above, a very broad peak, with a maxima at *ca.* 510 nm, can be observed, this tails off very slowly, with some intensity being observed until slightly above 600 nm. The sample stored at 43 %RH has again a different shape, with a maximum at 460 nm. The intensity of this peak then recedes, and, although close to the samples stored at lower %RH, it does reach zero intensity at a slightly lower wavelength. The sample identities can be predicted from the previous information: amorphous raffinose stored at 25° C and 32 %RH and lower has remained amorphous; stored above 57 %RH it has crystallised, probably to raffinose pentahydrate; at 43 %RH it has either partially crystallised, or has crystallised into a different polymorph of raffinose (*i.e.* less hydrated)

Due to the difficulties encountered attempting FT-Raman spectroscopy of trehalose, and further repeats of sucrose and lactose, it was not expected that raffinose would prove any more successful. It was attempted, but the spectra were identical to those for trehalose, in that there was no peak discernible in any

of the 16 spectra of raffinose (with and without the probe). Data are therefore not shown.

#### 4.28 DSC of raffinose

There is considerably less information available about distinguishing between polymorphs of raffinose than for the other excipients previously discussed. Literature concerning DSC data for raffinose is unfortunately contradictory, with one source stating there is a  $T_m$  of  $78^\circ\text{C}$  for raffinose pentahydrate,<sup>[48]</sup> and another stating there are a series of endotherms as water is lost from the pentahydrate (at  $56$ ,  $73$ , and  $85^\circ\text{C}$ ).<sup>[56]</sup> It is claimed the amorphous material has a  $T_g$  greater than the  $T_m$  of the pentahydrate, at  $90^\circ\text{C}$ .<sup>[57]</sup> It was therefore decided to measure the DSC thermogram of raffinose pentahydrate, as received, and compare the thermograms of the eight samples from the desiccators to the commercial sample of raffinose pentahydrate (Figure 4.34).

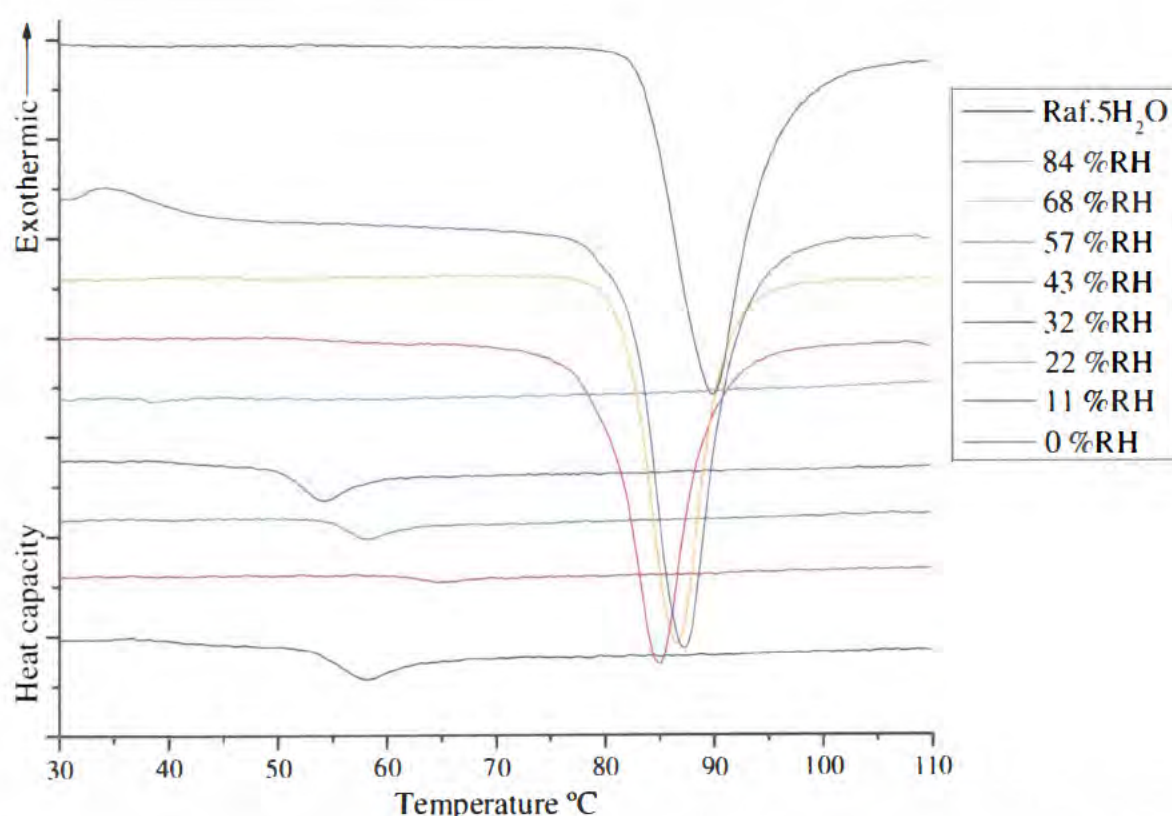


Figure 4.34 DSC of raffinose with 0.1% w/w phenol red, stored for one week at  $25^\circ\text{C}$  and controlled %RH. Note that Raf.5H<sub>2</sub>O is the DSC thermogram of commercial raffinose pentahydrate (without the probe molecule for comparative purposes). Thermograms collected once.

The first thermogram of interest above is that of raffinose pentahydrate. In this thermogram, it can be seen that the onset of the  $T_m$  is 80° C, which agrees with the literature value of 78° C.<sup>[48]</sup> However, there is no evidence for the sequential loss of water as suggested by Cheng *et al.*<sup>[56]</sup> Of the eight samples of lyophilised raffinose with phenol red, there are two distinct types of thermograms visible. Firstly the samples stored at 43 %RH and below are amorphous, as evidenced by the presence of a  $T_g$  in the thermogram (values shown in table 4.6). Lyophilised raffinose stored at 57 %RH and above has crystallised to raffinose pentahydrate, as can be seen by the thermograms. There is however, an unexpected result with these samples: water acts as a plasticiser, and should lower melting temperature ( $T_m$ ), as can be seen (Figure 4.34), storage at increasing %RH has *raised* the  $T_m$ , (Table 4.8) It is also seen again that the  $T_g$  for the sample stored at 0 %RH is lower than for the sample stored at 11 %RH, and in this case, also 22 %RH. The hygrometer reading for the desiccators suggested that the actual values for these three desiccators were within 2 %RH of the stated value. The reason for the low  $T_g$  of the sample at 0 %RH is therefore unknown, and could be caused by any of numerous effects, from contamination, to leaving exposed to ambient conditions before analysis or the salt solution exchanging water with the sample. Repetition of the DSC analysis may eliminate some of these possibilities (for example, experimental error).

Sample (% RH)	$T_g$ (° C)	$T_m$ (° C)
0	53.2	-
11	61.6	-
22	54.9	-
32	49.3	-
43	37.4	-
57	-	72.4
68	-	75.4
84	-	75.7

Table 4.6  $T_g$  and  $T_m$  peak onset values for amorphous raffinose and raffinose pentahydrate.

The DSC thermogram for raffinose stored at 43 %RH suggests that the sample is probably amorphous (a very small  $T_g$  could be assigned at 37.4° C); this does not agree with the DRUV spectra, which is different to the other amorphous samples. It is possible that there may be some crystallisation of this sample, like with trehalose, but it will have to be seen if the XRD diffractograms (section 4.30) are able to confirm the identity of this sample.

#### 4.29 DSC of raffinose without dye

The DSC thermograms of lyophilised raffinose without the probe molecule were collected to determine if the earlier observed result of increasing  $T_m$  with increased storage humidity could be repeated for samples without the probe molecule. It was also required to discover if phenol red was having any effect upon the crystallisation of amorphous raffinose, although from previous work shown in this chapter, this is considered unlikely. The thermograms are shown below (Figure 4.35).

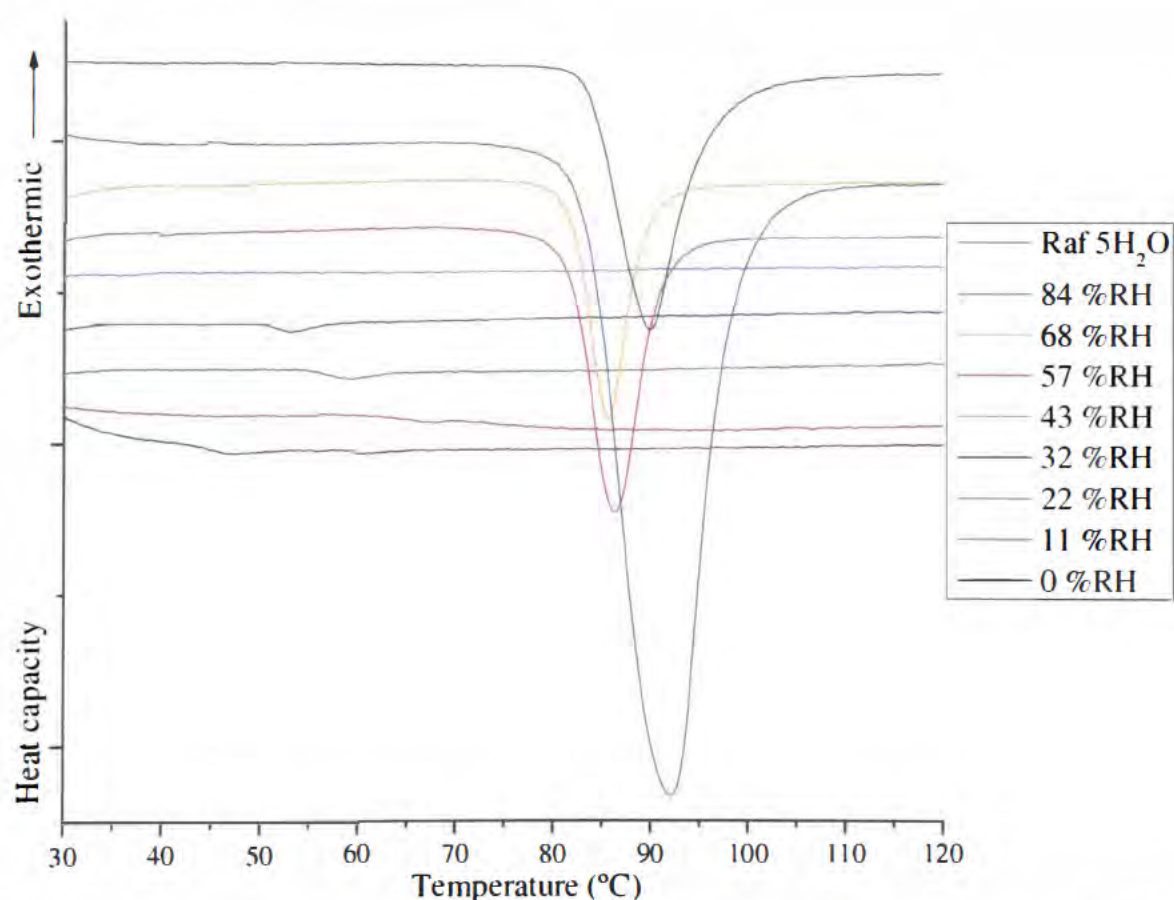


Figure 4.35 DSC of raffinose stored for one week at 25° C and controlled %RH. Thermograms collected once.

The three crystalline samples, 57, 68 and 84 %RH are all of raffinose pentahydrate, but intriguingly, the onset of the  $T_m$  for all three is greater than

when the dye was present, at 79° C compared to the values in table 4.8. The lack of the probe (acting as an impurity) would explain this – however this is the only time this has been observed in the DSC for any excipient. The pattern of increasing  $T_m$  with increasing relative humidity has not been observed, but it is still apparent from the thermograms that the samples are raffinose pentahydrate.

### 4.30 XRD of raffinose

After searching the literature, no evidence for distinguishing between different polymorphs of raffinose could be discovered by powder x-ray diffraction. However, the crystal structure and diffraction data for raffinose pentahydrate has been determined.<sup>[58]</sup> Therefore, it is possible to identify both amorphous raffinose (by the halo effect) and raffinose pentahydrate by comparing the diffractograms (Figure 4.36) to the literature. In the unlikely event that the diffractogram does not fit either of these, then a different polymorph of raffinose has been generated, and this will need to be identified, and the DSC thermograms re-examined.

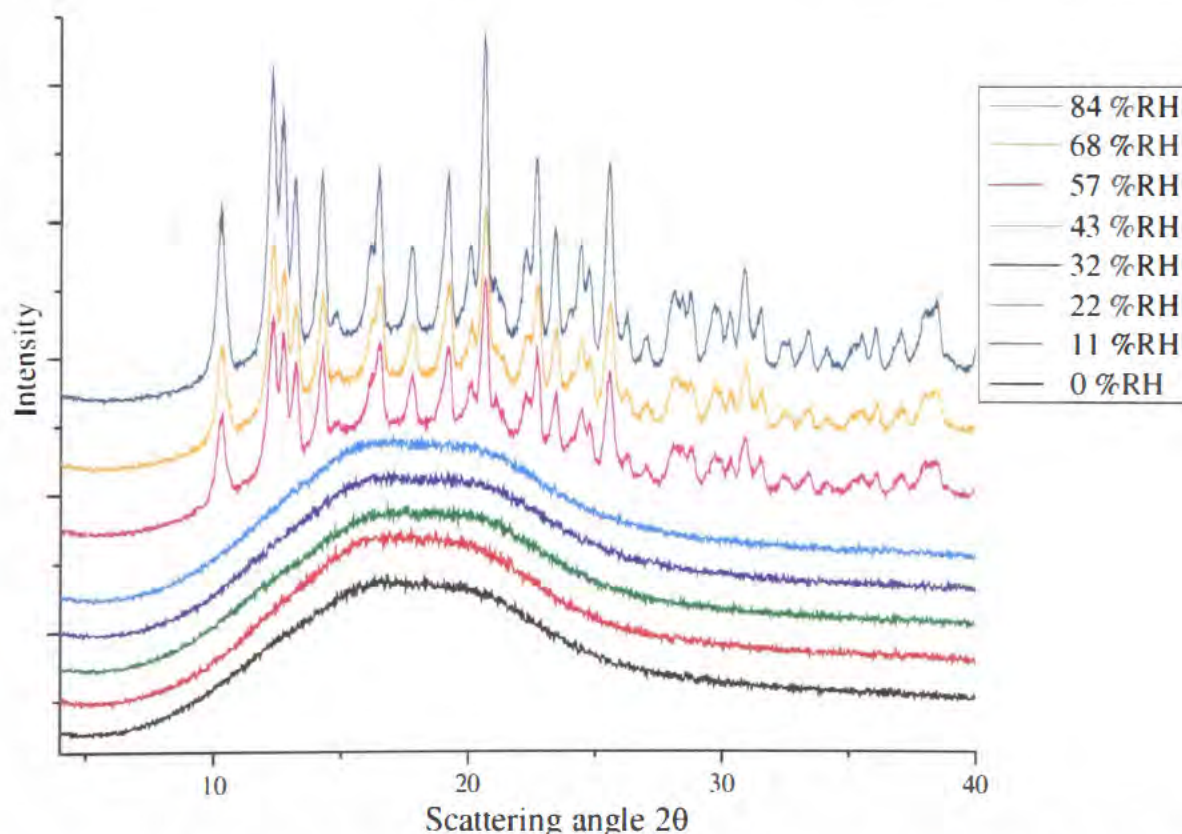


Figure 4.36 XRD of raffinose with 0.1% w/w phenol red, stored for one week at 25° C and controlled %RH. Diffractograms collected once.

The peaks in the diffractograms for samples stored at 57% RH and above in figure 4.36 were compared to those of the diffractogram of raffinose

pentahydrate in the literature.<sup>[58]</sup> It was confirmed that the samples stored at 57% RH and above are raffinose pentahydrate. The samples stored at 43 %RH, and below, are identified as amorphous, by virtue of the halo effect.

#### 4.31 XRD of raffinose without dye

The DRUV spectrum for raffinose stored at 43 %RH (figure 4.32) being different to all other DRUV spectra of raffinose, makes it important to discover if the XRD diffractogram is also different (Figure 4.37). It is predicted to appear amorphous, particularly after considering the DSC thermogram for this sample - DSC having a greater limit of detection for low level amorphous (or crystalline) content than XRD.

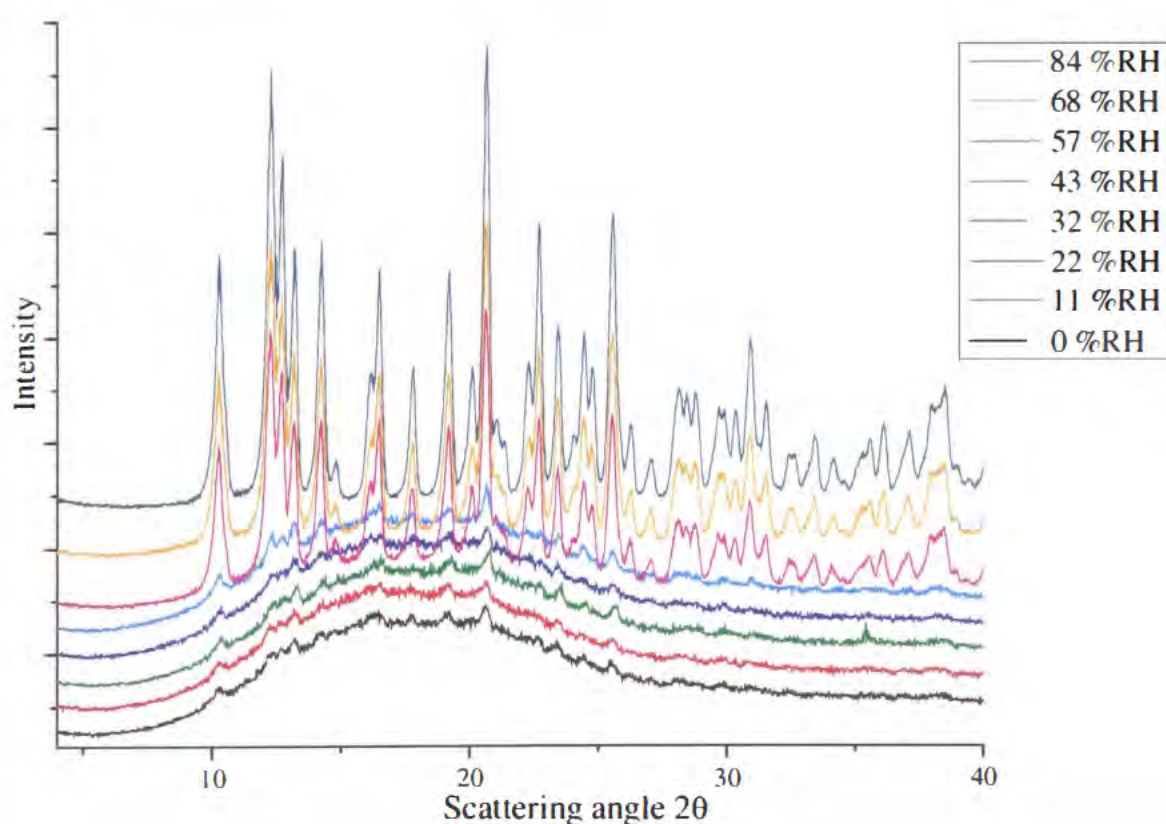


Figure 4.37 XRD of raffinose stored for one week at 25° C and controlled %RH. Diffractograms collected once.

The samples stored at 57 %RH and above are again raffinose pentahydrate, and the samples stored below this are predominantly amorphous. It should be noted that there are some minute peaks present in all the amorphous diffractograms, but the overall shape of them is of a single broad peak, *i.e.* the halo effect. The peaks observed may have been caused by contamination from a crystalline sample.



This was previously suggested in section 4.12, and would indicate that DRUV spectroscopy, and therefore perichromism, has a limit of detection considerably below 5 % amorphous content, or is capable of distinguishing between an amorphous glass and an amorphous rubber.

### 4.33 The saccharides

In all cases for the saccharides, the only polymorph that has been produced by storing at 25° C and crystallisation at controlled %RH has been the most hydrated form previously reported in the literature. Obviously lowering the  $T_g$  by increasing the humidity causes enough water to be available for the saccharide to crystallise into the most hydrated form. It would be interesting to determine if raising the temperature, and slowly raising the humidity would allow for the crystallisation of less hydrated sugars for example raffinose trihydrate or  $\alpha$ -lactose anhydrous. The opposite approach to this, maintaining the samples at lower levels of humidity for extended periods would probably not allow for any crystallisation as the  $T_g$  would still be above the storage temperature. Given more time this could be an interesting investigation.

Upon comparing the DRUV spectra of the four amorphous saccharides (Figure 4.38) it is apparent that they are all, surprisingly, very similar. It might have been anticipated that raffinose would have a different spectrum, being a trisaccharide, but in fact the only difference in wavelength, between any of the spectra, is that of sucrose. The maximum reflectance for amorphous lactose, trehalose and raffinose is *ca.* 515 nm. Sucrose is represented by a very broad peak, which tails off at *ca.* 540 nm. The wavelength of maximum reflectance for phenol red is 579 nm (Chapter 5, Figure 5.1) which means that the presence of the amorphous saccharide has caused a blue shift of 65 nm – for sucrose it is at least 40 nm.

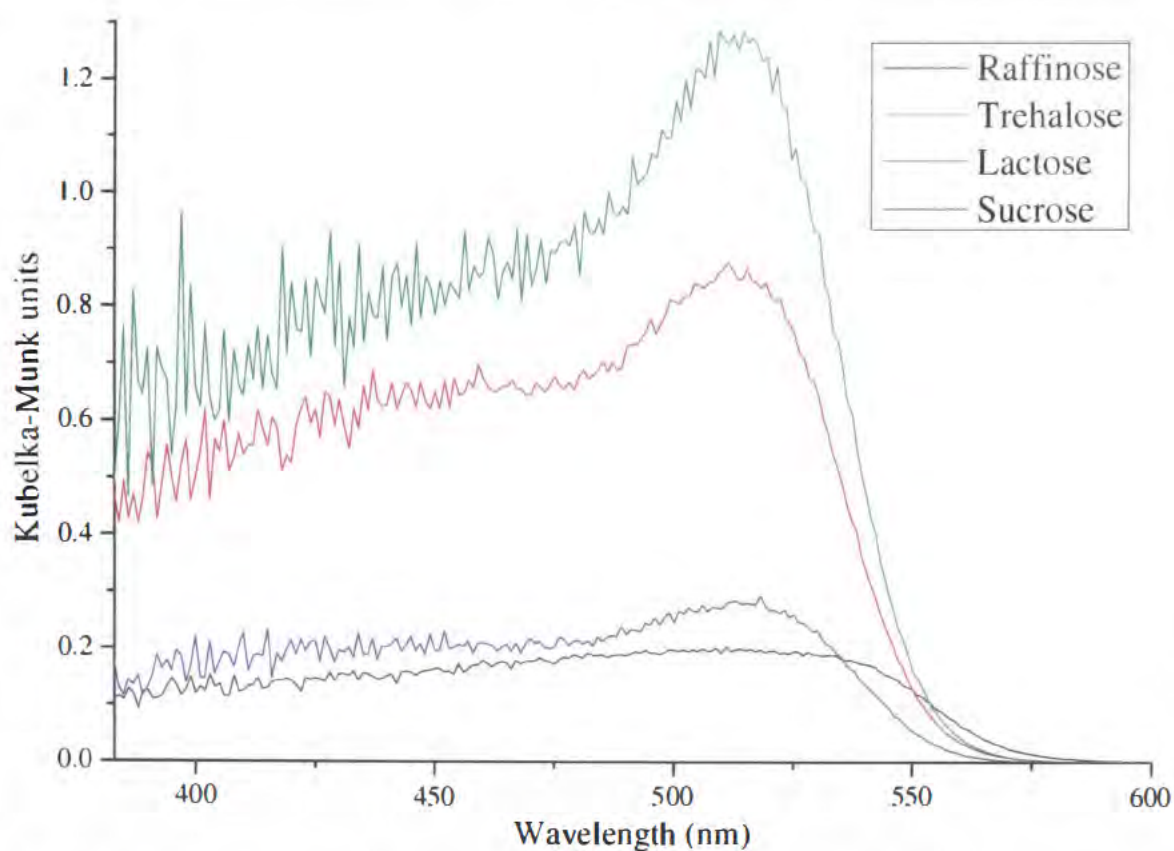


**Figure 4.38** A comparison of four amorphous saccharides, each with 0.1 %w/w phenol red. (Samples stored at 11 %RH chosen to represent amorphous samples).

The lack of capability to distinguish between amorphous saccharides is not altogether surprising. Neither FT-Raman, nor XRD are able to do so, and DRUV spectroscopy, like these, is dependant on the interaction of a photon on a particle surface. However, the DRUV spectra of the crystalline saccharides (Figure 4.39) should be different, as they are for FT-Raman and XRD. This is because an amorphous surface is random, and the functional groups in these four saccharides are identical. However, in their crystalline phases different functional groups will be present at the surface in different, fixed ratios, and as phenol red should, theoretically, preferentially bond to one group (due to spatial and chemical preferences) it could be expected that the amorphous spectra would all be very similar, but the crystalline spectra must be different from one another.

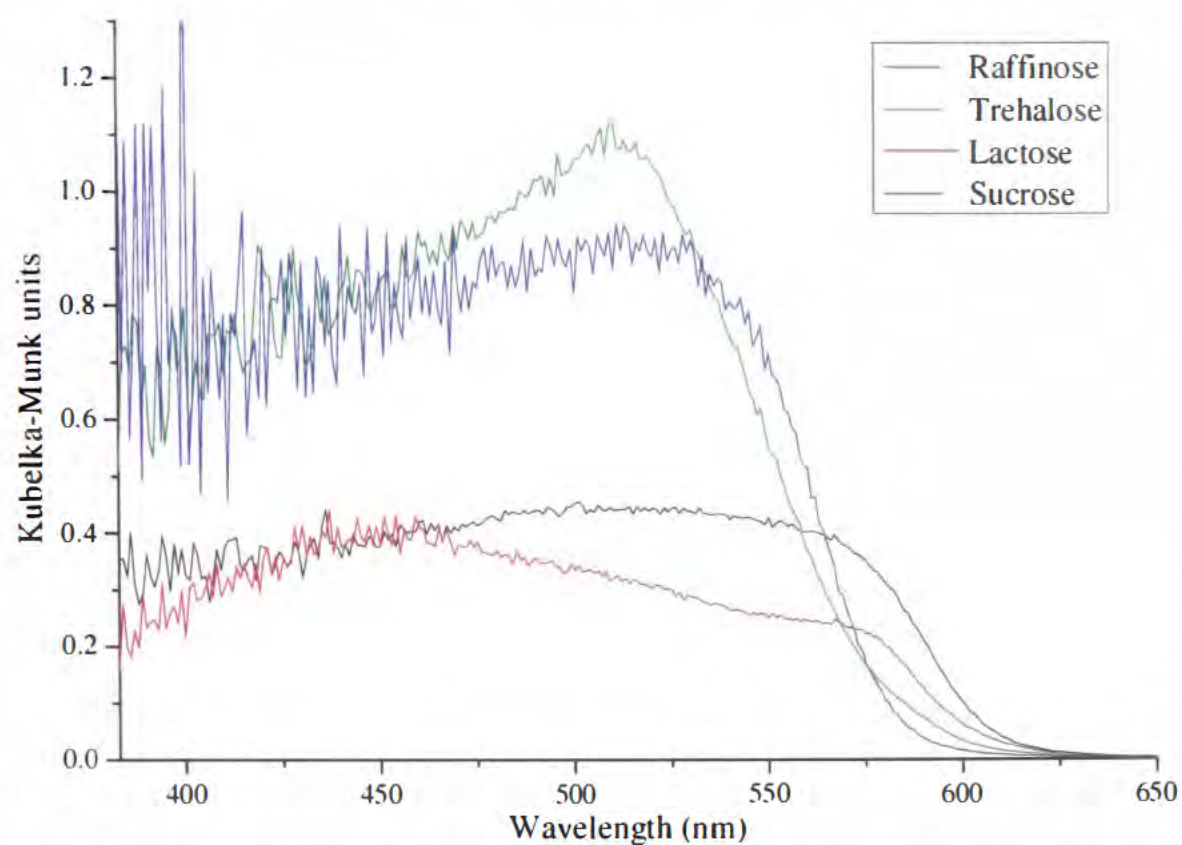


Figure 4.39 A comparison of four crystalline saccharides, each with 0.1 %w/w phenol red. (Samples stored at 57 %RH chosen to represent crystalline samples).

The DRUV spectra of the four crystalline saccharides are dissimilar, possibly reflecting different surface acidity between the samples. The intensities of trehalose and raffinose are much greater than for sucrose and lactose. Trehalose has a peak maximum at 510 nm, raffinose at *ca.* 520 nm, sucrose is again a broad peak, tailing off at 570 nm and lactose appears to have two peaks, the first at 451 nm and the second tailing off at 575 nm. The intensity of the spectra has already been shown to be potentially misleading, for example in figure 4.6, it is observed that the least intense spectrum is for the sample stored at 84 %RH, but the next least intense is for the sample stored at 11 %RH. These spectra were repeated, and although the wavelengths observed were reproducible the intensities were not. The peak of lactose at 451 nm could be said to be observed in the other samples to a significantly lesser degree, and this possible peak will be discussed in greater detail in section 5.5.

Sample	11 %RH	57 %RH
Phenol red	579	579
Sucrose	~540	~570
Lactose	515	~575
Trehalose	515	510
Raffinose	515	~520

Table 4.8. Wavelength (nm) of maximum reflectance of four different saccharides, with 0.1 %w/w phenol red, after lyophilisation and storage for one week at 25° C and controlled %RH. Note trehalose has a different spectrum above 550nm between the amorphous and crystalline forms.

#### 4.34 References

- [1] F. J. Green, *The Sigma-Aldrich Handbook of Stains, Dyes and Indicators*, **1991**.
- [2] X. Dong, Q. Hong, L. He, X. Jiang, S. Li, *International Biodeterioration and Biodegradation* **2008**, *62*, 257.
- [3] B. Makower, W. B. Dye, *Agricultural and Food Chemistry* **1956**, *4*, 72.
- [4] *The Pharmaceutical Codex*, 11th ed., The Pharmaceutical Press, London, **1979**.
- [5] J. T. Cartensen, K. Van Scoik, *Pharmaceutical Research* **1990**, *7*, 1278.
- [6] S. T. Beckett, M. G. Francesconi, P. M. Geary, G. Mackenzie, A. P. E. Maulny, *Carbohydrate Research* **2006**, *341*, 2591.
- [7] N. Faria, M. N. Pons, S. Feyo de Azevedo, F. A. Rocha, H. Vivier, *Powder Technology* **2003**, *133*, 54.
- [8] H. D. Goff, E. Verespej, D. Jermann, *Thermochimica Acta* **2003**, *399*, 43.
- [9] I. Hopkinson, R. A. L. Jones, P. J. McDonald, B. Newling, A. Lecat, S. Livings, *Polymer* **2001**, *42*, 4947.
- [10] T. P. Labuza, P. S. Labuza, *Journal of Food Processing Preservation* **2004**, *28*, 274.
- [11] M. Lappalainen, I. Pitkanen, P. Harjunen, *International Journal of Pharmaceutics* **2006**, *307*, 150.
- [12] M. Mathlouthi, A. L. Cholli, J. L. Koenig, *Carbohydrate Research* **1986**, *147*, 1.
- [13] M.-A. Ottenhof, W. MacNaughtan, I. A. Farhat, *Carbohydrate Research* **2003**, *338*, 2195.
- [14] A. Saleki-Gerhardt, G. Zograf, *Pharmaceutical Research* **1994**, *11*, 1166.
- [15] A. D. Gift, L. S. Taylor, *Journal of Pharmaceutical and Biomedical Analysis* **2007**, *43*, 14.
- [16] A. M. Gil, P. S. Belton, V. Felix, *Spectrochimica Acta Part A: Molecular and Biomolecular Spectroscopy* **1996**, *52*, 1649.

- [17] J. H. Kirk, S. E. Dann, C. G. Blatchford, *International Journal of Pharmaceutics* **2007**, 334, 103.
- [18] P. W. Atkins, J. de Paula, *Elements of Physical Chemistry*, 4th ed., Oxford University Press, Oxford, UK, **2005**.
- [19] G. Xue, *Prog. Polymer Science* **1997**, 22, 313.
- [20] C. J. Kedward, W. MacNaughtan, J. R. Mitchell, *Carbohydrate Research* **2000**, 329, 423.
- [21] K. Kawakami, K. Miyoshi, N. Tamura, T. Yamaguchi, Y. Ida, *Journal of Pharmaceutical Sciences* **2005**, 95, 1354.
- [22] G. Buckton, P. Darcy, *International Journal of Pharmaceutics* **1995**, 123, 265.
- [23] D. Gao, J. H. Rytting, *International Journal of Pharmaceutics* **1997**, 151, 183.
- [24] D. M. M. Jaradat, S. Mebs, L. Chęcińska, L. P., *Carbohydrate Research* **2007**, 342, 1480.
- [25] B. M. Murphy, S. W. Prescott, I. Larson, *Journal of Pharmaceutical and Biomedical Analysis* **2005**, 38, 186.
- [26] J. Bronlund, T. Paterson, *International Dairy Journal* **2004**, 14, 247.
- [27] G. Buckton, E. Yonemochi, J. Hammond, A. Moffat, *International Journal of Pharmaceutics* **1998**, 168, 231.
- [28] X. Chen, S. Bates, K. R. Morris, *Journal of Pharmaceutical and Biomedical Analysis* **2001**, 26, 63.
- [29] N. Drapier-Beche, J. Fanni, M. Parmentier, M. Vilasi, *Journal of Dairy Science* **1997**, 80, 457.
- [30] A. Gombas, I. Antal, P. Szabo-Revesz, S. Marton, I. Eros, *International Journal of Pharmaceutics* **2003**, 256, 25.
- [31] M. K. Haque, Y. H. Roos, *Carbohydrate Research* **2005**, 340, 293.
- [32] S. E. Hogan, G. Buckton, *International Journal of Pharmaceutics* **2000**, 207, 57.
- [33] E. Katainen, P. Niemela, P. Harjunen, J. Suhonen, K. Jarvinen, *Talanta* **2005**, 68, 1.
- [34] L. Norgaard, M. T. Hahn, L. B. Knudsen, I. A. Farhat, S. B. Engelsens, *International Dairy Journal* **2005**, 15, 1261.
- [35] R. Ramos, S. Gaisford, G. Buckton, *International Journal of Pharmaceutics* **2005**, 300, 13.
- [36] Y. Roos, M. Karel, *Journal of Food Science* **1992**, 57, 775.
- [37] M. D. Ticehurst, P. York, R. C. Rowe, S. K. Dwivedi, *International Journal of Pharmaceutics* **1996**, 141, 93.
- [38] A. B. Richards, S. Krakowka, L. B. Dexter, H. Schmid, A. P. M. Wolterbeek, D. H. Waalkens-Berendsen, A. Shigoyuki, M. Kurimoto, *Food and Chemical Toxicology* **2002**, 40, 871.
- [39] J. F. Willart, A. De Gusseme, H. G. Odou, F. Danede, M. Descamps, *Solid State Communications* **2001**, 119, 501.
- [40] H. Nagase, T. Endo, H. Ueda, M. Nakagaki, *Carbohydrate Research* **2002**, 337, 167.
- [41] S. S. Pinto, H. P. Diogo, J. J. Moura-Ramos, *Journal of Chem. Thermodynamics* **2006**, 2006, 1130.
- [42] R. Lefort, A. De Gusseme, J. F. Willart, F. Danede, M. Descamps, *International Journal of Pharmaceutics* **2004**, 280, 209.

- [43] A. Moran, G. Buckton, *International Journal of Pharmaceutics* **2007**, 343, 12.
- [44] H. Z. Cummins, H. Zhang, J. Oh, J.-A. Seo, H. K. Kim, Y.-H. Hwang, Y. S. Yang, Y. S. Yu, Y. Inn, *Journal of Non-Crystalline Solids* **2006**, 352, 4464.
- [45] T. Furuki, A. Kishi, M. Sakurai, *Carbohydrate Research* **2005**, 340, 429.
- [46] M. Takahashi, Y. Kawazoe, Y. Ishikawa, H. Ito, *Chemical Physics Letters* **2006**, 429, 371.
- [47] A. M. Gil, P. S. Belton, V. Felix, *Spectrochimica Acta Part A: Molecular and Biomolecular Spectroscopy* **1996**, 52, 1649.
- [48] Collins, *Carbohydrate*, Chapman and Hall Chemistry Sourcebooks, Bristol, **1987**.
- [49] A. Bouchard, N. Jovanovic, G. W. Hofland, W. Jiskoot, E. Mendes, D. J. A. Crommelin, G.-J. Witkamp, *European Journal of Pharmaceutics and Biopharmaceutics* **2007**, 68, 781.
- [50] S. S. Pinto, H. P. Diogo, J. J. Moura-Ramos, *Journal of Chemical Thermodynamics* **2006**, 38, 1130.
- [51] K. Kajiwara, F. Franks, P. Echlin, A. L. Greer, *Pharmaceutical Research* **1999**, 16, 1441.
- [52] H. Levine, *Amorphous food and Pharmaceutical systems*, Royal Society of Chemistry, **2002**.
- [53] W.-T. Cheng, S.-Y. Lin, *Carbohydrate Polymers* **2006**, 64, 212.
- [54] S. E. Hogan, G. Buckton, *International Journal of Pharmaceutics* **2001**, 227, 57.
- [55] M. Kacurakova, M. Mathlouthi, *Carbohydrate Research* **1996**, 284, 145.
- [56] W.-T. Cheng, S.-Y. Lin, *Carbohydrate Polymers* **2006**, 64, 212.
- [57] J. H. Crowe, F. A. Hoekstra, K. H. N. Nguyen, L. M. Crowe, *Biochimica et Biophysica Acta* **1996**, 1280, 187.
- [58] G. A. Jeffrey, D.-B. Huang, *Carbohydrate Research* **1990**, 206, 173.

## **Chapter 5**

### **Mechanistic studies and sample set expansion**

#### **5.1 Introduction**

A new technique, like perichromism, is developed for one of several possible reasons. These could be that there is currently no technique to examine a particular phenomenon, that current techniques are not sensitive or inclusive enough, or that they are not facile, cost-effective or fast enough. Results in the previous chapter show that perichromism is capable of distinguishing between amorphous and crystalline material, the equipment to do this is much simpler than any of the other techniques used. Obviously, a great deal more work needs to be done before perichromism could become an industrially viable technique, some of which is shown in this chapter. The aim of running a series of control experiments is to determine that the perichromic shifts observed in chapter 4 could only have been caused by the crystallisation of the amorphous excipient, and no other factor is being erroneously ignored.

#### **5.2 Control experiments**

It has been shown that perichromism is a viable technique for distinguishing between amorphous and crystalline material. The presence of the probe does not appear to be affecting the crystallisation of the sample. It now needs to be ascertained if the DRUV results given in chapter 4 are measuring a property of the excipient, or of the probe. The FT-Raman, DSC and XRD of sucrose without the probe have only shown that the dye is not affecting the sucrose. The DRUV spectra in chapter 4 could be generated if phenol red (and not a change to the excipient) has a different DRUV spectrum when freeze-dried and stored at different relative humidity. If, upon freeze-drying an aqueous solution of phenol red and storing it under identical conditions as *per* sucrose for one week, the

DRUV spectra (Figure 5.1) are the same, thus the observed perichromism is not a measure of how the probe itself is being changed in response to humidity. Therefore it is measuring how the interaction with the excipient changes after a morphological change, affecting the bonding of the probe molecule to the surface which alters the wavelength in the spectrum.

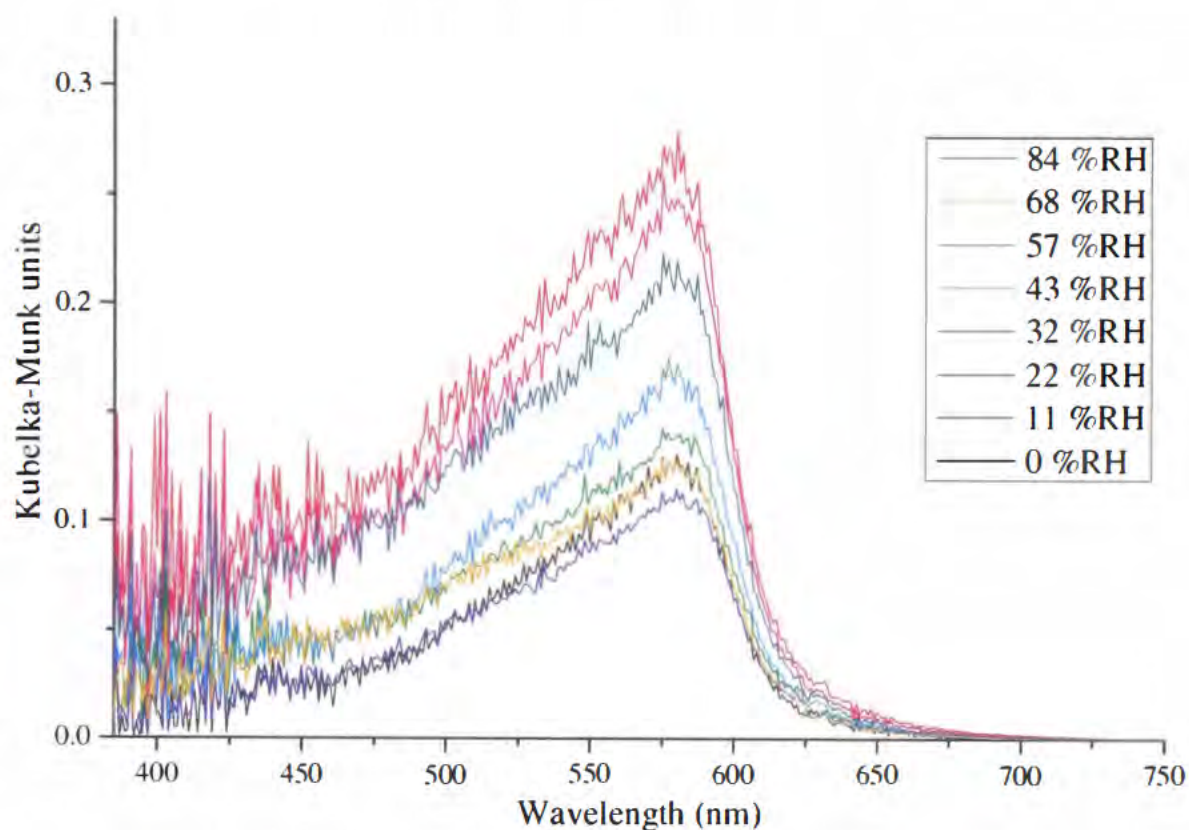


Figure 5.1 DRUV spectra of freeze-dried phenol red stored for one week at constant temperature (25° C) and %RH.

Freeze-drying, and storing at different %RH for one week, causes no change in the wavelength of maximum reflectance,  $\lambda_{\max}$ , (579 nm) of phenol red. Therefore, the DRUV spectra of sucrose with phenol red are showing the morphological form of sucrose present is causing perichromism. This maximum reflectance agrees exactly with the crystalline samples of sucrose with 0.1% w/w phenol red (Figure 4.6). This would suggest that phenol red is being changed by the presence of amorphous sucrose, which is then reversed as the sample crystallises. This is shown by the blue shift of over 30 nm when compared to the DRUV spectrum of phenol red (at any %RH) of the amorphous samples in figure 4.6.

### 5.3 Low-level amorphous content determination of sucrose.

To be an industrially viable technique, perichromism needs to be able to determine low-level amorphous content in a predominantly crystalline solid, and *vice versa*. To test this, known masses of amorphous and crystalline material, with phenol red already incorporated, were gently mixed to produce a homogenous mixture and the DRUV spectra obtained (Figure 5.2). No method of mixing two powders gives a perfectly homogenous mixture, and mixing may cause further generation of amorphous material, it was decided that no content of less than 5 % could be examined with confidence, (table 5.1) as this percentage content can be determined by several techniques. It is expected that for a mixture, two peaks will be observed in the spectrum, one for the amorphous material, and one for the crystalline. Furthermore, the intensities of the peaks will hopefully correspond to the amount of each species in the mixture, allowing for, at least, a rudimentary quantification of amorphous content.

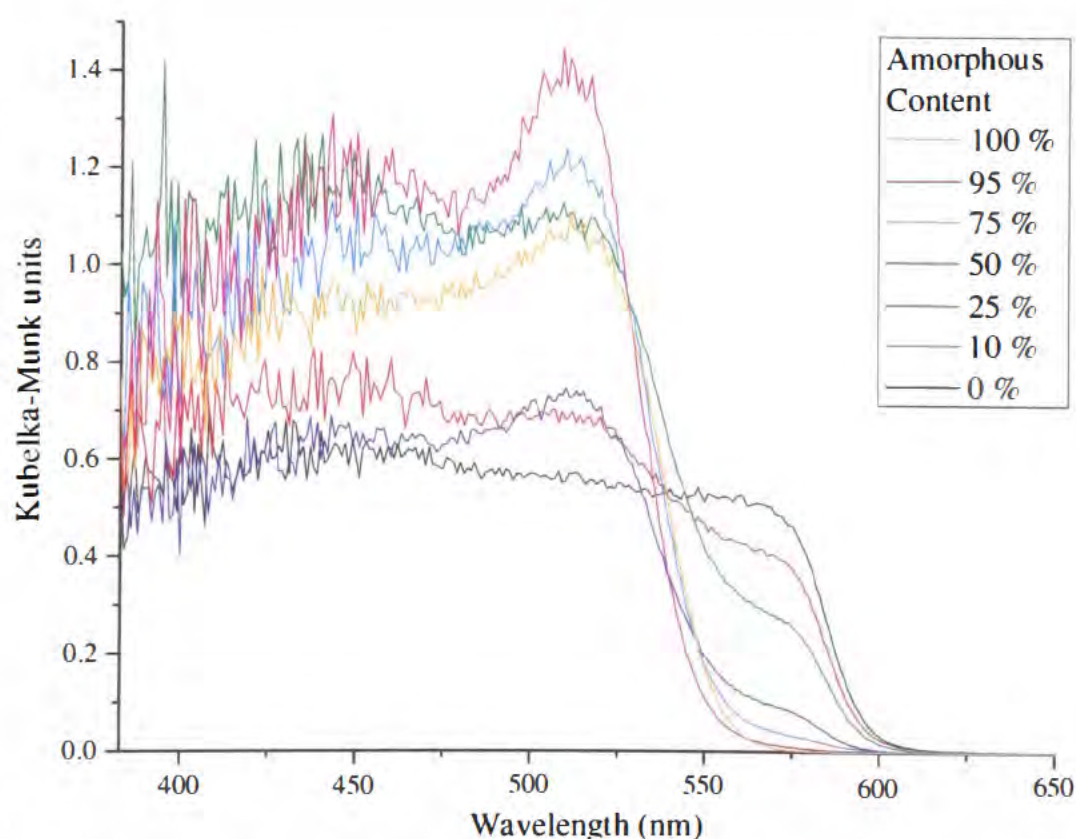


Figure 5.2. DRUV spectra of mixtures of amorphous and crystalline sucrose, (both with 0.1% w/w phenol red).

As predicted, the DRUV spectra has two peaks, one for the amorphous sucrose, the other for crystalline, as observed in figure 5.2. The intensity of reflectance for

the crystalline sample, measured at 565 nm, can be seen to decrease as amorphous content is introduced to the sample. The amorphous peak, measured at 510 nm, does not increase in proportion to amorphous content of the sample. It should be remembered that the intensity of crystalline samples in the DRUV spectra in chapter 4 were not sequential, however this was for 100% crystalline samples. A linear relationship between observed intensity and crystalline material could be reasonably expected. Increasing the amount of crystalline material should give a greater intensity to the peak that is indicative of crystalline material. It should also be the same for amorphous material, but a glance at Figure 5.2 shows this not to be the case. This may be because there are more than one amorphous species available, or that the probe molecule is at the surface of the crystalline samples, but spread throughout the amorphous one (this will be investigated by SEM in section 5.7). However, due to the observed continual decrease in the peak intensity of the crystalline sample it may be possible to predict % amorphous content by plotting the peak intensity of the crystalline sample (at 565 nm) against measured amorphous content. This might be true from plotting the ratio of the intensity of the crystalline peak (at 565 nm) and the intensity of the amorphous peak against amorphous content.

<b>% amorphous content</b>	<b>Peak intensity at 510 nm</b>	<b>Adjusted intensity at 510 nm*</b>	<b>Peak intensity at 565 nm</b>	<b>Adjusted intensity at 565 nm<sup>†</sup></b>	<b>Ratio 510 nm : 565 nm</b>	<b>Log ratio</b>
0	0.565	0.000	0.510	0.492	0	-
10	0.690	0.125	0.414	0.396	0.316 : 1	-0.50
25	1.114	0.549	0.302	0.284	1.933 : 1	0.29
50	0.740	0.175	0.106	0.088	1.989 : 1	0.30
75	1.236	0.671	0.052	0.034	19.74 : 1	1.30
95	1.435	0.870	0.023	0.005	174 : 1	2.24
100	1.090	0.525	0.018	0.000	Infinite	-

Table 5.1. Peak ratios of amorphous and crystalline material in figure 5.2.

\*Adjusted by subtracting 0.565 from all values. <sup>†</sup>Adjusted by subtracting 0.018 from all values.

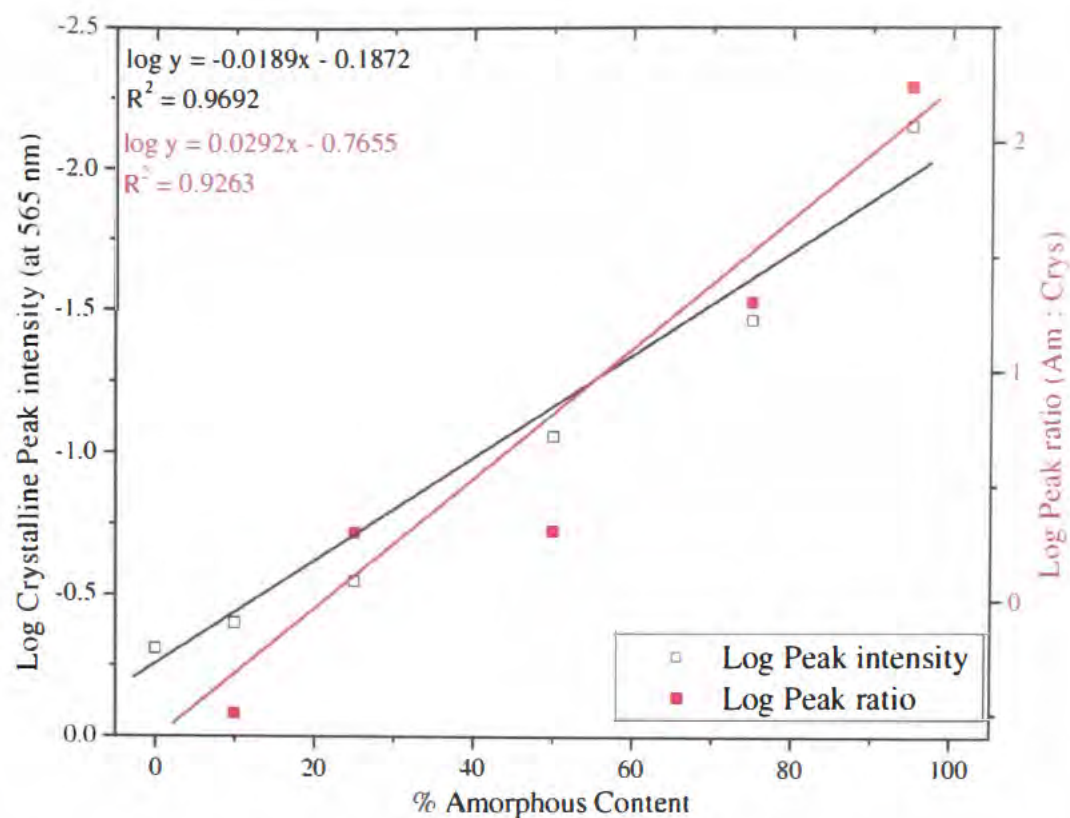


Figure 5.3. Correlation between amorphous content of sucrose and the ratios of crystalline peak intensity to amorphous peak intensity

Although the correlation of the two data sets shown in Figure 5.3 are not quite as good as hoped for – this appears to be mostly due to an unexpectedly low value for the crystalline peak intensity in the 50:50 mixture, the following equations can be used to determine % amorphous content of an unknown sample, from (Equation 9) peak intensity (KM) at 565 nm, and from the peak ratio at 510 nm with 565 nm (Equation 10).

$$\% \text{ Amorphous content} = \frac{\log \text{ KM} - 0.1872}{-0.0189} \quad \text{Equation 9}$$

$$\% \text{ Amorphous content} = \frac{\log (\text{ratio}) - 0.7655}{0.0292} \quad \text{Equation 10}$$

A linear relationship between the log peak intensity and the % amorphous content could give a quantification of the level of crystallinity of a sample – but it probably will have to be analysed on a series of standard amorphous content samples for every sample, and also for each perichromic dye. This could become a very useful tool, but due to time constraints, and the primary aim of

determining if perichromism was actually a genuine phenomena, this possibility could not be continued for the other samples or probes (See section 6).

#### **5.4 Effect of mechanical friction on crystallinity.**

Amorphous content determination is important to the pharmaceutical industry because amorphous material may be an unwanted and unexpected side-product when manufacturing a medicine, affecting the drug profile<sup>[1, 2]</sup> (*i.e.* solubility, stability *etc.*). The manufacturing process most likely to generate unwanted amorphous material is grinding. Grinding is required to reduce particle size, which is of particular importance for a route of administration by inhalation.<sup>[3]</sup> To investigate the effect of grinding, a crystalline solid was ground in a mortar and pestle. Although this does not allow for a high degree of reproducibility, it will give an insight into whether grinding (or other processes that apply a similar mechanical force) does cause the generation of amorphous material on the surface of a crystalline material. It will also determine if the addition of a probe molecule facilitates the measurement of the amount of this amorphous material generated.

The DRUV spectrum of crystalline sucrose, with 0.1 %w/w phenol red, was measured. The sample was then ground using a mortar and pestle. A spectrum was taken after every 10 revolutions of the pestle (Figure 5.4). It was attempted to maintain even pressure throughout grinding. However it should be re-iterated that this experiment is only designed for the qualification of a change in the DRUV spectrum and not quantification.

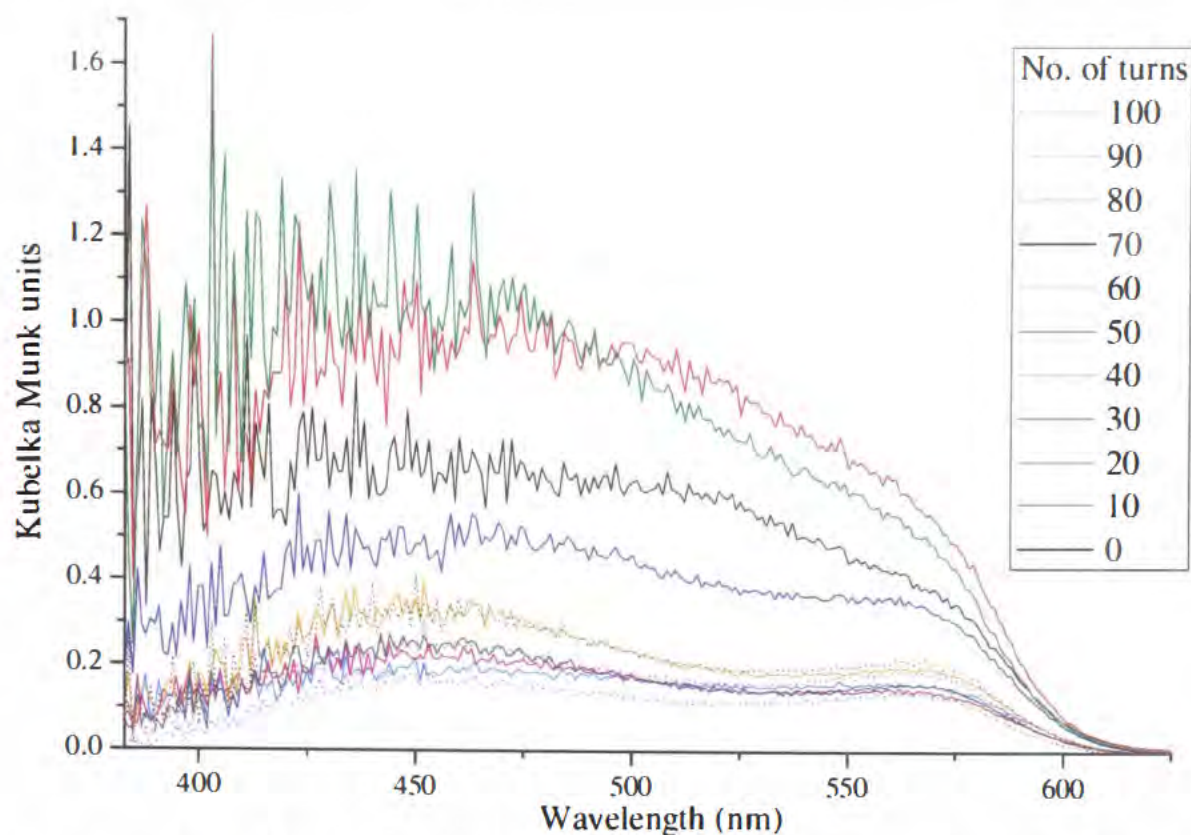


Figure 5.4. DRUV spectra of sucrose with 0.1 %w/w phenol red, each spectrum taken after grinding in a mortar in pestle.

The initial spectrum in figure 5.4, before grinding has occurred, has the same form as that of crystalline sucrose in figure 4.6. As grinding commences, the respective spectra (10 and 20 revolutions) are very noisy in the 400 - 475 nm range. However, it is at 30 revolutions and after, that a noticeable difference in the spectrum occurs, with a new, albeit shallow, peak at  $\approx 450$  nm. After 40 revolutions, the spectrum for ground sucrose does not significantly alter. This means two things; firstly, grinding sucrose has potentially produced amorphous material on the surface of the crystalline sucrose. Secondly, the amount of amorphous sucrose being generated by grinding must reach a finite point quite quickly, otherwise the spectra would continue to change until eventually it was identical to amorphous sucrose produced by freeze-drying. One of the reasons that this does not happen is once the surface contains amorphous material, further grinding of the amorphous regions will not cause any more amorphous material to be generated, secondly grinding with a mortar and pestle will not produce an ultra fine powder, and is not a particularly efficient technique (compared to jet milling for example) so some crystalline material will remain at the surface.

The other reason for the change in spectra may not be due to the generation of amorphous material, but rather the reduction in particle size, and as stated above,

there is a finite limit to how small an average particle size grinding in a mortar and pestle can generate. DRUV spectroscopy is known to be affected by particle size.<sup>[4]</sup> It was decided to see if XRD would be able to detect any difference between crystalline sucrose (with the probe) and the sucrose that had been ground for 100 revolutions, figure 5.5.

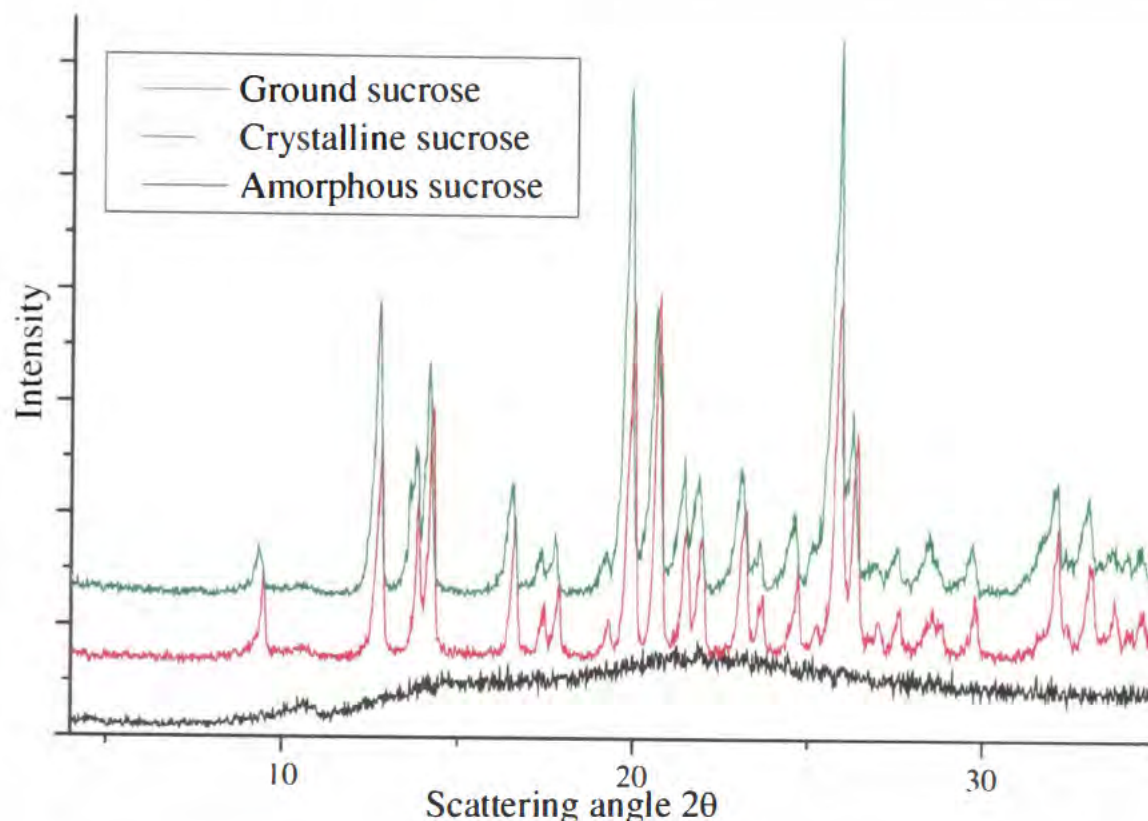


Figure 5.5 XRD of ground, and crystalline sucrose with 0.1 %w/w phenol red.

Remembering that to prepare a sample for XRD requires it to be ground, it was necessary to determine if XRD would be capable of distinguishing between the “crystalline” diffractogram and the “ground”, and as can be seen from figure 5.5 there is no observable difference in the diffractogram. This is very interesting given the fact that DRUV spectroscopy is able to record a noticeable difference (Figure 5.4), suggesting that DRUV spectroscopy is a more sensitive technique than XRD and is able to detect much lower levels of amorphous content than XRD.

## 5.5 Dye concentration.

DRUV spectra of sucrose (Section 4.3) shows that perichromism is observable using phenol red as a probe molecule to distinguish between amorphous and crystalline material. Thus far, only 0.1 %w/w phenol red has been incorporated into the excipient. This allows for determination of amorphous and crystalline species, without causing any unwanted side effects, and is easily measured into a mass of excipient ideal for laboratory use without the risk of excessive errors being introduced. However, there may be more information available in the spectra. It is important to discover the optimum probe concentration, the maximum amount of probe molecule that can be added, such that the reflectance can be reliably measured, and the minimum amount of probe that can be added allowing perichromism to be observed, a range of different probe concentrations were selected, and the DRUV spectra of each is shown in figure 5.6.

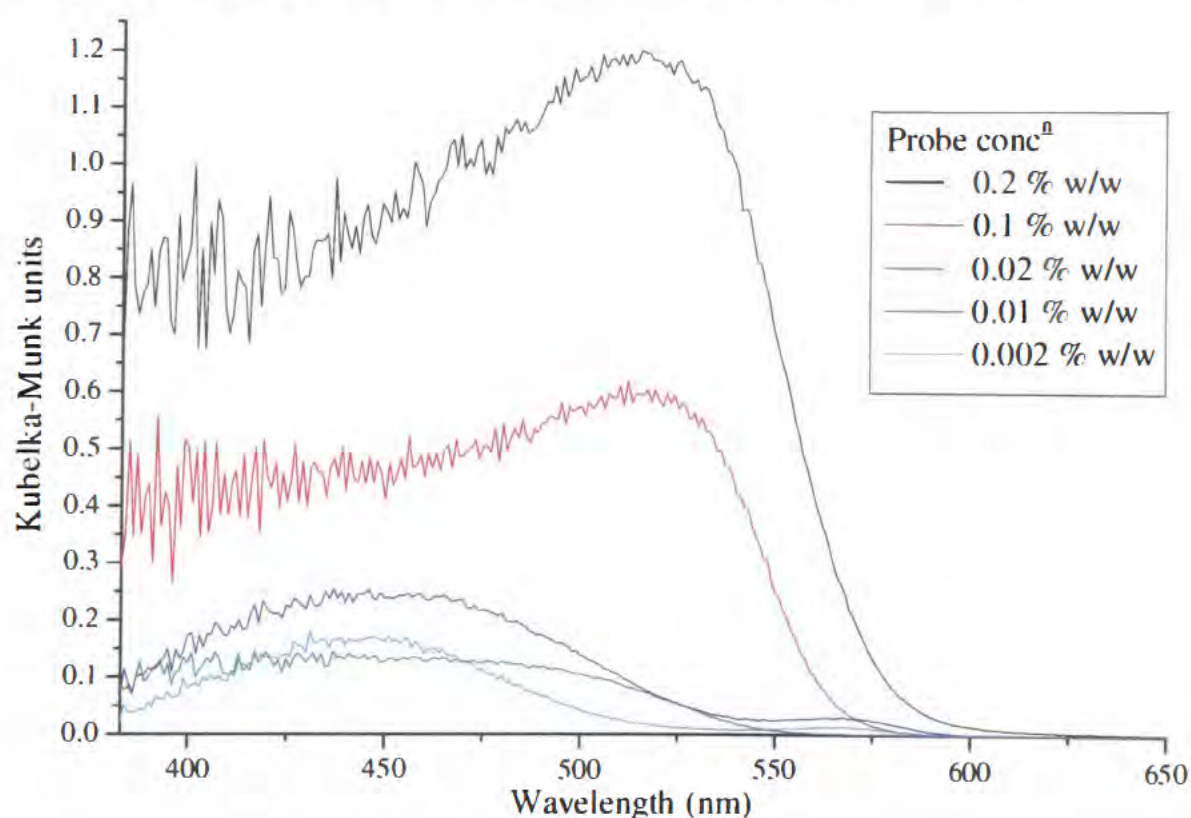


Figure 5.6 DRUV spectra of amorphous sucrose with various concentrations of phenol red.

Figure 5.6 shows that increasing the probe concentration to 0.2 %w/w still allows for perichromism to be measured. However, the region below 450 nm becomes noisy, suggesting that this is near the maximum amount of probe that can be added. Reducing the concentration of the probe shows that amorphous sucrose with 0.02 %w/w, or 0.01 %w/w phenol red has two peaks in the DRUV spectra.

These are at 448 nm and at 567 nm, which correspond exactly to the two peaks that are observed when crystalline sucrose, with 0.1 %w/w phenol red, is ground (Figure 5.4), supporting the theory that the ground samples contain amorphous material. However, as the intensities shown in figure 5.6 are not reproducible, the order of results shown is the same but the actual positions vary noticeably, and the sample with 0.02 %w/w phenol red has a lower intensity than the sample with 0.01 %w/w it would not be logical to attempt to measure the ratio between the two peak intensities for either concentration, and compare for “pH-equivalence” by comparing with the solution UV spectra of phenol red. The change in intensity may be due to small errors with pipetting small volumes of a stock solution or attempting to weigh exactly 0.002% of the mass of sucrose used to produce the concentrations of phenol red as used in figure 5.6.

From figure 5.6, it could be said that the maximum level of probe concentration (for phenol red) is only a little greater than 0.2 %w/w as the peak observed is broad and the baseline is noisy. DRUV spectra for concentrations of 0.002 %w/w phenol red give a reproducible peak position, however, errors occur trying accurately to replicate measurements of the mass of probe (even by taken an aliquot from a stock solution) to give such low concentrations limit its viability for small-scale work. The minimum dye level that could be used with confidence in the accuracy of weighing the probe (for 5 g of excipient) is at best 0.01 %w/w. The concentration that has been used thus far, 0.1 %w/w is in the middle of these two extremes, making it an ideal choice for probe concentration.

## **5.6 Dispersive Raman analysis of trehalose**

Due to the problems that were encountered with FT-Raman spectroscopy of trehalose, dispersive Raman spectroscopy of the samples was attempted. The results for this can be seen in Figure 5.7, and as predicted, was partly obscured by fluorescence from the dye, as observed by the rising baseline.

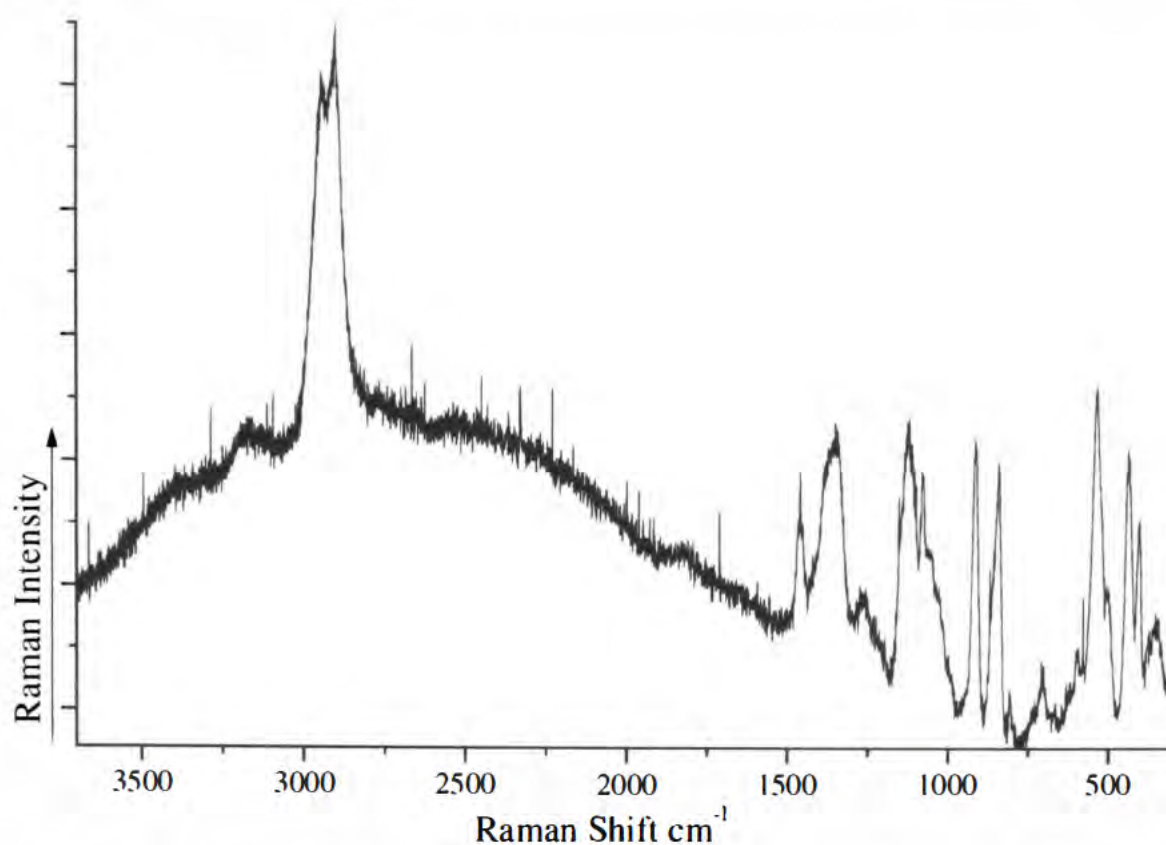


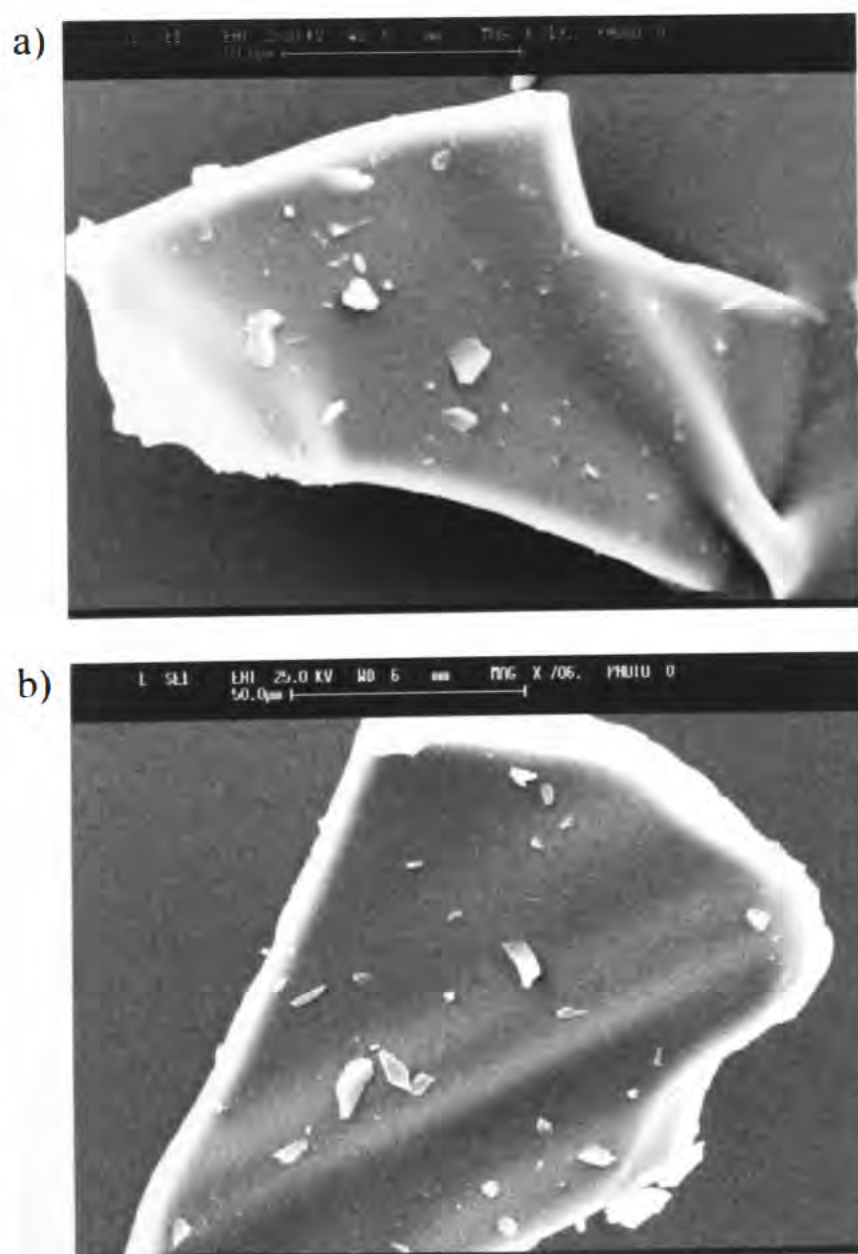
Figure 5.7. Dispersive Raman of trehalose with 0.1 %w/w phenol red stored for one week at 25° C and 57 %RH.

The baseline in figure 5.7 starts to rise at *ca.* 800  $\text{cm}^{-1}$ , which is the point where fluorescence is affecting the spectrum. However, it can be seen from the peaks observed that this sample of trehalose is crystalline, with bands at 842 and 915  $\text{cm}^{-1}$  which correspond to literature data.<sup>[5]</sup> Presumably amorphous material would be determined by the absence of these peaks meaning dispersive Raman could have potentially been used to distinguish between amorphous and crystalline material. This was not done due to both time constraints and the strong level of fluorescence is still a cause of concern when interpreting this data. This area is discussed in more detail in chapter 6.

## 5.7 SEM of trehalose

The four techniques (DRUV, FT-Raman, DSC and XRD) utilised so far for the study of polymorphs of disaccharides have yielded complementary data, and allowed for a clear determination of polymorphic form. A technique that has not yet been used that may reveal further information is scanning electron microscopy (SEM). SEM is capable of giving an image of the surface of the crystal or amorphous region. This may also give an insight into what is occurring to the probe molecule as the excipient crystallises (at high %RH). There are three

possible options: the first is that the probe remains evenly distributed; secondly the probe migrates to either the surface, or the inside, of the crystal; thirdly, the probe molecule is incorporated into the crystal lattice. Of these possibilities, the third option would almost certainly have caused obvious differences to the diffractograms and thermograms. The first option is also less likely, as the amorphous excipient collapses and cakes before crystallising, a process that is reliant on the mobility of the sample. Therefore the probe has probably collated on either the surface of the crystal, inside the crystal or a combination of the two (but no longer evenly distributed). As water is expelled when sucrose crystallises,<sup>[6]</sup> it is most likely that the probe will migrate to the surface rather than inside the crystal, which might be visible in the SEM micrograph. The probable mechanism will be addressed later in this chapter, but SEM will hopefully give an interesting insight as to the surface morphology of both the amorphous powder, and the crystals. SEM images were collected for amorphous and crystalline trehalose, both with and without the probe molecule (Figure 5.8).



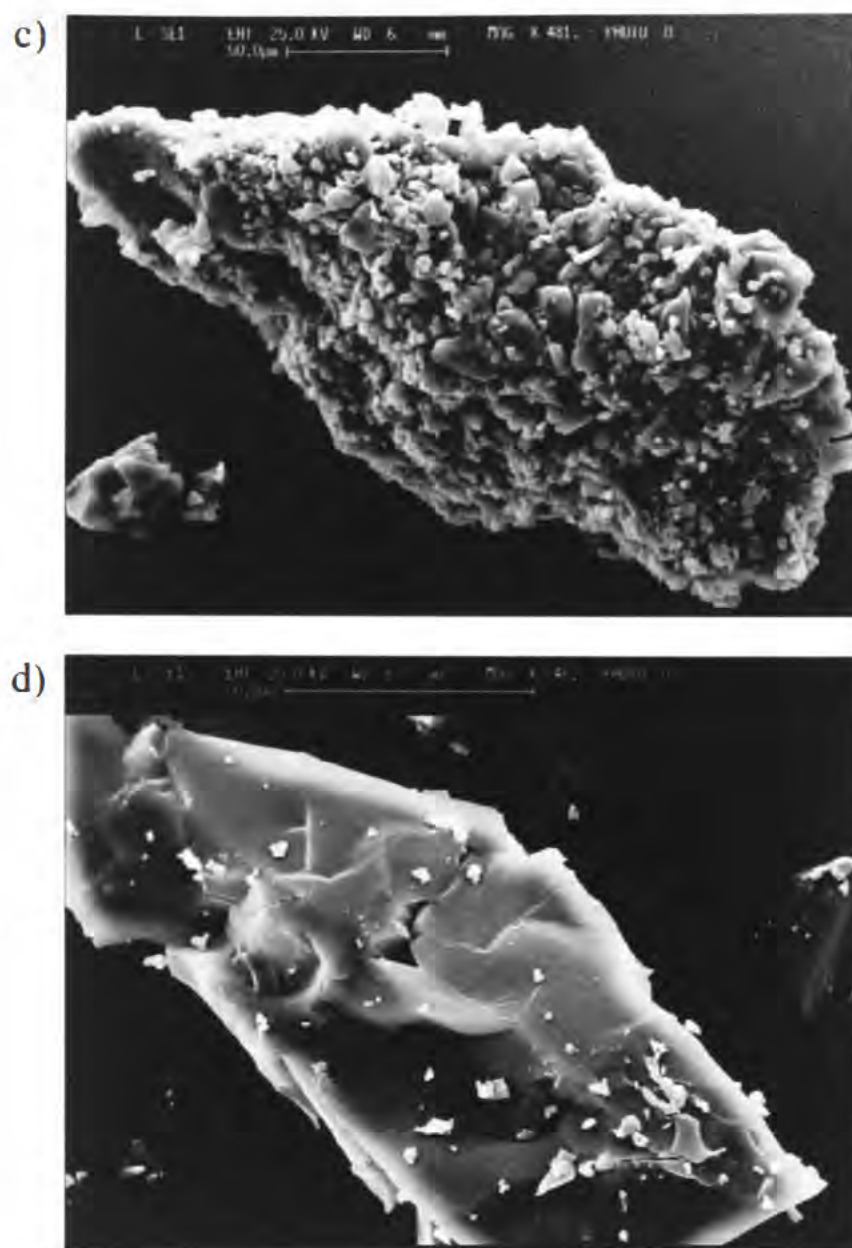


Figure 5.8. SEM of a) amorphous trehalose with 0.1 %w/w phenol red; b) amorphous trehalose; c) crystalline trehalose with 0.1 %w/w phenol red; and d) crystalline trehalose. The scale bar on each micrograph represents 50 µm.

Comparing the two micrographs of amorphous trehalose (Figure 5.8a and 5.8b) reveals an extremely similar picture. Both micrographs look identical, there is no obvious difference to the size of the particles shown, and they both have a smooth “glassy” appearance. This suggests that the probe molecule is not having any effect on the surface of the material (in the amorphous state). If this is the same for all materials then the fact that the surface techniques (FT-Raman and XRD) are unable to distinguish between amorphous samples with or without the probe molecule is explained, as the surface in both cases is the same.

It is immediately clear, upon examination of the four micrographs shown above (Figure 5.8) that one of them is considerably different than the other three – it should also be noted that all four micrographs are representative of each sample,

the particles viewed looked as shown in Figure 5.8 throughout the sample. Trehalose dihydrate with 0.1 %w/w phenol red (Figure 5.8c) appears to be a greatly disrupted surface in comparison with the dihydrate without the probe (Figure 5.8d). The most obvious explanation for this difference is the presence of the probe. The surface of the sample in figure 5.8c is probably not the probe – as it is only present at 0.1% w/w, and is more likely to be trehalose that has reacted to the presence of the probe during crystallisation. The micro-crystallisation seen in figure 5.8c could be indicative of a sample that has not fully crystallised, or maybe that the probe has crystallised sporadically (and separately from the trehalose) throughout the sample, and where these crystals of phenol red appear, the crystallisation of the trehalose is fractured, giving rise to the very disrupted surface. This micrograph does give one final piece of information. The vastly disrupted surface would strongly suggest that this is contributing in some part, at least, to the change in the DRUV spectra (Figure 4.25) between the samples shown in figure 5.8a and figure 5.8c. Assuming this is the case, then the mechanism of perichromism can not be solely due to surface acidity, and the position of the probe (and its 3D arrangement) must therefore play a part in the observable difference in DRUV spectra.

The two amorphous micrographs (Figures 5.8a and 5.8b) have indistinguishable differences in their surface morphology. Trehalose dihydrate is only being affected during crystallisation, but not to the extent where it is crystallising as a different polymorph. The vastly disrupted surface may cause some of the physical properties of trehalose to alter. Possible changes may occur to sample friability and fragility. This will only be an issue if the perichromic probe was used on-line during manufacture of, for example, a tablet, which required a change in morphological form. This is unlikely, as the main purpose of adding the probe is to act as an indicator to show unwanted changes in morphological form. Comparing the surfaces of amorphous and crystalline trehalose with the probe molecule (Figures 5.8a and 5.8c) would lead to the conclusion that a surface active technique utilised to differentiate between these two samples would produce very different results. This has been borne out by DRUV spectroscopy (Figure 4.24) particularly in the 550-600 nm range.

## 5.8 EDX of trehalose

Given the differences observable in the micrographs above (Figures 5.8a-d) a technique that could show where the probe was in figures 5.8a and 5.8c would potentially detail how the probe migrates through the sample as it crystallises. Energy dispersive x-ray analysis (EDX) was attempted on trehalose with 0.1 %w/w phenol red. The aim of this was to discover where the probe molecule was within, and its distribution throughout, the sample. SEM microscopy (Figure 5.8c) suggests that the probe is at, or near the surface when trehalose crystallises, but did not reveal how evenly the probe is distributed the probe was. EDX would be able to determine elemental distribution (as long as the element has an atomic mass greater than 11) within a micrograph, thus an image of the surface of a sample can be constructed. Both the probe and the excipient are organic and the only element present in the probe that is not present in trehalose is sulphur. This means that only *ca.* 9 %w/w of the probe (the probe has a molar mass of 354,<sup>[7]</sup> of which sulphur, with atomic mass 32, provides *ca.* 9 %), present at 0.1 %w/w of the total sample, could be used to distinguish between probe and excipient. This proved to be far too small for EDX to be able to image (it is suggested that it would have required 100 times greater concentration of sulphur within the sample to find it). The EDX results are therefore not shown.

## 5.9 Perichromism with other materials?

It has been observed that it is possible to distinguish between morphological forms of different saccharides, as well as the different crystalline excipients by adding a probe molecule, and comparing the DRUV spectra of each material. Saccharides are carbohydrates, and, as can be seen from their respective structures (Chapter 3) contain many hydroxyl groups. Perichromism may occur through hydrogen bonding between probe and excipient, and if this is the case, a material with a myriad of hydroxyl groups will present a much greater opportunity for perichromism to occur, than a material lacking hydroxyl groups. Testing other materials also affords the opportunity to examine possible perichromism with materials that were used in the literature<sup>[8, 9]</sup> to examine “pH-

equivalence” (comparing diffuse reflection UV with solution UV at different pH and from this calculating the surface acidity, or “pH-equivalence”).

The materials selected were talc, citric acid, sodium bicarbonate and potato starch, which have “pH-equivalence” values of 6.08, 1.45, 8.27 and 4.49, respectively.<sup>[9]</sup> Therefore the DRUV spectra for each of these materials, with phenol red used to determine this value should be super-imposable on the solution UV/vis spectra of phenol red at the aforementioned pH (*i.e.* the DRUV spectra for talc, pH-equivalence value of 6.1, should be comparable to the solution UV/vis spectra of phenol red at pH 6.1 as the talc is equivalent to a solution with a pH of 6.1). The point of maximum reflectance of the probe in the solid state is being compared to the  $\lambda_{\max}$  in the solution state, the “pH-equivalence” value should be independent of the probe used, *i.e.* the same “pH-equivalence” should be determined irrespective of probe molecule used, so comparing the solution UV/vis spectra of phenol red to the DRUV spectra of talc *et al.* (with phenol red) should also allow for “pH-equivalence” values along with any perichromic shift being observed as a change in wavelength. The solution UV/vis spectra of phenol red is shown below (Figures 5.9 and 5.10).

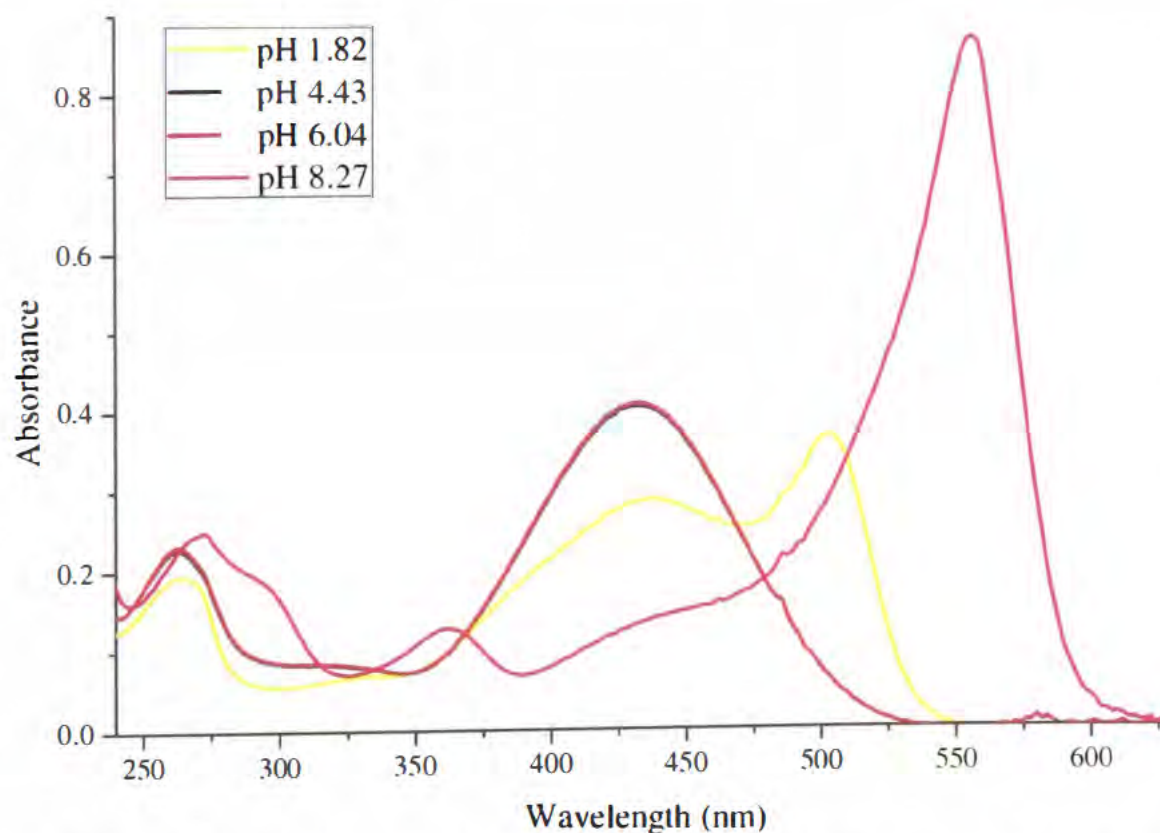


Figure 5.9 Solution UV/Vis spectra of phenol red at four different pH values.

From figure 5.9 it can be seen that there is very little difference between spectra of phenol red at pH 4.43 and pH 6.04. However the spectra at pH 1.82 and pH 8.31 are noticeably different. From the graph above (Figure 5.9) we can observe two successive equilibria, when many more spectra are taken (Figure 5.10) it should hopefully be possible to determine the pH of these equilibria and observe any trends in the solution UV spectra.

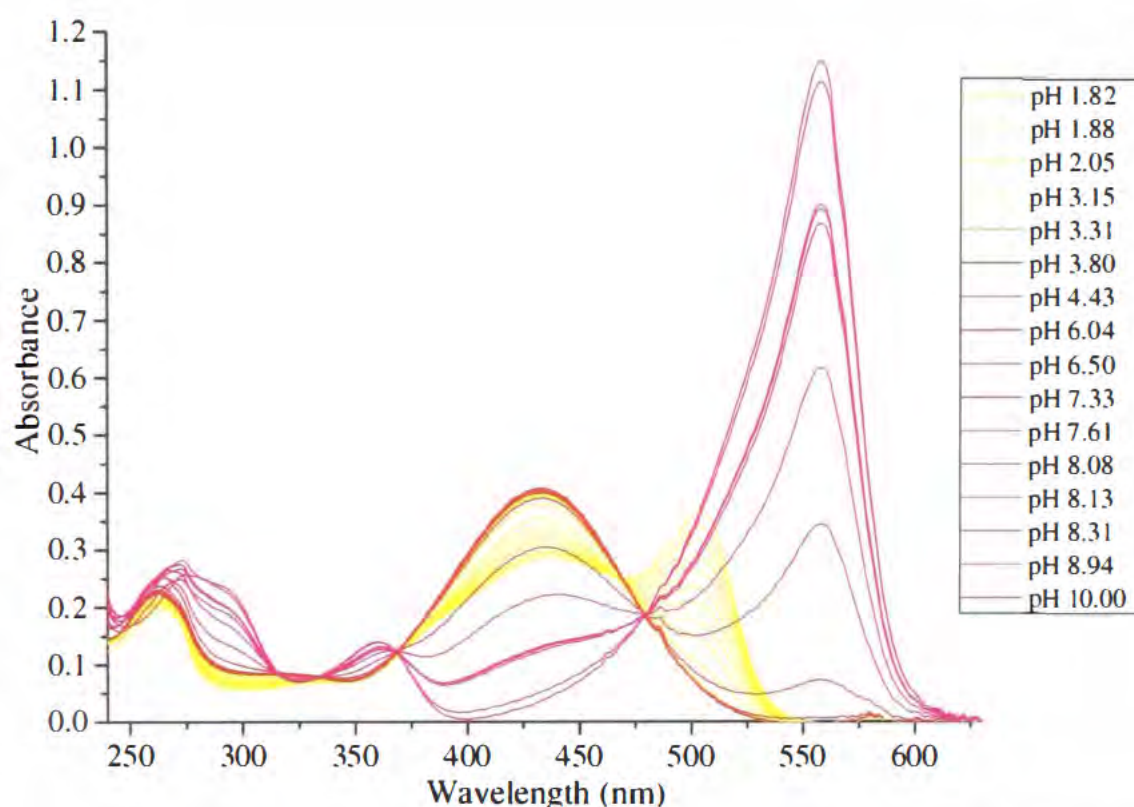


Figure 5.10. Electronic absorbance spectra of phenol red in aqueous solution, buffered to different pH with NaOH and HCl. The colours (yellow, red, magenta) are approximately the colour of the aqueous solution of phenol red at the pH given in the key, which is an incomplete list of pH, to aid clarity.

From the above figure (5.10) it can again be seen that three species of phenol red exist, depending on the pH of the solution, *i.e.* there are two equilibria. Increasing the solution pH from pH 1.8 to pH 3.2 causes the peak at 504 nm to disappear, and the peak at 432 nm to increase in intensity. Between pH 3.2 and pH 6.5, the spectra are identical with one peak, of roughly constant intensity at 432 nm. Increasing the pH above 6.5 causes the peak at 432 nm to rapidly lose intensity, and a new peak, at 558 nm to appear, which increases in intensity as the pH of the solution is further increased.

It would therefore be expected that the DRUV spectra of the four excipients of given “pH-equivalence” values to have comparable peak positions to the corresponding pH of the above spectra from the solution state. It is therefore anticipated that the DRUV spectrum for talc will have a maximum reflectance at 432 nm; for citric acid, 504 nm, with a small peak at 432 nm; for sodium bicarbonate, 557 nm; and for potato starch, 432 nm. In fact it should not be possible, according to “pH-equivalence”, to be able to distinguish between talc and potato starch using phenol red as a perichromic probe. The DRUV spectra of the four excipients are shown below (Figure 5.11).

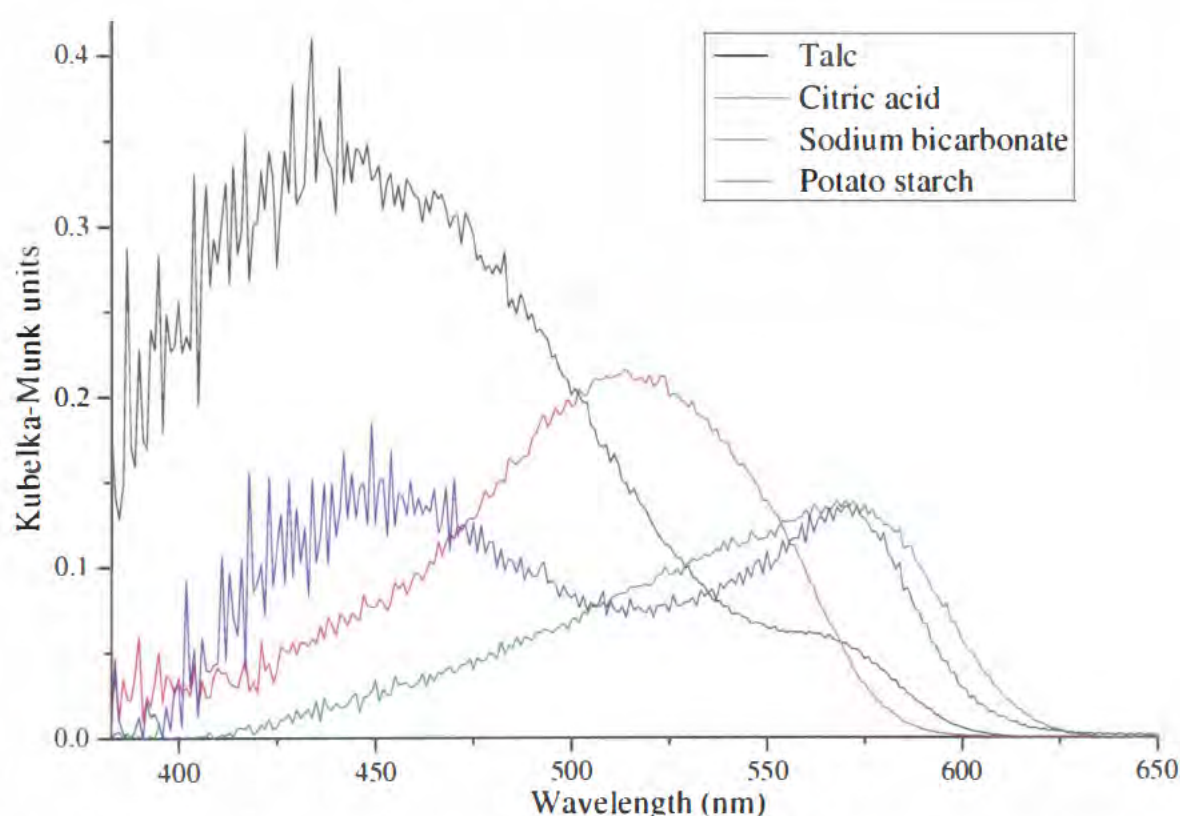


Figure 5.11 DRUV spectra of four excipients with 0.1 %w/w phenol red that were used in the literature<sup>[8, 9]</sup> to examine “pH-equivalence”

Excipient	Predicted peaks (nm)	Actual peak maximum (nm)
Talc	432	438 (and 564)
Citric acid	504 (and 432)	514
Sodium bicarbonate	557	570
Potato starch	432	448 and 570

Table 5.2 A comparison between predicted (from “pH-equivalence” data and spectra shown in figure 5.9) and actual DRUV spectra from figure 5.11.

Excipient	Literature “pH-equivalence” <sup>[9]</sup>	Determined “pH-equivalence”
Talc	6.1	6.6
Citric acid	1.45	≤1.82 <sup>a</sup>
Sodium bicarbonate	8.3	7.3
Potato starch	4.4	6.6

Table 5.3 A comparison between literature and predicted “pH-equivalence” values, determined from figure 5.11. <sup>a</sup>Probably lower than 1.82, but unable to determine an actual value from figure 5.11

The predicted and actual peak maxima are within 15 nm of each other, however, there are two peaks present for talc, which would give a “pH-equivalence” of *ca.* 6.6, (0.5 above the literature value) and two for potato starch, at different wavelengths to those of talc, also given a “pH-equivalence” of *ca.* 6.6 (2.2 above the literature value), the absence of the second peak for citric acid, is not surprising, as this peak was only present in low levels at a greater pH than the surface of citric acid is purported to be. The low intensity of the peak for sodium bicarbonate (about the same as for starch) would suggest that the “pH-equivalence” for this is *ca.* 7.3 (Some 1.0 below the literature value). It should be re-iterated that the absolute intensity of each DRUV spectrum is variable, dependant on many factors including particle size, and only the peak position remains the same. For this reason, “pH-equivalence” values should (if they are to be used at all) be determined from as many probes, with different ionization pH ranges, as possible, using the peak position and possibly the ratio of the intensities, rather than the absolute value determined

This result highlights that “pH-equivalence” data should only be used as a crude estimate as to whether a solid surface is strongly/weakly acidic/basic or approximately neutral. The data is too variable to justify any greater level of confidence, unless using a multitude of different probe molecules in a trial-and-error batch process enabling a much closer determination of the “pH-equivalence”. This suffers from the potential drawbacks of being both time-consuming, and also wasteful. Having different coloured batches of product is

not viable for the pharmaceutical industry, so whatever materials were tested with different probes would then have to be discarded. This is not a serious issue when examining excipients such as sucrose, but could be if an (much more expensive) API is considered.

This result also shows that the mechanism for perichromism is most likely to be affected by the acidity of the surface and how the probe molecule is able to interact with it. Although similar to how “pH-equivalence” values are determined, it is not dependant on the intensity observed in the DRUV spectrum.

### **5.10 Sample preparation**

There is a difference in the sample preparation between samples prepared in this work, and those prepared to measure “pH-equivalence”. Samples herein have been prepared by freeze-drying an aqueous solution of the material (excipient and probe together), but in the literature, the removal of the solvent was achieved through using a vacuum oven<sup>[8]</sup> *i.e.* the probe has been added as a coat and the solvent removed by evaporation of the solvent. It was decided to investigate how sample preparation might affect the DRUV spectra.

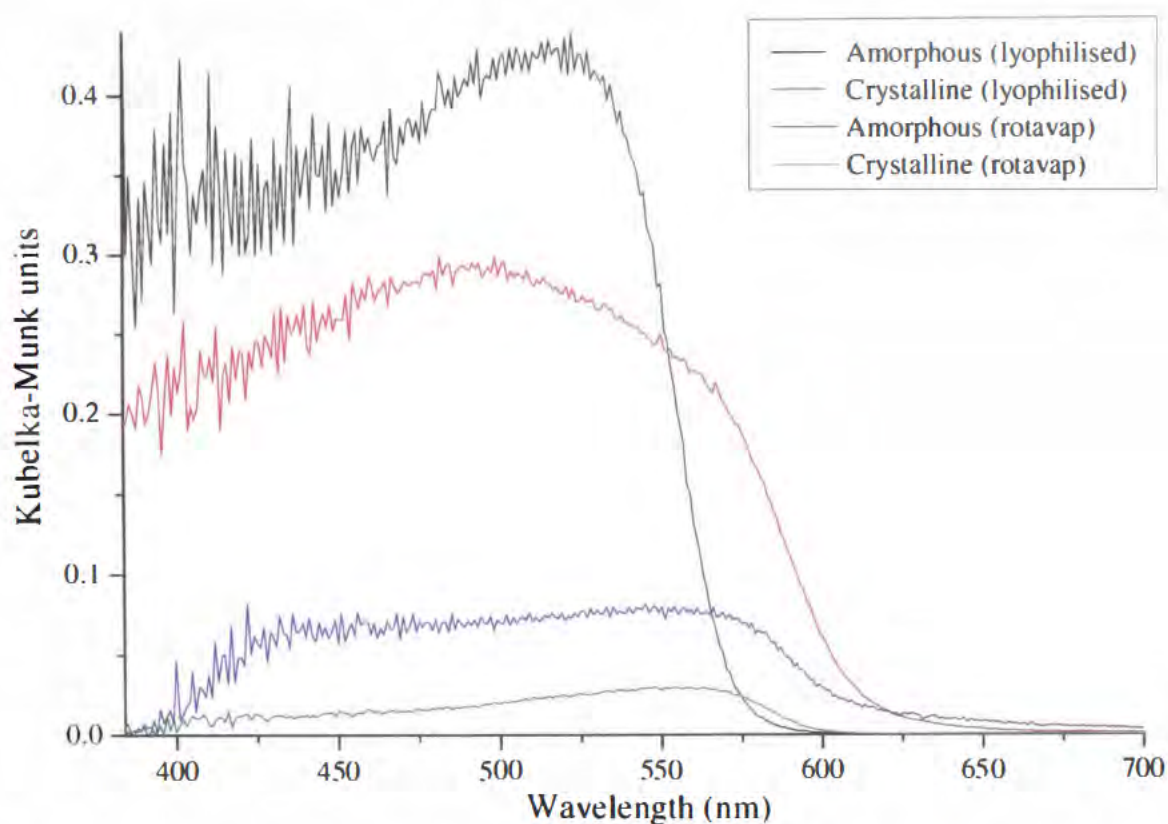


Figure 5.12 Comparison between processing methods (Recrystallisation of lyophilised sucrose and rotary evaporation) for sucrose, with 0.1 %w/w phenol red.

The first thing that can be seen from the spectra in figure 5.12 is that the intensity of the spectra for rotary evaporated sucrose is only a fraction of that for the recrystallised after freeze-drying. This again shows that the “pH-equivalence” values calculated in the literature by comparing the intensity of the peaks are open to interpretation. However, it also appears that the peak position for the two techniques is different. This may be because the probe molecule is not able to interact with the surface of the excipient in the same manner. It should be noted that the sample did not look a uniform colour after removal from the rotary evaporator. Secondly, the spectra shown in figure 5.12 for amorphous sucrose which has had the probe added by rotary evaporation (amorphous rotavap) looks almost identical to the crystalline sample (crystalline rotavap), suggesting that rotary evaporation has caused the amorphous sucrose to crystallise. This was tested by DSC (not shown) where a  $T_c$  could clearly be observed. This means that the bulk of the material was amorphous. It is hypothesised that the addition of the dye by rotary evaporation to amorphous sucrose has caused the *surface* of the sucrose to crystallise, but the interior of the bulk has been unchanged, presumably because there was insufficient time for penetration of the anti-solvent and therefore crystallisation (if the anti-solvent allows for minimal absorption of

the excipient, then crystallisation at the surface of the excipient would be expected to occur).

This is actually a very important result for the viability of perichromism. It has been suggested from earlier results that the sensitivity of DRUV spectroscopy for detecting low-level amorphous (or crystalline) content is much greater than for traditional techniques like XRD and DSC, but this is the first possible case with a sample that has no other polymorphic forms (sucrose is either amorphous or an anhydrous crystal). It has also occurred with a sample that has been extensively examined: although not shown, the DRUV spectra of sucrose has been repeated many times (greater than ten) throughout the course of this work. This is the only time that a sample that is amorphous sucrose as determined by either DSC or XRD has shown to be crystalline in the DRUV spectra. This highlights the sensitivity of DRUV spectroscopy, when compared to DSC, and although it does not show what happens to the bulk material, this is actually irrelevant, as the generation of a different polymorph during manufacture will occur *at the surface* of the material.

### 5.11 Reichardt's dye

The work thus far presented would suggest that the addition of a probe molecule to a solid-surface can generate a qualitative answer to the identity of a polymorph, and to some degree a quantitative answer as to the polymorphic homogeneity of the surface. Perichromism relies on how the probe molecule interacts with the surface, and the most probable interaction for phenol red, is *via* hydrogen bonding due to the two hydroxyl groups (and the sulphonic acid group), this will be discussed in greater detail in a following section (5.12). The idea originates from solvatochromism, and in particular to the visible colour change that Reichardt's phenolate betaine dye displays when dissolved in different solvents. Reichardt's dye has the largest  $\Delta\lambda_{\max}$  with changing polarity.<sup>[10]</sup> It would therefore, be a logical assumption to attempt perichromism using Reichardt's dye as the probe molecule. The reason that this was decided against, was that Reichardt's dye has very poor aqueous solubility, and it has a

permanent dipole<sup>[11]</sup> (*i.e.* is polar), was predicted to be less likely to ionise (lose an electron) which was expected to be necessary for perichromism to be effective.

It was suggested that the name perichromism (*peri* – around; *chromism* – colour) was not the most apt term when using Reichardt's dye. However, there are many other terms ending with “*chromism*” none of which seemed remotely suitable and perichromism *is* still suitable by virtue of the probe interacting with the external surface of the solid.

Using phenol red as a perichromic probe has allowed for the differentiation between amorphous and crystalline forms of the same material, and between a crystalline polymorph of different molecules, but there is also substantial grouping, *i.e.* three amorphous saccharides have a  $\lambda_{\max}$  at 515nm (Table 4.8). It has not been possible to distinguish between these three amorphous saccharides, and there is also some question as to how different the spectra of surfaces with supposedly different “pH-equivalence” values actually are. Using Reichardt's dye, it might be possible to separate these groups, if in solution, they have different polarity, and when freeze-dried the change to the dye remains. Due to its poor aqueous solubility, and the difficulty in protonating the probe, it was deemed a poor candidate for initial experimentation. Indeed, because of its extremely poor aqueous solubility, method 2, (dissolving the probe in aqueous solution with the excipient then freeze-drying) proved to be unsuccessful at introducing the probe molecule to the surface of a pharmaceutical excipient (if a solvent could be found that both Reichardt's dye and the excipient were soluble in, then it would be possible to use this solvent in place of water in method 2, but probably not to freeze-dry). Therefore the method was adapted to become method 3.

Due to the limited aqueous solubility in water, a stock solution of Reichardt's dye was prepared by dissolving 5.0 mg of Reichardt's dye in 50 mL of dichloromethane (DCM). This was then added to each lyophilised saccharide. The DCM was removed by rotary evaporation. The amorphous saccharide with

the probe was then stored for one week at either 0 %RH, or 57 %RH to allow for a comparison between the amorphous and crystalline sample. The DRUV spectra (Figure 5.13) were then measured. It would have been preferable to simply substitute DCM for water in the original method, except it would have damaged the seals in the freeze-drier.

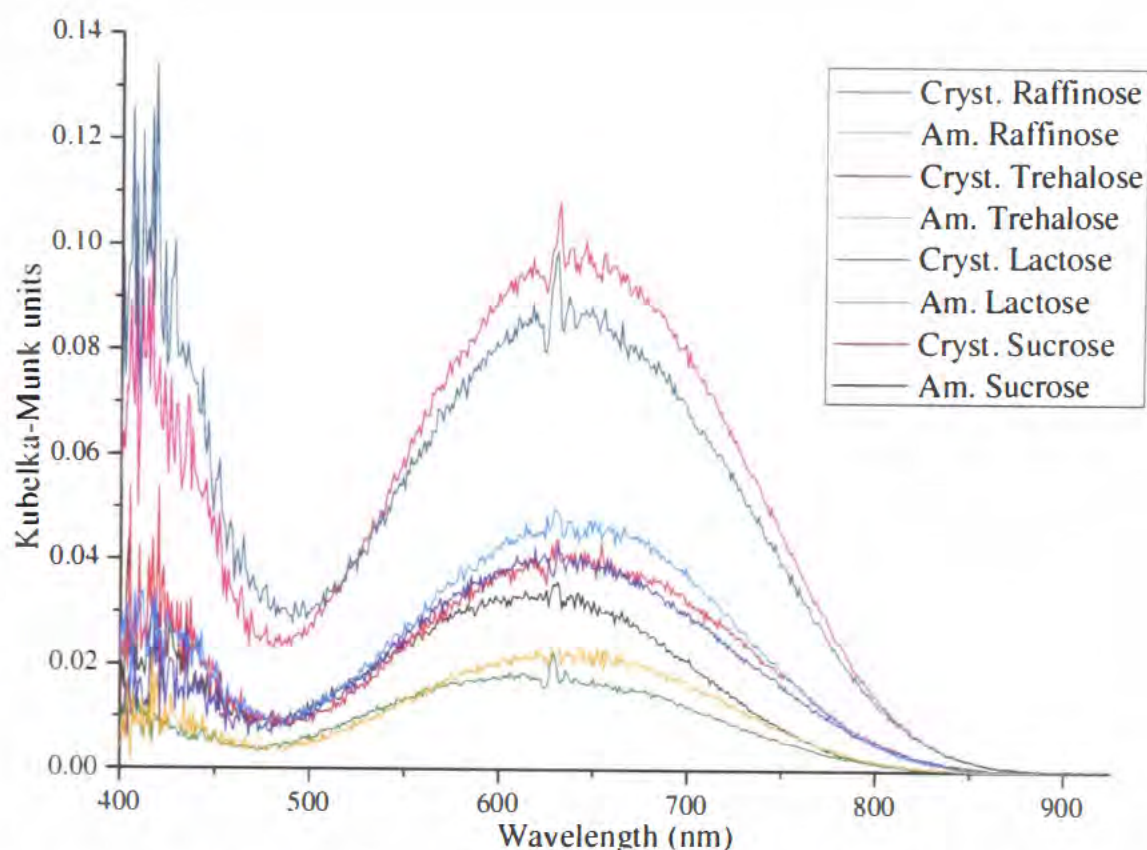


Figure 5.13 DRUV spectra of four saccharides with 0.1 %w/w Reichardt's dye, freeze dried and stored for 1 week at 25° C and controlled %RH. Am. = Amorphous; Cryst. = Crystalline

The DRUV spectra above show that the addition of Reichardt's dye as a probe molecule does not allow for the differentiation between an amorphous and crystalline polymorph of a saccharide, nor to be able to distinguish between the saccharides. All eight of the spectra have two peaks, the first at 410 nm, and the second at 630 nm (although it does look like amorphous sucrose is blue-shifted, it is actually identical in shape and position to both amorphous lactose and raffinose, amorphous trehalose is, much more intense, although it is the same shape). Other DRUV spectra of these excipients, with phenol red, show that there is a difference in the surface depending on polymorphic form, which means that Reichardt's dye is unable to report a phenomenon that phenol red can. The most likely reason for this is the ability of phenol red to hydrogen bond to the

surface of the sugars, which Reichardt's dye is unable to do. The other conclusion that can be drawn from this experiment is that a solvatochromic probe is not necessarily a perichromic one.

As the method had been modified, and no difference between amorphous and crystalline saccharides had been observed by DRUV, it was necessary to determine the morphological form of each compound by a different technique. It was decided to use DSC to determine this, and the thermograms (Figure 5.14) are shown below.

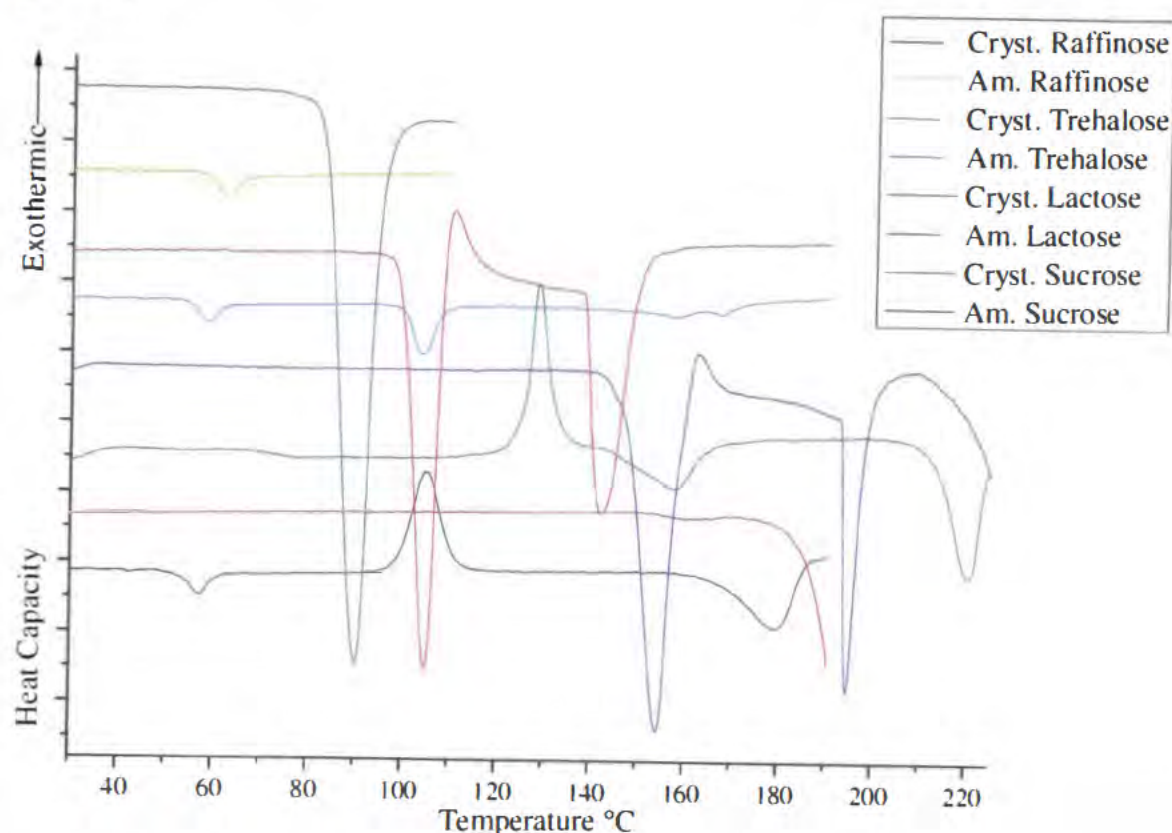


Figure 5.14 DSC of four saccharides with 0.1 %w/w Reichardt's dye stored for one week at 25° C and controlled %RH. Am. = Amorphous; Cryst. = Crystalline.

The DSC thermograms above (Figure 5.14) allow for easy identification of the polymorph of each saccharide. All of the amorphous polymorphs, except for lactose have a  $T_g$  present at *ca.* 60° C, and both amorphous sucrose and lactose show a large exothermic  $T_c$  at 100° C and 125° C respectively. The samples that were presumed crystalline show a  $T_m$  (and decomposition) and for lactose and trehalose, an endothermic peak for the loss of water. It is also very apparent from the above figure that the DSC thermograms of sucrose, which were quite noisy earlier (Figure 4.10) are now much clearer, the cause for this remains unclear, but

one possibility is that the addition of DCM has removed all non-essential water from the samples, which could significantly alter the DSC thermograms.

Although no difference in the DRUV spectra (Figure 5.13) of an amorphous or crystalline saccharide was observed, it is possible that the presence of humidity may still cause a difference to the spectrum of Reichardt's dye and as the amorphous sample was stored in a "dry" atmosphere, and the crystalline in a "wet" one, the lack of change in the spectra, could, although unlikely, have been two effects cancelling each other out. To determine this the DRUV spectra of Reichardt's dye stored at ambient conditions was compared to the DRUV spectra of Reichardt's dye stored in a desiccator at 57 %RH for 1 week (Figure 5.15). It was observed before measuring this latter spectrum that water had actually condensed upon the surface of the Reichardt's dye but did not appear to have interacted in any way.

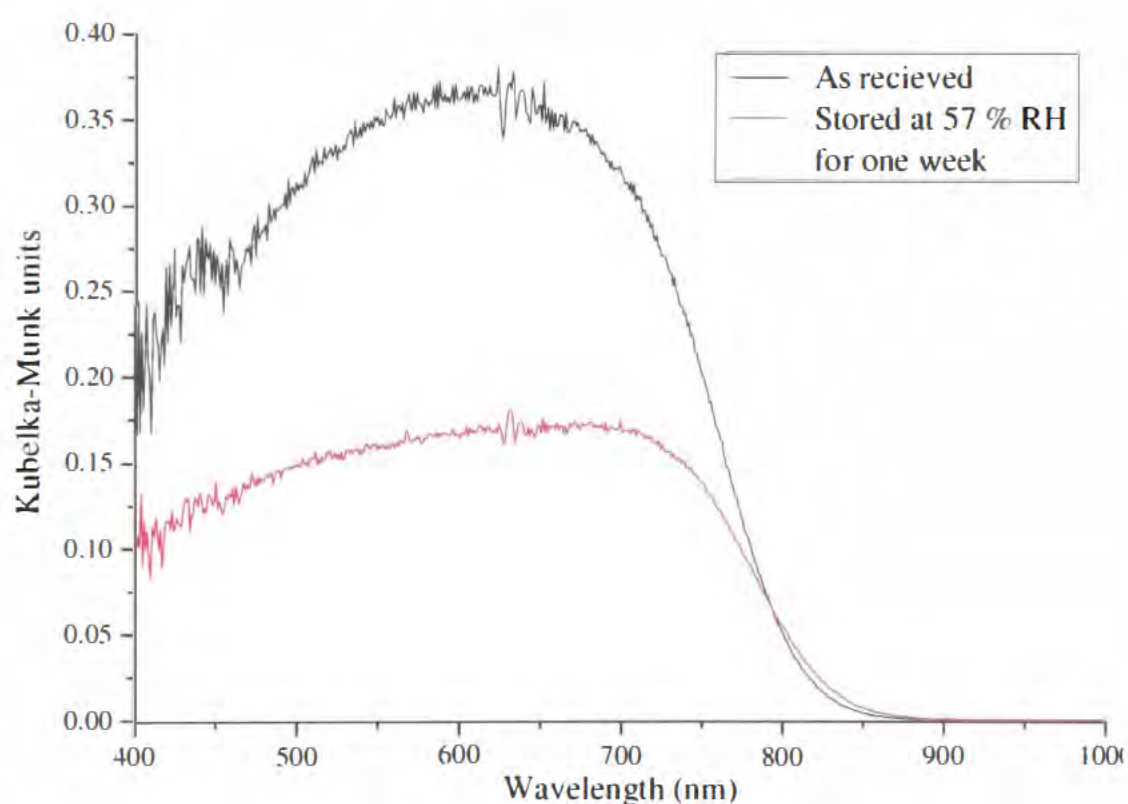


Figure 5.15 DRUV spectra of Reichardt's dye

The presence of water has not had any discernible effect upon the DRUV spectrum of Reichardt's dye. The spectra do look different below 600 nm when compared to those measured with the saccharides (Figure 5.13). In fact, a small shoulder can be observed in the spectrum for Reichardt's dye as received at 450 nm, meaning this difference is almost certainly due to the greater intensity caused by the much larger mass of the dye, as the spectra with the sugars have

only 0.1 % the concentration of probe as the spectra of neat Reichardt's dye above.

### 5.11.1 A comparison of the three methods.

Three methods were ultimately used in this work; the first, methods 1a and 1b, were soon discarded as they were over-complicated, and did not produce amorphous and crystalline material with a measurable amount of probe molecule. The second, recrystallisation of lyophilised material, with the probe incorporated before freeze-drying, was used for the majority of the experimentation, and allowed for the greatest confidence in the results. The third method, adding the probe *via* rotary evaporation, was then chosen to compare the methodology of adding the dye after processing, to see if the fears of causing unwanted changes to the sample would be validated. From results of this third method, this concern appears to have been unnecessary, however, a different, and unanticipated processing problem from rotary evaporation was discovered. Once the solvent has been removed, the probe and the analyte will be left behind in the round-bottomed flask, meaning that there are two problems with this method: firstly, it was unknown if the addition of an anti-solvent had affected the surface of the sample; and secondly, rotary evaporation led to an uneven distribution of the probe throughout the sample.

Whether or not this was also observed for the similar “pH-equivalence” method has not been discussed in the respective literature.<sup>[8, 9]</sup>

## 5.12 Mechanism

The data that has been presented in the preceding sections reveal that the concept of perichromism, *i.e.* the addition of a probe molecule to a material to determine if colour change in response to morphological change, is valid. By careful interpretation of the results, a strong hypothesis can be put forward to describe the mechanism of action of perichromism. This is best observed from the control experiments that have been performed.

DRUV spectra of the probe molecule post lyophilisation and storage at controlled relative humidity and 25° C show that any observed change in the DRUV spectrum involving probe addition to an excipient is not being caused by a change in the probe molecule upon storage at elevated humidity (Section 5.2). Therefore it must be recording an influence exerted by a change in the excipient. It has also been observed that the presence or absence of the probe molecule has no bearing upon the crystallisation or otherwise of the excipient as determined by the other techniques used.

It has been shown that perichromism is not dependant on the direction of morphological form change, *i.e.* perichromism will be observed if a crystalline material becomes amorphous, on the surface at least (Section 5.3) as well as when an amorphous material crystallises. It has also been shown that perichromism is not limited to disaccharides, as raffinose (a trisaccharide) also exhibits perichromism. The excipients so far investigated, however, all have one common factor. They all consist of Carbon, Hydrogen and Oxygen, indeed they are all carbohydrates, and all have multiple hydroxyl groups for hydrogen bonding. Phenol red has also exhibited perichromism with other solid surfaces (Section 5.9), which literature<sup>[9]</sup> states have different surface acidity.

The choice of probe is also very important. Phenol red was chosen because it is a pH indicator, and is also injected in a medical procedure<sup>[12]</sup>, so it should be safe if perichromism were to become a PAT test and this probe was added to pharmaceutical formulations. Being a pH indicator means that solutions containing phenol red as a probe molecule are coloured based on the presence (or absence) of hydrogen ions. Reichardt's dye, does not appear to be influenced by hydrogen bonding, and did not exhibit perichromism in the solid state on any of the four saccharides (Section 5.11) whereas phenol red did give a positive result for perichromism. Therefore perichromism must be being caused by a feature of phenol red that Reichardt's dye does not have. The obvious candidate is the capability of phenol red to hydrogen bond.

It is here that perichromism could be confused with "pH-equivalence". The two ideas are similar but where "pH-equivalence" suggests that the probe molecule is

able to measure the pH of a solid (as one would a liquid), perichromism is suggesting that as the material crystallises, molecules at the surface of the excipient change from a random arrangement to a very well defined lattice. This could induce perichromism in one of two ways: firstly the hydrogen bonds between the saccharide and the probe could be broken and reformed, causing a change in how the probe is bonded to the surface; or secondly, the probe does not break away from the surface, and as the molecule crystallises, the probe is either stretched or compressed, which changes the wavelength of photons that have interacted with these bonds.

Another, arguably less-probable, cause of the perichromic shift is the expulsion of water from the amorphous sample as it crystallises. This non-essential water could quite conceivably interact with the probe molecule at the surface, and the difference in the spectra could be a “dry” probe molecule versus a “wet” probe molecule. If this water is interacting with the probe then a pH measurement is possible. The reason this is considered less probable is that as water is expelled, the probe would have to migrate with it. This would mean that material near the centre of the re-crystallised mass would have a much lower probe concentration. No evidence of this could be observed either visually or spectrophotometrically. The dye could, theoretically crystallise at the surface of the excipient without the excipient crystallising, however, storage of the dye at elevated humidity did not show a change in the DRUV spectra (Section 5.2) or there could be a migration of the probe to the surface during crystallisation, as this would explain the SEM images (Figure 5.8).

To understand how phenol red is able to exhibit a colour change with change of morphological form, it is beneficial to examine how it changes colour in solution. Phenol red, as an indicator can be written as  $\text{In}^{2-}$  when it is completely unionized above pH 8.1. The addition of acid ( $\text{H}^+$ ) will cause a reaction (as well as reducing the pH) and  $\text{HIn}^-$  will be produced when the pH of the solution is below pH 6.6. This is accompanied by a colour change, from fuchsia to yellow. Between pH 6.6 and pH 8.1 both species will be present and the solution appears red. If enough acid is added, and the pH of the solution drops below pH 1.8, then the product is  $\text{H}_2\text{In}$  and the colour of the solution is orange.

The colour change is possibly caused by a ring opening and/or closing – phenol red is mentioned as a zwitterionic material, based on changes to its absorption spectra, in the literature<sup>[13]</sup> which would affect its DRUV spectrum. As the indicator is ionized, the ring structure is closed, and due to steric hindrance (Figure 5.16) the 3D structure of the dye becomes less planar. This ring formation removes the double bond at the pivotal carbon atom, allowing all three benzene rings to rotate around it. This means that phenol red is no longer fully conjugated, and that the  $\pi$ -electron cloud is less able to spread evenly across the entirety of the molecule. Therefore the wavelengths of the photons that is absorbed is lower so the light that is seen visually is of a higher wavelength and a corresponding red-shift in the colour absorbed is seen (fuchsia to yellow). It should also be noticed that this molecule is chiral.

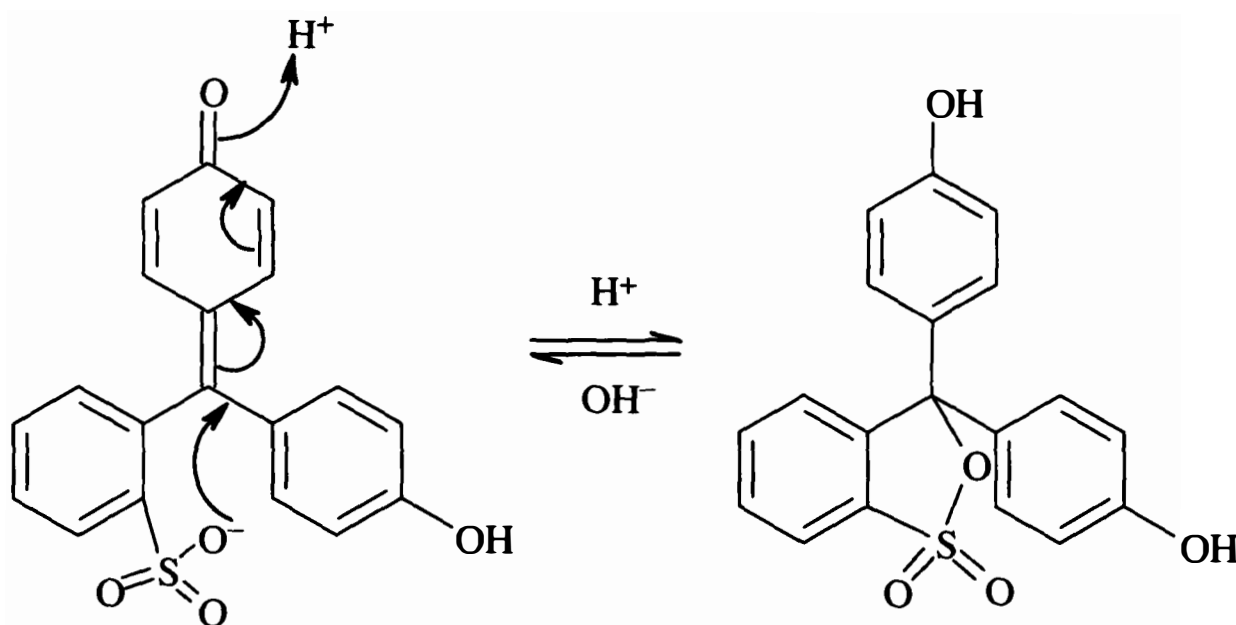


Figure 5.16 Phenol red, ring formation.

The change in planarity mechanism would suggest that the probe may undergo changes in dihedral angles around a central atom, for example the triarylmethane classification of dyes (which includes phenol red) will be perichromic, but a dye that is not, for example neutral red ( $C_{15}H_{17}N_4Cl$ ) a eurhodin dye, will probably not be perichromic. A triarylmethane dye consists of three benzene rings attached to a central carbon atom, allowing for the benzene rings to rotate; a eurhodin dye has three benzene rings that are all bonded in a series (see Figure 5.17 for the structure of neutral red) which would mean they are not able to rotate. It also

means that it would be expected that methyl green (also a triarylmethane dye) should be perichromic. It is believed that this dye may indeed be perichromic using method 2 (storage at elevated humidity), and a re-investigation with this probe would have been implemented given further time.

This theory is quite different from that proposed for “pH-equivalence” which is that of a surface acidity, and is simply a mechanical process as the greater volume of the amorphous solid cakes, and the sample crystallises, the dye is no longer able to maintain its original shape. There will be a finite level to this, but interestingly, this should allow for a perichromic dye with a visual colour change at any pH transition for example, between pH 0.0 and 2.0 like methyl violet to be employed, even if the “surface acidity” of the material under investigation is much greater than this.

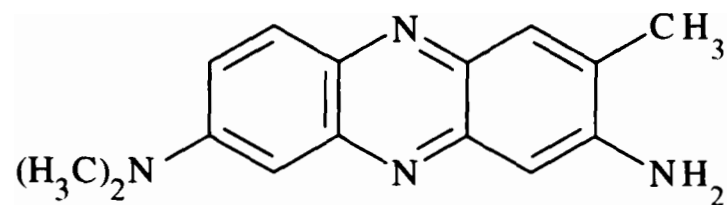


Figure 5.17 Neutral red

Perichromism, will, if this mechanism is correct, only be successful with dyes that are either able to rotate, or are chiral. It may also be that a red-shift is indicative of an amorphous material that has crystallised, and, probably of more import to the pharmaceutical industry, if a blue-shift is detected, then a crystalline material has become amorphous – these shifts certainly appear to be the case for phenol red. This simple difference may allow for the addition of a probe molecule into a pharmaceutical formulation, *e.g.* a tablet, and by taking DRUV spectra before and after processing, allow for a quick, facile determination of the morphological phase of the material being assessed.

Perichromism is not observed because a solid is ionizing another solid, and water has been removed from the system by freeze-drying, therefore ionization is extremely unlikely. Figure 5.16 would suggest that the change in structure from the ring-opened to ring-closed phenol red would be enough to cause a change in

the planarity of the probe molecule and hence a change in the colour as the  $\pi$ -electron cloud will be altered by the probe being out of plane. However, this would be expected to occur at random within the amorphous phase, which would mean that the wavelength of the amorphous material-probe matrix would not be repeatable. The data presented herein show that this is not the case. Therefore this is unlikely to be the mechanism of perichromism, or that a second phenomenon is concurrently causing a repeatable “folding” of the probe structure.

It should be reiterated that most of the excipients studied here are low molecular weight carbohydrates. These molecules have been used extensively in recent years as cryo-protectants when freeze-drying proteins.<sup>[14]</sup> It has therefore been suggested that the excipients could be cryo-protecting the probe molecule, and that hydrogen bonding between the amorphous excipient is preserving the structure of the probe molecule. This would mean that the wavelengths in the DRUV spectra would be reproducible. It would also mean that a change in the DRUV spectra must be caused by an event that affects the amorphous nature of the excipient, for example crystallisation. This mechanism would also explain why there are two distinct groupings of the observed wavelength when using phenol red as the probe molecule; the amorphous wavelength, and the crystalline wavelength, which appears to be unique for each material. Amorphous material of molecules with similar structures, would, according to this theory, have the same wavelength, and indeed, this was observed as the wavelength of the amorphous samples of sucrose, lactose and trehalose, which all have the same molecular formula. All had a  $\lambda_{\max}$  of 515nm, whereas amorphous raffinose, which has a different molecular formula, had a different  $\lambda_{\max}$ . When they crystallised into different, defined structures, the observed  $\lambda_{\max}$  differed between all excipients.

### 5.13 References

- [1] J. J. Seyer, P. E. Luner, M. S. Kemper, *Journal of Pharmaceutical Sciences* **2000**, 89, 1305.

- [2] M. Lappalainen, I. Pitkanen, P. Harjunen, *International Journal of Pharmaceutics* **2006**, 307, 150.
- [3] B. M. Murphy, S. W. Prescott, I. Larson, *Journal of Pharmaceutical and Biomedical Analysis* **2005**, 38, 186.
- [4] H. H. Willard, J. L. L. Merritt, J. A. Dean, J. F. A. Settle, *Instrumental Methods of Analysis*, 6th ed., Wadsworth Publishing Company, Belmont, California, **1981**.
- [5] A. M. Gil, P. S. Belton, V. Felix, *Spectrochimica Acta Part A: Molecular and Biomolecular Spectroscopy* **1996**, 52, 1649.
- [6] B. Makower, W. B. Dye, *Agricultural and Food Chemistry* **1956**, 4, 72.
- [7] F. J. Green, *The Sigma-Aldrich Handbook of Stains, Dyes and Indicators*, **1991**.
- [8] R. Govindarajan, A. Zinchuk, B. C. Hancock, E. Y. Shalaev, R. Suryanarayanan, *Pharmaceutical Research* **2006**, 23, 2454.
- [9] C.-A. Scheef, D. Oelkrug, P. C. Schmidt, *European Journal of Pharmaceutics and Biopharmaceutics* **1998**, 46, 209.
- [10] C. Reichardt, *Chemical Reviews* **1994**, 94, 2319.
- [11] C. Reichardt, *Chemical Society Reviews* **1992**, 147.
- [12] *The Pharmaceutical Codex*, 11th ed., The Pharmaceutical Press, London, **1979**.
- [13] K. Yamaguchi, Z. Tamura, M. Maeda, *Analytical Sciences* **1997**, 13, 521.
- [14] S. D. Allison, B. Chang, T. W. Randolph, J. F. Carpenter, *Archives of Biochemistry and Biophysics* **1999**, 365, 289.

## Chapter 6

### Conclusions and Future work

#### 6.1 Conclusions

The aim of this work was to investigate whether a rapid, facile method for determining morphological phases could be developed. The idea was to utilise a cheap probe molecule that would give one response when a solid was crystalline, and another when amorphous - this would then be detected using DRUV spectroscopy, or a colour change visible to the naked eye, of a similar magnitude to that seen for Reichardt's dye in the solution state.<sup>[1]</sup> The obvious candidate for a visual transition in colour is a pH indicator.

To be able to measure a change in morphological phase, it is necessary to be able to produce crystalline and amorphous polymorphs of a material for comparison. This was achieved by freeze drying an aqueous solution of a pharmaceutical excipient to render it amorphous. The crystallinity could then be tailored by storing the amorphous material at controlled temperature and relative humidity. As the %RH is increased, the  $T_g$  of the amorphous material decreased, until below room temperature, allowing for crystallisation to occur. By adding the probe before freeze-drying, it meant that there was no further processing required to the amorphous or crystalline material, thereby allowing for a simple comparison of each morphological form.

It can be seen in the photographs in chapter 4 (figures 4.5, 4.15 and 4.24) that a noticeable change can be observed visually between an amorphous solid with a probe (phenol red) and its crystalline derivatives. This was further revealed by DRUV spectroscopy, which showed a change in the wavelength of maximum reflectance of up to 50 nm going from the amorphous phase to the crystalline. In all work performed, this change in wavelength was observed as a red-shift on

conversion to the crystalline material. Confirmation of the morphological identity of the materials examined by DRUV was independently established by several techniques, notably XRD and DSC.

To simulate some of the pharmaceutical manufacturing stresses that can be applied to a material, grinding of the crystalline phase was implemented. The DRUV spectra revealed that upon grinding, a second peak could be observed. This peak was at the same wavelength as the amorphous peak. By calculating the peak ratios of the crystalline peak and amorphous peak, it is possible to approximate how much of the crystalline material has been rendered amorphous. Furthermore, a point was reached (surprisingly quickly – *ca.* 40 revolutions of the pestle, see figure 5.4) where the ratios of the peaks no longer changed, *i.e.* continued grinding elicited no further generation of amorphous material.

By storing the amorphous samples at different levels of humidity, it raised the possibility that the pH indicator was responding to this stimulus. However, this was realised not to be the case as the freeze-dried probe did not crystallise on its own (figure 5.1). If incremental increases in %RH were responsible for the red-shift of the probe in the DRUV spectrum, then this red-shift would either: a) also be incremental; or b) would always occur at the same relative humidity. A comparison of the DRUV spectra of sucrose (Figure 4.6) and lactose (Figure 4.22) show that neither of these scenarios is evident. Therefore the level of humidity is not effecting the probe molecule, and the red-shift observed is solely caused by the conversion of the amorphous form to the crystalline form of the excipient. Theoretically, although not tested, raising the storage temperature of the sample stored at 0 %RH above  $T_g$  (also causing crystallisation) would show the same red shift as storing at 25° C and elevating relative humidity.

Perichromism was observed using phenol red on four different saccharides, sucrose, lactose, trehalose and raffinose using phenol red as a probe molecule. Initial experimentation using sucrose and two different probe molecules, methyl green and methyl red did not elicit a perichromic response. It should be reiterated here that the method used at this stage (method 1) was different, particularly when preparing crystalline material to that used when phenol red was

the probe molecule. For methyl green and methyl red, a ten-fold concentration of dye was used and the sample frozen for a short period to prepare amorphous material, for crystalline material it was re-crystallised from warm water and ethanol. For phenol red both amorphous and crystalline material were prepared by freeze-drying an aqueous solution of the probe and excipient, before storing at controlled temperature and humidity allowing some samples to crystallise and others to remain amorphous. It is believed that perichromism would probably have been observed with methyl green (like phenol red, a triarylmethane dye) and possibly methyl red using the same method as employed when phenol red was the probe molecule.

The initial idea for perichromism stemmed from a well-reported phenomenon called solvatochromism, where a probe molecule is different colours in solvents of differing polarity.<sup>[1]</sup> The probe used most solvatochromism is Reichardt's dye,<sup>[2]</sup> which exhibits very noticeable colour change dependant on the solvent dissolved in, for example red in methanol and green in acetone.<sup>[1]</sup> Reichardt's dye was not originally chosen as a model probe for perichromism as it has very poor aqueous solubility. However, once perichromism had been consistently observed for phenol red, it was decided to examine the use of Reichardt's dye, which, if it is, as perichromic as it is solvatochromic, would be an ideal candidate for detecting low levels of morphological change on the surface of an excipient.

Due to the almost complete insolubility of Reichardt's dye in aqueous media, a different method, similar to that used in "pH-equivalence"<sup>[3, 4]</sup> studies was devised. Reichardt's dye was dissolved in a solvent that was also an anti-solvent to the excipient being studied. The solvent was then removed by rotary evaporation, distributing the probe molecule on the surface. Immediately it became apparent that an unknown amount of the dye had not adsorbed on the surface of the excipient, but instead coated the glass vessel. This added a significant error to any method which used peak intensity to identify the morphological form (as in "pH-equivalence") if quantitative data is required. Further more, the addition of an anti-solvent may have caused morphological changes to the surface of the excipient. No perichromic shift could be observed between the DRUV spectra of different morphological forms of excipients

containing Reichardt's dye. Whether this is due to the possibilities discussed above, or Reichardt's dye not being perichromic, was not determined.

As well as investigating Reichardt's dye for perichromic potential, the dataset of excipients was expanded to include a selection of solid surfaces with a wide range of surface acidities as determined by "pH-equivalence" in an attempt to discover if perichromism was a report of surface acidity, or of a difference between an amorphous and crystalline material (assuming that these materials have identical surface acidity). Four materials were chosen, citric acid, talc, potato starch and sodium bicarbonate - ranging in purported surface acidity from pH 1.45 (citric acid<sup>[3]</sup>) to pH 8.3 (sodium bicarbonate<sup>[3]</sup>). Although a small difference in the spectra was observed, the surface acidity of the material (calculated by comparing the DRUV spectra to the solution spectra of phenol red at known pH) gave a broad agreement with the literature surface acidity (table 5.3). The results obtained had large margins of error, leaving little confidence in the ability to claim any surface "pH-equivalence" as determined using phenol red to 2 decimal places, but possibly enabling claims of one surface to be more acidic than another.

It is suggested that the probe molecule is being "cryo-protected" by the excipient and hydrogen bonded to the surface. As the amorphous material crystallises, the hydrogen bonds are broken, and the dihedral angle around the central carbon atom in the probe is able to change, hence change the planarity. There is less 3-dimensional space available in the packing of an amorphous material, as the random alignment of the molecules will cause irregular gaps in the packing which may cause the dye to be forced into a less optimal conformation. Conversely as the amorphous material crystallises, regular gaps form between the molecules of the excipient, and the probe molecule is able to un-fold into a more planar shape, aided by the increased motility of the excipient undergoing crystallisation. This means the probe is less sterically hindered, and able to adopt a more planar shape and a more uniform distribution on the surface of the excipient. This change in planarity affects the  $\pi$ -electron clouds of the phenol groups and results in distortion of the molecular orbitals, giving rise to a visual

change in the colour of the sample. When the crystalline sample is ground, the mechanical stress is great enough to render the surface of the crystalline material amorphous, which acts in a similar way to lyophilisation to a percentage of the probe molecule, the greater the period of grinding, the greater the percentage of amorphous material generated. This gradual change could be seen clearly in Figure 5.4.

The work shown in chapter 4 proves that the addition of a probe molecule to a pharmaceutically important material allows for rapid, facile, identification of any changes that may then occur to the materials morphological form. This would suggest that a PAT can be developed. However, before this can be implemented, there is a lot more work that needs to be performed.

## 6.2 Future Work

The data presented in the preceding chapters has shown that perichromism is a genuine phenomenon and in principle can be used to differentiate between amorphous and crystalline material. It has not, however, shown that it will be a viable PAT test. Before this can happen, further investigation needs to be performed. A strategy of how to move this forward is proposed below, along with some ideas which have developed through the study of perichromism, which will further the scientific understanding of the phenomenon.

One of the first things that can be done is to expand the dataset of pharmaceutical excipients to include a broad range of materials that are used in solid-state formulations and serve a variety of different roles within a formulation. This would have the purpose of expanding the number of surfaces investigated where hydrogen bonding could not be the cause. Candidates to start this could include Teflon or magnesium stearate which is used as a lubricant to prevent frictional problems, *i.e.* capping and fragmentation during tableting.<sup>[5]</sup>

Another area for expansion is in probe selection. Methyl red and methyl green have both been unsuccessfully used as perichromic probes. However, this may have been due to the method used rather than a feature of the probe. Indeed,

methyl green, a triarylmethane dye like phenol red, should be capable of exhibiting perichromism, assuming the mechanism (section 5.13) is correct. If methyl green was added to the excipient the same way as phenol red was (method 2) it would be expected to exhibit some level of perichromism. Once the ideal probe has been found, then further investigation into probe concentration can be undertaken. The optimal concentration of phenol red appears to be 0.1 %w/w although perichromism can be observed at one-tenth of this probe concentration (section 5.5). Different probes may have optimum probe concentrations, with lower concentrations able to be accurately produced from diluting stock solutions of the dye.

One method to find the ideal probe molecule would be firstly to use several triarylmethane probes as perichromic dyes. It is predicted that in this scenario a red-shift will be observed between the DRUV spectra of this probe on a crystalline surface compared to the same probe on an amorphous surface of the same material. Secondly, find (if possible) several probe molecules that will not alter conformation (*i.e.* remain in the same 3-dimensional plane). One possibility is neutral red (Figure 5.23), a euryhodin dye. Ideally of course, several candidate dyes from all dye classifications would be tested.

In section 5.3, it is stated that a linear relationship between a known amorphous content and the intensity of the DRUV spectra at specific wavelengths was observed. This was for sucrose, and could be expanded to include the other excipients used in chapter 4. It would also be beneficial if a more accurate method for producing a homogenous mixture of amorphous and crystalline material could be produced, otherwise using a technique that measures the surface, such as these, errors can be easily introduced. Ideally, being able to produce a material that was a homogenous mixture of 0.1% amorphous content, then a next of 0.2% amorphous content, and so forth, would enable two aims to be realised: is there a linear relationship observable in the DRUV spectra, and the determination of the limit of detection of perichromism, although this will change by both probe and excipient. Data presented in chapter 4 suggests the limit is considerably better than both XRD (10% amorphous content) and DSC

(5% amorphous content) and may even surpass FT-Raman (1% amorphous content).

Grinding of crystalline sucrose has been used to simulate some of the possible mechanical stresses that a pharmaceutical solid may undergo. This has generated some amorphous content on the surface. If it is possible to analyse accurately very small changes in amorphous content, then it could be possible to determine how much amorphous content is generated in a given manufacturing process, and at which stage, enabling the manufacturing process to be modified accordingly so no, or very little unwanted amorphous material is generated. An ideal scenario would be a sample with a probe attached that displayed a distinct colour change before and after a given processes (*i.e.* grinding) as a function of any amorphous material produced during this process. This is a very large change, so is unlikely, but a smaller, but equally obvious colour change could be possible, as it is with Reichardt's dye in solution.

The choice and possible effects of the storage temperature, have not, thus far, been mentioned. The choice for temperature is for the obvious reason that it is near to ambient – and also because the humidity generated by the saturated salt solutions at 25° C is known, adjusting the temperature will cause the relative humidity in the desiccator to change. An investigation could be undertaken to attempt to observe if the amorphous saccharides stored in the desiccators would crystallise in a desiccator that previously it remained amorphous in, or *vice versa* at different temperature, but the same saturated salt solution (thus altering the %RH). It may cause the %RH to try to “buffer” the affect of the temperature change, and no affect be seen, or a cumulative %RH and temperature change could be witnessed, causing faster, more facile crystallisation.

When an amorphous material is maintained at low %RH, the motility of the material is impaired, raising the glass transition temperature of the amorphous material. If the storage temperature of an amorphous sample maintained at very low %RH is well below the  $T_g$ , then the sample will remain amorphous. An interesting experiment that could be conducted would be to store the amorphous saccharides at 0 %RH but at a temperature above  $T_g$  (and  $T_c$ ) but below  $T_m$ . This

should allow the amorphous material to crystallise, without exposing the probe to any water. Theoretically, assuming the mechanism given in section 5.13 is correct, then the DRUV spectra of, for example, crystalline sucrose prepared this way would be identical to the DRUV spectra of crystalline sucrose stored at 57 %RH and 25° C. If it is not, then the probe is (partially or fully) responding to the change in humidity – although as already stated, an incremental change in the wavelength of maximal reflectance would have been expected for all samples at increasing humidity if this was the case.

It would be very interesting to observe the DRUV spectra of a compound with multiple polymorphs. To do this, it may be necessary to add the probe molecule and prepare an amorphous sample (Method 2 as detailed in chapter 3) and then to process this amorphous material so that several different crystalline polymorphs are prepared, as was attempted with raffinose. However, as seen throughout chapter 4, the amorphous material will only crystallise into its most stable form, so additional processing will be required – this may mean that the probe concentration becomes variable across samples, but this will only affect the intensity, and not the position of the maximum reflectance, so perichromism could still be qualified between samples.

Extension of the FT-Raman spectroscopy studies to include trehalose and raffinose samples (with and without the probe) would be of interest. This was originally not possible due to detector issues. Results would be expected to confirm the DRUV, DSC and XRD results of these samples. The SEM of sucrose, lactose and raffinose could be collected as well, as they were for trehalose (section 5.7). There would be no benefit of EDX of these excipients, as the probe is not concentrated enough to determine where in any of the samples it is (section 5.8). It would also be a good idea to get more XRD data of all the samples at relative humidity near to where the samples crystallise, particularly sucrose, at 32 %RH. The diffractogram in figure 4.13 was noticeably different to the other samples – the reason for this is unknown, but further diffractograms might enable the reason for this anomaly to be discovered.

Once perichromism has been established in a range of excipients using a variety of probes, then active pharmaceutical ingredients (API) should also be examined. Investigation could also be attempted to discover the feasibility of one or more perichromic probe molecules being employed to distinguish between two or more surfaces, to determine which of the surfaces is becoming amorphous, and to what extent, thereby opening the possibility of multiple analysis. As has been stated numerous times, the generation of amorphous material can have an unwanted side-effect on the properties of a tablet.<sup>[6-9]</sup> If it is possible to isolate which of these materials causes this, then it is possible to either stop this material becoming amorphous, or to replace it with a different excipient that does not change the properties of a tablet if it is made amorphous. If it is the reduction of crystallinity in the API that results in poorer performance, and the cause(s) of this can not be eliminated from the manufacturing process, then it may be necessary to change how the drug is to be administered, for example instead of as a tablet, it may be better to administer the drug as a capsule.

Another interesting area for expansion would be to research the potential of perichromism to distinguish between different conformers of a material (*i.e.* change at a chiral centre). It would be expected that diastereoisomers for instance, would show different perichromism as many differences between diastereomers have previously been established, not least melting points.<sup>[10, 11]</sup> The ability to distinguish between diastereomers is of major importance to the pharmaceutical industry due to the vastly different properties two diastereomers may have, a well-known example of this being thalidomide, where one diastereomer is an effective antiemetic, and the other (S-thalidomide) a potent teratogen responsible for causing large numbers of birth defects in the late 1950's to early 1960's.<sup>[12]</sup>

### 6.3 References

- [1] C. Reichardt, *Chemical Reviews* **1994**, *94*, 2319.
- [2] K. Stadnicka, P. Milart, A. Olech, P. Olszewski, *Journal of Molecular Structure* **2002**, *604*, 9.
- [3] C.-A. Scheef, D. Oelkrug, P. C. Schmidt, *European Journal of Pharmaceutics and Biopharmaceutics* **1998**, *46*, 209.

- [4] R. Govindarajan, A. Zinchuk, B. C. Hancock, E. Y. Shalaev, R. Suryanarayanan, *Pharmaceutical Research* **2006**, 23, 2454.
- [5] M. E. Aulton, *Pharmaceutics: The science of dosage form design*, Second ed., Churchill Livingstone, **2002**.
- [6] J. J. Seyer, P. E. Luner, M. S. Kemper, *Journal of Pharmaceutical Sciences* **2000**, 89, 1305.
- [7] M. Lappalainen, I. Pitkanen, P. Harjunen, *International Journal of Pharmaceutics* **2006**, 307, 150.
- [8] D. Al-Hadithi, G. Buckton, S. Brocchini, *Thermochimica Acta* **2004**, 417, 193.
- [9] E. Katainen, P. Niemela, P. Harjunen, J. Suhonen, K. Jarvinen, *Talanta* **2005**, 68, 1.
- [10] *CRC Handbook of Chemistry and Physics*, 75th ed., CRC Press, Boca Raton, Florida, **1994**.
- [11] *The Pharmaceutical Codex*, 11th ed., The Pharmaceutical Press, London, **1979**.
- [12] M. E. Bosch, A. J. Ruiz Sanchez, F. Sanchez Rojas, C. Bosch Ojeda, *Journal of Pharmaceutical and Biomedical Analysis* **2008**, 46, 9.